Conformations and Charge Fluctuations in Polyelectrolyte Solutions

Thesis by
Kevin Shen

In Partial Fulfillment of the Requirements for the
Degree of
Doctor of Philosophy

CALIFORNIA INSTITUTE OF TECHNOLOGY
Pasadena, California

2019
Defended July 12, 2018

Kevin Shen
ORCID: 0000-0001-9715-7474

To my dad, Liang-Ping Shen
Thank you for introducing me to the
beauty and magic
that is math and science.
Thank you for teaching me to love
both the natural and human world.

ACKNOWLEDGEMENTS

I would like to thank Caltech and many wonderful people for these formative PhD years of mine. First and foremost I want to thank my advisor, Zhen-Gang Wang. The lucidity of Professor Wang's lectures, and the piercing curiosity and insight he brings to science never cease to amaze and inspire me; our discussions always lead to new answers and questions that bring fun and energy to the pursuit of science. Outside of science, I want to thank Professor Wang for being an incredibly supportive advisor and mentor, and for providing me with a space to grow. Professor Wang is a model scholar and mentor, and I will always remember his reminder to our group to take a step back, look at the clouds, and wonder.

Next, I want to thank my thesis committee – John Brady, Mikhail Shapiro, and Tom Miller. They have all been inspiring scientists and have given me valuable scientific and career advice that will guide me for the rest of my life.

I would like to thank the Chemical Engineering Staff for making the department feel like home. Special shout-outs to Kathy Bubash, Martha Hepworth, Allison Ouelette, Sohee Lee, and Suresh Guptha for their smiles and assistance.

I thank the many people that I have worked and laughed with over the years – Dr. Issei Nakamura, Dr. Xiaofei Xu, Dr. Umi Yamamoto, Dr. Pengfei Zhang, Dr. Huikuan Chao, Dr. JJ (Jian Jiang), Dr. Rui Wang, Dr. Bilin Zhuang, Ahmad Omar, Hyeongjoo Row, Andy Ylitalo, Rachel Krueger, Alex Vaschillo, Dr. Nuo Wang, Dr. Marco Heinen, Dr. Mu Wang, Charlie Slominski, Eric Burkholder, Austin Dulaney, Dr.Stewart Mallory, Camilla Kjeldberg, Zhiwei Peng. Rui and Bilin were instrumental mentors when I was first getting started at Caltech, and they treated me to much delicious food. Issei and Umi brought a zany goofiness that kept work fun. Ahmad always prompted the most amazing discussions, from deep science questions to timely social commentary. Life also would not have been the same without the amazing classmates and friends – Yufeng Huang, Joey Kim, Isaac Fees, Kevin Marshall, Travis Schlappi, Sho Takatori – with whom I studied for quals, grabbed late night food, rode bikes, and shot the breeze.

I want to thank my wife Wanwan for being the most wan-derful partner I could ask for. She has been a shining beacon in my life these past years, a refuge and constant source of endless love, support, wisdom, and laughs. I thank her for the joy and beauty she brings to my life, and I am excited for the many adventures ahead of us.

Above all I want to thank my family for their enduring love and support. I want to thank Stephanie for being a rock and reminder of what's important in life. I thank my mom for her calming, irreverent humor. And last but not least, I want to thank my dad for inspiring and supporting me my whole life, for fostering my deep interest in science when I was a child, and for tirelessly sacrificing throughout life so that my sister and I could be the best we could be. I strive to be as fearlessly supportive and loving as he is.

Lastly, I want to express gratitude for the support by National Science Foundation Graduate Research Fellowship (NSF-GRFP Grant) DGE-1745301 and the Jacobs Institute for Molecular Engineering for Medicine. Their support afforded me the space and time to ask and explore the deep questions I seek to answer.

ABSTRACT

From DNA and RNA encoding life to flocculation agents used in water remediation, charged polymers (polyelectrolytes) are prevalent in nearly all facets of our lives. The charged nature of polyelectrolytes has rendered them useful in many applications, from the stabilization of colloids to the formation of nanoparticles for drug or gene delivery. There are open questions regarding the factors that dictate polyelectrolyte stability, and electrostatic fluctuations, first elucidated by Debye and Hückel for simple electrolytes, are key to the thermodynamic description of such charged systems. Electrostatic fluctuations lead to ionic clouds around charges, leading to favorable energy decreases. While charge-fluctuations are well-described for simple electrolytes, the impact of polyelectrolyte (PE) charge connectivity on charge fluctuations is much less well understood: a huge number of degrees of freedom must be considered in order to describe the multicomponent nature of polyelectrolyte solutions and the large number of conformations the polyelectrolytes themselves can assume. Past theories have both under- and over-estimated the connectivity effects on electrostatic fluctuations, and do not give a clear picture of the transition from weak to strong electrostatic fluctuations.

My work has focused on coming up with a theory that self-consistently accounts for the coupling of chain connectivity and electrostatic fluctuations, thus spanning electrostatic fluctuations from weak to intermediate fluctuation strengths. In particular, I present a novel renormalized Gaussian fluctuation (RGF) theory that identifies the renormalization of chain structure as a key physical consequence of intermediate-strength electrostatic fluctuations. The theory self-consistently couples chain structure with the thermodynamics, and mediates the transition from weak, linearized fluctuations to the onset of stronger fluctuation effects like ion pairing. While the onset of these different fluctuation effects has a clear sequence, they are all coupled and must be determined self-consistently. A key concept introduced by the theory is the notion of the polyelectrolyte self energy, which describes the electrostatic work required to charge the molecule in solution, and provides a useful perspective from which to understand and rationalize the effects of chain conformation on thermodynamic behavior. We use the theory to study the phase behavior of polyelectrolyte solutions and connect theory to experimental results.

PUBLISHED CONTENT AND CONTRIBUTIONS

[1]K. Shen, and Z.-G. Wang, "Polyelectrolyte chain structure and solution phase behavior", Macromolecules **51**, 1706–1717 (2018) DOI:10.1021/acs.macromol.7b02685.

[2]P. Zhang, N. M. Alsaifi, J. Wu, and Z.-G. Wang, "Salt partitioning in complex coacervation of symmetric polyelectrolytes", Macromolecules **51**, 5586 (2018) DOI:10.1021/acs.macromol.8b00726.

[3]K. Shen, and Z.-G. Wang, "Electrostatic correlations and the polyelectrolyte self energy", J. Chem. Phys. **146**, 084901 (2017) DOI:10.1063/1.4975777.

In all the above, K.S. participated in the conception of the project, conducted calculations, analyzed the data, and participated in the writing of the manuscript.

TABLE OF CONTENTS

Chapter 1

INTRODUCTION: CHARGED SYSTEMS

This introductory chapter gives an overview of the basic features of charged systems and a sense of the range of contexts where charged molecules, in particular charged polymers (polyelectrolytes), might appear. We outline the classical theoretical descriptions of such systems in order to give context to the open theoretical challenges that need to be addressed and the physical questions that must be answered. Subsequent chapters present our new theoretical framework and its application to polyelectrolyte systems.

This chapter includes content from our previously published article:

[1]K. Shen, and Z.-G. Wang, "Electrostatic correlations and the polyelectrolyte self energy", J. Chem. Phys. **146**, 084901 (2017) DOI:10.1063/1.4975777.

1.1 Charged Molecules in Nature

Our lives abound with polymers and colloids – insoluble large molecules and micron-sized particles "suspended" in solution. To write or paint in the past millennia one had to grind inkstone or other mineral pigments and suspend the resulting particles in water. Without further additives, the resulting inks and paints did not stay suspended in solution nor did they last long on the writing substrates. The innovation of adding gum arabic, a natural mixture of polysaccharide polymers, or other natural binders like egg yolk greatly improved the stability of inks and paints and their durability when applied [1]. During the Renaissance, painters like Jan van Eyck exploited another colloidal suspension innovation – oil-based paints, which could suspend more pigments for increased vibrancy and would dry more slowly to allow more precise mixing of colors – to achieve ever-increasing realism in paintings [2]. Literally entire eras of art and human culture can be characterized by innovations in colloidal suspensions.

It comes as no surprise then that the control of colloidal suspensions is of great interest, and electrostatic interactions provide a crucial physical handle on these systems. Some colloids, like the tannins in wine and pigments in ink are lyophobic and not stable in solution [3]. The work of dispersing these colloids in suspension is often

achieved by charging these colloids by coating them with charged polymers, also known as polyelectrolytes [4]. In other applications, for example, when removing organic contaminants from wastewater, polyelectrolytes are again used to aggregate the (oftentimes charged) contaminants into larger, more easily separable flocs, thus avoiding more energy-intensive filtration processes [5, 6].

In addition to serving as powerful additives to control colloidal suspension behavior, polyelectrolytes are themselves a ubiquitous class of molecules with interesting behaviors of their own. For one, most naturally occurring polymers are charged – our genetic material, DNA and RNA, has negatively charged backbones endowed by their phosphate groups. Polysaccharides, such as the anticogulant heparin [7], can carry carboxyl, amine, and/or sulfuric groups that endow the polysaccharide with charge. Proteins almost invariably have charged amino acid groups. For broad reviews of polyelectrolytes we refer the interested reader to recent works[8, 9]; here we only highlight some of the physical questions we are interested in.

Charged interactions are long-ranged and lead to important correlations between positive and negative charges which can manifest in many different ways. For example, polyelectrolytes attract oppositely charged salt ions to maintain a nearly constant effective charge, a phenomenon known as counterion condensation [10–12]. Similarly, correlations also exist between oppositely charged polyelectrolytes, leading to polyelectrolyte complexation. For example, the assembly of many RNA viruses is believed to be driven primarily by charge-driven complexation between the negatively charged genetic material RNA and positively charged portions of virus capsid tails [13–16]. In fact, even charged, synthetic polyelectrolytes and even gold particles can be packaged by virus capsids, a testament to the importance of charged interactions [17, 18].

These complexation behaviors can be rich with questions and puzzles. Studies of the aforementioned RNA viruses found that the RNA packaged by viruses often contain *more* negative backbone charge than the positive charge on the virus capsid tails [13, 15]! What governs this overcharging behavior? Another related question is, what concentrations and kinds of positive charges are needed to compact our (negatively-charged) DNA within the small confines of our nuclei [19, 20]? The idea of DNA compaction has even been used in a new class of next-generation antibiotics based on polyelectrolytes, whose mechanism of action is a charge-facilitated penetration of bacteria and a subsequent charge-induced aggregation of DNA within the bacterial cytoplasm into useless aggregates [21].

Inspired by natural nanoparticles created from polyelectrolyte complexes, many synthetic nanoparticles are likewise being developed from polyelectrolytes. A prototypical example is the use of polyethylenimine, a positively charged polyelectrolyte, to complex with RNA/DNA and form "synthetic viruses" that protect the RNA/DNA and deliver them to cells [22–24]. These nanoparticle systems can be further tailored using block copolymers, i.e. polymers with more than one functional group. For example, such a block copolymer can have a charged domain responsible for complexing with the nanocargo of interest, and a second neutral block to endow such nanoparticles with a relatively well-defined size [23, 25].

In addition to the formation of nanoparticles by polyelectrolyte complexation, another interesting class of materials formed by polyelectrolytes are complex coacervates. Coacervates are a broad class of materials where lyophilic colloids aggregate, but because of their affinity for the solvent, the resulting colloid-enriched, coacervate phase still has a high solvent content, notably resulting in a liquid phase, in contrast to lyophobic colloids that form solid aggregates and precipitate out of solution [3]. Coacervates were first reported in the early 1900s (Fig. 1.1), and the term was coined by Bungenberg de Jong and Kruyt, from the prefix "co" and Latin word "acervus" meaning "heap" [26]. The word coacervate thus literally means, "to heap together," and the additional prefix of "complex" to the phrase " complex coacervation" is meant to highlight the charge-complexation process that underlies the coacervation of polyelectrolytes. Complex coacervates need not contain polyelectrolytes – even rigid charged particles and multivalent ions may form such a coacervate phase – but polyelectroltyes do constitute a large class of complex coacervates [8].

Coacervates are prevalent and are employed in many industrial settings [3]. Yogurt and milk drinks stabilize naturally-occurring (negatively charged) casein micelles in milk by the addition of positively charged metyl esterified pectins. The resulting complex-coacervate aggregates stay stable in solution [27]. In addition, complex coacervates are being explored as potential fat-replacement droplets [28] and self-healing coatings [29]. The ability of coacervates to maintain a distinct, stable phase and uptake solid particles and oil has sparked interest in using complex coacervates for separations and enhanced oil recovery [26, 30].

This last feature of complex coacervates – that they are well-defined phases that can maintain a chemical environment distinct from the dilute aqueous phase – may have many implications for how cellular activity is organized. A hypothesis sometimes called the "garbage bag world" hypothesis posits that life may have

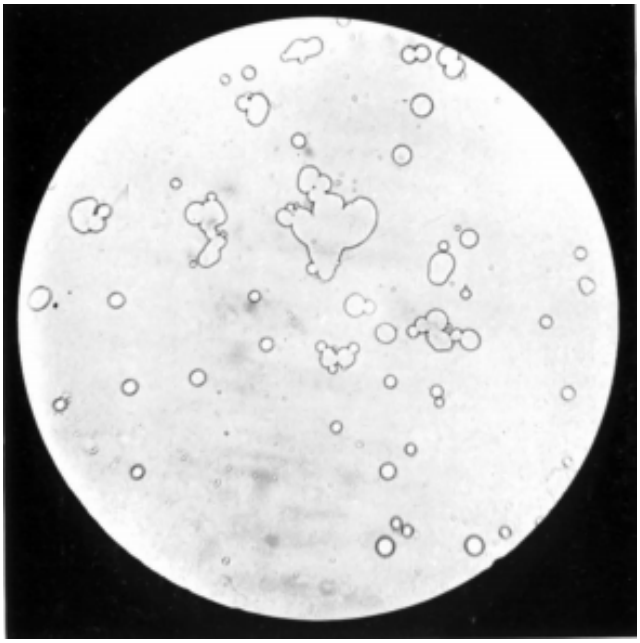

Figure 1.1: Reproduced from Bungenberg de Jong and Kruyt, a picture of a coacervate phase formed by gum arabic and serum albumen [26].

originated from complex coacervates [31–35]. The idea is that small coacervate droplets can accumulate small molecules in a well-defined environment, increasing their concentration and facilitating possible reactions and the formation of more complicated molecular or proto-cellular structures. The appeal of this hypothesis is that a membrane would not be a pre-requisite for early chemical life to proceed [35]. Although the "garbage bag" world does not address many issues of the origin of life, such as the development of systematic reproduction, recent work has highlighted the role of intrinsically disordered proteins in forming phase-separated-domains within cells [36–38]. These domains, such as nucleoli, Cajal bodies, and RNA granules, are associated with localized cellular activity and have been aptly named "membraneless organelles" (Fig. 1.2) [39–42]. The intrinsically disordered proteins are typically 10-15% charged, and currently workers are trying to address to what extent these membraneless organelle phases are driven by charge interactions [43].

A key question to ask in such polyelectrolyte systems is the nature and strength of the charge correlations. In general, the balance of electrostatic attraction and repulsion is not trivial – studies have shown that increasing multivalent ion concentration at first shrinks polyelectrolyte sizes, before leading to a re-entrant expansion at even higher salt concentration [44].

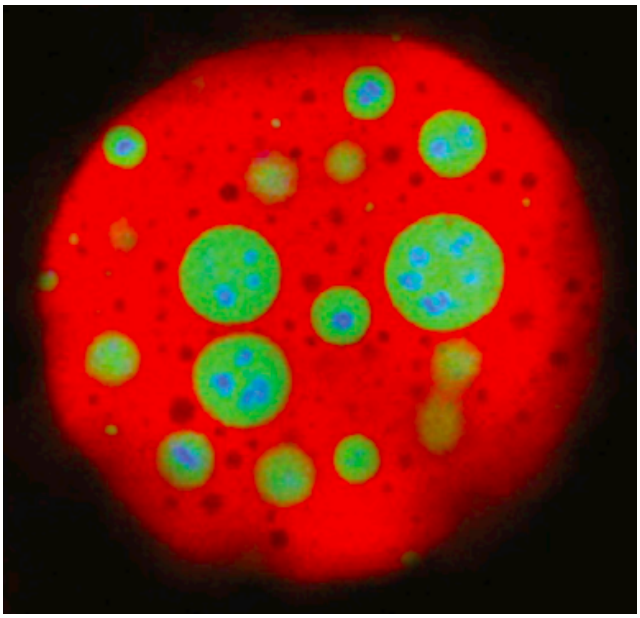

Figure 1.2: Reproduced from Feric et al. 2016 (DOI: 10.1016/j.cell.2016.04.047, CellPress open access, Creative Commons License), a picture of the nucleolus, a membraneless organelle [42].

Much of the recent experimental work done on polyelectrolytes has centered around improved characterization of such polyelectrolyte systems. Early experimental work typically employed naturally occurring polyelectrolytes [26, 45], which introduced complicating factors, such as complex molecular structure or polydispersity. One important advancement was the characterization of simpler, better-characterized polyelectrolyte systems. A series of important works explored the complexation process between poly(acrylic acid) and poly(allylamine), systematically varying parameters such as the stoichiometric mixing ratio, salt concentration, pH, and chain length ratios. Turbidity and optimal microscopy were used to identify polyelectrolyte complex formation, distinguish between precipitates and coacervates, and form phase diagrams [46, 47]. Their results were rationalized by consideration of screening by salt and bridging effects between chains. Subsequent studies of polypeptides were even better controlled – chain length can be precisely controlled and the backbones are the same in both cationic and anionic polypeptides, with the difference all ascribable to the side group [48–50]. These studies further characterized the phase boundary by determining the critical amount of salt needed to dissolve the coacervate as well as used isothermal calorimetry to calculate the enthalpy and entropy change upon mixing polycation and polyanion solutions. Consistent with past work and simulation [51], they found that the *mixing* free energy was largely

endothermic, suggesting that the *mixing* process is dominated by the entropy gain of counterion release.

Before discussing the state of comparison between theory and experiment, we discuss some key ideas in the theoretical description of charged systems.

1.2 Simple Electrolytes: Fluctuations and Debye-Hückel

We first consider simple electrolyte solutions, such as solutions of NaCl or KCl, where there are only cations and their associated anions.

The main interaction governing charged systems is the Coulomb interaction, where the energy between two charges of valence z_1 and z_2 are

$$U = \frac{z_1 z_2}{4\pi\epsilon_0\epsilon_r r_{12}} \tag{1.1}$$

where $r_{12} = |\mathbf{r}_1 - \mathbf{r}_2|$ is the separation distance between the two charges, $\epsilon_0 = 8.854... \cdot 10^{-12} F/m = 4.76 \cdot 10^{-6} e^2/nm \cdot k_B \cdot K$ is the vacuum permittivity, and ϵ_r is the relative permittivity of the medium in a linear dielectric description. At room temperature, water has $\epsilon_r \approx 80$.

It is helpful to compare the Coulomb interaction energy to the thermal energy scale $k_B T = 1/\beta$, which identifies the Bjerrum length

$$l_b = \frac{e^2}{4\pi\epsilon_0\epsilon_r k_B T} \tag{1.2}$$

as a characteristic length scale at which two elementary charges interact with energy $k_B T$. The interaction energy is then $\beta U = l_b \frac{z_1 z_2}{r_{12}}$. For aqueous solution at room temperature, $l_b \approx 0.7nm$, which is roughly $1-3$ atoms or molecular diameters. The Bjerrum length characterizes the strength of electrostatic interactions, with higher l_b corresponding to stronger electrostatic coupling.

The total Coulombic energy in a system is obtained by summing up all pair interactions between charges. In a continuous representation of charges, this is written as

$$\beta U = \int d\mathbf{r}_1 d\mathbf{r}_2 l_b \frac{\rho_e(\mathbf{r}_1)\rho_e(\mathbf{r}_2)}{|\mathbf{r}_1 - \mathbf{r}_2|} \tag{1.3}$$

where the net charge density $\rho_e = \sum_i z_i \rho_i$ is the sum of the charge contributions from each species i.

In practice, it is difficult to keep track of the locations of all charges, which constantly fluctuate in space, and so a very useful theoretical technique is to apply a *mean-field*

description where, instead of tracking the instantaneous location all particles in the system, one instead only keeps track of the average (mean) fields. Mean field descriptions can successfully describe a range of interesting phenomena, such as the van der Waals liquid-vapor or polymer blend phase separation [52, 53]. When applied to charged systems, we keep track of the species charge densities $\bar{\rho}_i$ and the net charge density $\bar{\rho}_e$.

An interesting consequence of the long-ranged nature of the Coulomb energy is that macroscopic charge separation has a prohibitive energy cost. In other words, on average the system must be charge neutral ($\bar{\rho}_e = 0$), and charge separation must be confined to small regions in space. For bulk solutions, there are no special interfaces for charges to be localized, and so $\bar{\rho}_e = 0$ everywhere. One then immediately finds that the mean-field Coulombic energy is identically zero everywhere, independent of the Bjerrum length and charge density!

This signals that, unless the charge neutrality symmetry is broken by external fields or charges, the leading order effect of charged systems lies in higher-order fluctuation effects. Electrostatics is all about how charges are *correlated* with each other. This is fundamentally different from the mean-field nature of many other phase separating systems.

Seeing that the simplest mean-field description is inadequate for describing the thermodynamics of charged systems, one must employ more advanced tools of statistical mechanics.

A physically motivated approach to describe such correlations employs a clever use of the mean-field theory. As noted earlier, the mean-field description gives the trivial solution unless some symmetry in the system is broken. The idea, then, is to *tag* an ion in bulk solution and study the distribution about or correlation to the other charges in solution. Although one is still studying bulk solution, the choice of reference frame breaks the symmetry of the system, and a suitable use of mean field theory would capture the correlations of the bulk solution *with respect to* the tagged ion, even while ignoring the correlations between the rest of the ions.

For concreteness, let us specify to a monovalent 1:1 salt solution, and let the tagged charge be positive. Formally, the distribution of the $+/-$ species is characterized by a pair-distribution function

$$\rho_{\pm}(r) = \rho_{+0} g_{+\pm}(r) = \rho_{+0} e^{-\beta w_{+\pm}(r)} \tag{1.4}$$

where $w_{+\pm} = -\ln g_{+\pm}$ is the potential of mean force between the (+) tagged ion and the $+/-$ species of interest. The Poisson-Boltzmann approximation is the assumption that the potential of mean force is related to the mean electrostatic potential ψ about the tagged ion [54]

$$w_{+\pm} = \pm\beta\psi \tag{1.5}$$

where $\beta\psi$ is given by the Poisson equation:

$$-\nabla\epsilon(r)\nabla\psi(r) = \rho_+(r) - \rho_-(r) \tag{1.6}$$

In 1923, Debye and Hückel approximately solved the Poisson-Boltzmann equation for the charge distribution about a tagged ion by linearizing the Boltzmann relation characterizing the pair distribution function $g_{+\pm} = e^{-\beta w_{+\pm}}$ [54, 55]. The resulting mean potential is characterized by a *screened* Coulomb interaction

$$\beta\psi(r) = l_b\frac{e^{-\kappa r}}{r} \tag{1.7}$$

where $\kappa = (4\pi l_b \sum_i \rho_{i0} q_i^2)^{1/2}$ is the Debye screening constant whose inverse is the Debye screening length $\lambda_D = \kappa^{-1}$.

The ion distribution similarly follows a screened-Coulomb Yukawa form, and this ion distribution is called the "ionic" atmosphere about the tagged ion, with oppositely-charged ions enriched and same-charged ions depleted about the tagged ion (Fig. 1.3).

The tagged ion, however, is representative of all charges in the bulk solution – they will all be preferentially surrounded by opposite charges, thus leading to a *lower* interaction energy relative to the mean-field result. The free energy decrease of the ion relative to the mean field result gives the excess chemical potential of the ion, which, within the DH approximation is

$$\beta\mu_i^{DH} = -q_i^2\frac{l_b\kappa}{2} \tag{1.8}$$

and the bulk solution Helmholtz free energy has an excess electrostatic contribution

$$\beta f^{DH} = -\frac{\kappa^3}{12\pi}. \tag{1.9}$$

Note that the factor of κ in the numerator of both expressions increases in magnitude with density, meaning that the electrostatic correlation energy becomes increasingly

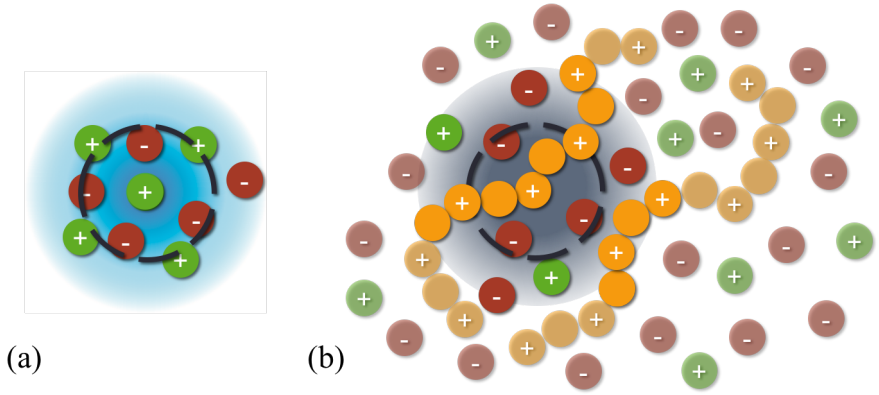

(a) (b)

Figure 1.3: Schematic of the ion cloud, or distribution, about a tagged charge of interest. The self energy is the electrostatic work required to build up a charge in this environment. (a) For simple ions the ion cloud is well-described by the Debye-Hückel theory. (b) For polyelectrolytes, the ionic atmosphere is modified by neighboring monomers along the same and other chains, and depends on the chain structure. Reproduced from Shen and Wang JCP 2017.[60] DOI:10.1063/1.4975777

negative with increasing concentration. This provides a driving force for the system to separate into a phase with a higher concentration of charges.

A theory using the DH Helmholtz free energy as the driving force found that the critical interaction strength at which ions will phase separate into a liquid phase is $\sigma/l_b \approx 0.0625$ (with sigma a characteristic ion diameter) [56], corroborated by simulations that found a critical value of about $\sigma/l_b \approx 0.057$ [57]. Although this liquid-liquid phase separation has not been observed in solution for monovalent ions, we note that the critical temperature at which the NaCl vapor-molten liquid transition appears is $\sigma/l_b \approx 0.055$ [58, 59], remarkably close to the results predicted by the simple DH theory for the restricted primitive model with symmetric ion sizes!

1.3 Theory of Polyelectrolytes

A salient feature of the DH theory is that electrostatic correlations increase with increasing ion valency z_i. Thus, polyelectrolytes, being inherently multivalent, have increased correlation effects compared to simple electrolyte systems. However, the magnitude of the multivalency effect is unclear because the spatial extent of the polyelectrolyte chains introduces new length scales and the conformation degrees of freedom of the polymers (Fig. 1.3).

Any theoretical attempt to understand the effective multivalency effect arising from chain connectivity in polyelectrolytes is immediately faced with a daunting increase

in the number of variables to study, the most salient of which include: backbone architecture, backbone flexibility and Kuhn length, and charge sequence. In an effort to achieve physical clarity and reduce the number of variables, many theories and simulations take their starting point to be linear polyelectrolytes with N monomers of Kuhn length b and only some fraction α of *same*-charged monomers.

The foundational (and still widely used) [61–64] theory of polyelectrolyte coacervation put forth by Voorn and Overbeek [65] chooses to completely ignore the contribution of chain connectivity to electrostatic correlations, directly borrowing the DH expressions for charge correlations and hence treating the backbone charges as disconnected free ions. In the Voorn-Overbeek theory, chain connectivity is only manifested in the translational entropy term:

$$f^{VO} = \sum_i \frac{\rho_i}{N_i}\left(\ln\frac{\rho_i}{N_i} - 1\right) + f^{\text{ex. vol.}} + f^{DH} \tag{1.10}$$

where N_i is the chain length of species i, ρ_i is the monomer density of species i. The correlation energy term is treated assuming it is the same as if all the charged monomers were disconnected, and approximated by the Debye-Hückel form $f^{DH} = -\kappa^3/12\pi$ with $\kappa^2 = 4\pi l_b \sum_i \alpha_i z_i^2 \rho_i$, and α_i the fraction of charged monomers of species i.

The idea of approximating the backbone charge as disconnected ions has been adopted in recent theories of polyelectrolytes, either using the VO-DH approximation as a starting point for constructing inhomogeneous theories [64], or replacing the DH correlation using more advanced treatments of *simple* electrolytes [66].

Attempts to connect experiment to theoretical predictions have often started with the VO theory [62, 65] or the Debye-Hückel screening ideas applied in different ways. These early theoretical comparisons with experiments test the limits of minimal, physical models. Because of its conceptual simplicity and seemingly severe assumptions, the VO theory truly serves as an important test of "how much we can get away with." If one does not expect quantitative accuracy, VO theory was found to give qualitatively reasonable phase boundary dependence on added salt [62], the agreement of which improves significantly if one allows for fitting parameters in the VO theory. Another interesting problem was explaining the ultra-low surface tensions of polyelectrolyte coacervates [64, 67]. Voorn-Overbeek ideas were borrowed and combined with a local-density approximation to predict the surface tension of polyelectrolyte coacervates, where it was found to give qualitatively cor-

rect salt-dependent scaling [64], and the surface tension was found to decrease with increasing chain length.

A time-salt superposition principle for polyelectrolyte coacervate rheology has also been proposed based on the idea that the relaxation time in coacervates is governed by "sticky attractions" characterized by Debye-Hückel screened interactions [68]. This identified time scale produced surprisingly good collapses of rheological measurements of the polyelectrolyte coacervate frequency response [50, 68]. However, many puzzles still persist: chain-length effects on the rheology were found to be asymmetric for polycations versus polyanions [68], and simulations have yet to reproduce the same salt-dependent frequency response.

Despite the VO theory's wide use and many successes, its treatment of electrostatic correlations and neglect of chain connectivity effects on charge correlations likely benefits from cancellation of errors; the VO approximation is still poorly understood, and as a result obscures the influence of one of the most important design parameters of polyelectrolytes – the chain architecture. In some instances, VO theory can even be qualitatively wrong. The most recent example of the VO theory's failure is its predictions for the tie lines of polyelectroltye coacervation in the salt-polymer plane. The VO *always* predicts salt enrichment in the coacervate phase, whereas recent experiments and simulations suggest that the tie line can indicate both enrichment and depletion of salt [69]. How might chain connectivity qualitatively modify the tie-line behavior of polyelectrolyte complexation?

A more systematic and descriptive theory is clearly desirable to understand both the merits and shortcomings of VO theory and the true underlying physics governing polyelectrolyte solutions and complexes. Over the decades much effort has been put into developing improved polyelectrolyte theories, many of which are described in a couple of recent reviews [9, 70]. These theories can be broadly categorized by the different physical effects that they seek to consider.

A widely used theory is the thermodynamic perturbation theory (TPT), which aims to capture the effects due to chain connectivity through a leading order perturbation expansion around the simple electrolyte results [71–76]. The first-order TPT (TPT-1) forms the basis for a widely used density-functional framework for the study of inhomogeneous polyelectrolyte systems [77–80]. While producing reasonable agreements for bulk properties and inhomogeneous systems at higher densities, like the VO theory and its variants, TPT-1 offers no insight into how one can use polymer characteristics – like backbone architecture and charge distribution on the backbone

– to control electrostatic interactions in materials. Only recently has there been a proposal to use TPT with a polymer one-component plasma as the reference system to better describe the connectivity effects [81].

An approach that tries to capture the effects of chain connectivity from the outset is the one-loop expansion/Random Phase Approximation (RPA) based on a leading order treatment of fluctuations in the field theoretic partition function [82–84]. RPA theories require a chain structure as input, and for prescribed chain structure provide explicit expressions describing how chain-connectivity generates extra charge correlations. Recent work has applied the RPA to macromolecules of arbitrary fractal dimensions with fixed intrachain structure factors [85]. However, for flexible chains, the use of a fixed Gaussian-chain structure factor for all concentrations (hereafter referred to as **f**ixed **g**aussian-**RPA**) leads to overestimation of the correlation effects, particularly at dilute concentrations. As a result, for flexible chains fg-RPA predicts critical concentrations that vanish with increasing chain length [86], in contradiction to simulation results [87]. Previous work has tried to fix this deficiency by introducing an *ad hoc* mesoscopic wavevector cut-off while still keeping the Gaussian structure factor for the long-wavelength fluctuation contributions [88].

The RPA theories of polyelectrolytes typically only consider fluctuations in the electrostatic interactions. In order to account for excluded volume fluctuations that are important even for neutral polymer systems [89], a variational method [90] was employed to treat the "double screening" [91], due to both excluded volume and electrostatic interactions. This theory by Muthukumar and coworkers has been used to study phase separation [92], adapted to account for counterion condensation [93, 94], and applied to study polyelectrolyte coil-globule transitions [95]. Unlike the fg-RPA, this approach allows the polyelectrolyte conformation to self-adapt. However, in the interest of obtaining analytical expressions, the double-screening theory pre-integrates the salt degrees of freedom, resulting in the Debye-Hückel description of screened interactions between monomer units, which does not feed back on the effective interaction between the salt ions. We note that such an approximation of using a screened Couloumb interaction for macroions is a common practice in many analytical and simulation studies [14, 96, 97].

Another method that bypasses the fixed-structure assumption is the *self-consistent* PRISM (sc-PRISM) integral equation approach [98, 99] that employs a structure-dependent effective medium-induced potential, and such an approach has been applied to polyelectrolytes by Yethiraj and coworkers [97, 100–103]. The sc-PRISM

has been quite successful for studying polyelectrolyte solution structure, but there have been limited studies on the thermodynamics [104–107]. Further, PRISM theories require the use of closures, the choice of which is guided by experience and comparisons to experiment and theory [97]. Finally, to date, sc-PRISM studies have been limited to only one polyelectrolyte species. To our knowledge the only application of PRISM to complex coacervates *ignored* the self-consistent determination of chain structure, and inconsistently borrowed thermodynamic expressions from theories of monomeric solutions [108].

A variational theory close in spirit to the sc-PRISM was proposed by Donley, Rudnick, and Liu [109] to study the concentration-dependence of polyelectrolyte chain structure. In hindsight, the theory can be understood as a sc-PRISM where the form of the effective intrachain interaction is motivated by RPA theory using heuristic arguments. Their theory yields good agreement with available computer simulation data on the end-to-end distance of the polyeletrolyte chain as a function of the polyelectrolyte and salt concentrations.

Lastly, we highlight a few recent theories of polyelectrolytes that do not fall as neatly into the above discussion. There has been a series of works applying a field theoretic technique called the Gaussian Equivalent Representation to polyelectrolytes, which has been applied to study the osmotic pressure of homo-polylectrolyte solutions and would be interesting to apply to more complex polyelectrolyte systems [110–114]. Another recent series of works have tried to revisit and re-evaluate the importance of microscopic detail and close-range interactions on polyelectrolytes, through the application of a (no-chain-self-consistency) PRISM theory [108] and a phenomenological transfer matrix theory with parameters that explicitly account for counterion condensation and polyelectrolyte-polyelectrolyte monomer ion pairing effects [115]. There has also been interest in further extending VO theory to account for counterion condensation and ion pairing effects through a chemical binding theoretical picture [116].

1.4 Thesis Outline

Our interest in the theoretical description of polyelectrolytes can broadly be divided into two complementary themes. First, what are the ways by which electrostatic correlations manifest themselves in polyelectrolytes? We are aware of different limiting cases, such as Debye exponential screening in dilute, weakly correlated, simple electrolyte solutions and counterion condensation for highly charged, cylin-

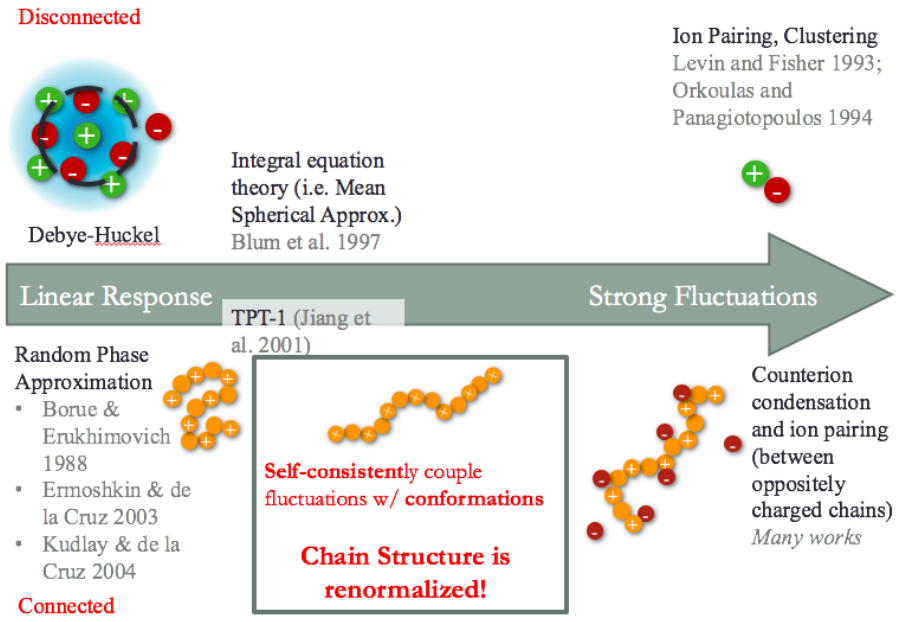

Figure 1.4: Schematic of two main factors dictating charged systems: chain connectivity and strength of electrostatic coupling. A central outcome of our work is the presentation of a unified theory that contextualizes how past theories are related to each other, and demonstrates the previously unappreciated coupling regime where changing chain conformations (boxed in the diagram) play a paramount role.

drical polyelectrolytes, but how do electrostatic correlations transition from one physical manifestation to another? Secondly, we want to understand the role of chain conformation in controlling these electrostatic correlations. How does the microscopic structure of a polyelectrolyte chain influence electrostatic attractions and the strength of complexation? The ultimate goal would be to construct a *unified* theory that self-consistently addresses both correlations and chain conformations and is consistent from weak to (modestly) high interaction strengths. A unified theory is crucial to understanding the relative importance and contributions of the many facets of electrostatic fluctuations.

A central contribution of my work is the presentation of just such a unified theory that clarifies the dual and complementary effects of chain connectivity and varying electrostatic coupling strength. In Fig. 1.4, we outline where some of the main physical effects are expected to be important, and some corresponding classical theories that describe these physical effects. On the simple electrolyte (disconnected charges) side of things, the two limits are a linear-screening regime characterized by the Debye Hückel theory, and ion pairing and clustering effects at strong coupling

strengths. Integral equation theories approximately handle the increasing electrostatic coupling strength, and their accuracy is dependent on the closure used. The TPT-1 theory outlined previously attempts to bridge from the disconnected to the connected side of this diagram in a perturbative way. On the connected-charge side of the diagram, past theories have tended to either focus on the weak-coupling limit, where chain connectivity can be treated using the RPA theory, which is essentially a generalized DH theory applicable for macromolecules, or directly jump to the polyelectrolyte analog of simple electrolyte strong coupling effects – counterion condensation and inter-chain pairing. Through the use of our unified theory, we demonstrate that there is actually a large range of electrostatic couplings where electrostatic fluctuations primarily act through *renormalized chain conformations*, though of course all correlation effects are coupled. Previous theories that fail to treat chain connectivity properly risk over-estimating the importance of stronger correlation effects. We explore the physical consequences of these renormalized chain conformations on polyelectrolyte solution thermodynamics.

To this end, in Chapter 2 I introduce the renormalized Gaussian fluctuation (RGF) and, for the first time in literature, apply it to polymers. A key theoretical result is that the physical effect of the leading non-perturbative fluctuations not considered in past perturbative theories is the renormalization, or self-consistency, of the chain structure with the charge fluctuations and solution thermodynamics. In particular, I apply the theoretical framework to study salt-free solutions of polyelectrolytes, and introduce a physical quantity we term the polyelectrolyte self energy, which can be understood as the electrostatic chemical potential, or the work it takes to assemble charge into a chain. In addition to the Born solvation energy and a generalized ionic cloud self-interaction energy which are present for simple electrolytes, the self energy also contains intra-chain charge interactions, which depend significantly on chain conformation. Our theory bridges the commonly used Voorn-Overbeek (VO) theory [65], which only accounts for the ionic cloud energy of disconnected charges, and Random Phase Approximation (RPA) theories which account for connectivity but ignore that electrostatic energy can be relaxed through conformational changes. The self energy highlights the importance and role of adapting chain structure, in particular highlighting how incorrect large-wavelenth behavior introduced artifacts in previous polyelectrolyte theories.

Our theory describes the infinite-dilution self energy appropriately, reproduces expected scalings of overall chain dimension at finite salt and polymer concentration,

and gives a N-dependent cross-over of the correlation energy from a renormalized Debye-Hückel concentration dependence to a weaker concentration dependence associated with chain connectivity. In particular, we find that chain conformational changes represent a significant mode through which electrostatic energy is relaxed in polyelectrolyte solutions; relaxing the inter-chain electrostatic energy through conformational changes subsequently reduces the magnitude of correlation energies. Accounting for these conformational changes allows our theory to appropriately capture the N-independent limit of the critical point in salt-free polyelectrolyte solutions. Also important is that for long chains our theory reproduces a N-independent plateau in the osmotic coefficient, which other theories are unable to predict.

Following, in Chapter 3 we apply our self-consistent theory to study the phase behavior of polyelectrolyte solutions. Our theory predicts re-entrant behavior with added-salt for polyelectrolyte (PE) solutions with a single PE species. For coacervate-forming solutions of oppositely charged polyelectrolytes, we predict salting-in and tie-line behaviors consistent with recent experiments. Importantly, we find that the phase diagrams of fully-charged flexible chains are *much* more similar to that of semiflexible rods than Gaussian chains, even in semi-dilute solution when the chain structure is overall Gaussian. We trace this to the local-stiffening of flexible chains by the electrostatics, which persists in semi-dilute solution and continues to play a big role in the thermodynamics and phase diagrams, thus emphasizing the importance of shorter wavelength electrostatic flutuations. We also show that at high polymer concentrations the correlation energy of flexible polyelectrolytes follows a functional form $\propto -\ln\rho$ that can be thought of as renormalizing the translational entropy of counterions. This kind of behavior was previously only predicted for polyelectrolyte rods [85].

In Chapter 4 we investigate the apparent similarity between the (renormalized) linearized fluctuations captured by our theory and counterion condensation. We propose a theory that self-consistently captures electrostatic fluctuations from weak to intermediate electrostatic couplings, and from our theory we identify a total electrostatic binding constant that captures counterion condensation's dependence on chain structure and anti-cooperative effects. We find an unexpectedly important contribution to the osmotic pressure from linearized fluctuations – in fact, above an electrostatic interaction strength of roughly $l_b/b \approx 1$, the relative contribution of counterion condensation *decreases* with increasing concentration. Further, by retaining the discrete nature of condensed counterions and backbone charge sites,

we reveal the importance of the "residiual" charge fluctuations of these condensed ion pairs in governing the phase behavior of polyelectrolyte solutions. Depending on the amount of residual fluctuations, counterion condensation can either stabilize *or* destabilize the solution.

Finally, in Chapter 5 we further discuss some nuances of the RGF framework and its relation to other theoretical approaches for studying fluctuations. We address the issue that statistical mechanical field theories feature complex-valued actions, whereas the Gibbs-Feynman-Bogoliubov (GFB) bound upon which the RGF procedure is based is based is only valid for real-valued actions. We demonstrate that the RGF self-consistency conditions do not need to be rooted in the GFB bound, but can also be understood as a self-consistent first order perturbation. Our work thus both establishes the RGF procedure on more secure footing as well as makes transparent the physical consequences of the newly-considered fluctuations. We further present a self-consistent first-order perturbation treatment of canonical ensemble systems, and discuss its connections with previous theories.

The contents of each chapter have been published, or have been prepared as a manuscript for submission.

BIBLIOGRAPHY

[1]P.-G. De Gennes, and J. Badoz, *Fragile objects: soft matter, hard science, and the thrill of discovery* (Springer Science & Business Media, 2012).

[2]E. H. Gombrich, and E. Gombrich, *The story of art*, Vol. 12 (Phaidon London, 1995).

[3]E. Spruijt, *Strength, structure and stability of polyelectrolyte complex coacervates* (PhD thesis, Wageningen University, The Netherlands, 2012).

[4]P. Pincus, "Colloid stabilization with grafted polyelectrolytes", Macromolecules **24**, 2912–2919 (1991).

[5]A. Rabiee, A. Ershad-Langroudi, and M. E. Zeynali, "A survey on cationic polyelectrolytes and their applications: acrylamide derivatives", Reviews in Chemical Engineering **31**, 239–261 (2015).

[6]Y. Adachi, "Sedimentation and electrophoresis of a porous floc and a colloidal particle coated with polyelectrolytes", Current Opinion in Colloid & Interface Science **24**, 72–78 (2016).

[7]A. Bentolila, I. Vlodavsky, C. Haloun, and A. J. Domb, "Synthesis and heparin-like biological activity of amino acid-based polymers", Polymers for Advanced Technologies **11**, 377–387 (2000).

[8]S. Srivastava, and M. V. Tirrell, "Polyelectrolyte complexation", Adv. Chem. Phys., 499–544 (2016).

[9]M. Muthukumar, "50th anniversary perspective: a perspective on polyelectrolyte solutions", Macromolecules **50**, 9528 (2017) 10.1021/acs.macromol.7b01929.

[10]G. S. Manning, "Limiting laws and counterion condensation in polyelectrolyte solutions i. colligative properties", J. Chem. Phys. **51**, 924 (1969).

[11]G. S. Manning, "Limiting laws and counterion condensation in polyelectrolyte solutions ii. self-diffusion of the small ions", J. Chem. Phys. **51**, 934–938 (1969).

[12]G. S. Manning, "Counterion binding in polyelectrolyte theory", Accounts of Chemical Research **12**, 443–449 (1979).

[13]C. L. Ting, J. Wu, and Z.-G. Wang, "Thermodynamic basis for the genome to capsid charge relationship in viral encapsidation", P. Natl. Acad. Sci. USA **108**, 16986 (2011).

[14]J. D. Perlmutter, C. Qiao, and M. F. Hagan, "Viral genome structures are optimal for capsid assembly", Elife **2**, e00632 (2013).

[15]V. A. Belyi, and M. Muthukumar, "Electrostatic origin of the genome packing in viruses", Proceedings of the National Academy of Sciences **103**, 17174–17178 (2006).

[16]M. F. Hagan, "A theory for viral capsid assembly around electrostatic cores", J. Chem. Phys. **130**, 114902 (2009).

[17]J. Sun, C. DuFort, M.-C. Daniel, A. Murali, C. Chen, K. Gopinath, B. Stein, M. De, V. M. Rotello, A. Holzenburg, et al., "Core-controlled polymorphism in virus-like particles", Proceedings of the National Academy of Sciences **104**, 1354–1359 (2007).

[18]Y. Hu, R. Zandi, A. Anavitarte, C. M. Knobler, and W. M. Gelbart, "Packaging of a polymer by a viral capsid: the interplay between polymer length and capsid size", Biophysical Journal **94**, 1428–1436 (2008).

[19]R. de Vries, "Dna condensation in bacteria: interplay between macromolecular crowding and nucleoid proteins", Biochimie **92**, 1715–1721 (2010).

[20]S. Cunha, C. L. Woldringh, and T. Odijk, "Polymer-mediated compaction and internal dynamics of isolated escherichia coli nucleoids", Journal of Structural Biology **136**, 53–66 (2001).

[21]W. Chin, G. Zhong, Q. Pu, C. Yang, W. Lou, P. F. De Sessions, B. Periaswamy, A. Lee, Z. C. Liang, X. Ding, et al., "A macromolecular approach to eradicate multidrug resistant bacterial infections while mitigating drug resistance onset", Nature Communications **9**, 917 (2018).

[22]F. Pittella, and K. Kataoka, *Polymeric micelles for sirna delivery* (Springer, 2013), p. 161.

[23]D. W. Pan, and M. E. Davis, "Cationic mucic acid polymer-based sirna delivery systems", Bioconjugate Chem. **26**, 1791 (2015).

[24]K. A. Black, D. Priftis, S. L. Perry, J. Yip, W. Y. Byun, and M. Tirrell, "Protein encapsulation via polypeptide complex coacervation", ACS Macro Lett. **3**, 1088 (2014).

[25]H. M. van der Kooij, E. Spruijt, I. K. Voets, R. Fokkink, M. A. Cohen Stuart, and J. van der Gucht, "On the stability and morphology of complex coacervate core micelles: from spherical to wormlike micelles", Langmuir **28**, 14180–14191 (2012).

[26]H. Bungenberg de Jong, and H. Kruyt, "Coacervation (partial miscibility in colloid systems)", P. K. Ned. Akad. Wetensc. **32**, 849 (1929).

[27]R. H. Tromp, C. G. de Kruif, M. van Eijk, and C. Rolin, "On the mechanism of stabilisation of acidified milk drinks by pectin", Food Hydrocolloids **18**, 565–572 (2004).

[28]C. Schmitt, and S. L. Turgeon, "Protein/polysaccharide complexes and coacervates in food systems", Adv. Colloid Interface Sci. **167**, 63 (2011).

[29]G. Decher, "Fuzzy nanoassemblies: toward layered polymeric multicomposites", Science **277**, 1232–1237 (1997).

[30]F. Weinbreck, M. Minor, and C. De Kruif, "Microencapsulation of oils using whey protein/gum arabic coacervates", Journal of Microencapsulation **21**, 667–679 (2004).

[31]H. Okihana, "Formation and catalytic activity of high molecular weight soluble polymers produced by heating amino acids in a modified sea medium", Origins of Life and Evolution of Biospheres **12**, 153–163 (1982).

[32]A. I. Oparin, *The origin of life, translated by s. margulis*, 1953.

[33]J. D. Bernal, *The origin of life*, tech. rep. (1967).

[34]T. Evreinova, T. Mamontova, V. Karnauhov, S. Stephanov, and U. Hrust, "Coacervate systems and origin of life", in *Cosmochemical evolution and the origins of life* (Springer, 1974), pp. 201–205.

[35]F. Dyson, *Origins of life* (Cambridge University Press, 1999).

[36]P. Li, S. Banjade, H.-C. Cheng, S. Kim, B. Chen, L. Guo, M. Llaguno, J. V. Hollingsworth, D. S. King, S. F. Banani, et al., "Phase transitions in the assembly of multivalent signalling proteins", Nature **483**, 336 (2012).

[37]H. Walter, and D. E. Brooks, "Phase separation in cytoplasm, due to macromolecular crowding, is the basis for microcompartmentation", FEBS letters **361**, 135–139 (1995).

[38]A. A. Hyman, and K. Simons, "Beyond oil and water—phase transitions in cells", Science **337**, 1047–1049 (2012).

[39]T. J. Nott, T. D. Craggs, and A. J. Baldwin, "Membraneless organelles can melt nucleic acid duplexes and act as biomolecular filters", Nature chemistry **8**, 569 (2016).

[40]C. P. Brangwynne, C. R. Eckmann, D. S. Courson, A. Rybarska, C. Hoege, J. Gharakhani, F. Jülicher, and A. A. Hyman, "Germline p granules are liquid droplets that localize by controlled dissolution/condensation", Science **324**, 1729–1732 (2009).

[41]C. P. Brangwynne, T. J. Mitchison, and A. A. Hyman, "Active liquid-like behavior of nucleoli determines their size and shape in xenopus laevis oocytes", Proceedings of the National Academy of Sciences **108**, 4334–4339 (2011).

[42]M. Feric, N. Vaidya, T. S. Harmon, D. M. Mitrea, L. Zhu, T. M. Richardson, R. W. Kriwacki, R. V. Pappu, and C. P. Brangwynne, "Coexisting liquid phases underlie nucleolar subcompartments", Cell **165**, 1686–1697 (2016) 10.1016/j.cell.2016.04.047.

[43]Y.-H. Lin, J. D. Forman-Kay, and H. S. Chan, "Sequence-specific polyampholyte phase separation in membraneless organelles", Phys. Rev. Lett. **117**, 178101 (2016) 10.1103/PhysRevLett.117.178101.

[44]P.-Y. Hsiao, and E. Luijten, "Salt-induced collapse and reexpansion of highly charged flexible polyelectrolytes", Phys. Rev. Lett. **97**, 148301 (2006).

[45]C. G. de Kruif, F. Weinbreck, and R. de Vries, "Complex coacervation of proteins and anionic polysaccharides", Curr. Opin. Colloid Interface Sci. **9**, 340 (2004).

[46]R. Chollakup, W. Smitthipong, C. D. Eisenbach, and M. Tirrell, "Phase behavior and coacervation of aqueous poly(acrylic acid)-poly(allylamine) solutions", Macromolecules **43**, 2518–2528 (2010).

[47]R. Chollakup, J. B. Beck, K. Dirnberger, M. Tirrell, and C. D. Eisenbach, "Polyelectrolyte molecular weight and salt effects on the phase behavior and coacervation of aqueous solutions of poly (acrylic acid) sodium salt and poly (allylamine) hydrochloride", Macromolecules **46**, 2376–2390 (2013).

[48]D. Priftis, N. Laugel, and M. Tirrell, "Thermodynamic characterization of polypeptide complex coacervation", Langmuir **28**, 15947 (2012).

[49]D. Priftis, and M. Tirrell, "Phase behaviour and complex coacervation of aqueous polypeptide solutions", Soft Matter **8**, 9396–9405 (2012).

[50]D. Priftis, K. Megley, N. Laugel, and M. Tirrell, "Complex coacervation of poly(ethylene-imine)/polypeptide aqueous solutions: thermodynamic and rheological characterization", Journal of Colloid and Interface Science **398**, 39–50 (2013).

[51]Z. Ou, and M. Muthukumar, "Entropy and enthalpy of polyelectrolyte complexation: langevin dynamics simulations", The Journal of Chemical Physics **124**, (2006).

[52]D. McQuarrie, "Statistical mechanics", Sausalito, Calif.: University Science Books **12**, 641 (2004).

[53]R. Colby, and M. Rubinstein, "Polymer physics", New-York: Oxford University **100**, 274 (2003).

[54]T. L. Hill, *An introduction to statistical thermodynamics* (Courier Corporation, 1986).

[55]P. Debye, and E. Hückel, "De la théorie des électrolytes. i. abaissement du point de congélation et phénomènes associés", Phys. Zeitschrift **24**, 185 (1923).

[56]M. E. Fisher, and Y. Levin, "Criticality in ionic fluids: debye-hückel theory, bjerrum, and beyond", Phys. Rev. Lett. **71**, 3826 (1993).

[57]G. Orkoulas, and A. Z. Panagiotopoulos, "Free energy and phase equilibria for the restricted primitive model of ionic fluids from monte carlo simulations", The Journal of chemical physics **101**, 1452–1459 (1994).

[58]P. Keblinski, J. Eggebrecht, D. Wolf, and S. Phillpot, "Molecular dynamics study of screening in ionic fluids", J. Chem. Phys. **113**, 282–291 (2000).

[59]Y. Guissani, and B. Guillot, "Coexisting phases and criticality in nacl by computer simulation", J. Chem. Phys. **101**, 490–509 (1994).

[60]K. Shen, and Z.-G. Wang, "Electrostatic correlations and the polyelectrolyte self energy", J. Chem. Phys. **146**, 084901 (2017) DOI:10.1063/1.4975777.

[61]R. de Vries, and M. A. Cohen Stuart, "Theory and simulations of macroion complexation", Curr. Opin. Colloid Interface Sci. **11**, 295 (2006).

[62]E. Spruijt, A. H. Westphal, J. W. Borst, M. A. Cohen Stuart, and J. van der Gucht, "Binodal compositions of polyelectrolyte complexes", Macromolecules **43**, 6476 (2010).

[63]J. van der Gucht, E. Spruijt, M. Lemmers, and M. A. Cohen Stuart, "Polyelectrolyte complexes: bulk phases and colloidal systems", J. Colloid Interface Sci. **361**, 407 (2011).

[64]J. Qin, D. Priftis, R. Farina, S. L. Perry, L. Leon, J. Whitmer, K. Hoffmann, M. Tirrell, and J. J. de Pablo, "Interfacial tension of polyelectrolyte complex coacervate phases", ACS Macro Lett. **3**, 565 (2014).

[65]J. T. G. Overbeek, and M. J. Voorn, "Phase separation in polyelectrolyte solutions. theory of complex coacervation", J. Cell Compar. Phys. **49**, 7 (1957).

[66]C. E. Sing, J. W. Zwanikken, and M. O. de la Cruz, "Interfacial behavior in polyelectrolyte blends: hybrid liquid-state integral equation and self-consistent field theory study", Phys. Rev. Lett. **111**, 168303 (2013).

[67]E. Spruijt, J. Sprakel, M. A. Cohen Stuart, and J. van der Gucht, "Interfacial tension between a complex coacervate phase and its coexisting aqueous phase", Soft Matter **6**, 172–178 (2010).

[68]E. Spruijt, M. A. Cohen Stuart, and J. van der Gucht, "Linear viscoelasticity of polyelectrolyte complex coacervates", Macromolecules **46**, 1633–1641 (2013).

[69]L. Li, S. Srivastava, M. Andreev, A. Marciel, J. de Pablo, and M. Tirrell, *Submitted*, 2018.

[70]C. E. Sing, "Development of the modern theory of polymeric complex coacervation", Advances in Colloid and Interface Science **239**, 2–16 (2017).

[71]L. Blum, Y. V. Kalyuzhnyi, O. Bernard, and J. N. Herrera-Pacheco, "Sticky charged spheres in the mean-spherical approximation: a model for colloids and polyelectrolytes", J. Phys. Condens. Matter **8**, A143 (1996).

[72]I. Protsykevytch, Y. Kalyuzhnyi, M. Holovko, and L. Blum, "Ion-ion, ion-solvent and solvent-solvent interactions in electrolyte solutions: solution of the polymer mean spherical approximation for the totally flexible sticky two-point electrolyte model", J. Mol. Liq. **73**, 1 (1997) http://dx.doi.org/10.1016/S0167-7322(97)00053-6.

[73]O. Bernard, and L. Blum, "Thermodynamics of a model for flexible polyelectrolytes in the binding mean spherical approximation", J. Chem. Phys. **112**, 7227 (2000) http://dx.doi.org/10.1063/1.481287.

[74]N. von Solms, and Y. C. Chiew, "Analytical integral equation theory for a restricted primitive model of polyelectrolytes and counterions within the mean spherical approximation. i. thermodynamic properties", J. Chem. Phys. **111**, 4839 (1999) http://dx.doi.org/10.1063/1.479246.

[75]N. von Solms, and Y. C. Chiew, "A model for polyelectrolytes", J. Stat. Phys. **100**, 267 (2000) 10.1023/A:1018652031157.

[76]J. Jiang, L. Blum, O. Bernard, and J. M. Prausnitz, "Thermodynamic properties and phase equilibria of charged hard sphere chain model for polyelectrolyte solutions", Mol. Phys. **99**, 1121 (2001).

[77]Z. Li, and J. Wu, "Density functional theory for planar electric double layers: closing the gap between simple and polyelectrolytes", J. Phys. Chem. B **110**, 7473 (2006) 10.1021/jp060127w.

[78]Z. Li, and J. Wu, "Density functional theory for polyelectrolytes near oppositely charged surfaces", Phys. Rev. Lett. **96**, 048302 (2006) 10.1103/PhysRevLett.96.048302.

[79]T. Jiang, Z.-G. Wang, and J. Wu, "Electrostatic regulation of genome packaging in human hepatitis b virus", Biophys. J. **96**, 3065 (2009) http://dx.doi.org/10.1016/j.bpj.2009.01.009.

[80]L. Wang, H. Liang, and J. Wu, "Electrostatic origins of polyelectrolyte adsorption: theory and monte carlo simulations", J. Chem. Phys. **133**, 044906, 044906 (2010).

[81]Y. A. Budkov, A. L. Kolesnikov, N. Georgi, E. A. Nogovitsyn, and M. G. Kiselev, "A new equation of state of a flexible-chain polyelectrolyte solution: phase equilibria and osmotic pressure in the salt-free case", J. Chem. Phys. **142**, 174901 (2015).

[82]V. Y. Borue, and I. Y. Erukhimovich, "A statistical theory of weakly charged polyelectrolytes: fluctuations, equation of state and microphase separation", Macromolecules **21**, 3240 (1988).

[83]A. Khokhlov, and K. Khachaturian, "On the theory of weakly charged polyelectrolytes", Polymer **23**, 1742 (1982).

[84]M. Castelnovo, and J.-F. Joanny, "Complexation between oppositely charged polyelectrolytes: beyond the random phase approximation", Eur. Phys. J. E **6**, 377 (2001).

[85]J. Qin, and J. J. de Pablo, "Criticality and connectivity in macromolecular charge complexation", Macromolecules **49**, 8789 (2016).

[86]K. A. Mahdi, and M. O. de la Cruz, "Phase diagrams of salt-free polyelectrolyte semidilute solutions", Macromolecules **33**, 7649 (2000).

[87]G. Orkoulas, S. K. Kumar, and A. Z. Panagiotopoulos, "Monte carlo study of coulombic criticality in polyelectrolytes", Phys. Rev. Lett. **90**, 048303 (2003).

[88]A. V. Ermoshkin, and M. Olvera de la Cruz, "A modified random phase approximation of polyelectrolyte solutions", Macromolecules **36**, 7824 (2003).

[89]S. F. Edwards, "The theory of polymer solutions at intermediate concentration", P. Phys. Soc. **88**, 265 (1966).

[90]M. Muthukumar, and S. Edwards, "Extrapolation formulas for polymer solution properties", J. Chem. Phys. **76**, 2720 (1982).

[91]M. Muthukumar, "Double screening in polyelectrolyte solutions: limiting laws and crossover formulas", J. Chem. Phys. **105**, 5183 (1996).

[92]M. Muthukumar, "Phase diagram of polyelectrolyte solutions: weak polymer effect", Macromolecules **35**, 9142 (2002).

[93]M. Muthukumar, "Theory of counter-ion condensation on flexible polyelectrolytes: adsorption mechanism", J. Chem. Phys. **120**, 9343 (2004).

[94]R. Kumar, A. Kundagrami, and M. Muthukumar, "Counterion adsorption on flexible polyelectrolytes: comparison of theories", Macromolecules **42**, 1370 (2009).

[95]A. Kundagrami, and M. Muthukumar, "Effective charge and coil-globule transition of a polyelectrolyte chain", Macromolecules **43**, 2574 (2010).

[96]M. J. Stevens, and K. Kremer, "Structure of salt-free linear polyelectrolytes in the debye-hückel approximation", J. Phys. II **6**, 1607 (1996).

[97]A. Yethiraj, "Conformational properties and static structure factor of polyelectrolyte solutions", Phys. Rev. Lett. **78**, 3789 (1997).

[98]C. J. Grayce, and K. S. Schweizer, "Solvation potentials for macromolecules", J. Chem. Phys. **100**, 6846 (1994).

[99]C. J. Grayce, A. Yethiraj, and K. S. Schweizer, "Liquid-state theory of the density dependent conformation of nonpolar linear polymers", J. Chem. Phys. **100**, 6857 (1994).

[100]A. Yethiraj, "Theory for chain conformations and static structure of dilute and semidilute polyelectrolyte solutions", J. Chem. Phys. **108**, 1184 (1998).

[101]C.-Y. Shew, and A. Yethiraj, "Monte carlo simulations and self-consistent integral equation theory for polyelectrolyte solutions", J. Chem. Phys. **110**, 5437 (1999).

[102]C.-Y. Shew, and A. Yethiraj, "Self-consistent integral equation theory for semiflexible chain polyelectrolyte solutions", J. Chem. Phys. **113**, 8841 (2000).

[103]T. Hofmann, R. Winkler, and P. Reineker, "Self-consistent integral equation theory for solutions of finite extensible semiflexible polyelectrolyte chains", J. Chem. Phys. **118**, 6624 (2003).

[104]R. Chang, and A. Yethiraj, "Osmotic pressure of salt-free polyelectrolyte solutions: a monte carlo simulation study", Macromolecules **38**, 607 (2005).

[105]K. S. Schweizer, and J. G. Curro, "Equation of state of polymer melts: general formulation of a microscopic integral equation theory", J. Chem. Phys. **89**, 3342 (1988).

[106]K. S. Schweizer, and J. G. Curro, "Equation of state of polymer melts: numerical results for athermal freely jointed chain fluids", J. Chem. Phys. **89**, 3350 (1988).

[107]J. P. Donley, J. G. Curro, and J. D. McCoy, "A density functional theory for pair correlation functions in molecular liquids", J. Chem. Phys. **101**, 3205 (1994).

[108]S. L. Perry, and C. E. Sing, "Prism-based theory of complex coacervation: excluded volume versus chain correlation", Macromolecules **48**, 5040 (2015).

[109]J. P. Donley, J. Rudnick, and A. J. Liu, "Chain structure in polyelectrolyte solutions at nonzero concentrations", Macromolecules **30**, 1188 (1997).

[110]Y. A. Budkov, A. I. Frolov, M. G. Kiselev, and N. V. Brilliantov, "Surface-induced liquid-gas transition in salt-free solutions of model charged colloids", J. Chem. Phys. **139**, 194901 (2013).

[111]Y. A. Budkov, A. Kolesnikov, E. Nogovitsyn, and M. Kiselev, "Electrostatic-interaction-induced phase separation in solutions of flexible-chain polyelectrolytes", Polymer Science Series A **56**, 697–711 (2014).

[112]G. V. Efimov, and E. A. Nogovitsin, "The partition functions of classical systems in the gaussian equivalent representation of functional integrals", Physica A: Statistical Mechanics and its Applications **234**, 506–522 (1996).

[113]S. A. Baeurle, M. Charlot, and E. A. Nogovitsin, "Grand canonical investigations of prototypical polyelectrolyte models beyond the mean field level of approximation", Phys. Rev. E **75**, 011804 (2007).

[114]E. A. Nogovitsyn, and Y. A. Budkov, "Development of the theory of a self-consistent field for polyelectrolyte solutions", Russ. J. Phys. Chem. A **85**, 1363–1368 (2011).

[115]T. K. Lytle, and C. E. Sing, "Transfer matrix theory of polymer complex coacervation", Soft Matter **13**, 7001–7012 (2017).

[116]A. Salehi, and R. G. Larson, "A molecular thermodynamic model of complexation in mixtures of oppositely charged polyelectrolytes with explicit account of charge association/dissociation", Macromolecules **49**, 9706–9719 (2016).

Chapter 2

THE POLYELECTROLYTE SELF ENERGY

We address the effects of chain connectivity on electrostatic fluctuations in polyelectrolyte solutions using a field-theoretic, renormalized Gaussian fluctuation (RGF) theory. As in simple electrolyte solutions (Z.-G. Wang, Phys. Rev. E. **8**1, 021501 (2010)), the RGF provides a unified theory for electrostatic fluctuations, accounting for both dielectric and charge correlation effects in terms of the self energy. Unlike simple ions, the polyelectrolyte self energy depends intimately on the chain conformation, and our theory naturally provides a self-consistent determination of the response of intramolecular chain structure to polyelectrolyte and salt concentrations. The effects of the chain-conformation on the self energy and thermodynamics are especially pronounced for flexible polyelectrolytes at low polymer and salt concentrations, where application of the wrong chain structure can lead to a drastic misestimation of the electrostatic correlations. By capturing the expected scaling behavior of chain size from dilute to semi-dilute regimes, our theory provides improved estimates of the self energy at low polymer concentrations and correctly predicts the eventual N-independence of the critical temperature and concentration of salt-free solutions of flexible polyelectrolytes. We show that the self energy can be interpreted in terms of an infinite-dilution energy $\mu^{\mathrm{el}}_{m,0}$ and a finite concentration correlation correction μ^{corr} which tends to cancel out the former with increasing concentration.

This chapter includes content from our previously published article:

[1] K. Shen, and Z.-G. Wang, "Electrostatic correlations and the polyelectrolyte self energy", J. Chem. Phys. **146**, 084901 (2017) DOI:10.1063/1.4975777.

2.1 Introduction

Polyelectrolytes are widely used for many applications, ranging from energy materials [1] to solution additives (e.g. for food, cosmetics, and healthcare products). [2] Polyelectrolytes are also ubiquitous in biology, as many naturally occurring polymers – DNA/RNA, proteins, and some polysaccharides – are charged. Consequently, understanding the interplay of electrostatics with polyelectrolyte functionality is central for understanding many biological processes [3] and guides the

design of materials such as adhesives, [4] drug-delivery microencapsulants, [5–7] and micro/nanoactuators. [8]

The long-range nature of electrostatic interactions gives rise to nontrivial correlation effects in polyelectrolyte systems such as ion-condensation [9] and complex coacervation. [10–12] A key challenge in the theoretical study of polyelectrolytes is the proper description of electrostatic correlations and their consequences on the structure and thermodynamics.

The physical origin of electrostatic correlation is the preferential interaction between opposite charges. For simple electrolyte solutions this correlation is manifested in the "ionic atmosphere" (Fig. 1.3) first proposed by Debye and Hückel (DH). [13] As the result of the favorable interaction of an ion with its ionic atmosphere, the free energy of the system is lowered. Theoretically, for point charges, the spatial extent of the ion atmosphere is characterized by the well-known inverse Debye screening length

$$\kappa^2 = \lambda_D^{-2} = 4\pi l_b \sum_i z_i^2 c_i, \tag{2.1}$$

where the Bjerrum length $l_b = e^2/4\pi\varepsilon kT$ is the length scale at which two unit charges interact with energy kT and characterizes the strength of charge interactions. These charge correlations modify a host of properties such as osmotic pressure, ionic activities, and mobilities. For dilute electrolyte solutions, the electrostatic free energy density and the associated excess chemical potential are given respectively by:

$$\begin{aligned} \beta f^{el} &= -\frac{\kappa^3}{12\pi} \\ \beta \mu_i^{el} &= -z_i^2 \frac{l_b \kappa}{2}. \end{aligned} \tag{2.2}$$

A key question we wish to address is how the connectivity of polyelectrolytes will modify this classic Debye-Hückel correlation behavior. The DH expression gives a prediction for both the concentration and valency-dependence of correlation energies. Polyelectrolytes, being inherently multivalent, should on physical grounds be expected to also have increased correlation effects compared to simple electrolyte systems. However, the magnitude of this multivalency effect is unclear due to the spatial extent of the polyelectrolytes, and the concentration dependence of correlation energies is also unclear. We will find, at extremely low concentrations, that flexible polyelectrolytes follow a renormalized DH concentration-scaling, before

transitioning to more rod-like polyelectrolyte concentration dependences at higher concentrations.

In this chapter, we study electrostatic fluctuations in polyelectrolyte solutions by extending the field-theoretic renormalized Gaussian fluctuation theory (RGF) derived in the previous chapter for polymers to a general case with charged interactions an arbitrary number of charged species. In this theory, the key thermodynamic quantity that captures the electrostatic fluctuations is the self energy of an effective single chain. For simple electrolytes, the self energy is the electrostatic work required to assemble charge from an infinitely dispersed state onto an ion and is given by [14]

$$\beta\mu^{el}_{\text{chg}} = \frac{z^2_{\text{chg}}}{2}\int d\mathbf{r}'d\mathbf{r}'' h_{\text{chg}}(\mathbf{r}-\mathbf{r}')G(\mathbf{r}',\mathbf{r}'')h_{\text{chg}}(\mathbf{r}''-\mathbf{r}) \tag{2.3}$$

where h_{chg} is the charge distribution on an ion, and $G(\mathbf{r},\mathbf{r}')$ is a self-consistently determined Green's function characterizing electrostatic field fluctuations, which can be thought of as an effective interaction between two test charges in an ionic environment. Eq. (2.3) is a unified expression accounting for *both* the polarization of the dielectric medium (e.g. Born solvation and image charge interactions) and correlations due to the ionic atmosphere.

For polyelectrolytes, we will see that the self energy is analogously the work required to assemble charge onto the polyelectrolyte. However, because of the conformational degrees of freedom, part of the work is due to the entropic change of deforming the chain. The internal energy contribution to the self energy resembles Eq. (2.3) and involves the single-chain structure factor, reflecting the spatial extent of the polyelectrolyte chain. The RGF theory prescribes a *s*elf-consistent determination of the effective intrachain structure along with the effective interaction $G(\mathbf{r},\mathbf{r}')$ as an inherent part of the theory.

To demonstrate the new physical content embodied in our theory and its effect on polyelectrolyte solution thermodynamics, we compare our results to several classical theories. The first theory to which we compare to is the thermodynamic perturbation theory, in particular the so-called first-order theory (TPT-1), which attempted to capture chain connectivity through a leading order perturbation expansion around the *simple* electrolyte results [15–24]. This is only expected to give good results in very dense systems, and the connectivity information in TPT-1 is limited, giving little qualitative insight into the effect of more complicated polymer architectures.

We also compare to the Random Phase Approximation (RPA), which is essentially the perturbation theory foundation upon which our RGF approach tries to improve.

Unlike the TPT-1, the RPA also tries to capture the complete effects of chain connectivity from the outset [25–27], and is based on a leading order treatment of fluctuations in the field theoretic partition function. The key limitation of RPA theories is that they require a chain structure as input, but for prescribed chain structure the RPA provides explicit expressions describing how chain-connectivity generates extra charge correlations. However, for flexible chains, the use of a fixed Gaussian-chain structure factor for all concentrations (hereafter referred to as **f**ixed **g**aussian-**RPA**) leads to the overestimation of the correlation effects, particularly at dilute concentrations, predicting critical interactions and concentrations that vanish with increasing chain length, [28, 29] in contradiction to simulation results [30]. A key contribution of the work of this chapter is to explain this spurious behavior in physical terms.

The rest of this chapter is organized as follows. In Section II we present a full derivation of the RGF theory for polyelectrolyte solutions. At this stage, our derivation is general for arbitrary charged macromolecules. A key part of the variational calculation is the natural emergence of a self-consistent calculation of single-chain averages and chain structure under an effective interaction $G(\mathbf{r}, \mathbf{r}')$. We then specify to a bulk system and provide expressions for the osmotic pressure and electrostatic chemical potential of polyelectrolytes, the latter being identified as the average self energy. In Section III we apply our theory to study flexible, discretely charged chains, and demonstrate how the self-consistent procedure and single-chain averages can be approximated with a variational procedure. In Section IV we present and discuss numerical results for the intrachain structure, effective interaction, polyelectrolyte self energy, osmotic coefficient, and critical point. We demonstrate the crucial importance of intrachain structure in determining the self energy and thermodynamics. We compare our results with those from several existing theories, with particular attention paid to the chain length dependence in the various properties. Finally, in Section V we conclude with a summary of the key results and future outlook.

2.2 General Theory

2.2.1 Field-Theoretic Formulation

We consider a general solution of polyelectrolytes (charged macromolecules with arbitrary internal connectivity and charge distribution) and salt ions in a solvent. We start with the microscopic density operator for species γ (which indexes over all

solvent, polyelectrolyte, and salt ion species)

$$\hat{\rho}_\gamma(\mathbf{r}) = \sum_{A=1}^{n_\gamma} \sum_{j=1}^{N_\gamma} \delta(\mathbf{r} - \mathbf{r}_{\gamma A j}), \tag{2.4}$$

where A refers to the A-th molecule of species γ, running up to the total number n_γ of molecules of species γ, and j refers to the j-th "monomer" out of a total number N_γ of monomers in a molecule A of species γ. For monomeric species, such as the small ions and solvent, $N_\gamma = 1$ and the index j only takes the value of 1.

Following previous work on the self energy of simple electrolytes, [14] individual charges (i.e. salt ions or charged monomers) are described by a short-ranged charge distribution $ez\,h(\mathbf{r} - \mathbf{r}')$, for an ion located at $\mathbf{r}'$, where we have factored out the elementary charge e and the (signed) valency z. A convenient choice for h is a Gaussian

$$h = \left(\frac{1}{2a^2}\right)^{3/2} \exp\left[-\frac{\pi(\mathbf{r} - \mathbf{r}')^2}{2a^2}\right]. \tag{2.5}$$

This distribution gives the ion a finite radius, not of excluded volume, but of charge distribution. Doing so avoids the diverging interactions in point-charge models and captures the Born solvation energy of individual ions in a dielectric medium, as well as finite-size corrections to the ion correlation energy. [14] This feature allows our coarse-grained theory to capture the essential thermodynamic effects of finite-size ions at higher densities without having to resolve the microscopic structure.

For simple salt, the charge density of the A-th molecule of species γ in unit of the elementary charge e is simply $\hat{\rho}^{\text{chg}}_{\gamma A} = z_\gamma h_\gamma(\mathbf{r} - \mathbf{r}_A)$. However, for polyelectrolytes we need to sum over all monomers j of a particular macromolecule A of species γ. In addition, to allow for arbitrary charge distribution along the polymer backbone, we introduce the signed valency $z_{\gamma j}$ such that an uncharged monomer in the polyelectrolyte chain has $z_{\gamma j} = 0$. The charge density due to the A-th molecule of the γ-th species is

$$\hat{\rho}^{\text{chg}}_{\gamma A}(\mathbf{r}) = \sum_j z_{\gamma j} h_{\gamma j}(\mathbf{r} - \mathbf{r}_{\gamma A j}), \tag{2.6}$$

where the sum runs over each monomer j of object A of species γ. With this definition, the charge density of each species γ is given by

$$\hat{\rho}^{\text{chg}}_\gamma(\mathbf{r}) = \sum_A \hat{\rho}^{\text{chg}}_{\gamma A}. \tag{2.7}$$

Allowing for the presence of external (fixed) charge distribution ρ_{ex}, we then define a total charge density

$$\hat{\rho}^{\text{chg}} = \rho_{\text{ex}} + \sum_{\gamma} \hat{\rho}_{\gamma}^{\text{chg}}. \tag{2.8}$$

Treating the charged interactions as in a linear dielectric medium with electric permittivity ε (which can be spatially dependent), the Coulomb energy of the system is written as

$$H_C = \frac{e^2}{2} \int d\mathbf{r} d\mathbf{r}' \hat{\rho}^{\text{chg}}(\mathbf{r}) C(\mathbf{r}, \mathbf{r}') \hat{\rho}^{\text{chg}}(\mathbf{r}'), \tag{2.9}$$

where $C(\mathbf{r}, \mathbf{r}')$ is the Coulomb operator given by

$$-\nabla \cdot [\varepsilon \nabla C(\mathbf{r}, \mathbf{r}')] = \delta(\mathbf{r} - \mathbf{r}'). \tag{2.10}$$

To complete the description of the system, we add the excluded volume interactions and polyelectrolyte conformation degrees of freedom. The excluded volume between all the species is accounted for by an incompressibility constraint $\sum_{\gamma} \hat{\phi}_{\gamma}(\mathbf{r}) = 1$ that applies at all $\mathbf{r}$.[31] This constraint is enforced by a Dirac δ-function in its familiar exponential representation $\delta(1 - \sum_{\gamma} \hat{\phi}_{\gamma}) = \int \mathcal{D}\eta e^{i\eta(1-\sum_{\gamma} \hat{\phi}_{\gamma})}$, which introduces an incompressibility field η and the volume fraction operator $\hat{\phi}_{\gamma}$, which is related to the density operator via $\hat{\phi}_{\gamma} = v_{\gamma} \hat{\rho}_{\gamma}$, where v_{γ} is the monomer volume of species γ (for simplicity, we have implicitly assumed that all monomers on the polyelectrolyte chain have the same volume).

The conformation degrees of freedom of the polyelectrolyte is accounted for by an (arbitrary) chain connectivity bonded interaction hamiltonian H_B which depends on the relative positions of the monomers in a polyelectrolyte chain. To focus on the electrostatic correlation, we ignore other interactions, such as the Flory-Huggins interaction.

The canonical partition function is

$$\mathcal{Q} = \prod_{\gamma} \frac{1}{n_{\gamma}! v_{\gamma}^{n_{\gamma} N_{\gamma}}} \prod_{A,j} \int d\mathbf{r}_{\gamma A j} \int \mathcal{D}\eta \exp(-\beta H), \tag{2.11}$$

where the effective “Hamiltonian" is

$$\beta H = \beta H_C - i\eta \left(1 - \sum_{\gamma} \hat{\phi}_{\gamma}\right) + \beta H_B \tag{2.12}$$

and includes the incompressibility constraint. In Eq. (2.12) the species index γ runs over all species (solvent, simple salt ions, and polyelectrolyte). We use the monomer

volume v_γ instead of the usual cube of the thermal de Broglie wavelength to avoid introducing nonessential notations; this merely produces an immaterial shift in the reference chemical potential.

We then introduce the scaled Coulomb operator

$$C = \beta e^2 C$$

and the scaled permittivity

$$\epsilon = \varepsilon/(\beta e^2),$$

which has units of inverse length and is related to the Bjerrum length by

$$l_b = \frac{1}{4\pi\epsilon}.$$

For an inhomogeneous dielectric medium, ϵ will be more convenient to use than l_b. The scaled permittivity also leads naturally to the scaled inverse Coulomb operator

$$C^{-1}(\mathbf{r}, \mathbf{r}') = -\nabla_{\mathbf{r}} \cdot [\epsilon(\mathbf{r})\nabla_{\mathbf{r}'}\delta(\mathbf{r} - \mathbf{r}')],$$

which is related to the Coulomb operator by

$$\int d\mathbf{r}_1 C^{-1}(\mathbf{r}, \mathbf{r}_1)C(\mathbf{r}_1, \mathbf{r}') = \delta(\mathbf{r} - \mathbf{r}')$$

To further simply notation, we henceforth use k_BT as the unit of energy and e as the unit of charge, so we set $\beta = 1$ and $e = 1$.

Next, we use the Hubbard-Stratanovich (HS) transformation to decouple the Coulomb interaction, which introduces the electrostatic potential $\Psi(\mathbf{r})$ (non-dimensionalized by βe) and renders the canonical partition function as

$$\mathcal{Q} = \frac{1}{\Omega_C} \prod_\gamma \frac{1}{n_\gamma! v_\gamma^{n_\gamma N_\gamma}} \int \mathcal{D}\Psi \mathcal{D}\eta \exp(-Y), \tag{2.13}$$

where Ω_C is a normalization factor from the HS transformation given by

$$\begin{aligned} \Omega_C &= \int D\Psi \exp\left[-\frac{1}{2}\int d\mathbf{r}d\mathbf{r}' \;\; \Psi(\mathbf{r})C^{-1}(\mathbf{r}, \mathbf{r}')\Psi(\mathbf{r}')\right] \\ &= \int D\Psi \exp\left[-\frac{1}{2}\int d\mathbf{r}\epsilon(\nabla\Psi)^2\right] = [\det C]^{1/2} \end{aligned} \tag{2.14}$$

and the canonical “action" is

$$\begin{aligned} Y = \frac{1}{2}\int d\mathbf{r}d\mathbf{r}'\Psi(\mathbf{r})C(\mathbf{r}, \mathbf{r}')^{-1}\Psi(\mathbf{r}') \\ - \int d\mathbf{r}(i\eta - i\rho_{\text{ex}}\Psi) - \sum_\lambda n_\gamma \ln \mathcal{Q}_\gamma[\eta, \Psi], \end{aligned} \tag{2.15}$$

where Q_γ is the single-particle/polymer partition function given shortly below.

Transforming to the grand canonical ensemble by introducing the species fugacities λ_γ, we obtain the grand canonical partition function

$$\Xi = \frac{1}{\Omega_C} \int \mathcal{D}\Psi \mathcal{D}\eta e^{-L[\Psi,\eta]} \tag{2.16}$$

with the grand canonical "action" L

$$\begin{aligned} L[\Psi,\eta] = \frac{1}{2} \int d\mathbf{r} d\mathbf{r}' \Psi(\mathbf{r}) C(\mathbf{r},\mathbf{r}')^{-1} \Psi(\mathbf{r}') \\ - \int d\mathbf{r} (i\eta - i\rho_{\text{ex}}\Psi) - \sum_\lambda \lambda_\gamma Q_\gamma[\eta,\Psi]. \end{aligned} \tag{2.17}$$

It is useful to notationally distinguish between the three basic types of species: solvent (s), simple salt ($\pm$), polymer (p). Correspondingly, the single-particle/polymer partition functions of the three basic types of species are:

$$Q_s = \int d\mathbf{r}_s e^{-iv_s\eta} \tag{2.18}$$

$$Q_\pm = \int d\mathbf{r}_\pm e^{-iv_\pm\eta - iz_\pm h_\pm * \Psi} \tag{2.19}$$

$$Q_p = \int \mathcal{D}\mathcal{R} e^{-H_B - iv_p \int d\mathbf{r}\eta\hat{\rho}_p - i\int d\mathbf{r}\Psi\hat{\rho}_{p1}^{\text{chg}}} \tag{2.20}$$

where we have introduced $\mathcal{R}$ to denote collectively the positions of all monomers in a single polyelectrolyte. For economy of notation, it is to be understood that $\hat{\rho}_{p1}^{\text{chg}}$ refers to the charge density of a *single* chain only, defined as in Eq. (2.6). We also write $h * \Psi$ to denote a convolution, or spatial averaging by the distribution h:

$$h * \Psi = \int d\mathbf{r}' h(\mathbf{r} - \mathbf{r}')\Psi(\mathbf{r}'). \tag{2.21}$$

Thus far, Eq. (2.16) is the formally exact expression for the partition function of our system. It forms the starting point for field-based numerical simulations such as the Complex Langevin methods [31] as well as approximate analytical theories.

2.2.2 Renormalized Gaussian Fluctuation Theory

For analytical insight, we seek to develop an approximate theory for evaluating Ξ, Eq. (2.16). The lowest-order saddle-point approximation would lead to a self-consistent mean-field theory, [32] in which the saddle-point condition on Ψ results in a Poisson-Boltzmann (PB) level description where correlations between

fixed charges ρ_{ex} and mobile charges ρ_γ^{chg} are included, but correlations between mobile charges themselves are ignored. The standard RPA theory accounts for the quadratic fluctuations around the saddle-point. In doing so, however, one is left with a *fixed* structure factor determined solely by the saddle-point condition. For uniform systems of polyelectrolytes, the chain structure factor that enters the RPA is independent of polyelectrolyte and salt concentrations. To circumvent this shortcoming, we approximate the partition function Eq. (2.16) as in our previous RGF theory, using a *non-perturbative* variational calculation.

The RGF theory follows the Gibbs-Feynman-Bogoliubov (GFB) variational approach by introducing a general Gaussian reference action L_{ref}. As written, Eq. (2.16) involves two fields η and Ψ to which we may apply the variational method. Allowing fluctuations in both fields will lead to the so-called double screening of both electrostatic and excluded volume. [33, 34] However, in this chapter, we focus on the fluctuation effects due to electrostatics and thus perform the variational calculation only for the Ψ field; the excluded volume interaction will be treated at the mean-field level by the saddle-point approximation for the η field. For the Ψ field, we make the following Gaussian reference action:

$$L_{\text{ref}} = \frac{1}{2}\int d\mathbf{r}d\mathbf{r}'[\Psi(\mathbf{r}) + i\psi(\mathbf{r})]G^{-1}(\mathbf{r},\mathbf{r}')[\Psi(\mathbf{r}') + i\psi(\mathbf{r}')] \tag{2.22}$$

which is parametrized by a mean electrostatic potential $-i\psi(\mathbf{r})$ and a variance, or Green's function $G(\mathbf{r},\mathbf{r}')$ which we will later show to correspond to an effective electrostatic interaction that generalizes the familiar screened-Coulomb interaction. This reference action thus accounts for the deviation $\chi = \Psi - (-i\psi) = \Psi + i\psi$ from the mean electrostatic potential.

Using L_{ref} we rewrite the grand canonical partition function Eq. (2.16) as

$$\begin{aligned}\Xi =& \frac{1}{\Omega_C}\int \mathcal{D}\Psi\mathcal{D}\eta e^{-L_{\text{ref}}[\Psi]}e^{-(L[\Psi,\eta]-L_{\text{ref}}[\Psi])} \\ =& \frac{\Omega_G}{\Omega_C}\int \mathcal{D}\eta \left\langle e^{-(L[\Psi,\eta]-L_{\text{ref}}[\Psi])}\right\rangle_{\text{ref}}\end{aligned} \tag{2.23}$$

where $\langle\cdots\rangle_{\text{ref}}$ denotes an average over Ψ with respect to the reference action L_{ref}, and Ω_G the corresponding partition function of L_{ref}, defined analogously to Ω_C in Eq. (2.14) with G in place of C. For notational clarity, we will henceforth write $\langle\cdots\rangle_{\text{ref}}$ as $\langle\cdots\rangle$.

To implement the GFB procedure (for more discussion of the nuances, see Ch. 5), we begin with approximating the field integral over Ψ with a leading order cumulant

expansion

$$\Xi \approx \int \mathcal{D}\eta \ \ \frac{\Omega_G}{\Omega_C} e^{-\langle L - L_{\text{ref}} \rangle} \equiv \Xi_{GFB}. \tag{2.24}$$

The first cumulant in the exponent can be readily evaluated owing to the Gaussian nature of the fluctuating field, and is given by:

$$\begin{aligned}
\langle L - L_{\text{ref}} \rangle =& \frac{1}{2} \int d\mathbf{r} d\mathbf{r}' \left\langle \Psi \cdot C^{-1} \cdot \Psi \right\rangle - \int d\mathbf{r} (i\eta - i\rho_{\text{ex}} \langle \Psi \rangle) \qquad (2.25) \\
& - \sum_j \lambda_j \left\langle Q_j \right\rangle - \frac{1}{2} \int d\mathbf{r} d\mathbf{r}' G^{-1}(\mathbf{r}, \mathbf{r}') \langle \chi(\mathbf{r}) \chi(\mathbf{r}') \rangle \\
=& \frac{1}{2} \int d\mathbf{r} d\mathbf{r}' [C^{-1} - G^{-1}] G - \frac{1}{2} \int d\mathbf{r} d\mathbf{r}' \psi \cdot C^{-1} \cdot \psi \qquad (2.26) \\
& - \int d\mathbf{r} (i\eta - \rho_{\text{ex}} \psi) - \sum_\gamma \lambda_\gamma \left\langle Q_\gamma \right\rangle
\end{aligned}$$

where we have used $\langle \Psi \rangle = -i\psi$ and $\langle \chi(\mathbf{r}) \chi(\mathbf{r}') \rangle = G(\mathbf{r}, \mathbf{r}')$. The grand partition function Ξ_{GFB} and *variational* grand free energy W_v are found to be:

$$\Xi_{GFB} = \int \mathcal{D}\eta e^{-W_v[G, \psi; \eta]} \tag{2.27}$$

$$\begin{aligned}
W_v[G, \psi; \eta] =& -\frac{1}{2} \ln \left(\frac{\det G}{\det C} \right) + \frac{1}{2} \int d\mathbf{r} d\mathbf{r}' [C^{-1} - G^{-1}] G \\
& - \frac{1}{2} \int d\mathbf{r} d\mathbf{r}' \psi \cdot C^{-1} \cdot \psi - \int d\mathbf{r} (i\eta - \rho_{\text{ex}} \psi) - \sum_\gamma \lambda_\gamma \left\langle Q_\gamma \right\rangle . \qquad (2.28)
\end{aligned}$$

In Eq. (2.28), the Ψ-field averaged single-particle/polymer partition functions are:

$$\langle Q_s \rangle = \int d\mathbf{r}_s \ \ \exp\left[-i v_s \eta \right] \tag{2.29}$$

$$\langle Q_\pm \rangle = \int d\mathbf{r}_\pm \ \ \exp\left[-i v_\pm \eta - z_\pm h_\pm * \psi \right] \cdot \exp\left[-\frac{1}{2} z_\pm^2 h_\pm * G * h_\pm \right] \tag{2.30}$$

$$\begin{aligned}
\left\langle Q_p \right\rangle =& \int \mathcal{D}\mathcal{R} \ \ \exp\left[-H_B - \int d\mathbf{r} \ (i v_p \eta \hat{\rho}_{p1} + \psi \hat{\rho}_{p1}^{\text{chg}}) \right] \qquad (2.31) \\
& \cdot \exp\left[-\frac{1}{2} \int d\mathbf{r} d\mathbf{r}' \ \hat{\rho}_{p1}^{\text{chg}} \cdot G \cdot \hat{\rho}_{p1}^{\text{chg}} \right].
\end{aligned}$$

For the small ions, the electrostatic fluctuations characterized by $G(\mathbf{r}, \mathbf{r}')$ enter as an instantaneous self-interaction which defines the self energy of the ion [14]

$$\begin{aligned}
u_\pm(\mathbf{r}) \equiv& \frac{1}{2} z_\pm^2 h_\pm * G * h_\pm \\
=& \frac{1}{2} z_\pm^2 \int d\mathbf{r}_1 d\mathbf{r}_2 h_\pm(\mathbf{r} - \mathbf{r}_1) G(\mathbf{r}_1, \mathbf{r}_2) h_\pm(\mathbf{r}_2 - \mathbf{r}). \qquad (2.32)
\end{aligned}$$

Similarly, the calculation of the single-chain partition function now features $G(\mathbf{r}, \mathbf{r}')$ as an effective *intra*chain interaction

$$u_p^{\text{inst}}(\mathcal{R}) \equiv \frac{1}{2} \int d\mathbf{r} d\mathbf{r}' \hat{\rho}_{p1}^{\text{chg}}(\mathbf{r}) G(\mathbf{r}, \mathbf{r}') \hat{\rho}_{p1}^{\text{chg}}(\mathbf{r}'). \tag{2.33}$$

In the limit where the polymer has only one monomer, $\hat{\rho}_{p1}^{\text{chg}}(\mathbf{r}) = z_p h(\mathbf{r} - \hat{\mathbf{r}})$, and the polyelectrolyte expression reduces to that of the simple electrolytes above. In the general case, however, this *instantaneous* (hence the superscript 'inst') interaction is clearly conformation dependent and *non-local*; Eq. (2.31) further suggests that there will also be chain conformation entropy contributions.

We emphasize that although our theory has the structure of independent particles and chains, the single-particle/chain partition functions involve the fluctuation-mediated effective intra-particle/chain interaction $G(\mathbf{r}, \mathbf{r}')$ that is missing in self-consistent mean-field (SCMF) theories. For polymeric species, it is precisely this intrachain interaction that is able to generate chain structures that adapt to the solution conditions.

For transparency and notational simplicity, in the following part we specify to a system of solvent, salt, and one polyelectrolyte species, but the expressions can be trivially extended to treat the general case with more salt and polyelectrolyte species.

To proceed, we first make the saddle-point approximation for the field η. Anticipating that the saddle-point value of η is purely imaginary, we define a real field $\mathcal{P} = i\eta$. The saddle-point condition is

$$\frac{\delta W_v}{\delta \mathcal{P}(\mathbf{r})} = 0 \tag{2.34}$$

which yields

$$1 - v_s \rho_s - v_+ \rho_+ - v_- \rho_- - v_p \rho_p = 0. \tag{2.35}$$

The densities of the species are given by:

$$\begin{aligned}
\rho_s(\mathbf{r}) &= -\frac{\lambda_p}{v_s} \frac{\delta \langle Q_s \rangle}{\delta \mathcal{P}(\mathbf{r})} = \lambda_s e^{-v_s \mathcal{P}} \\
\rho_\pm(\mathbf{r}) &= -\frac{\lambda_\pm}{v_\pm} \frac{\delta \langle Q_\pm \rangle}{\delta \mathcal{P}(\mathbf{r})} = \lambda_\pm e^{-v_\pm \mathcal{P} - z_\pm h_\pm * \psi - u_\pm} \\
\rho_p(\mathbf{r}) &= -\frac{\lambda_p}{v_p} \frac{\delta \langle Q_p \rangle}{\delta \mathcal{P}(\mathbf{r})}.
\end{aligned} \tag{2.36}$$

Eq. (2.35) is just the condition of incompressibility, and $\mathcal{P}$ can be solved to yield

$$\mathcal{P} = -\frac{1}{v_s} \log \frac{1 - \phi}{\lambda_s v_s} \tag{2.37}$$

where ϕ is the total volume fraction $\phi = \sum_{\gamma \neq s} v_\gamma \rho_\gamma$ of non-solvent species. It is customary to set $\lambda_s = 1/v_s$, which gives

$$\mathcal{P} = -\frac{1}{v_s} \log(1 - \phi) \tag{2.38}$$

We note that, at the saddle-point level, our theory can be easily adapted to accommodate other models of excluded volume and hard sphere equations of state.

With the excluded volume effects taken care of, we now discuss the determination of the variational parameters (G, ψ) describing the electrostatic fluctuations and interactions. The self-consistency of the GFB procedure comes from determining the values of (G, ψ) such that $W_v[G, \psi; \mathcal{P}]$ is stationary at fixed pressure field $\mathcal{P}$, by a partial functional differentiation with respect to the variational parameters G and ψ.[1][35]

Performing the variation with respect to the mean electrostatic potential

$$\frac{\delta W_v}{\delta \psi(\mathbf{r})} = 0 \tag{2.39}$$

leads to a Poisson-Boltzmann type expression

$$-\nabla \cdot \epsilon(\mathbf{r}) \nabla \psi = \rho_{\text{ex}} + \rho_+^{\text{chg}} + \rho_-^{\text{chg}} + \rho_p^{\text{chg}}, \tag{2.40}$$

where the species charge densities are given by:

$$\begin{aligned} \rho_\pm^{\text{chg}}(\mathbf{r}) &= -\lambda_\pm \frac{\delta \langle Q_\pm \rangle}{\delta \psi(\mathbf{r})} = \lambda_\pm z_\pm h_\pm * e^{-v_\pm \mathcal{P} - z_\pm h_\pm * \psi - u_\pm} \\ \rho_p^{\text{chg}}(\mathbf{r}) &= -\lambda_p \frac{\delta \langle Q_p \rangle}{\delta \psi(\mathbf{r})} \end{aligned} \tag{2.41}$$

Finally, the stationarity condition on G

$$\frac{\delta W_v}{\delta G(\mathbf{r}, \mathbf{r}')} = 0 \tag{2.42}$$

leads to an integro-differential equation

$$\delta(\mathbf{r} - \mathbf{r}') = \int d\mathbf{r}_1 \, [C^{-1}(\mathbf{r}, \mathbf{r}_1) + 2I(\mathbf{r}, \mathbf{r}_1)] G(\mathbf{r}_1, \mathbf{r}') \tag{2.43}$$

[1] While procedurally the same as the saddle-point evaluation of $\mathcal{P}$, we stress that while $\mathcal{P}$ is an original field variable of the exact partition function, (G, ψ) have a distinct origin in the GFB variational approximation of fluctuations in the Ψ field.

where the ionic strength term is given by

$$\begin{aligned} 2I(\mathbf{r},\mathbf{r}') = &\sum_{\gamma} \lambda_\gamma \frac{\delta \left\langle Q_\gamma \right\rangle}{\delta G(\mathbf{r},\mathbf{r}')} \\ =&z_+^2 \int d\mathbf{r}_1 \;\; h_+(\mathbf{r}-\mathbf{r}_1)\rho_+(\mathbf{r}_1)h_+(\mathbf{r}_1-\mathbf{r}') \\ &+ z_-^2 \int d\mathbf{r}_1 \;\; h_-(\mathbf{r}-\mathbf{r}_1)\rho_-(\mathbf{r}_1)h_-(\mathbf{r}_1-\mathbf{r}') \\ &+ \lambda_p \left\langle Q_p \right\rangle \left\langle \hat{\rho}_{p1}^{\mathrm{chg}} \hat{\rho}_{p1}^{\mathrm{chg}} \right\rangle . \end{aligned} \tag{2.44}$$

In the last line above we have used the identity for the *single-chain* charge correlation

$$\left\langle \hat{\rho}_{p1}^{\mathrm{chg}} \hat{\rho}_{p1}^{\mathrm{chg}} \right\rangle = \frac{1}{\left\langle Q_p \right\rangle} \frac{\delta \left\langle Q_p \right\rangle}{\delta G(\mathbf{r},\mathbf{r}')} \tag{2.45}$$

of a single chain with partition function $\left\langle Q_p \right\rangle$ to rewrite the differentiation with respect to G

$$\begin{aligned} \lambda_\gamma \frac{\delta \left\langle Q_p \right\rangle}{\delta G(\mathbf{r},\mathbf{r}')} &= \lambda_p \frac{\left\langle Q_p \right\rangle}{\left\langle Q_p \right\rangle} \frac{\delta \left\langle Q_p \right\rangle}{\delta G(\mathbf{r},\mathbf{r}')} \\ &= \lambda_p \left\langle Q_p \right\rangle \left\langle \hat{\rho}_{p1}^{\mathrm{chg}} \hat{\rho}_{p1}^{\mathrm{chg}} \right\rangle \; . \end{aligned} \tag{2.46}$$

In the case where the polymer only consists of one monomer, the polymer contribution to the ionic strength reduces to the simple electrolyte case.

Equations (2.38), (2.40), (2.43), and (2.44) constitute the central expressions of our self-consistent theory. The self-consistent determination of polymer conformation originates from the fact that the Green's function $G(\mathbf{r},\mathbf{r}')$ Eq. (2.43) itself depends on the single-chain charge correlations $\left\langle \hat{\rho}_{p1}^{\mathrm{chg}}(\mathbf{r}) \hat{\rho}_{p1}^{\mathrm{chg}}(\mathbf{r}') \right\rangle$, which in turn comes from the average single-chain partition function $\left\langle Q_p \right\rangle$ determined by $G(\mathbf{r},\mathbf{r}')$, Eq. (2.31).

Although the idea of a self-consistent determination of chain structure is not new, it is gratifying that our derivation of the RGF naturally prescribes how to perform the self-consistent calculation.

2.2.3 Bulk Solution Thermodynamics: Self Energy and Osmotic Pressure

To demonstrate the nature of this self-consistent calculation, we now specify to a bulk solution with $\rho_{\mathrm{ex}} = 0$. For a bulk solution, the single-particle/polymer partition

functions simplify to:

$$\begin{aligned}
\langle Q_\pm \rangle =& V e^{-v_\pm \mathcal{P} - z_\pm \psi} q_\pm \\
q_\pm =& e^{-\frac{1}{2}\int dr dr'\ z_\pm h_\pm * G * z_\pm h_\pm} = e^{-u_\pm} \\
\left\langle Q_p \right\rangle =& V e^{-N_p v_p \mathcal{P} - z_p^{tot}\psi} q_p \\
q_p =& \frac{1}{V}\int \mathcal{D}\mathcal{R}\ e^{-H_B - \frac{1}{2}\int dr dr'\ \hat{\rho}_{p1}^{\text{chg}} \cdot G \cdot \hat{\rho}_{p1}^{\text{chg}}}
\end{aligned} \tag{2.47}$$

where z_p^{tot} is the total charge carried by a chain. $q_\gamma = Q_\gamma / V$ is the single-particle/chain partition function excluding the translational degrees of freedom; for simple ions $q_\pm$ is simply the Boltzmann weight given by the simple ion self energy $u_\pm$ in Eq. (2.32).

Using Eq. (2.36), we evaluate the density and determine the fugacities to be:

$$\begin{aligned}
\lambda_\pm &= \frac{n_\pm}{\langle Q_\pm \rangle} = \frac{\rho_\pm}{\exp[-u_\pm]\exp[-v_\pm \mathcal{P} - z_\pm \psi]} \\
\lambda_p &= \frac{n_p}{\left\langle Q_p \right\rangle} = \frac{\rho_p / N_p}{q_p \exp[-v_p N_p \mathcal{P} - z_p^{tot}\psi]}
\end{aligned} \tag{2.48}$$

where $\rho_p = n_p N_p / V$ is the monomer density. Using the fugacity relation, the polymer contribution Eq. (2.46) to the ionic strength is simply

$$\begin{aligned}
\lambda_p \left\langle Q_p \right\rangle \left\langle \hat{\rho}_{p1}^{\text{chg}} \hat{\rho}_{p1}^{\text{chg}} \right\rangle &= n_p \left\langle \hat{\rho}_{p1}^{\text{chg}} \hat{\rho}_{p1}^{\text{chg}} \right\rangle \\
&= \frac{n_p}{V} V \left\langle \hat{\rho}_{p1}^{\text{chg}} \hat{\rho}_{p1}^{\text{chg}} \right\rangle \\
&= \frac{\rho_p}{N_p} S_p^{\text{chg}}.
\end{aligned} \tag{2.49}$$

Recognizing that the *single*-chain structure $\left\langle \hat{\rho}_{p1}^{\text{chg}} \hat{\rho}_{p1}^{\text{chg}} \right\rangle$ scales as the density of a single chain N/V, we have pre-emptively regrouped a factor of V/V in anticipation that the single-chain charge structure factor defined as $S_p^{\text{chg}} \equiv V \left\langle \hat{\rho}_{p1}^{\text{chg}} \hat{\rho}_{p1}^{\text{chg}} \right\rangle$ is independent of volume.

The fugacity is related to the chemical potential by $\mu_\gamma = \ln(\lambda_\gamma v_\gamma)$, whence we can identify the per-ion and per-*chain* chemical potentials as:

$$\begin{aligned}
\mu_\pm &= \ln(\rho_\pm v_\pm) + v_\pm \mathcal{P} + z_\pm \psi + u_\pm \\
\mu_p &= \ln\left(\frac{\rho_p v_p}{N_p}\right) + v_p N_p \mathcal{P} + z_p^{tot}\psi + u_p
\end{aligned} \tag{2.50}$$

where

$$u_p = -\ln q_p. \tag{2.51}$$

The first three terms in both chemical potential expressions of Eq. (2.50) are the same as in a mean-field analysis of a bulk solution. The physical content of the last term u_p is the free energy of a chain interacting with itself via the effective potential G, and within our theory u_p is easily identifiable as the *per-chain*, chemical potential attributable to electrostatic fluctuations. We thus define $\mu_p^{el} \equiv u_p$ and term it the (bulk) *per-chain self energy*.

It can be easily verified that all the polymer expressions above reduce to those of simple electrolytes in the single-monomer limit $N_p = 1$, since then $z_p^{tot} = z_p$, H_B can be set to zero, $\hat{\rho}_{p1}^{\text{chg}}(\mathbf{r}) = z_p h(\mathbf{r} - \hat{\mathbf{r}})$, and by translation invariance $\int \mathcal{DR} \to \int dr \to V$. Clearly, in this limit $u_p \xrightarrow{N_p=1} u_\pm$.

In the bulk, it is also useful to define the self energy per monomer (note subscript 'm' for 'monomer') as

$$\mu_m^{el} \equiv \frac{u_p}{N_p}. \tag{2.52}$$

Further, the self-consistent set of Equations (2.38), (2.40), (2.43), and (2.44) are simple in the bulk case: the constitutive equation (2.40) for ψ is just the global charge neutrality constraint, while in Eq. (2.43) the structure factors and $G(\mathbf{r}, \mathbf{r}')$ become translation-invariant, allowing a simple Fourier representation. Further, because of the rotational symmetry, only the magnitude of the wavevector matters, and Eqs. (2.43) and (2.44) become:

$$1 = \epsilon k^2 \tilde{G}(k) + 2\tilde{I}(k)\tilde{G}(k) \tag{2.53}$$

$$\tilde{2}I(k) = \rho_+ \tilde{S}_+^{\text{chg}}(k) + \rho_- \tilde{S}_-^{\text{chg}}(k) + \frac{\rho_p}{N_p} \tilde{S}_p^{\text{chg}}(k) \tag{2.54}$$

which can be easily solved to obtain

$$\tilde{G}(k) = \frac{1}{\epsilon[k^2 + \tilde{\kappa}^2(k)]}, \tag{2.55}$$

where we identify $\tilde{\kappa}^2(k) = 2\tilde{I}(k)/\epsilon$ as the *wave-vector dependent* screening function, a generalization of the Debye screening constant. In our spread-charge model, even simple salt ions have some internal charge structure

$$\tilde{S}_\pm^{\text{chg}} = z_\pm^2 \tilde{h}_\pm^2(k). \tag{2.56}$$

For point charges $\tilde{h}_\pm = 1$, recovering the same ionic strength contribution as in DH theory. Therefore in the absence of polymers, in the point charge limit for simple electrolyte, $\tilde{G}(\mathbf{k})$ is precisely the DH screened Coulomb interaction.

In bulk solution, a polyelectrolyte with discrete charges has a charge structure factor that can generally be divided into a self and non-self piece

$$\tilde{S}_p^{\mathrm{chg}}(k) = \sum_l z_{pl}^2 \tilde{h}_{pl}^2(k) + \sum_l \sum_{m \neq l} z_{pl} \tilde{h}_{pl}(k) z_{pm} \tilde{h}_{pm}(-k) \tilde{\omega}_{lm}(k). \tag{2.57}$$

The first sum is the $l = m$ self piece, and the second sum is over all other terms. The structure is characterized by the intramolecular correlation $\tilde{\omega}_{lm}$ between two monomers l and m on the same chain. [36] While $\tilde{\omega}_{lm}(k)$ has unknown analytical form, we know that $\tilde{\omega}_{lm}(k) \to 1$ as $k \to 0$, and $\tilde{\omega}_{lm}(k) \to 0$ as $k \gg 1/a$. We thus see that in the large wavelength limit the polyelectrolyte charges contribute collectively to the screening $\tilde{\kappa}^2(k)$ as a high-valency object $\sim (z^{tot})^2$ where $z^{tot} = \sum_l z_{pl}$ is the total valency. In contrast, in the small wavelength limit the charges screen as independent charges, which for historical reasons we call the Voorn-Overbeek (VO) limit (only in the sense of treating the charges as disconnected from each other – the original VO theory used DH theory with point charges, while we leave open the possibility of giving charges internal structure).

It has been previously noted that the magnitude of collective screening by polyelectrolyte charges should be wave-vector dependent and described by the charge structure (contained in $\tilde{I}$): [26, 37] at different wavelengths portions of chains screen as independent objects, and the size of these screening portions is set by the structure. These discussions correctly identified that with increasing density, screening will be increasingly controlled by higher-k structure. However, previous discussions, with few exceptions,[38] often smear out the charges on a chain, thus treating simple ions and polymer charges on different footing and missing the approach to the VO-limit at high wavevectors.

We now present the osmotic pressure Π. We can use $\lambda_\gamma \left\langle Q_\gamma \right\rangle / V = \rho_\gamma / N_\gamma$ to identify the ideal osmotic contribution. Then, using Fourier integrals to evaluate the determinants in W_v Eq. (2.28), the osmotic pressure is:

$$\Pi = -\left[\frac{W_v - W_v^0}{V}\right] = -\frac{1}{4\pi^2}\int_0^\infty k^2\, dk \left[\ln\left(1 + \frac{\tilde{\kappa}^2(k)}{k^2}\right) - \frac{\tilde{\kappa}^2(k)}{k^2 + \tilde{\kappa}^2(k)}\right] - \frac{1}{v_s}\left(1 + \log(1-\phi)\right) + \frac{1-\phi}{v_s} + \rho_\pm + \frac{\rho_p}{N_p} \tag{2.58}$$

where W_v^0 is the grand free energy of a pure solvent system.

An important feature of the theory is the necessity of self-consistently determining the chain charge structure $\tilde{S}_p^{\text{chg}}(k)$ Eq. (2.57) and $\tilde{G}(k)$ Eq. (2.55). The Green's function $\tilde{G}(k)$ itself depends on the chain structure; the latter is in turn determined by a chain interacting with itself through G in the single-chain partition function $\langle Q_p \rangle$, Eq. (2.31). The self-consistency is typically solved by iteratively approximating G and the chain structure until convergence is achieved.

The last piece required to implement our theory is an evaluation of the single-chain partition function and corresponding intramolecular charge structure. The exact evaluation of single-chain partition functions is difficult even for simpler pair interactions, and in general should be done by numerical simulation. [39] In Sec. 2.3 we demonstrate how $\langle Q_p \rangle$ can be approximately and simply evaluated, but we point out that such an approximation is not itself inherent to the general theory.

2.3 Self-Consistent Calculation of Flexible Chain Structure

Our discussion has heretofore been general for macromolecules of arbitrary internal connectivity and charge distribution. To illustrate one way of carrying out the self-consistent calculation and facilitate comparison to previous theories, we specify to study flexible polyelectrolyte chains with Kuhn length b, equally spaced (discrete) charges of the same valency z_p, and overall charged monomer fraction f, such that the total polymer charge is $z_p^{tot} = Nfz_p$. Again, the discrete nature of the charges will be reflected in the charge structure factor and is important at high wavevectors.

Given this chain model, the expressions for the per-monomer chemical potential, density, and charge structure factor $\tilde{S}_\gamma^{\text{chg}}(k)$ are now:

$$\mu_m = \frac{1}{N_p} \ln \frac{\rho_p v_p}{N_p} - v_p \mathcal{P} + f z_p \psi + \frac{u_p}{N_p} \tag{2.59}$$

$$\rho_p = \lambda_p N_p e^{-N_p v_p \mathcal{P} - N_p f z_p \psi - u_p} \tag{2.60}$$

$$\tilde{S}_p^{\text{chg}}(k) = z_p^2 Nf[1 + (Nf - 1)\tilde{\omega}(k)]\tilde{h}_p^2(k) \tag{2.61}$$

where we have re-expressed the sum over all monomer-monomer pair correlations $\tilde{\omega}_{lm}$ with an average per-monomer structure $\tilde{\omega}$. Following our previous discussion, one can check that when $k \to 0$, $\tilde{S}_p^{\text{chg}} \sim (Nfz_p)^2$ as for a Nfz_p-valent object, and when $ka \gg 1$, $\tilde{S}_p^{\text{chg}} \sim Nfz_p^2$ as for Nf independent charges of valency z_p.

Returning to the task of calculating the single-chain partition function, we resort to a commonly used variational technique. There are many variations reported in the literature, [36, 37, 40–44] but they all essentially reduce to a Flory-type

decomposition of the single-chain free energy into entropic F_{ent} and interaction F_{int} contributions

$$u_p = -\ln q_p \approx \min_{\zeta} \left[F_{\text{ent}}(\zeta) + F_{\text{int}}(\zeta) \right] \tag{2.62}$$

where ζ indicates some conformational parameterization of a reference chain. In Flory's treatment of the excluded volume of a single chain, for example, ζ would be the average end-to-end distance. For our case, we take our reference chain to be a wormlike chain parameterized by an effective persistence length $\zeta \equiv l_{\text{eff}}$. Under this model, l_{eff} controls the chain expansion $\alpha^2 = \left\langle R_{ee}^2 \right\rangle / R_{ee,0}^2$

$$\alpha^2 = 2\frac{l_{\text{eff}}}{b}\left[1 - \frac{l_{\text{eff}}}{Nb}\left(1 - e^{-Nb/l_{\text{eff}}}\right)\right]. \tag{2.63}$$

The variational parameter l_{eff} also controls the per-monomer structure $\tilde{\omega}(k; l_{\text{eff}})$ in the charge structure factor $\tilde{S}_p^{\text{chg}}$. We note, however, l_{eff} introduced here cannot be simply interpreted as the mechanical persistence of the polymer, since it is defined by the overall chain size rather than reflecting the local bending stiffness. [41] While exact expressions of the worm-like-chain (WLC) structure factor exist in literature, [45] to facilitate calculations we use a simple analytical form:

$$\tilde{\omega}(k) = \frac{\exp[-kl_{\text{eff}}/2]}{1 + k^2 Nbl_{\text{eff}}/6} + \frac{1 - \exp[-kl_{\text{eff}}/2]}{1 + kNb/\pi} \tag{2.64}$$

which interpolates between the appropriate asymptotic limits of $\tilde{\omega}(k; l_{\text{eff}})$: [46, 47]

$$\tilde{\omega}(k) \sim \begin{cases} 1, & k < \sqrt{6/Nbl_{\text{eff}}} \\ 6/k^2 Nbl_{\text{eff}}, & \sqrt{6/Nbl_{\text{eff}}} < k < 1/l_{\text{eff}} \\ \pi/kNb, & k > 1/l_{\text{eff}} \end{cases} \tag{2.65}$$

Like a previously proposed expression, [46] our expression interpolates between Gaussian-chain behavior $\tilde{\omega} \sim 6/Nbl_{\text{eff}}k^2$ at low wavevector and rodlike behavior $\tilde{\omega} \sim \pi/kNb$ at high wavevector, with a crossover set by l_{eff}. An important feature of the WLC chain structure captured by our expression is that the *magnitude* of $\tilde{\omega}$ at high wavevector is negligibly affected by l_{eff}, reflecting the intuition that while electrostatics can greatly deform overall chain structure, smaller scale structure is less affected, [41] consistent with blob-theory arguments [48] and simulation observations. [49] As long as we work in the regime where electrostatic blobs have only $g \sim (b/f^2 l_b)^{2/3} \sim O(1)$ monomer each, the WLC structure persists down to the monomer length scale so that smaller length-scale structures do not need to be resolved.

We are thus able to write a one-parameter (l_{eff}) model for the single-polyelectrolyte free-energy Eq. (2.62) with entropic and interaction terms given by:

$$F_{\text{ent}} = -\frac{3}{2}N\ln\left(1-\frac{\alpha^2}{N}\right) - 3\ln(\alpha) \tag{2.66}$$

$$F_{\text{int}} = \frac{1}{4\pi^2}\int k^2 dk\ \tilde{G}(k)\tilde{S}_p^{\text{chg}}(k;l_{\text{eff}}) \tag{2.67}$$

The first term of the entropic free energy is a finite extensibility approximation that lies between the elastic free energies obtained from integrating the worm-like-chain (WLC) and freely-jointed-chain (FJC) force-extension relationships. [50, 51] The second term $-3\ln(\alpha)$ is a term that resists chain compression, first deduced by Flory and used by several subsequent authors. [52–55]

We also note that the expression for the interaction energy Eq. (2.67) is an improvement upon typical scaling estimates of the Coulomb energy. When the effective interaction G is a bare Coulomb interaction, for an extended structure ($R \sim N$) the usual scaling estimate gives an energy of $N^2/R \sim N$. [48] The structure factor of an extended chain is roughly $\tilde{S}^{\text{chg}}(k) \sim N^2/(1+kN/\pi)$, and Eq. (2.67) gives an interaction energy of $\sim N\ln N$ with the correct logarithmic correction. [56, 57]

An interesting consequence of this decomposition of the single-chain partition function is that the electrostatic fluctuation contribution to the self energy is decomposed into two contributions: 1) entropic work of deforming the chains and 2) average interaction energy. The presence of an entropic contribution to the fluctuation-induced excess chemical potential is a special feature of flexible chains.

With the structure factor specified, we solve for self-consistency iteratively: for given Green's function $\tilde{G}$ we minimize the single-chain free energy Eq. (2.62) to approximate l_{eff} and estimate the charge structure factor $\tilde{S}_p^{\text{chg}}(k)$ via Eq. (2.61) and (2.64), which we then use as input to update $\tilde{G}$ using Eq. (2.55). We stop when the rms relative error of l_{eff} between iterations is below 10^{-10}. Results of our calculations are presented in Sec. 2.4.

2.4 Numerical Results and Discussion

For numerical calculations, we consider fully-charged chains with $f = 1, z_p = 1$, monovalent salt, set all ion sizes to be the same diameter $\sigma = 2a = 1$, and set the Kuhn length $b = \sigma$. We also study systems with Bjerrum length $l_b \sim 1$, ensuring that electrostatic blobs only have $g \sim (b/f^2 l_b)^{2/3} \sim 1$ Kuhn monomers each. To facilitate comparison with the restricted primitive model, the parameters v_γ are

chosen to reproduce the divergence in the excluded volume free energy at the closest packing number density of hard spheres with diameter σ.

We start by examining salt-effects on the structure of isolated chains, then finite-concentration effects on chain size in salt-free polyelectrolyte solutions. Subsequently, we present the effective self-interaction G, demonstrate the presence of charge oscillations, and compare to screening predictions under the DH and fixed-Gaussian structure approximations. Next, we examine the polymer self energy of *salt-free* polyelectrolyte solutions and compare our predictions to alternative theories for electrostatic correlations. Finally, we study the consequences of our theory on the osmotic coefficient and phase separation behavior.

2.4.1 Chain Structure

The scaling behavior of linear homopolyelectrolytes is well-known for both the single-chain [48] and semidilute regimes.[57, 58]

In the single-chain, salt-free limit, scaling theory predicts that the long range electrostatic forces elongate flexible chains into a "cigar" of electrostatic blobs with chain size scaling linearly with chain length as $R \sim N$. [48] At finite concentrations of salt, the screened Coulomb interaction effectively acts as an excluded volume interaction for chain segments separated by distances greater than κ^{-1}, where κ is the inverse Debye length of the added salt. Consequently, while short chains still exhibit the "cigar" scaling, sufficiently long chains behave as self-avoiding walks, [57, 58] with the crossover determined by the salt concentration. These expectations are borne out in Fig. 2.1, where we plot results for the chain size as function of chain length for several different salt concentrations $\rho_{\pm}$.

For our theory, in the single-chain limit the polyelectrolyte does not contribute to the screening $\tilde{\kappa}(k)$, and the Green's function reduces to a modified screened Coulomb interaction $\tilde{G} = 4\pi l_b/(k^2+\tilde{\kappa}(k)^2)$. Since in the single-chain limit $\tilde{G}$ is independent of polymer conformation, the self-consistent calculation only requires us to minimize the free energy of a single effective chain Eq. (2.62).

Because the salt concentrations considered are still dilute enough for finite ion-size effects to be negligible, the DH expression $\kappa^2 = 4\pi l_b z^2(2\rho_{\pm}) = 8\pi l_b z^2 \rho_{\pm}$ is a good estimate of the screening length, and the crossover condition $\kappa R > 1$ predicts a crossover salt concentration $\rho_{\pm}^* \sim N^{-2}$, where we have used that in the dilute salt limit $R \sim N$. In the inset of Fig. 2.1 we locate the crossover by the intersection of fits to the asymptotic scaling limits, and verify this scaling expectation of the

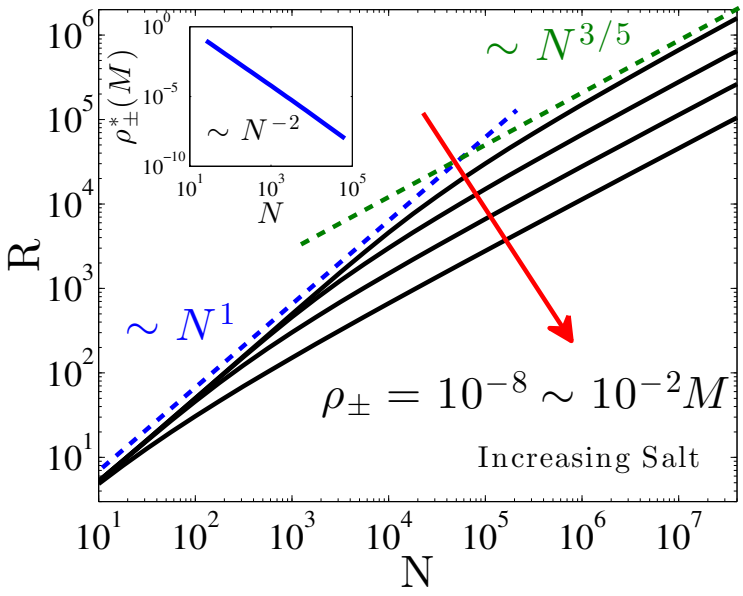

Figure 2.1: End-to-end distance in the single-chain limit, with parameters $l_b = 0.7$, $f = 1$, $z_p = 1$, at different salt concentrations $\rho_\pm$. The blue and green dashed lines represent, respectively, the $R \sim N$ and $R \sim N^{3/5}$ scalings in the zero and high salt limits. The inset shows the crossover salt concentration $\rho^*_\pm \sim N^{-2}$.

crossover concentration.

At finite concentrations of polyelectrolyte, there is a new scaling regime for the polymer size when the monomer concentration ρ_p becomes sufficiently high. This concentration is usually taken to be at the physical overlap, $\rho^*_p \sim 1/N^2$, with new scaling behavior given by the semidilute prediction of ideal random walk statistics $R \sim N^{1/2}$. [57, 58]

We plot our results for salt-free polyelectrolyte solutions in Fig. 2.2 at several polymer concentrations. For sufficiently high concentrations, we recover the ideal random walk scaling. Further, the crossovers happen below physical overlap, in accord with limited simulation data, [40, 49] and are attributed to the fact that the Coulomb interactions are long-ranged and that chains repel each other even below physical overlap.

The crossover appears to be extremely gradual (more than two decades). Nevertheless, for given concentration we can approximately locate the crossover chain length by again finding the intersection of the asymptotic limits. We plot these results in the inset of Fig. 2.2 and find that the crossover concentration goes as $\rho^*_p \sim N^{-3}$.

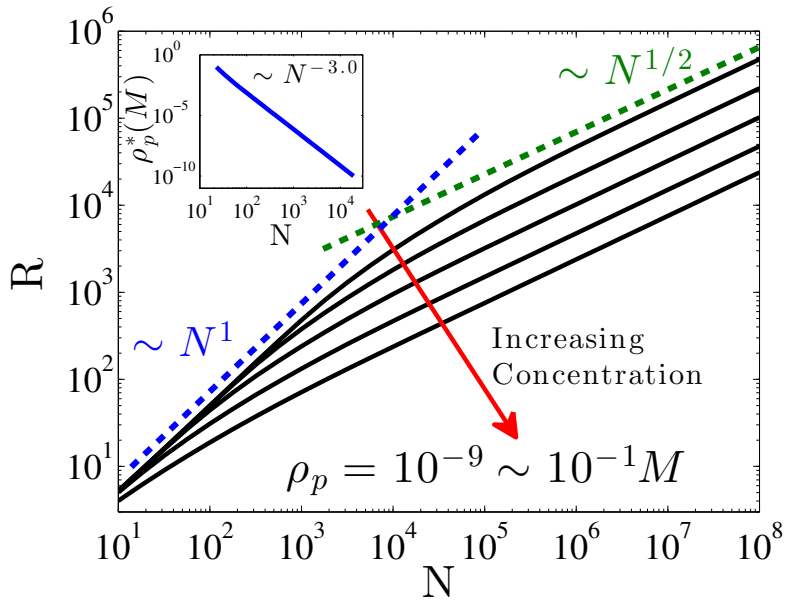

Figure 2.2: End-to-end distance of a polyelectrolyte in salt-free solutions at finite monomer concentration ρ_p, with parameters $l_b = 0.7, f = 1, z_p = 1$. The blue and green dashed lines represent, respectively, the $R \sim N$ scaling in the dilute regime, and the $R \sim N^{1/2}$ scaling in the semidilute regime. The inset shows the crossover monomer concentration $\rho_p^* \sim N^{-3}$.

To understand this apparently strong N-dependency, we will have to first understand the nature of screening in solutions with finite concentrations of polyelectrolyte, of which we will give a more detailed discussion in Section 2.4.3. We do mention, however, that if one uses the most conservative estimate of screening where only counterions contribute to the screening length, chains are expected to interact at concentrations a factor of $1/(4\pi l_b f)^3$ below physical overlap, [58] which is several orders of magnitude for parameters studied in this chapter ($4\pi l_b f \approx 10$). This is in qualitative agreement with our results that chains begin contracting far below physical overlap.

Thus, we have shown that our theory is able to correctly capture asymptotic chain size scaling behavior and reproduce qualitatively reasonable crossovers. We will show that correctly capturing these asymptotic limits is sufficient to give correct behavior for the osmotic coefficient and critical properties.

2.4.2 Effective Interaction $G(k)$

For simple electrolytes, the field fluctuations and effective screened interaction are well-described by the Debye-Hückel screened Coulomb function. The Voorn-Overbeek approximation of neglecting chain connectivity takes Debye-Hückel as its starting point, and describes electrostatic fluctuations in polyelectrolyte solution by a screened Coulomb with screening constant $\kappa_{\mathrm{vo}}^2 = 4\pi l_b(\rho_+ + c_p N) = 8\pi l_b \rho_p$, where the monomer number density ρ_p is related to the chain number density c_p by $\rho_p = c_p N$, and $\rho_+ = \rho_p$ in salt-free solution of polyelectrolyte (recall $f = 1, z_p = 1$). The opposite limit is to treat polyelectrolytes as point charges of valency $z_{tot} = N$. [49] In this case, the electrostatic fluctuations are characterized by the screened Coulomb with a renormalized screening constant $\kappa_{\mathrm{N}}^2 = 4\pi l_b(\rho_+ + c_p N^2) = 4\pi l_b \rho_p(1 + N)$. Clearly, the effect of chain connectivity on screening should lie somewhere between these two limits. In Fig. 2.3, we plot the Fourier-transformed Green's function G for salt-free solutions of (1) chains with adaptable structure (our theory, RGF) and for (2) chains with fixed Gaussian-chain structure (fg-RPA), and compare to the two aforementioned limits.

For sufficiently dilute systems, the Green's function G for both our theory and RPA fall on the screened Coulomb line with screening constant κ_{N}^2 – information about the chain connectivity is reflected only through the total charge z_{tot}. We argue that this is the correct limiting law – for sufficiently dilute systems translational entropy opposes any ion condensation and the counterions can be considered a constant background charge. As long as the polymers are sufficiently far apart, they appear to each other essentially as point charges with valency z_{tot}, and can be treated using results from the one-component plasma (OCP) theory once one scales the charges by z_{tot}. In the dilute limit, the OCP is known to be governed by the DH expressions [59] – when treating polyelectrolytes as a single z_{tot}-valent object the OCP theory gives a screening length λ that scales as $\sim (l_b \rho N)^{-1/2}$, which is consistent with screening constant $\kappa_{\mathrm{N}}^2 = 4\pi l_b \rho_p(1 + N)$ for $N \gg 1$.

At higher concentrations, the finite-extent of the polyelectrolyte begins impacting the Green's function, and leads to a peak in $G(k)$ at finite wavenumbers that depend on the concentration. This peak can be shown to lead to attractive wells in $G(\mathbf{r} - \mathbf{r}')$, which allow for positively charged chains to assume random walk statistics; the random-walk conformation would not be possible with a purely repulsive screened Coulomb interaction. This is the reason our RGF is able to reproduce the Gaussian-chain scaling in semidilute solution. On the other hand, the fg-RPA *a*ssumes a

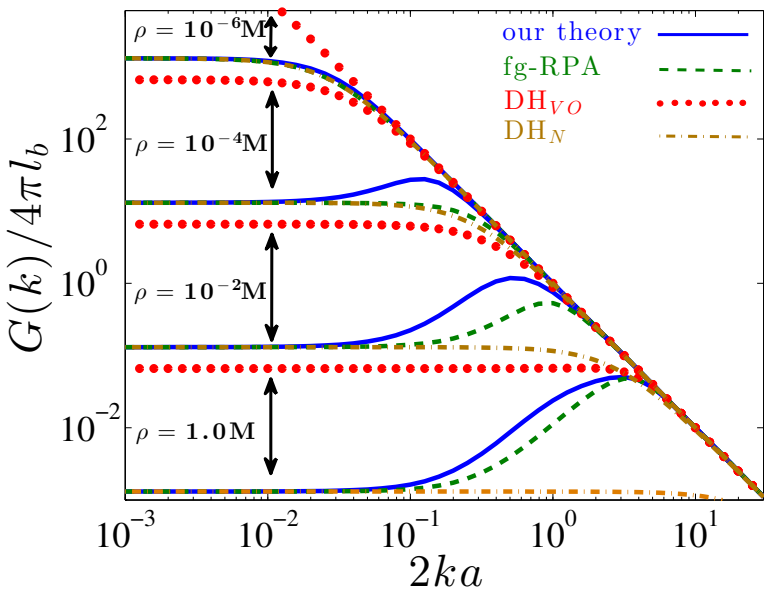

Figure 2.3: Green's function $G/4\pi l_b$ characterizing electrostatic field fluctuations, at different polyelectrolyte concentrations, from our RGF theory (blue solid), fg-RPA (green dashed), DH prediction with VO screening strength $\kappa^2_{\rm VO} = 8\pi l_b \rho_p$ ($DH_{\rm VO}$, red dotted), and DH prediction using the N-valent screening strength $\kappa^2_N = 4\pi l_b \rho_p (1+N)$ ($DH_{\rm N}$, brown dot-dashed). Results are for salt-free solutions ($l_b = 1, f = 1, z_p = 1, N = 100$) at different monomer densities ρ_p. Relative to the RGF, the fg-RPA over-predicts screening, has a delayed crossover, and predicts a peak at higher wavenumber (smaller wavelength).

Gaussian-chain structure $f$or all concentrations, and there is no feedback of G onto the chain structure.

The peak in $G(k)$ is also associated with decreased screening compared to DH expectations using the dilute limit κ^2_N as the screening strength. The onset of a peak is actually also present for simple electrolyte solutions and corrects for the over-prediction of correlations within the DH approximation at higher concentrations. It can be generally shown that the peak sets in at lower concentrations for larger ion sizes: at higher concentrations, only sub-portions of spatially extended charged objects screen independently, hence decreasing the effective valency and screening strength.

Polyelectrolytes have their charge greatly extended across space, and correspondingly their peak sets in at a much lower concentration than simple electrolytes. The RGF, which predicts an adaptable chain size that becomes expanded relative to the

ideal Gaussian chain, predicts an earlier onset of a peak in $G(k)$ and less screening (larger $G(k)$ values) than the fg-RPA theory at all concentrations. However, the peaks of the two theories do approach each other with increasing concentration, as expected of the semidilute regime.

2.4.3 Electrostatic Self Energy and Correlations

We now examine the self energy per polyelectrolyte monomer Eq. (2.52), which depends on both the chain structure and Green's function. We first give the *total* self energy, where the zero energy of the electrostatics is taken to be the state where charges are dispersed into infinitesimal bits at infinity in vacuum. This perspective highlights the energetic consequences of connecting charges onto a chain, which is especially important in dilute solution. Further, this reference energy includes the energy of assembling charge onto each charged monomer, thus ensuring we account for both dielectric effects of solvation and interactions between charges.

To study correlation effects due to finite polymer concentration, we argue that the most natural definition involves subtracting out the infinite-dilution energy. We are then able to distinguish a dilute limit following a renormalized DH-like scaling, and a crossover to less effective screening due to the overlap of polyelectrolyte chains in space.

To simplify the parameter space to one density variable and highlight the role of chain structure in modifying the self energy, below we only present results for salt-free solutions of flexible polyelectrolytes. However, the physical principles regarding screening and the correlation energy are generally applicable to more complicated systems.

2.4.3.1 Total Self Energy

One key feature of semidilute solutions is that the self energy should become independent of chain length for sufficiently long chain lengths. This is confirmed in Fig. 2.4a, where we plot the *total* self energy of salt-free solutions of polyelectrolytes. With increasing chain length, the self energies begin overlapping over greater concentration ranges, in agreement with our expectations for semidilute solutions.

Figure 2.4a also shows that the fg-RPA theory greatly over-estimates the self energy at low concentrations, and its value rapidly grows with chain length N. Having shown in Section 2.4.2 that with increasing dilution the Green's function G becomes

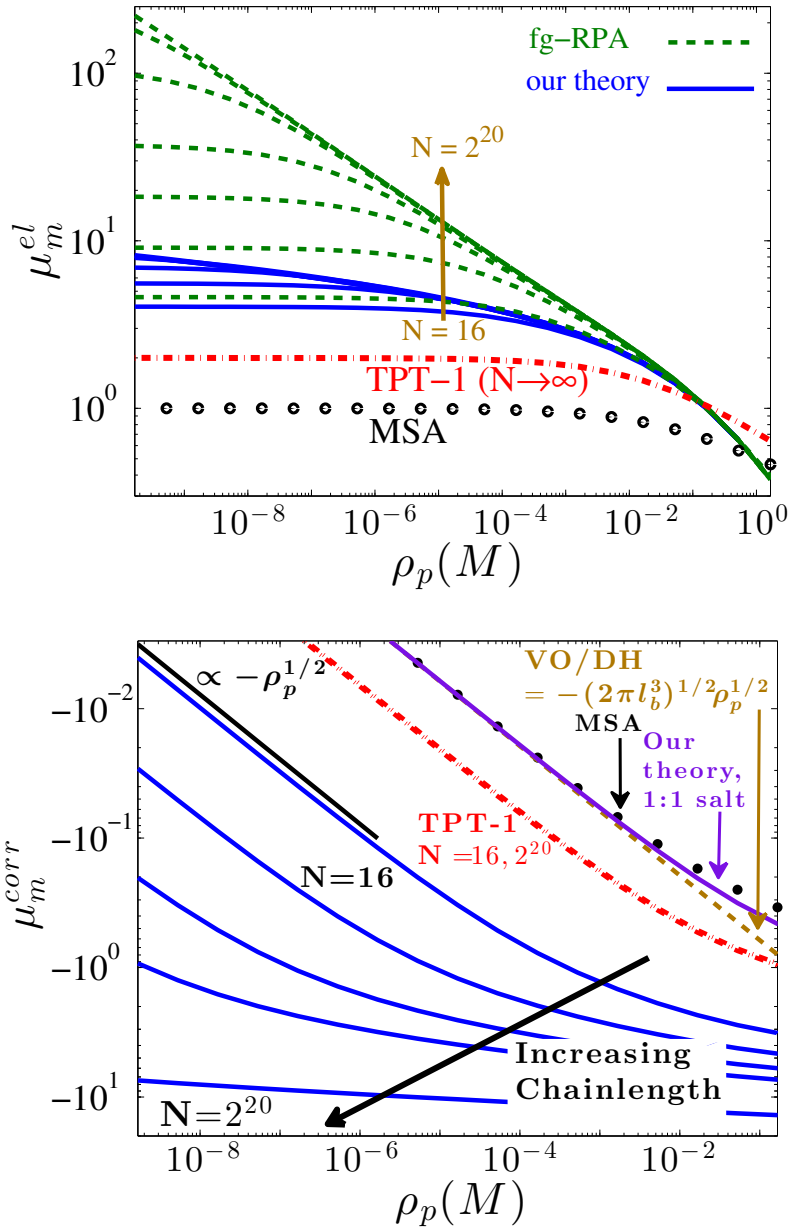

Figure 2.4: (a) Per-monomer total self energy μ_m^{el} of salt-free polyelectrolyte solutions, with parameters $l_b = 1, f = 1, z_p = 1$, comparing fg-RPA (dashed, green), RGF (solid, blue), MSA (dotted, black) and TPT-1 (dot-dashed, red) results. (b) Per-monomer correlation energy $\mu_m^{\text{corr}} = \mu_m^{el} - \mu_{m,0}^{el}$. In addition to MSA and TPT-1, we also plot the VO prediction using point-charge DH expression (dashed, brown), and our RGF theory for 1:1 salt (solid, purple). The fg-RPA correlation energy scales as $N^{1/2}$, and is omitted because it is not well-represented by the scales of the figure.

insensitive to chain structure, we conclude that the origin of this huge over-estimate of the self energy is the fg-RPA chain structure.

To understand the magnitude of the fg-RPA's over-estimate of the self energy, we consider the infinite-dilution limit. The self energy of a simple ion is the Born solvation energy given by $l_b/2a$, representing the work done against the dielectric background to assemble a charge into a region of size a. For polyelectrolytes, we expect the infinite-dilution per-monomer energy to be *higher* than the Born solvation energy of an isolated ion, due to the additional work (including chain elasticity) required to assemble multiple charges at finite separation from each other.

As confirmed in Section 2.4.1, the chain size of an isolated flexible polyelectrolyte scales linearly with chain length $R \sim N$. Elementary calculation of the energy of a line of charges gives an energy that scales as $\sim N \ln N$; as mentioned earlier in the context of our expression for the interaction energy Eq. (2.67), this is generally true of charges arranged in a structure that scales as $R \sim N$ for large N. Thus for flexible polyelectrolytes we expect that at infinite dilution, the per-monomer energy associated with connectivity grows logarithmically $\sim \ln N$.

In contrast, for a fixed-Gaussian structure $R \sim N^{1/2}$ and the infinite-dilution (chain) self energy scales as $\sim N^2/R \sim N^2/N^{1/2} \sim N^{3/2}$, leading to a per-monomer self energy that grows as $\sim N^{1/2}$. This is the origin of the rapidly diverging self energy in fg-RPA, and is attributed to the artificially compact conformation imposed by a fixed-Gaussian-chain structure. The self energies predicted by the fg-RPA at low concentrations lead to an artificially high driving force for phase separation into denser states. In contrast, our theory allows the chain conformation to relax, significantly reducing the self energy and increasing the stability of the single-phase region of a polyelectrolyte solution relative to fg-RPA theory.

For a constant dielectric background, the screening due to correlations (as a result of finite polymer concentration) reduces the amount of work required to assemble charge onto a chain, which we have defined as the self energy. The infinite-dilution self energy, then, contains information about the amount of correlation energy attributable to chain connectivity and provides an upper bound for its magnitude.

2.4.3.2 Electrostatic Correlation Energy

To isolate the correlation self energy μ_m^{corr} associated with finite concentrations of polyelectrolyte, for constant-dielectric backgrounds, it is most natural to subtract

out the infinite-dilution self energy $\mu^{el}_{m,0}$

$$\mu^{\text{corr}}_m = \mu^{el}_m - \mu^{el}_{m,0} \tag{2.68}$$

In the simple-electrolyte case, this is simply taking the single-ion Born solvation energy to be the reference energy, and is the usual reference used for studying simple electrolytes. For polyelectrolytes, however, one must be careful to subtract the infinite-dilution energy of an entire chain, not just the sum of the Born solvation energy of each of the charged monomers.

In Fig. 2.4b we plot the correlation energy μ^{corr}_m. For comparison we also plot the correlation energy results from the liquid-state integral equation Mean Spherical Approximation (MSA) theory of simple electrolytes, [20] TPT-1 chain perturbation theory, [20] the VO approximation, and our theory applied to 1:1 electrolytes. Here we focus on the behavior for our theory, and postpone comparison until Section 2.4.3.3.

At sufficiently low concentrations, our theory predicts a per-monomer correlation energy μ^{corr}_m that scales as $\sim (N\rho_p l_b)^{1/2} = (N^2 c_p l_b)^{1/2}$, where we remind the readers that ρ_p and c_p are the monomer and chain number densities, respectively. Comparison with the DH point charge result $\sim (z^2 c\ l_b)^{1/2}$ indicates that in sufficiently dilute solution, the correlations follow DH-scaling, with chains screening as N-valent ions – the entire chain behaves as a fundamental, N-valent screening unit. This is in accord with the dilute limit, renormalized-DH behavior of electrostatic fluctuations described by $G(k)$.

At first sight, this N-dependence may seem unusually strong. Examination of Fig. 2.4b shows that the dilute scaling quickly crosses over to a weaker concentration dependence at higher concentrations. The presence of a crossover is a generic feature of finite-sized charges, and is also present in the MSA theory for simple electrolytes and the RGF theory applied to simple electrolytes. However, the location of the crossover in simple electrolytes depends on the ion size a, which is much smaller than the size of a polyelectrolyte. As hinted by our examination of the chain structure and Green's function, the dilute solution DH behavior only persists while the chain size $R < \xi$, where ξ is some length scale that we attempt to identify below.

In general, the screening function $\tilde{\kappa}$ in our RGF theory is wavelength-dependent but, as demonstrated above in the dilute solution limit, DH behavior describes the thermodynamics, with an N-dependent screening constant $\kappa^2_{\text{N}} = 4\pi l_b \rho_p (1 + N)$, suggesting that the relevant length scale may be given by $\xi^{-2}_{\text{DH}} = \kappa^2_{\text{N}}$. Combined

with the dilute solution scaling $R \sim N$, the condition $R/\xi_{\mathrm{DH}} > 1$ is equivalent to $\rho_p < N^{-3} \equiv \rho_p^{*DH}$, which is the crossover scaling observed in Section 2.4.1 for the chain size. We note that this crossover scaling is in contrast to the physical overlap condition or "minimal" screening arguments that predict a crossover that scales as $\rho_p^* \sim N^{-2}$. [58] We leave the resolution of this discrepancy to future research.

Nevertheless, even if our RGF estimate of the location of crossovers is not accurate, the theory still reproduces the asymptotic limits in both dilute and semi-dilute solutions for the electrostatic correlations, both set by the scale of the infinite-dilution self energy. Thus the range of uncertainty in the intermediate concentrations is limited and we expect the theory to be able to reasonably describe the thermodynamic properties in this concentration range. The same cannot be said for the fg-RPA theory, which can severely overpredict correlations over a significant concentration range.

2.4.3.3 Comparison to Other Theories

We now compare our predictions for the correlation energy to other theories. Note that in Fig. 2.4b the fg-RPA results are not discussed because they are not well-represented on the axes used: the over-estimation of the correlation energy is too great.

As can be seen in Fig. 2.4b, classic VO theory approximates correlations with a solution of disconnected point charges using Debye-Hückel theory. DH theory predicts a self energy that scales linearly with the Debye screening constant $\kappa \sim \rho^{1/2}$ for all concentrations, without crossovers. Compared to our theory for polyelectrolytes, the VO theory underestimates correlations for most concentrations.

We also plot the MSA theory as an example of a liquid-state integral equation theory for the restricted primitive model of simple electrolytes, which accounts for ion size through a hard-core model. At low concentrations the integral equation theory matches the DH point charge theory; it is only at higher concentrations ($\kappa a > 1$) that there is a deviation, and correlations have a weaker concentration-dependence relative to the DH result. Recent polyelectrolyte theories that use integral equation results for the simple electrolyte [60] make the same VO approximation of treating the correlations with a solution of disconnected charges, and are expected to more or less coincide with the MSA results presented here. While for high concentrations the MSA correctly reduces correlations relative to point-charge VO, the lack of

any chain-length information means that the chain-length dependent crossover is completely neglected.

Thermodynamic perturbation theory (TPT-1) is an attempt at correcting for chain correlations by perturbing about liquid-state results for simple electrolytes. [20, 61] TPT-1 predicts a perturbation that grows with chain length as $\sim (N-1)/N$, [62] yielding a modest multivalency effect of chain-connectivity. However, the perturbation rapidly becomes insensitive to chain length. As shown in Fig. 2.4b, the TPT-1 results for chain lengths $N = 16$ and $N = 2^{20}$ are indistinguishable on the scale of the plot. Further, because the TPT-1 theory uses correlations of a simple electrolyte system, it is unable to capture the crossover behavior in the electrostatic correlations at low concentrations, an essential consequence of polymer chain connectivity. Instead, the crossover observed in TPT-1 theory is tied to the monomeric length-scale a.

2.4.4 Thermodynamics and Critical Point Behavior

The theory presented in this chapter is applicable to the study of the thermodynamics of general polyelectrolyte solutions, which will be the subject of future work. Below we illustrate its application to the osmotic coefficients and the critical properties for a fully charged ($f = 1$) salt-free polyelectrolyte solution with monovalent counterions.

With increasing chain length N, we expect the osmotic coefficient to become independent of N in semidilute solutions. The osmotic coefficient is defined as the ratio of the actual osmotic pressure of a solution to its ideal value (given by van't Hoff's law). For a salt-free polyelectrolyte solution with monovalent counterions, the osmotic coefficient is

$$\Phi = \frac{\Pi}{\rho_p + c_p} = \frac{\Pi}{\rho_p(1 + 1/N)} \tag{2.69}$$

In Fig. 2.5, we plot the RGF theory's predictions of Φ for salt-free polyelectrolyte solutions at $l_b = 1$, which can be seen to reproduce the expected convergence in the large-N limit. Our result for $N = 16$ is in good quantitative agreement with reported simulation data of salt-free polyelectrolyte solutions for that chain length. [63]

For large N, our predicted osmotic coefficient Φ exhibits a plateau at a value less than 1 over a wide range of concentration. (At sufficient dilution we expect Φ to return to 1.) Such a plateau is often interpreted as a signature of counterion condensation, which reduces the population of osmotically active counterions.[64] However, we believe that in our theory, the plateau is a reflection of the behavior of a semidilute

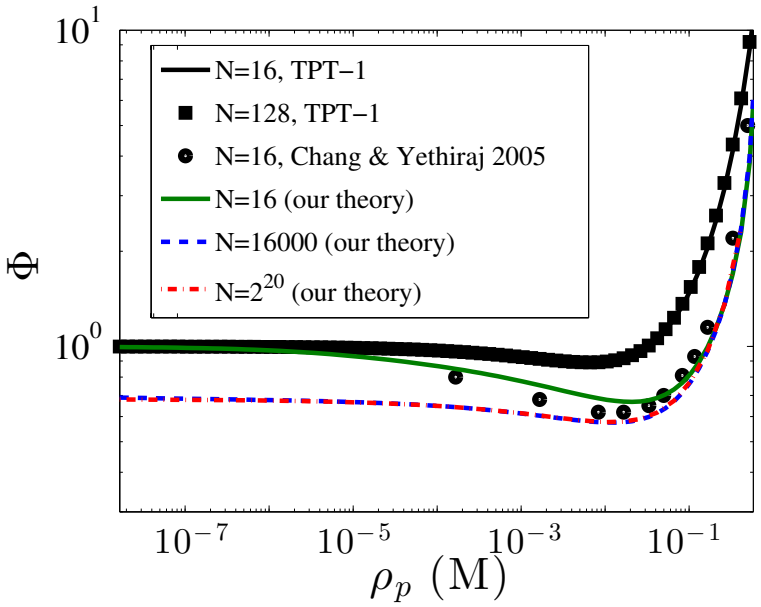

Figure 2.5: Osmotic coefficient $\Phi = \Pi/\rho_p(1 + 1/N)$ of salt-free polyelectrolyte solutions as a function of the monomer concentration ρ_p, with parameters $l_b = 1.0, f = 1, z_p = 1$. Our RGF results for $N = 16$ (solid, green) are shown in comparison with existing simulation data (circle, black).[63] In RGF theory, as the chain length increases the osmotic coefficients approach each other in semidilute solution ($N = 16000$ and $N = 2^{20}$ are nearly indistinguishable). TPT-1 underpredicts the chain-length dependence, with $N = 16$ (solid, black) nearly indistinguishable from $N = 128$ (squares, black).

solution of rods – we expect locally the chains to be stiff, up to some semidilute mesh size. Indeed, recently published work (without accounting for counterion condensation) found that infinite charged rods have a correlation energy that goes as $\sim \rho \ln \rho$, which serves to renormalize (reduce) the effective translational entropy of the counterions.[65] Such renormalization would lead the osmotic coefficient to exhibit a plateau at a value less than 1.

Importantly, though not obvious from the figure, it can be shown that at the presented $l_b = 1$, the solution remains stable against increased chain length. Our results are in contrast to those from the fg-RPA, where at any l_b, increasing the chain length will eventually turn the osmotic coefficient negative and drive the system to phase separation. [28] Lastly, although the TPT-1 involves a modest chain-length correction, it far underpredicts the dependence of correlations on chain length, reflecting its behavior for the self energy.

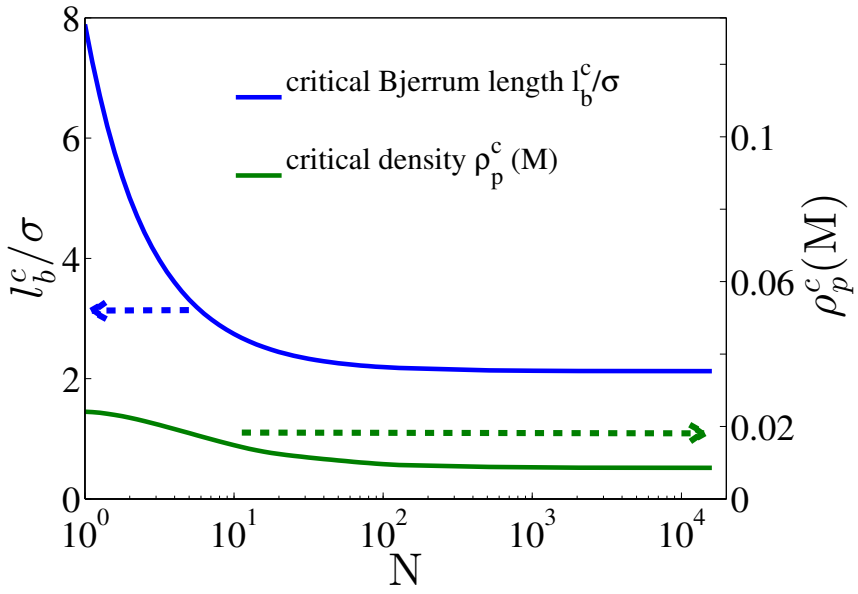

Figure 2.6: Chain-length dependence of the critical Bjerrum length ($\sim 1/T^c$) and critical concentration of salt-free polyelectrolyte solutions, with parameters $f = 1, z_p = 1$.

In Fig. 2.6, we plot the chain-length dependence of the critical Bjerrum length (~inverse temperature) l_b^c and critical monomer density ρ_p^c, for chain lengths up to $N = 10^4$. The predicted critical point appears insensitive to chain length for chain lengths $N \approx 30$; this insensitivity to chain length is in agreement with previous simulations and theories. [29, 30]

Previous literature suggested the origin of this critical behavior as either due to counterion condensation or other strong correlations on small length scales that cannot be accounted for by weak fluctuation theories.[29, 30] In contrast, our theory suggests that, in fact, accounting for chain conformational change is sufficient to explain the chain-length independence of the critical point of salt-free solutions of flexible polyelectrolytes. The conformational change is particularly important in dilute and low-concentration semidilute solution, where the unscreened Coulomb interactions can significantly distort the chain structure, and in doing so bound the correlation energy gain that drives phase separation. Application of the Gaussian chain structure at low concentrations drastically overestimates the correlation energy and hence the driving force for phase separation in salt-free solutions of flexible polyelectrolyte.

One might notice that the predicted critical Bjerrum length for long chains $l_b^c \approx 2$ is above 1 (the critical value for Manning condensation for $f = 1$) and hence expect counterion condensation to play a role in further stabilizing the dilute phase. [30] (At sufficiently large l_b, Brilliantov and coworkers [66, 67] showed that the chain can undergo a first-order coil-globule transition in a salt-free dilute solution. However, the value of l_b for such a transition is beyond the range of interest of our work in this chapter.) Although counterion condensation will undoubtedly further reduce the self energy, the magnitude of such reduction is still bounded by the same infinite-dilution self energy. Because the infinite-dilution self energy per monomer has only a weak dependence on the chain length (logarithmic vs. $N^{1/2}$ from fg-RPA), the energy range in the relevant range of the concentration where counterion condensation can play a role for large N in our theory is rather limited; we do not expect counterion condensation to substantially affect our conclusions. (In contrast, the magnitude of the counterion condensation contribution to the correlation energy would be much greater if the correlation energy followed the fg-RPA behavior. But even with the inclusion of counterion condensation, the fg-RPA theory does not predict the correct behavior of the critical properties without introducing additional modifications.)[29] Nevertheless, for quantitative prediction it would be important to account for counterion condensation, and this is planned for future work.

2.5 Conclusions

In this chapter, we have extended the field-theoretic renormalized Gaussian fluctuation (RGF) variational theory of simple electrolyte systems to systematically account for electrostatic fluctuations in polyelectrolytes. The key results of our theory can be summarized as follows:

1. Our theory *derives* a self-consistent procedure whereby electrostatic fluctuations characterized by G Eq. (2.43) are coupled to the intrachain structure and vice versa. The theory provides a unified framework for simultaneously describing the chain structure and thermodynamics in dilute *and* semidilute solutions.

2. Our theory correctly predicts the crossover from the $R \sim N$ scaling in the chain size to the $R \sim N^{3/5}$ scaling as a function of increasing salt in the single-chain limit. For finite concentrations of polyelectrolyte, the theory also predicts the dilute-limit scaling $R \sim N$ and the semidilute scaling $R \sim N^{1/2}$ in salt-free solutions.

3. The self-consistent procedure allows the clarification of the nature of screening, described by G. We confirm the screening behavior at long length scales, where the polyelectrolytes screen as polyvalent point charges, and at smaller length scales, where the charges on the polyelectrolyte chains behave as disconnected units (the VO limit). The onset and location of a peak in G is determined by the chain size, which is more accurately described by an adaptive chain structure.

4. Our theory features prominently the role of the polyelectrolyte self energy u_p, Eq. (2.51), which is the free energy of an independent chain interacting with itself through G, and is the work required to assemble charge onto a chain. The infinite-dilution self energy bounds the magnitude of connectivity contributions to the correlation energy, the latter tending to cancel out the former with increasing concentration.

5. We clarify that the correlation energy μ_m^{corr} is the difference of the self energy from its infinite-dilution value; μ_m^{corr} characterizes finite-concentration effects and reduces the self energy. With increasing polymer concentration, the correlation energy has a chain-size dependent crossover from a renormalized DH scaling in dilute solution to a weaker concentration dependence in the semidilute regime and beyond.

6. For salt-free polyelectrolyte solutions, we show that the chain structure can dramatically affect the self energy. By capturing the correct chain conformation in dilute and low-concentration semidilute solution, our theory correctly bounds the correlation energy and reproduces the N-insensitivity both in the osmotic coefficient in semidilute solution and the critical properties in the large-N limit.

We note that our physical picture of the self energy corroborates the self energy explanation used by some authors for "strong correlation" complexation. [68–70] These works treated polyelectrolyte complexation in the zero temperature limit where Coulomb interactions dominate. They identified the driving force for polyelectrolytes to aggregate into denser states as driven by a loss of an infinite-dilution self energy (which was estimated using the Coulomb energy of line charges $\sim N \log N$ per chain) upon entering a dense, neutralized state. Our theory works at finite temperature, and for a given concentration is able to *quantify* how much of the infinite-dilution self energy is lost. Being a weak coupling theory, our theory will

require further modification to include structures due to strong correlation effects, such as counterion condensation and ion-pairing.

The response of chain conformation to changing density is a key feature in our theory that is not present in theories of polyelectrolytes assuming fixed chain structures, such as fg-RPA [28, 29] or Ultra-Soft-Restricted-Primitive Model. [71, 72] Such theories predict, for Gaussian chains, spuriously strong N-dependencies of correlation energies, and this behavior is due to the failure of the assumed Gaussian structure at low concentrations. The fixed-Gaussian structure assumption artificially confines flexible chains to a radius that is too small by a factor of $\sqrt{N}$, thus raising the infinite-dilution self energy by the same factor. Thus, the fg-RPA theory predicts a higher infinite-dilution energy (which is a positive quantity), and there is correspondingly more electrostatic energy for the correlations (which contribute a negative energy) to reduce, leading to overestimations that persist into the semidilute regime. By a self-consistent determination of the single-chain structure, our theory avoids the artificially high energies appearing in the fg-RPA theory.

The self-consistency procedure derived in our theory is similar in spirit to sc-PRISM proposals [40] and the procedure employed by Donley et al,[37] all involving a single chain interacting through an effective pairwise additive interaction G. Indeed, our Green's function G would be the same as that prescribed by sc-PRISM theory if one used 1) the so-called "RPA" closure, [40, 73] 2) smeared charge distributions to regularize the electrostatic interactions, and 3) a commonly employed estimate of the medium-induced potential. [40, 74, 75] We note that Chandler demonstrated that RISM+RPA theory can be derived using a Gaussian Hamiltonian for density fluctuations, but no prescription was given on the self-consistent determination of a polymer's intrachain structure. [76]

A quantity of great interest for comparison with experimental scattering functions of polyelectrolyte solutions is the structure factor. Based on the similarity in G between our theory and the sc-PRISM+RPA theory, one might be tempted to assume the structure factor associated with our theory to be comparable to that of the sc-PRISM+RPA theory. However, we note that our theory is formulated without explicit density fields, and density is determined by conjugating an external field and taking the first functional derivative of the thermodynamic potential with respect to this field. It is thus most natural to calculate the structure factor using the conjugating field by taking the appropriate functional derivatives; this procedure is known to produce corrections that go beyond RPA,[27, 77] thus resulting in an improved

expression for the structure factor relative to sc-PRISM+RPA.

While in this chapter we have focused on linear homopolyelectrolyte solutions, our theory is applicable to general polyelectrolyte systems, such as polyelectrolyte coacervates, dendrimers, and gels. Promisingly, our theory gives a systematic framework for studying the impact of arbitrary polyelectrolyte architectures on electrostatic correlations, not achievable by many commonly-used theories of polyelectrolyte thermodynamics (i.e. TPT-1 and other theories that use the VO disconnected charges approximation). This feature of our theory is critical for advancing the theoretical design of novel polyelectrolyte materials, for which polymer architecture is a particularly important design parameter.

Finally, our theory retains many of the advantages of the original Gaussian variational theory applied to simple electrolytes, [14] providing a systematic framework for studying inhomogeneities in the dielectric medium and concentration profiles. Study of inhomogeneous systems will be the subject of future work.

BIBLIOGRAPHY

[1]D. T. Hallinan Jr, and N. P. Balsara, "Polymer electrolytes", Annu. Rev. Mater. Res. **43**, 503 (2013).

[2]C. Schmitt, and S. L. Turgeon, "Protein/polysaccharide complexes and coacervates in food systems", Adv. Colloid Interface Sci. **167**, 63 (2011).

[3]C. L. Ting, J. Wu, and Z.-G. Wang, "Thermodynamic basis for the genome to capsid charge relationship in viral encapsidation", P. Natl. Acad. Sci. USA **108**, 16986 (2011).

[4]D. S. Hwang, H. Zeng, A. Srivastava, D. V. Krogstad, M. Tirrell, J. N. Israelachvili, and J. H. Waite, "Viscosity and interfacial properties in a mussel-inspired adhesive coacervate", Soft Matter **6**, 3232 (2010).

[5]F. Pittella, and K. Kataoka, *Polymeric micelles for sirna delivery* (Springer, 2013), p. 161.

[6]D. W. Pan, and M. E. Davis, "Cationic mucic acid polymer-based sirna delivery systems", Bioconjugate Chem. **26**, 1791 (2015).

[7]K. A. Black, D. Priftis, S. L. Perry, J. Yip, W. Y. Byun, and M. Tirrell, "Protein encapsulation via polypeptide complex coacervation", ACS Macro Lett. **3**, 1088 (2014).

[8]M. A. Cohen Stuart, W. T. Huck, J. Genzer, M. Müller, C. Ober, M. Stamm, G. B. Sukhorukov, I. Szleifer, V. V. Tsukruk, and M. Urban, "Emerging applications of stimuli-responsive polymer materials", Nat. Mater. **9**, 101 (2010).

[9]G. S. Manning, "Limiting laws and counterion condensation in polyelectrolyte solutions i. colligative properties", J. Chem. Phys. **51**, 924 (1969).

[10]H. Bungenberg de Jong, and H. Kruyt, "Coacervation (partial miscibility in colloid systems)", P. K. Ned. Akad. Wetensc. **32**, 849 (1929).

[11]D. Priftis, N. Laugel, and M. Tirrell, "Thermodynamic characterization of polypeptide complex coacervation", Langmuir **28**, 15947 (2012).

[12]J. T. G. Overbeek, and M. J. Voorn, "Phase separation in polyelectrolyte solutions. theory of complex coacervation", J. Cell Compar. Phys. **49**, 7 (1957).

[13]P. Debye, and E. Hückel, "De la théorie des électrolytes. i. abaissement du point de congélation et phénomènes associés", Phys. Zeitschrift **24**, 185 (1923).

[14]Z.-G. Wang, "Fluctuation in electrolyte solutions: the self energy", Phys. Rev. E **81**, 021501 (2010).

[15]L. Blum, Y. V. Kalyuzhnyi, O. Bernard, and J. N. Herrera-Pacheco, "Sticky charged spheres in the mean-spherical approximation: a model for colloids and polyelectrolytes", J. Phys. Condens. Matter **8**, A143 (1996).

[16]I. Protsykevytch, Y. Kalyuzhnyi, M. Holovko, and L. Blum, "Ion-ion, ion-solvent and solvent-solvent interactions in electrolyte solutions: solution of the polymer mean spherical approximation for the totally flexible sticky two-point electrolyte model", J. Mol. Liq. **73**, 1 (1997) http://dx.doi.org/10.1016/S0167-7322(97)00053-6.

[17]O. Bernard, and L. Blum, "Thermodynamics of a model for flexible polyelectrolytes in the binding mean spherical approximation", J. Chem. Phys. **112**, 7227 (2000) http://dx.doi.org/10.1063/1.481287.

[18]N. von Solms, and Y. C. Chiew, "Analytical integral equation theory for a restricted primitive model of polyelectrolytes and counterions within the mean spherical approximation. i. thermodynamic properties", J. Chem. Phys. **111**, 4839 (1999) http://dx.doi.org/10.1063/1.479246.

[19]N. von Solms, and Y. C. Chiew, "A model for polyelectrolytes", J. Stat. Phys. **100**, 267 (2000) 10.1023/A:1018652031157.

[20]J. Jiang, L. Blum, O. Bernard, and J. M. Prausnitz, "Thermodynamic properties and phase equilibria of charged hard sphere chain model for polyelectrolyte solutions", Mol. Phys. **99**, 1121 (2001).

[21]Z. Li, and J. Wu, "Density functional theory for planar electric double layers: closing the gap between simple and polyelectrolytes", J. Phys. Chem. B **110**, 7473 (2006) 10.1021/jp060127w.

[22]Z. Li, and J. Wu, "Density functional theory for polyelectrolytes near oppositely charged surfaces", Phys. Rev. Lett. **96**, 048302 (2006) 10.1103/PhysRevLett.96.048302.

[23]T. Jiang, Z.-G. Wang, and J. Wu, "Electrostatic regulation of genome packaging in human hepatitis b virus", Biophys. J. **96**, 3065 (2009) http://dx.doi.org/10.1016/j.bpj.2009.01.009.

[24]L. Wang, H. Liang, and J. Wu, "Electrostatic origins of polyelectrolyte adsorption: theory and monte carlo simulations", J. Chem. Phys. **133**, 044906, 044906 (2010).

[25]V. Y. Borue, and I. Y. Erukhimovich, "A statistical theory of weakly charged polyelectrolytes: fluctuations, equation of state and microphase separation", Macromolecules **21**, 3240 (1988).

[26]A. Khokhlov, and K. Khachaturian, "On the theory of weakly charged polyelectrolytes", Polymer **23**, 1742 (1982).

[27]M. Castelnovo, and J.-F. Joanny, "Complexation between oppositely charged polyelectrolytes: beyond the random phase approximation", Eur. Phys. J. E **6**, 377 (2001).

[28]K. A. Mahdi, and M. O. de la Cruz, "Phase diagrams of salt-free polyelectrolyte semidilute solutions", Macromolecules **33**, 7649 (2000).

[29]A. V. Ermoshkin, and M. Olvera de la Cruz, "A modified random phase approximation of polyelectrolyte solutions", Macromolecules **36**, 7824 (2003).

[30]G. Orkoulas, S. K. Kumar, and A. Z. Panagiotopoulos, "Monte carlo study of coulombic criticality in polyelectrolytes", Phys. Rev. Lett. **90**, 048303 (2003).

[31]G. Fredrickson, *The equilibrium theory of inhomogeneous polymers* (Oxford University Press, USA, 2013).

[32]Q. Wang, T. Taniguchi, and G. H. Fredrickson, "Self-consistent field theory of polyelectrolyte systems", J. Phys. Chem. B **108**, 6733 (2004).

[33]M. Muthukumar, and S. Edwards, "Extrapolation formulas for polymer solution properties", J. Chem. Phys. **76**, 2720 (1982).

[34]M. Muthukumar, "Double screening in polyelectrolyte solutions: limiting laws and crossover formulas", J. Chem. Phys. **105**, 5183 (1996).

[35]D. Frydel, "Introduction to statistical field theory: from a toy model to a one-component plasma", Eur. J. Phys. **36**, 065050 (2015).

[36]C.-Y. Shew, and A. Yethiraj, "Self-consistent integral equation theory for semiflexible chain polyelectrolyte solutions", J. Chem. Phys. **113**, 8841 (2000).

[37]J. P. Donley, J. Rudnick, and A. J. Liu, "Chain structure in polyelectrolyte solutions at nonzero concentrations", Macromolecules **30**, 1188 (1997).

[38]I. I. Potemkin, and V. V. Palyulin, "Complexation of oppositely charged polyelectrolytes: effect of discrete charge distribution along the chain", Phys. Rev. E **81**, 041802 (2010).

[39]C.-Y. Shew, and A. Yethiraj, "Monte carlo simulations and self-consistent integral equation theory for polyelectrolyte solutions", J. Chem. Phys. **110**, 5437 (1999).

[40]A. Yethiraj, "Theory for chain conformations and static structure of dilute and semidilute polyelectrolyte solutions", J. Chem. Phys. **108**, 1184 (1998).

[41]M. Manghi, and R. R. Netz, "Variational theory for a single polyelectrolyte chain revisited", Eur. Phys. J. E **14**, 67 (2004).

[42]H. Li, and T. Witten, "Fluctuations and persistence length of charged flexible polymers", Macromolecules **28**, 5921 (1995).

[43]J.-L. Barrat, and J.-F. Joanny, "Persistence length of polyelectrolyte chains", Europhys. Lett. **24**, 333 (1993).

[44]T. Hofmann, R. Winkler, and P. Reineker, "Self-consistent integral equation theory for solutions of finite extensible semiflexible polyelectrolyte chains", J. Chem. Phys. **118**, 6624 (2003).

[45]A. J. Spakowitz, and Z.-G. Wang, "End-to-end distance vector distribution with fixed end orientations for the wormlike chain model", Phys. Rev. E **72**, 041802 (2005) 10.1103/PhysRevE.72.041802.

[46]A. V. Ermoshkin, A. N. Kudlay, and M. Olvera de la Cruz, "Thermoreversible crosslinking of polyelectrolyte chains", J. Chem. Phys. **120**, 11930 (2004).

[47]R. R. Netz, and D. Andelman, "Neutral and charged polymers at interfaces", Phys. Rep. **380**, 1 (2003).

[48]P. G. De Gennes, P. Pincus, R. M. Velasco, and F. Brochard, "Remarks on polyelectrolyte conformation", J. Phys. France **37**, 1461 (1976).

[49]M. J. Stevens, and K. Kremer, "The nature of flexible linear polyelectrolytes in salt free solution: a molecular dynamics study", J. Chem. Phys. **103**, 1669 (1995).

[50]P. K. Jha, F. J. Solis, J. J. de Pablo, and M. O. de la Cruz, "Nonlinear effects in the nanophase segregation of polyelectrolyte gels", Macromolecules **42**, 6284 (2009).

[51]J. F. Marko, and E. D. Siggia, "Stretching dna", Macromolecules **28**, 8759 (1995).

[52]P. J. Flory, *Principles of polymer chemistry* (Cornell University Press, 1953).

[53]D. Yang, and Q. Wang, "Unified view on the mean-field order of coil-globule transition", ACS Macro Lett. **2**, 952 (2013).

[54]O. Ptitsyn, and I. Eizner, "The theory of helix-coil transitions in macromolecules", Biofizika **10**, 3 (1965).

[55]P. G. De Gennes, "Collapse of a polymer chain in poor solvents", J. Phys. Lett. Paris **36**, 55 (1975).

[56]L. D. Landau, E. Lifshitz, and L. Pitaevskii, *Electrodynamics of continuous media*, trans. by J. Bell, M. Kearsley, and J. Sykes, 2nd ed., Vol. 8 (Pergamon Press, 1984).

[57]A. V. Dobrynin, and M. Rubinstein, "Theory of polyelectrolytes in solutions and at surfaces", Prog. Polym. Sci. **30**, 1049–1118 (2005).

[58]A. V. Dobrynin, R. H. Colby, and M. Rubinstein, "Scaling theory of polyelectrolyte solutions", Macromolecules **28**, 1859 (1995).

[59]N. V. Brilliantov, "Accurate first-principle equation of state for the one-component plasma", Contrib. Plasm. Phys. **38**, 489 (1998).

[60]C. E. Sing, J. W. Zwanikken, and M. O. de la Cruz, "Interfacial behavior in polyelectrolyte blends: hybrid liquid-state integral equation and self-consistent field theory study", Phys. Rev. Lett. **111**, 168303 (2013).

[61]M. Wertheim, "Fluids with highly directional attractive forces. ii. thermodynamic perturbation theory and integral equations", J. Stat. Phys. **35**, 35 (1984).

[62]Y. Zhou, and G. Stell, "Chemical association in simple models of molecular and ionic fluids. iii. the cavity function", J. Chem. Phys. **96**, 1507 (1992).

[63]R. Chang, and A. Yethiraj, "Osmotic pressure of salt-free polyelectrolyte solutions: a monte carlo simulation study", Macromolecules **38**, 607 (2005).

[64]Q. Liao, A. V. Dobrynin, and M. Rubinstein, "Molecular dynamics simulations of polyelectrolyte solutions: osmotic coefficient and counterion condensation", Macromolecules **36**, 3399 (2003).

[65]J. Qin, and J. J. de Pablo, "Criticality and connectivity in macromolecular charge complexation", Macromolecules **49**, 8789 (2016).

[66]N. V. Brilliantov, D. V. Kuznetsov, and R. Klein, "Chain collapse and counterion condensation in dilute polyelectrolyte solutions", Phys. Rev. Lett. **81**, 1433 (1998).

[67]A. M. Tom, S. Vemparala, R. Rajesh, and N. V. Brilliantov, "Mechanism of chain collapse of strongly charged polyelectrolytes", Phys. Rev. Lett. **117**, 147801 (2016).

[68]E. M. Mateescu, C. Jeppesen, and P. Pincus, "Overcharging of a spherical macroion by an oppositely charged polyelectrolyte", Europhys. Lett. **46**, 493 (1999).

[69]R. Zhang, and B. Shklovskii, "Phase diagram of solution of oppositely charged polyelectrolytes", Physica A **352**, 216 (2005).

[70]A. Y. Grosberg, T. T. Nguyen, and B. I. Shklovskii, "*Colloquium* : the physics of charge inversion in chemical and biological systems", Rev. Mod. Phys. **74**, 329 (2002).

[71]D. Coslovich, J.-P. Hansen, and G. Kahl, "Ultrasoft primitive model of polyionic solutions: structure, aggregation, and dynamics", J. Chem. Phys. **134**, 244514 (2011).

[72]P. B. Warren, and A. J. Masters, "Phase behaviour and the random phase approximation for ultrasoft restricted primitive models", J. Chem. Phys. **138**, 074901 (2013).

[73]K. S. Schweizer, and A. Yethiraj, "Polymer reference interaction site model theory: new molecular closures for phase separating fluids and alloys", J. Chem. Phys. **98**, 9053 (1993).

[74]C. J. Grayce, and K. S. Schweizer, "Solvation potentials for macromolecules", J. Chem. Phys. **100**, 6846 (1994).

[75]C. J. Grayce, A. Yethiraj, and K. S. Schweizer, "Liquid-state theory of the density dependent conformation of nonpolar linear polymers", J. Chem. Phys. **100**, 6857 (1994).

[76]D. Chandler, "Gaussian field model of fluids with an application to polymeric fluids", Phys. Rev. E **48**, 2898 (1993).

[77]B. P. Lee, and M. E. Fisher, "Density fluctuations in an electrolyte from generalized debye-hückel theory", Phys. Rev. Lett. **76**, 2906 (1996) 10.1103/PhysRevLett.76.2906.

Chapter 3

POLYELECTROLYTE PHASE BEHAVIOR

Using a recently developed renormalized Gaussian fluctuation (RGF) field theory that self-consistently accounts for the concentration-dependent coupling between chain structure and electrostatic correlations, we study the phase behavior of polyelectrolyte solutions, with a focus on the effects of added salts and chain structure. For solutions of a single polyelectrolyte species plus salt, the RGF theory predicts the existence of a loop in the phase boundary at Bjerrum lengths (inverse temperature) below (above) the critical value of the salt-free system. This loop behavior can occur at electrostatic interaction strengths l_b/b at which the loop no longer exists for the TPT-1 theory, and at fixed l_b/b the loop can persist for infinitely long chains, in contrast to theories using a fixed-Gaussian structure (fg-RPA). For systems of oppositely charged (but otherwise symmetric) chains, we again find that the fg-RPA greatly over-predicts the driving force for phase separation, especially at higher charge fractions (but still below the critical Manning charge density). In general, stiff chains have a narrower two-phase region than intrinsically-flexible chains, although intrinsically flexible chains can still experience a local stiffening which persists in semidilute solution; for higher charge fractions the local stiffening of flexible chains is crucial for reproducing qualitatively correct thermodynamics and phase diagrams. For fully charged flexible chains, we find that phase diagrams are quite similar to those for semiflexible rods, and that it is possible to capture the coacervate phase diagrams of the full self-consistent calculations using a constant, renormalized chain stiffness.

This chapter includes content from our previously published article:

[1] K. Shen, and Z.-G. Wang, "Polyelectrolyte chain structure and solution phase behavior", Macromolecules **51**, 1706–1717 (2018) DOI:10.1021/acs.macromol.7b02685.

3.1 Introduction

Polyelectrolytes are commonly found in both natural [1–5] and synthetic [6–12] polymer systems. Many applications (i.e. food, [4, 13, 14] pharmaceutical, [15–21] adhesives [8, 22–25]) of polyelectrolytes rely on their propensity to phase separate

into complexes, which can be fluid or solid, microscopic or macroscopic, and can often be structured. [20, 21, 26–29] In this chapter we focus on the electrostatic-correlation-induced liquid-liquid phase separation of polyelectrolytes in water or other polar solvent.

Electrostatic correlations in polyelectrolyte solutions continue to attract considerable theoretical efforts, as summarized in recent reviews.[28–30] One class of theories follows the spirit of Voorn and Overbeek (VO), and begins with a physical picture where the electrostatic correlations are based on an equivalent solution of disconnected charges. [31] The original VO work used the Debye-Hückel free energy density[32] for the electrostatic correlation, while more recent work use more detailed thermodynamic models of simple electrolytes,[33] or include the leading connectivity effects via a first-order thermodynamic perturbation (TPT-1) about the simple electrolyte reference.[34–39]

Another class of theories attempts to account for chain connectivity from the outset. [40–47] These theories use chain density correlation functions to characterize connectivity effects on electrostatic fluctuations. In the most basic form,[40, 44, 45] most commonly applied to flexible chains, a fixed, Gaussian chain structure (hereafter referred to as fg-RPA for fixed-Gaussian random phase approximation) is assumed for all concentrations. This approximation is only valid when the chain density is above $\rho^* b^3 \sim (l_b f^2/b)^{1/3}$,[40] where l_b/b characterizes the strength of electrostatic interactions and is $O(1)$ for typical aqueous solutions. At a modest charge fraction $f \lesssim 1$ where no Manning condensation occurs, this condition requires very high densities $\rho^* b^3 \approx 1$.

For typical systems, the fg-RPA approximation greatly overestimates the correlation contribution to the free energy, especially at low concentrations.[46] One insightful attempt to correct the failings of the fg-RPA recognized that fluctuations in fg-RPA are treated improperly on short length scales. However, rather than tackling the root problem associated with the chain structure, this "modified RPA theory" advocated for completely suppressing the short length scale fg-RPA fluctuations through the use of *ad hoc* cutoffs. [46] Another theory that is shown to yield significantly improved predictions of the critical parameters and osmotic coefficients was based upon decomposing the system into two one-component plasmas [48, 49] and using a neutral semi-dilute solution as the reference structure factor. [43]

We recently proposed a renormalized Gaussian fluctuation (RGF) theory using a *variational*, non-perturbative framework, that naturally prescribes a self-consistent

calculation of the chain structure. [50] In light of the RGF theory, many qualitative shortcomings of the VO, TPT-1, and fg-RPA theories have been demonstrated to be connected to their incorrect treatment of the chain structure. [50] The RGF was shown to correctly capture the crossovers in overall chain scaling as function of salt and polymer concentration, similar to some previous work that self-consistently accounted for the concentration-dependence of chain structure. [50–57]

Using the RGF we further elucidated the effects of conformation-concentration coupling on thermodynamics. A key observation was that the electrostatic correlation per monomer for linear flexible chains can, at most, increase logarithmically in chain length (stemming from the electrostatic energy of a linear object, which scales as $\ln N$ per unit length). A consequence of capturing this expected N-dependence is that, when applied to salt-free solutions of a single polyelectrolyte species, the RGF correctly predicts that there exists a critical Bjerrum length below which the solution is stable for all chain lengths, in agreement with simulations [58] and in *qualitative* contrast to the prediction from the fg-RPA theory. Below this critical Bjerrum length, the entropic penalty of partitioning counterions to a dense phase is too great for any chain length to overcome.

In this chapter, we apply the RGF to study the influence of added salt on the phase behavior of polyelectrolyte systems, with a focus on the role of the chain structure. An important conclusion is that small wavelength fluctuations are highly coupled to the chain structure at short length scales; stiff chains (semiflexible rods) have lower correlation energies and consequently narrower two-phase regions than flexible chains. Although in semidilute or high-salt solutions flexible polyelectrolytes are overall Gaussian, we find that their phase behavior is nevertheless much closer to that of semiflexible rods than that of ideal Gaussian chain. By renormalizing the chain structure, the RGF properly treats fluctuations on intrachain length scales and naturally suppresses the higher-wavenumber fluctuation modes without the introduction of an artificial cut-off as in “modified RPA". Thus, our theory can treat systems across a significantly wider density window and, importantly, can treat systems at much higher charge densities (up to $l_b f/b \simeq 1$) than previously possible with the commonly used fg-RPA theory or any other field theories that involve a bare Gaussian chain structure approximation. While we would have liked to compare the RGF to predictions from the “modified RPA” theory, the latter was developed and illustrated only for salt-free polyelectrolyte solutions, and no attempt was made to give a quantitative estimate of the cutoff nor to generalize the single cut-off

to solutions with multiple polyelectrolytes or small ions, making fair quantitative comparisons difficult. We thus do not attempt to compare the RGF to the "modified RPA."

The rest of the chapter is organized as follows. In Section 3.2 we present the essential results of the RGF relevant to bulk solutions. In Section 3.3 we examine the phase behavior of solutions of a single polyelectrolyte species, while in Section 3.4 we consider solutions with symmetric, oppositely charged polyelectrolytes. In both sections we compare phase diagrams predicted by the RGF for flexible chains with self-consistent chain structure to diagrams predicted for chains with fixed-Gaussian and semiflexible-rod structures. We follow in Section 3.5 by discussing the renormalization of chain structure and its effect on correlation energies. Finally, in Section 3.6 we conclude with a summary of the key results.

3.2 Theory

Although the RGF can be derived very generally for arbitrary polyelectrolytes and for inhomogeneous systems, we recapitulate only the key results relevant for discussion of bulk solution thermodynamics. We consider a general system with five species: neutral solvent, symmetric and oppositely charged salt ions (±), and symmetric polyelectrolytes ($p\pm$) of chain length N, with a fraction f of evenly-spaced, discrete charges. Systems having fewer components are just the special cases where one or more species are absent. For simplicity, all monomers are taken to have the same volume v, and Kuhn length of the polymer is taken to be $b = 1$, thus setting the unit of length.

The first subsection outlines the theory, introducing the renormalized Gaussian fluctuation theory and the self-consistent single-chain partition function of a flexible chain. The second subsection describes a second variational calculation used to estimate the single-chain partition function. For the full derivation and further details, we refer interested readers to our previous publication.[50]

3.2.1 Renormalized Gaussian Fluctuation (RGF) Theory

The main interaction considered in our system is the electrostatic interaction, which we model as taking place in a linear dielectric medium with constant scaled electric permittivity $\epsilon = \varepsilon/(\beta e^2)$. To simplify notation, we will use k_BT as the unit of energy and e as the unit of charge, so we set $\beta = 1$ and $e = 1$.

Individual monomeric charges are modeled with a short-ranged charge distribution

$z\,h(\mathbf{r}-\mathbf{r}')$ for a charged monomer of valence z located at $\mathbf{r}'$. The charge distribution is chosen to be a Gaussian with a radius a (not necessarily the same as the excluded volume size, but for simplicity we take $a = 0.5$ in this chapter). This smearing captures the Born solvation energy of individual ions in a dielectric medium, and produces finite-size corrections to the ion correlation energy. [50, 59]

The excluded volume between all species is accounted for by an incompressibility constraint $\sum_\gamma \hat{\phi}_\gamma(\mathbf{r}) = 1$ applied at all $\mathbf{r}$.[60] We express the constraint with a Dirac δ-function in its Fourier representation, $\delta\left(1-\sum_\gamma \hat{\phi}_\gamma\right) = \int \mathcal{D}\eta e^{i\eta(1-\sum_\gamma \hat{\phi}_\gamma)}$, introducing the incompressibility field η. The volume fraction operator $\hat{\phi}_\gamma$ is related to the monomer density operator via $\hat{\phi}_\gamma = v_\gamma \hat{\rho}_\gamma$, where v_γ is the monomer volume of species γ.

Finally, the chain connectivity and conformation degrees of freedom of the polyelectrolytes are accounted for by the bonding interaction modeled by the Hamiltonian H_B, which depends on the relative positions of the monomers in a polyelectrolyte chain. To focus on electrostatics we ignore other interactions such as the Flory-Huggins interaction.

Using the defined interactions, it is straightforward to write the corresponding field-theoretic, grand canonical partition function using standard field-theoretic identity transformations,[60] which introduces a fluctuating electrostatic potential field Ψ.[50] We approximate this partition function using the RGF procedure, which is *non-perturbative*. The RGF theory follows the Gibbs-Feynman-Bogoliubov[59] variational procedure and introduces a Gaussian reference action with a Green's function G characterizing the field fluctuations about a mean $-i\psi$; ψ and G are determined self-consistently by the RGF variational condition (for further discussion of the RGF see Ch. 5). (We note that there is a closely-related self-consistent approach that yields slightly different self-consistent equations, called the Gaussian equivalent representation (GER), first developed for quantum physics[61] and later applied to study thermodynamics[62–64] and conformational changes in polyelectrolyte solutions.[65])

To focus on the electrostatic field fluctuations, we perform the variational calculation only for the Ψ field; the excluded volume interaction will be treated at the mean-field level by the saddle-point approximation for the η field. If one formulated a full variational action that also considered fluctuations of the η field, with additional variational Green's functions characterizing such fluctuations, one would reproduce excluded volume fluctuations, leading to what is termed double-screening.[52]

Nevertheless, although our restricted electrostatic fluctuation theory does not have excluded volume screening, it was previously shown to correctly give self-avoiding-walk statistics and random walk statistics for the overall polymer conformation of isolated chains and semidilute solutions, respectively.[50]

The saddle-point condition for η leads to a pure imaginary value, so we henceforth define a real field $\mathcal{P} = i\eta$ satisfying:

$$\mathcal{P} = -\frac{1}{v}\log(1-\phi) \tag{3.1}$$

for the incompressibility condition, where ϕ is the total volume fraction $\phi = \sum_{\gamma \neq solv} v_\gamma \rho_\gamma$ of non-solvent species.

The RGF variational condition applied to ψ yields a charge neutrality condition and will not be further discussed. Meanwhile, the variational condition for $\tilde{G}(k)$ is expressed conveniently in Fourier space

$$\tilde{G}(k) = \frac{1}{\epsilon[k^2 + \tilde{\kappa}^2(k)]}, \tag{3.2}$$

from which we identify $\tilde{\kappa}^2(k) = 2\tilde{I}(k)/\epsilon$ as the *wavevector-dependent* screening *function*, a generalization of the Debye screening constant, with the ionic strength function $\tilde{I}(k)$ given by

$$2\tilde{I}(k) = \sum_\gamma \frac{\rho_\gamma}{N_\gamma}\tilde{S}_\gamma^{chg}(k) \tag{3.3}$$

where $\tilde{S}_\gamma^{chg}(k)$ is the *single-molecule* charge structure factor.

In our spread-charge model, even simple salt ions can have internal charge structure

$$\tilde{S}_\pm^{\mathrm{chg}} = z_\pm^2 \tilde{h}_\pm^2(k). \tag{3.4}$$

The single-chain charge structure factor for a polyelectrolyte with discrete charges is

$$\begin{aligned}\tilde{S}_{p\pm}^{\mathrm{chg}}(k) = &\sum_l z_{pl}^2 \tilde{h}_{pl}^2(k) \\ &+ \sum_l \sum_{m\neq l} z_{pl}\tilde{h}_{pl}(k) z_{pm}\tilde{h}_{pm}(-k)\tilde{\omega}_{lm}(k).\end{aligned} \tag{3.5}$$

The first sum is the $l = m$ self piece, and the second sum is over all other pairs. The structure is characterized by the intramolecular correlation $\tilde{\omega}_{lm}$ between two

monomers l and m on the same chain. [66] In general, $\tilde{\omega}_{lm}(k) \to 1$ as $k \to 0$, and $\tilde{\omega}_{lm}(k) \to 0$ for $k \gg 1/a$.

The structure factors $\tilde{S}^{\mathrm{chg}}(k)$ are obtained from differentiation of the single-particle/chain partition functions, which are:

$$\begin{aligned}
\langle Q_{\pm} \rangle &= V e^{-v_{\pm}\mathcal{P} - z_{\pm}\psi} q_{\pm} \\
q_{\pm} &= e^{-\frac{1}{2}\int d\mathbf{r} d\mathbf{r}'\ z_{\pm} h_{\pm} * G * z_{\pm} h_{\pm}} \\
\left\langle Q_{p\pm} \right\rangle &= V e^{-N_p v_p \mathcal{P} - z_{p\pm}^{tot}\psi} q_{p\pm} \\
q_{p\pm} &= \frac{1}{V}\int \mathcal{DR}\ e^{-H_B - \frac{1}{2}\int d\mathbf{r} d\mathbf{r}'\ \hat{\rho}_{p1}^{\mathrm{chg}} \cdot G \cdot \hat{\rho}_{p1}^{\mathrm{chg}}}
\end{aligned} \tag{3.6}$$

Note that the electrostatic partition functions q_γ feature $G(\mathbf{r}, \mathbf{r}')$ as a fluctuation-mediated, effective intra-molecular interaction, and is missing in self-consistent mean-field theories. This effective interaction is what allows chain structure to adapt to solution conditions.

The per-ion and per-*chain* chemical potentials are given as:

$$\begin{aligned}
\mu_{\pm} &= \ln(\rho_{\pm} v_{\pm}) + v_{\pm}\mathcal{P} + z_{\pm}\psi + u_{\pm} \\
\mu_{p\pm} &= \ln\left(\frac{\rho_p v_p}{N_p}\right) + v_p N_p \mathcal{P} + z_{p\pm}^{tot}\psi + u_{p\pm}
\end{aligned} \tag{3.7}$$

The first three terms in both chemical potential expressions Eq. (3.7) are the same as in a mean-field analysis of a bulk solution. The last terms u_γ are the self energies

$$u_\gamma = -\ln q_\gamma. \tag{3.8}$$

The self energy represents the free energy of an entity (an ion, or a polyelectrolyte chain) interacting with itself via the effective potential G, and reflects the effect of electrostatic correlations. We also define the average self energy per monomer (subscript 'm' for 'monomer') as

$$\mu_m^{el} \equiv \frac{u_{p\pm}}{N_p}. \tag{3.9}$$

Finally, the osmotic pressure is

$$\begin{aligned}
\Pi = &-\frac{1}{4\pi^2}\int_0^\infty k^2\ dk \left[\ln\left(1 + \frac{\tilde{\kappa}^2(k)}{k^2}\right) - \frac{\tilde{\kappa}^2(k)}{k^2 + \tilde{\kappa}^2(k)}\right] \\
&- \frac{1}{v}\left(1 + \log(1-\phi)\right) + \frac{1-\phi}{v} + \rho_{\pm} + \frac{\rho_{p\pm}}{N_p}
\end{aligned} \tag{3.10}$$

where the abbreviations $\rho_\pm$ and $\rho_{p\pm}$ are shorthand for summing over both positively and negatively charged species.

The exact evaluation of single-chain partition functions is difficult even for simpler pair interactions, and in general can be done by numerical simulation. [67] In Sec. 3.2.2 we describe an approximate scheme for calculating $\langle Q_p \rangle$ and $\tilde{S}_p^{\text{chg}}$, but such an approximation is not inherent to the general theory.

3.2.2 Calculation of Chain Structure Factor

For our specified model of flexible chains with fraction f of discrete charges of valence z_p, we write the charge structure factor as

$$\tilde{S}_p^{\text{chg}}(k) = z_{p\pm}^2 N f[1 + (Nf - 1)\tilde{\omega}(k)]\tilde{h}_p^2(k) \tag{3.11}$$

where we have re-expressed the sum over all monomer-monomer pair correlations $\tilde{\omega}_{lm}$ with an average per-monomer structure $\tilde{\omega}$.

Instead of performing a full simulation to calculate $\tilde{S}$, we perform a variational calculation[50] by decomposing the single-chain free energy u_p into entropic F_{ent} and interaction F_{int} contributions, parameterized by an effective persistence length l_{eff}, which controls the chain expansion

$$\alpha^2 = \langle R_{ee}^2 \rangle / R_{ee,0}^2 = 2(l_{\text{eff}}/b)\left[1 - (l_{\text{eff}}/Nb)\left(1 - e^{-Nb/l_{\text{eff}}}\right)\right]. \tag{3.12}$$

l_{eff} sets the per-monomer structure function $\tilde{\omega}(k; l_{\text{eff}})$ and is approximated as

$$\tilde{\omega}(k) = \frac{\exp[-kl_{\text{eff}}/2]}{1 + k^2 Nbl_{\text{eff}}/6} + \frac{1 - \exp[-kl_{\text{eff}}/2]}{1 + kNb/\pi}, \tag{3.13}$$

interpolating between Gaussian-chains $\tilde{\omega} \sim 6/(Nbl_{\text{eff}}k^2)$ at low k and rodlike behavior $\tilde{\omega} \sim \pi/kNb$ at high k, with a crossover set by l_{eff}. An important feature is that the *magnitude* of $\tilde{\omega}$ at sub-monomeric length scales is negligibly affected by l_{eff}, consistent with expectations and simulations. [68] If one uses the uniform expansion approximation for chain structure, the small wavelength fluctuations will be artificially suppressed, resulting in a non-physical effect of dampening the solvation energy of individual monomers.

We thus write a one-parameter (l_{eff}) model for $u_{p\pm} \approx \min_{l_{\text{eff}}}(F_{ent} + F_{int})$ with entropic and interaction terms:

$$F_{\text{ent}} = -\frac{3}{2}N \ln\left(1 - \frac{\alpha^2}{N}\right) - 3\ln(\alpha) \tag{3.14}$$

$$F_{\text{int}} = \frac{1}{4\pi^2}\int k^2 dk\ \tilde{G}(k)\tilde{S}_p^{\text{chg}}(k; l_{\text{eff}}) \tag{3.15}$$

The first term of the entropic free energy is elastic contribution accounting for finite extensibility. The second term $-3\ln(\alpha)$ is associated with the phase volume by the chain ends, first deduced by Flory[69, 70] and used by several subsequent authors.[71–73] We note that the interaction energy Eq. (3.15) is capable of reproducing the logarithmic factor for linear structures.[74, 75] Minimization of the free energy determines l_{eff} and in turn the charge structure factor $\tilde{S}_p^{\text{chg}}$.

3.2.3 Calculation Details

For a prescribed macroscopic condition set by l_b and $\{\rho_\gamma\}$, we solve for the Green's function $\tilde{G}$ and the persistence length l_{eff} self-consistent by an iterative procedure: for a given Green's function $\tilde{G}$ we minimize the single-chain free energy to determine l_{eff} and estimate the charge structure factor $\tilde{S}_p^{\text{chg}}$ via Eq. (3.11) and (3.13), which is then used to update $\tilde{G}$ using Eq. (3.2). We stop when the relative error of l_{eff} between iterations is below 10^{-10}.

The volumes for all monomers are taken to be the same. By assuming the liquid density to correspond to closest packing of effective hard spheres, $\rho_0 = \pi/3\sqrt{2}v_{hs}$, where v_{hs} is the volume of the sphere, the volume fraction for species γ is then $\phi_\gamma = \rho_\gamma/\rho_0$. For simplicity, we take $v_{hs} = b^3$ and report our results in terms of the dimensionless density ρb^3.

For phase equilibria, we solve for chemical potential equality for solutes $\mu_\gamma^I = \mu_\gamma^{II}$ (where $\gamma \neq s$) and mechanical equilibrium $\Pi^I = \Pi^{II}$ between the supernatant and coacervate phases, with both phases constrained to be charge-neutral. Further, for solutions with only one polyelectrolyte species, the asymmetry between positive and negative species requires that we consider the Donnan potential difference $\Delta\psi$ between the two phases.[76]

Results denoted "fg-RPA" in this chapter are calculated with the same expression as the reference WLC chain Eqs. (3.11) and (3.13) but with l_{eff} fixed at $l_{\text{eff}} = b/2$. We also compare our results with those of a semiflexible rod by setting $l_{\text{eff}} = Nb$. By using the same chain structure model for both the Gaussian and stiff limits, we ensure that fluctuations on monomer length scales are the same between all calculations, and the differences can be unambiguously attributed to different treatment of the chain structure at larger length scales.

3.3 Single Polyelectrolyte Species

We first study solutions with only a single polyelectrolyte species. As shown in our previous work (presented in Ch. 2), for salt-free solutions, there is a critical Bjerrum length l_b^c below which the solution is stable for all chain lengths. [50] The stability of the salt-free solution lies in the entropic penalty of phase-separating out the counterions required to neutralize the polyelectrolytes in the dense phase. At $l_b < l_b^c$ the correlations are not strong enough to overcome this entropic penalty in salt-free solutions.

Experiments and recent theory [76–78] have shown that low amounts of salt can lead to phase separation where the polyelectrolyte "salts out" into a denser phase. The added salt reduces the entropic penalty of phase-separating out the small ions that neutralize the polyelectrolyte charge. Once the amount of added salt is on the order of the charge concentration contributed by polyelectrolytes, the supernatant salt concentration no longer changes appreciably upon phase separation, and the polyelectrolyte is able to form a denser phase, even at at $l_b < l_b^c$. In Fig. 3.1 we plot the phase diagram in the salt-polymer concentration plane, where the salt concentration indicates the amount of *added* salt in excess of the neutralizing counterions, and zero salt concentration refers to a salt-free solution. In the inset of Fig. 3.1, we see that the coexistence curves for the different chain lengths converge to a boundary *linear* in polyelectrolyte concentration below which the solution is "effectively salt free" and does not phase separate.

Eventually, at higher salt concentrations, increasing the amount of added salt reduces the polyelectrolyte concentration in the dense branch of the phase diagram, and there is a critical salt concentration above which the solution no longer phase separates – in other words, the polyelectrolyte "salts in." The usual argument is that salt screens the electrostatic interactions.[79, 80] From the perspective of the self energy, [50] the salting-in behavior is explained by recognizing that with increasing salt, the correlation energies are increasingly dominated by the small ions. That is, the differential gain in the correlation energy (decrease in the energy) of the polyelectrolyte upon phase separation is diminished because the electrostatic environments in both the supernatant and polymer-rich phases are increasingly salt-controlled and hence similar.

Together, the salting-in and salting-out phenomena means that a loop is observable in the salt-polymer concentration phase diagram even when $l_b < l_b^c$, which we plot in Figure 3.1. This loop has also been predicted for simple electrolyte solutions

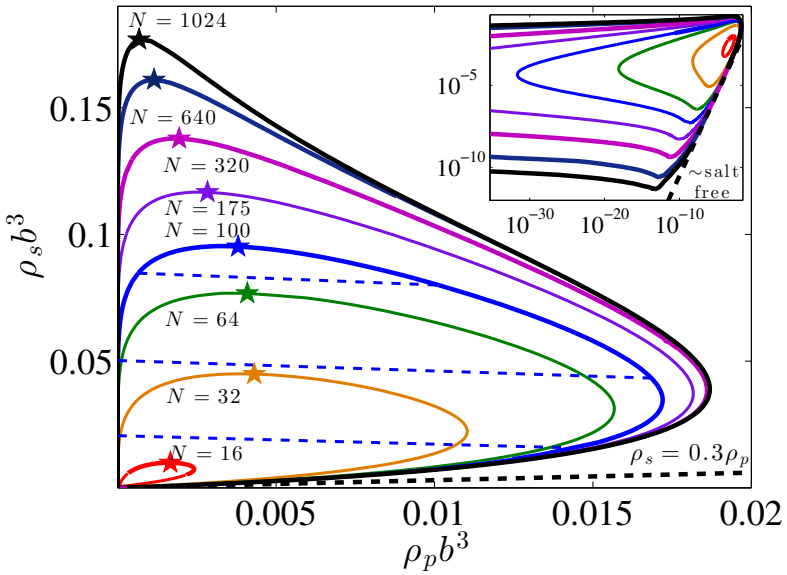

Figure 3.1: ρ_s vs. ρ_p phase diagram for single-species polyelectrolyte solution at $l_b = 1 < l_b^c$, $b = f = 1$. A linear boundary that is roughly $\sim 0.3\rho_s b^3$ demarcates an effectively salt free regime; below the line no phase separation happens. Increasing chain length increases the area of the two-phase region. The tie lines (blue dashed) are for N=100, and indicate a lower salt concentration in the polymer-rich phase.

with one multivalent species.[81] The tie lines predict a lower salt concentration in the dense than in the dilute phase, which is in agreement with previous work. [76] This tie line behavior has been attributed to the larger excluded volume interactions in the dense phase [82] but in our recent work can be understood more generally as the result of asymmetries between small ions and polyelectrolytes in the exchange chemical potential. [83]

The density of the dense phase increases with increasing chain length, but appears to approach a common envelope for long chains, consistent with the picture of a semidilute solution independent of chain lengths. For the longest chains studied at $l_b f/b = 1$, the polymer density remains low and never exceeds $0.02/b^3$. On the other hand, the supernatant phase continues to be rapidly depleted with increasing chain length due to the ever decreasing translational entropy of chains.

The upper critical salt concentration increases as a function of chain length N, again reflecting the increasing propensity for polyelectrolytes to phase separate. The upper critical polymer concentration is non-monotonic with chain length – it first

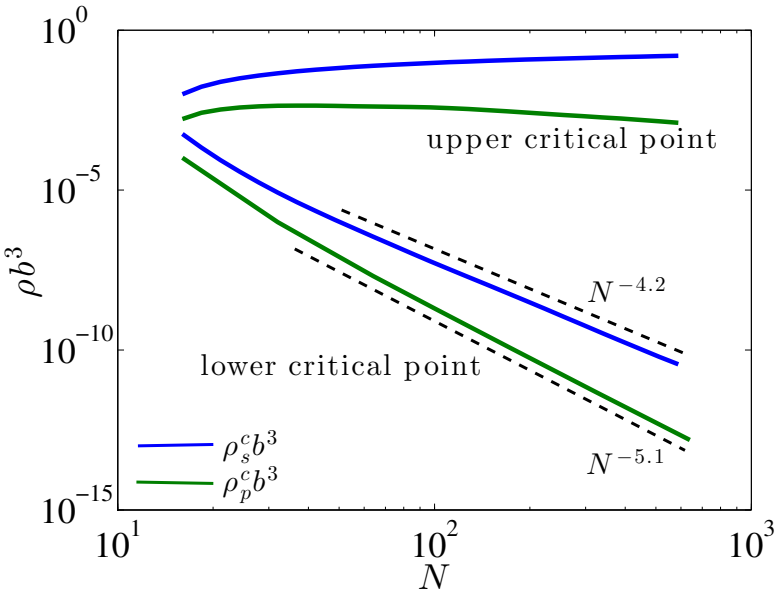

Figure 3.2: Lower and upper critical concentrations for both salt (ρ_s^c, blue) and polyelectrolyte (ρ_p^c, green), at $l_b = b = f = 1$. The upper critical polyelectrolyte concentration is non-monotonic with a maximum at $N \approx 38$. The lower critical concentration vanishes very rapidly with increasing chain length, with a N-dependence $\rho_s^{crit} \sim N^{-4}$. The lower critical polymer concentration has an even stronger N-dependence $\rho_p^{crit} \sim N^{-5}$.

increases (for $N < 38$) and then decreases (for $N > 38$). The decrease for long chain lengths reflects the decreasing translational entropy of long chains, which results in the longer chains phase separating at lower densities. Meanwhile, the correlation energy becomes independent of N for long chains in semidilute solution and has negligible chain-length effect on phase separation. The initial *increase* in the critical polymer concentration is because for short chains, increasing chain length initially increases the correlation energy faster than the translational entropy decreases. The behavior for these upper critical concentrations is shown by the two top curves in Fig. 3.2.

The lower critical salt concentration decreases with increasing chain length, consistent with the broadening of the phase separating region, and eventually vanishes for long chains (Fig. 3.2). In stark contrast, for chains with fixed Gaussian structure, sufficiently long chains do *not* have a lower critical point altogether. Increasing chain length in the fg-RPA leads to phase separation *even in* salt-free conditions, [50] as indicated by the "chimney" feature in the binodal of a Gaussian chain (Fig.

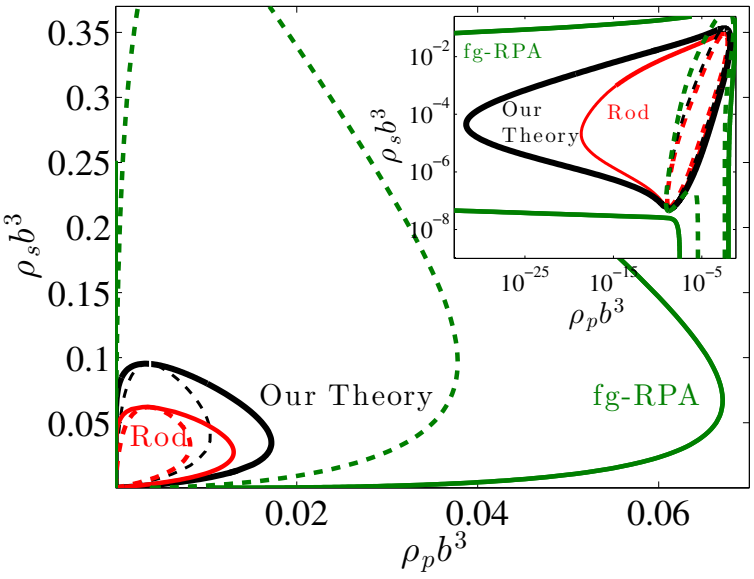

Figure 3.3: Phase diagram of phase separation at $l_b = b = f = 1$ for $N = 100$. For comparison, the results for semiflexible rod (red) and for Gaussian chain (green) structures are also included. The solid lines are for the binodal, while the dashed lines are for the spinodal. The Gaussian chains phase separates for all salt concentrations studied.

3.3).

From Fig. 3.2, we see that the lower critical polymer concentration has a stronger N-dependence than the critical salt concentration. Although we cannot explain the scaling exponents for the lower critical concentrations, we suggest that the critical concentration and thus exponents may be insensitive to chain structure. To support this suggestion, we plot the binodal and spinodal for rods ($l_{\text{eff}} = Nb$) and note that they have a similar shape to the RGF for the flexible chains, with a lower critical point nearly coinciding with that of the flexible chain (our theory). Remarkably, even the spinodal of the fg-RPA ($l_{\text{eff}} = 0.5$), which features an instability that persists to zero salt concentration, has an ellipsoidal region with a lower apex near the lower critical point of the stiffer chains. The insensitivity of this apex to the chain structure can be understood by noting that the polymer concentration at the critical point $\rho_p \sim N^{-5}$ is far below overlap, in a regime where the polyelectrolyte predominantly screens as an Nf-valent ion, independent of chain structure.[50] At higher concentrations, however, chain structure has a stronger impact on the electrostatic correlation and the spinodal of the fg-RPA deviates significantly from that of stiffer chains.

We also point out that at the conditions presented ($l_b f/b = 1$), the TPT-1 theory does *not* predict a loop in the phase diagram. The electrostatic correlation energies in TPT-1 theory are much weaker than in the RGF theory. For a polyelectrolyte solution where all monomers have diameter b and are charged, TPT-1 predicts a lower critical Bjerrum length $l_b/b \approx 2.8$ below which the loop in the phase diagram ceases to exist.[76] For the parameters we investigated, we did not yet encounter the lower critical l_b for which the loop vanishes, though the loop does shrink with decreasing l_b (and should cease to exist for $l_b = 0$).

Lastly, in Fig. 3.3 one can clearly see that increasing stiffness reduces the two-phase region of the phase diagram. Within the RGF theory, this is largely because stiffer chains have smaller correlation energies. Stiffer chains naturally tend to conformations with lower electrostatic energy than more flexible chains, meaning there is consequently less correlation energy to be gained by phase separation. Also important to note is that fully flexible chains can behave much more similarly to rods than to chains with fixed Gaussian structure. As will be shown later, at sufficiently high (but still modest) charge fractions, flexible chains will locally stiffen and expand, meaning their charge environment will more closely resemble rods than truly ideal chains.

3.4 Symmetric Polyelectrolyte Species

Next we study solutions of oppositely charged but otherwise symmetric polyelectrolytes. The oppositely charged polyelectrolytes are known to phase separate together into liquid phases called complex coacervates.[31]

We begin by examining the salt-free limit, where for chains of *fixed* fractal dimension $d > 3/2$, RPA theory predicts that the critical monomer density scales as $\rho_p^c \sim N^{-1}$ and that the critical charge fraction scales as $f^c \sim N^{-2/3}$.[42] Our results (Fig. 3.4) show a slightly weaker N-dependence for ρ_p^c and slightly stronger dependence for the charge fraction f^c, but are in general quite close to the RPA predictions.

The origin of this surprising agreement lies in the extremely low critical charge fractions. At such low charge fractions, the polyelectrolyte structure is essentially unperturbed by the charge interaction. The number of monomers in an electrostatic blob scales as $g \sim (b/l_b f^2)^{2/3}$ in theta solution and $g \sim (b/l_b f^2)^{5/7}$ in good solvent. The good solvent scaling means that the critical charge fraction scaling $f^c \sim N^{-0.695}$ produces $g \sim N^{0.993} \approx N$, i.e., the electrostatic blob is essentially the entire chain and overall $R/b \sim N^{-3/5}$. Even the theta solution scaling yields $g \sim N^{0.927}$. Further

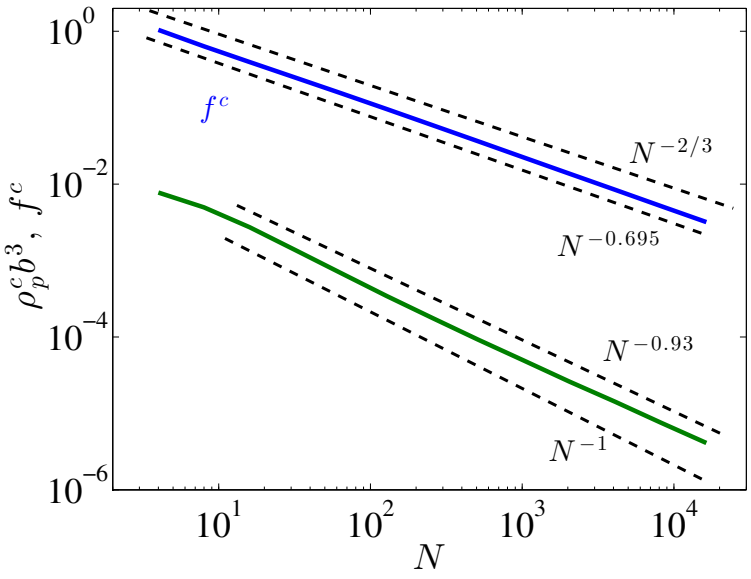

Figure 3.4: Scaling of the critical charge fraction f^c (blue) and critical monomer density ρ_p^c (green) for salt-free solutions of oppositely charged, symmetric polyelectrolytes with $l_b = b = 1$. The exponents $-2/3$ and -1 respectively for f^c and ρ_p^c are the RPA predictions[42] for salt-free solutions of chains with fractal dimension $d > 3/2$.

assuming that the blobs are linearly aligned then yields $R/b \sim N/g^{1-\nu} \sim N^{0.537}$ overall. This assumption of linearly aligned blobs yields an overlap concentration $\rho^* \sim N^{-0.61}$, which is consistently above the critical lower concentration. It is thus not surprising that for the salt-free symmetric polyelectrolyte system, our theory yields scaling results that are so close to the RPA predictions. Again, to match the cited scaling predictions, the chain structure does not need to be strictly Gaussian $d = 2$ ($\nu = 1/2$), but merely needs to satisfy $d > 3/2$ (i.e., the Flory exponent $\nu < 2/3$).[42]

At higher charge fractions, the deviation from Gaussian behavior becomes more significant. In particular, at low concentrations we expect flexible chains to stretch to relax their electrostatic energy, reducing the correlation energy gain (relative to chains with fixed Gaussian structure) upon complexation.[50] In other words, the fg-RPA's picture of an ideal Gaussian chain over-predicts the per-chain electrostatic energy in dilute solution, which is screened upon complexation. Consequently, one expects the fg-RPA to greatly overpredict the window of phase separation. This is confirmed in Fig. 3.5, where one can see that the dense branch of the binodal is

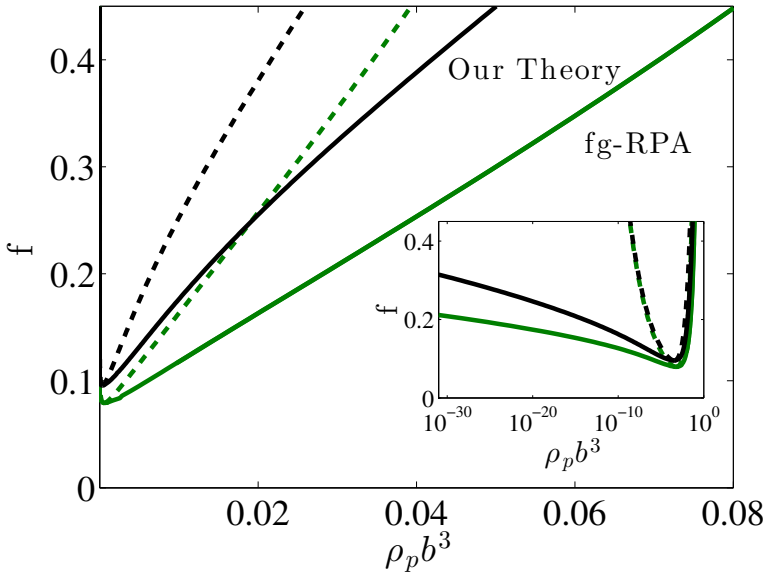

Figure 3.5: Phase diagram of salt-free solutions of oppositely charged, symmetric polyelectrolytes with length $N = 128$, $l_b = b = 1$. Solid lines are for the binodal, while dashed lines are for the spinodal. We compare the RGF theory (black) to the fg-RPA (green).

denser in fg-RPA than in the RGF theory. In addition, the critical charge fraction is slightly higher in the RGF theory, in agreement with the increased stability when chains are allowed to relax their chain structure.

For the dilute branch, by assuming an ideal Gaussian structure the fg-RPA predicts polyelectrolyte concentrations that are many orders of magnitude too dilute. Recent work by Delaney and Fredrickson has shown that in coacervate-forming systems, the supernatant phase is composed of clusters of oppositely charged chains, which lower the magnitude of the per-monomer electrostatic energy in the dilute phase.[84] Although this clustering effect is currently not captured by the RGF, the RGF still hints at the drastic over-estimate of the per-chain electrostatic energy in the fg-RPA theory and its overly dilute predictions for concentration in the supernatant phase.

We now consider adding salt under conditions where the salt-free solution already phase separates (Fig. 3.6). Similarly to solutions of only a single polyelectrolyte species, the added salt screens electrostatic interactions and decreases the window for phase separation. At any reasonable overall salt concentration, the salt is depleted in the coacervate phase, as indicated by the tie lines. (Interestingly, at *extremely*

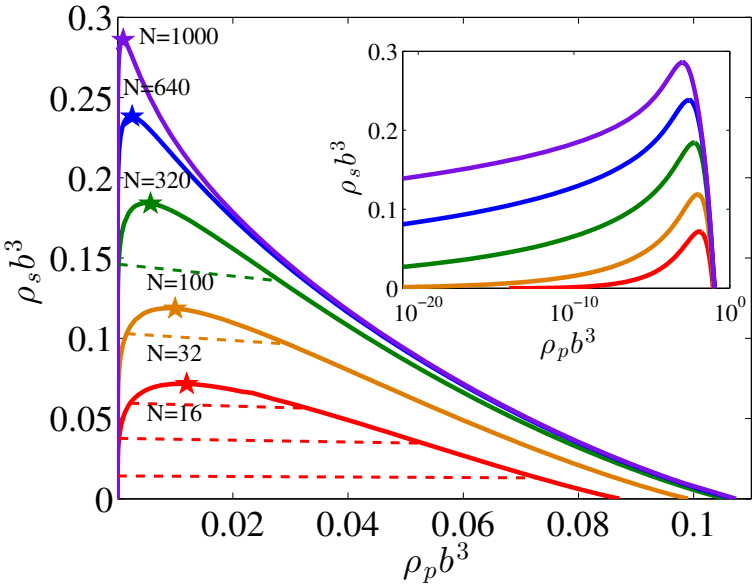

Figure 3.6: Phase diagram of complex coacervation with added salt at $l_b = 0.7$, $b = f = 1$. There is an N-independent envelope for the dense branch, and the tie lines indicate that the coacervate phase has a lower salt concentration than the supernatant phase.

low salt concentrations, the salt can actually be *enriched* in the dense phase, but these concentrations are too low to be shown clearly on the scale of the figure.) This behavior of the tie line is in contrast to theories that use the VO picture of disconnected charges,[85] but consistent with other theories that incorporate connectivity effects [76, 82, 83] and experiments and simulation.[86, 87]

Increasing chain length should, again, decrease the translational entropy of the chains and marginally increase the electrostatic correlation, leading to wider binodal curves (Fig. 3.6). Consequently, the critical salt concentration increases with increasing chain length, while the critical polymer concentration decreases for long chains. For shorter chains, the same competition between the correlation energy and translational entropy seen in the single polyelectrolyte species case is still operative, and there is a non-monotonicity in the critical polymer concentration with a peak around $N = 12$ (Fig.3.7) for the conditions presented in this chapter.

Away from the critical point, the dense branch of the polyelectrolyte approaches an N-independent curve (Fig. 3.6) with increasing chain length. This behavior is again consistent with the eventual N-independence of the correlation energies in

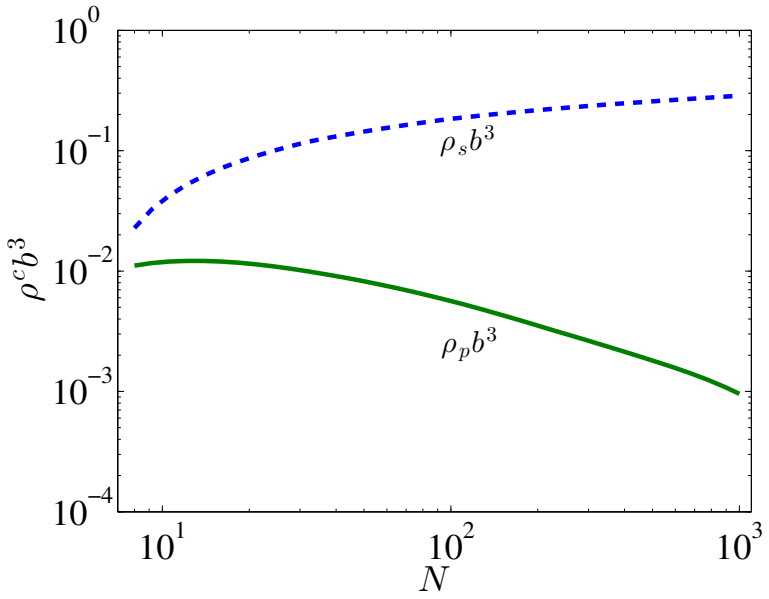

Figure 3.7: Critical salt ρ_s^c (blue, dashed) and polymer ρ_p^c (green, solid) densities for symmetric polyelectrolyte solutions at $l_b = 0.7$, $b = f = 1$.

semidilute solution.

When comparing chain structures, we again find that stiffer chains experience smaller correlation energies, and consequently have narrower two-phase regions in their phase diagram. In Fig. 3.8 one can clearly see this stiffness effect by comparing the semiflexible rods with flexible chains (whose structures are adaptively estimated by the RGF). Interestingly, one may also note that away from the critical point, the phase boundaries of the RGF theory of flexible chains is quantitatively quite close to those of polyelectrolyte rods. In fact, if we fix $l_{\text{eff}} \approx 2.0$ by its value at the RGF critical point, the resulting phase boundary nearly overlaps with that of the full RGF prediction (orange line, Fig. 3.8).

This similarity between stiff and semiflexible chains may be surprising – the dense phase of polyelectrolyte coacervates are semidilute and chains are overall Gaussian, which may lead one to expect the fg-RPA to give a good description of the dense phase. While this may be true for a qualitative understanding, we remark that the fg-RPA can lead to significant numerical discrepancies. Not only is the dilute branch of the binodal overly dilute, the dense branch can also be overly dense. In fact, the entire binodal region of the fg-RPA can be so wide that a significant phase unstable region persists up until the excluded volume limit for the parameters studied (Fig.

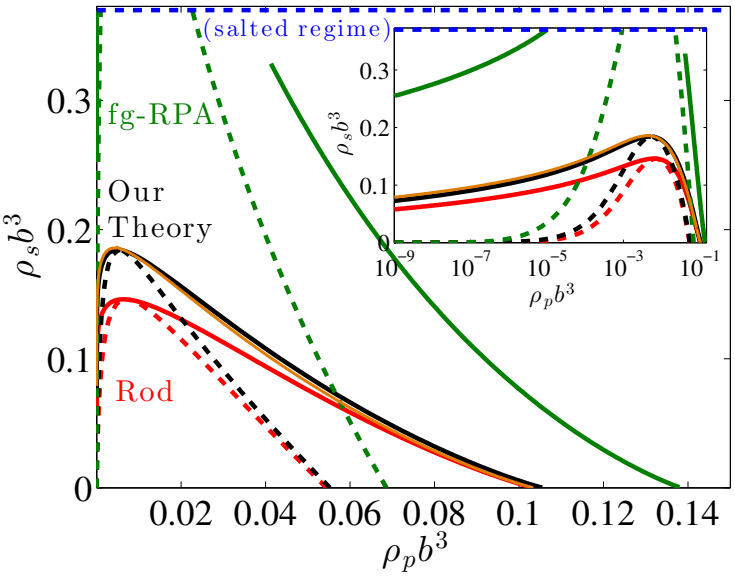

Figure 3.8: Phase diagram of complex coacervation at $l_b = 0.7$, $b = f = 1$ for $N = 100$. For comparison, the results for semiflexible rod (red) and for Gaussian chain (green) structures are also included. The solid lines are for the binodal, while the dashed lines are for the spinodal. For the parameters chosen, the fg-RPA fails to salt back in before the salt saturates (salted regime, blue dashed). The orange line uses a fixed value of $l_{\text{eff}} \approx 2.0$, the value of l_{eff} obtained from RGF at the critical point.

3.8). Further, the fg-RPA calculation for $N = 100$ has such strong correlations that the instability window is even wider than predicted by the RGF for $N = 1000$ (compare to Fig. 3.6). This overestimate of the electrostatic energy is most severe for the dilute phase, but the overestimate in the dense phase is still quantitatively significant.

Further, the dilute branch of the RGF theory and rods are both orders of magnitude higher than the fg-RPA theory, but we anticipate that in reality all three phase boundaries exhibit an overly dilute supernatant phase because none account for the formation of clusters.[84] Nevertheless, we expect the correct supernatant densities to still be so dilute that the osmotic pressure due to polymers is very nearly zero. Correspondingly, we believe that even with a corrected dilute branch, the dense branch will continue to be a good estimate away from the critical point.[42]

3.5 Effects of Chain Structure

The significant overestimate of flexible chain electrostatic correlation effects accompanying ideal Gaussian chain assumptions (fg-RPA) in both cases studied (single polyelectrolyte species and oppositely charged symmetric polyelectrolytes) and the quantitative closeness of RGF predictions to those for semiflexible rods can be explained by changes in the flexible chain structure. These changes persist even in semidilute solution and are sufficient to lead to a marked increase in thermodynamic stability of flexible polyelectrolyte solutions predicted by the RGF as compared to fg-RPA.

To quantify the change in chain structure, we plot the polyelectrolyte size along the binodal curves of both types of systems for a sample chain length $N = 100$ in Fig. 3.9. Along the dilute branch, the chains are much more extended than the ideal Gaussian chain, and in both systems R_{ee} decays monotonically with increasing salt. This may at first be surprising for the single polyelectrolyte species system, where the polymer concentration is non-monotonic in salt concentration along the dilute branch. However, along the portion of the dilute branch where the polymer concentration decreases with increasing salt, the polymer is so dilute that the screening is mostly dictated by the monotonically increasing salt concentration, leading to the monotonic decrease in chain size.

Along the dense branch, in the single polyelectrolyte system and away from the upper critical point, the chain size decreases monotonically. Away from the upper critical point, the polymer concentration seems to be around or below the overlap of self-avoiding chains, meaning that continued decrease in chain size is likely mostly due to the increased salt screening. On the other hand, the chain size *increases* monotonically along the dense branch of the symmetric polyelectrolyte system. This is because for nearly the entire branch, the polymer concentration remains above overlap and the polymer size is essentially controlled by the polymer concentration. As the polymer concentration drops monotonically with increasing salt, the correlation length of the semidilute solution increases and the chain size increases monotonically.

We note that for both the single polyelectrolyte species and the symmetric polyelectrolyte mixtures, the polyelectrolyte is still noticeably swollen relative to the Gaussian chain even along the dense branch. In particular, even in the coacervate-forming system where the dense phase can reach 10% volume fraction, the polyelectrolyte is still nearly twice as large as the ideal chain.

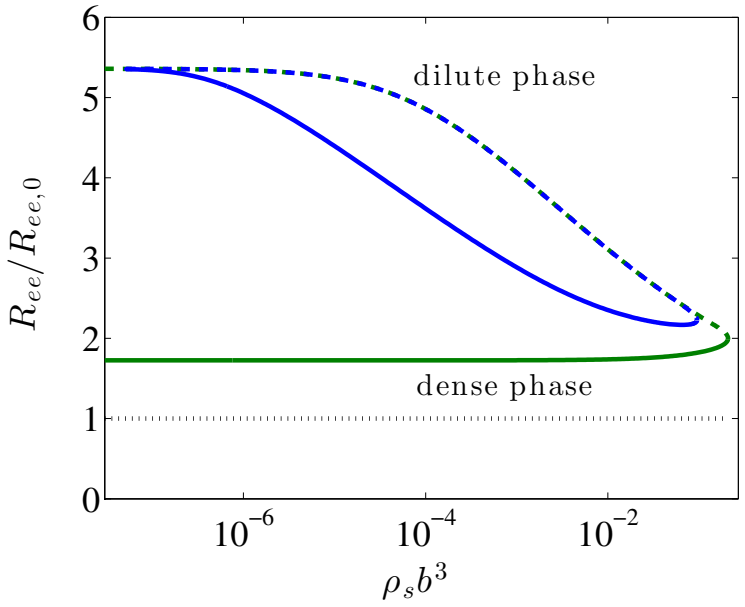

Figure 3.9: Polyelectrolyte end-to-end distance relative to the Gaussian chain for chain length $N = 100$ at $l_b = b = f = 1$, along the binodal of supernatant (dashed) and dense (solid) phases in solutions of single polyelectrolyte species (blue) and oppositely charged symmetric chains (green).

The change in the chain structure with the polyelectrolyte and salt concentrations has huge effects on the electrostatic correlation energies. As an example, in Fig. 3.10, we present the per-monomer correlation energy at fixed salt chemical potential, i.e. we consider a semi-grand system where the salt concentration equilibrates with a salt-only reservoir. To isolate the correlation energy associated with finite concentration of polyelectrolyte and hence the driving force for the formation of a dense polyelectrolyte phase, we subtract off the polyelectrolyte self energy in the limit of zero polyelectrolyte concentration from the electrostatic part of the per-monomer chemical potential[50]

$$\mu_m^{corr} = \mu_m^{el} - \mu_m^{el}(\rho_p = 0) \tag{3.16}$$

At low polymer concentrations, the correlations are primarily due to the salt ions and μ_m^{corr} is insensitive to polymer concentration. At a cross-over polymer concentration that increases with increasing salt, the electrostatic environment becomes eventually dominated by the polyelectrolytes, which produces a negative change in the correlation energy. The fg-RPA confines charges to an artificially small ideal Gaussian chain volume, down to the monomeric scale, and hence greatly overes-

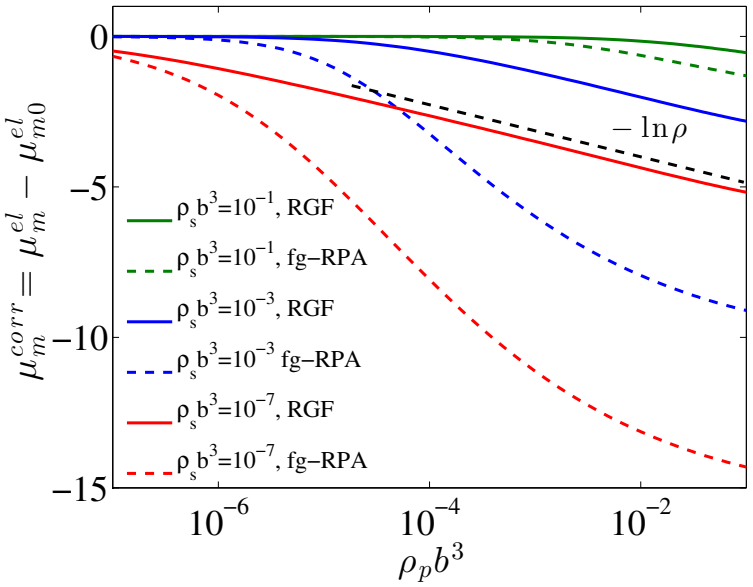

Figure 3.10: Correlation energy per monomer as a function of polyeletrolyte concentration for chains of $N = 100$ at $l_b = b = f = 1$ and at fixed salt chemical potential with reservoir salt concentration $\rho_s b^3 = 10^{-3}$ (red), $\rho_s b^3 = 10^{-2}$ (blue), $\rho_s b^3 = 10^{-1}$ (green). Our RGF results are shown as solid curves and the fg-RPA results are given as dashed curves.

timates the magnitude of the correlation energy (primarily by overestimating the positive $\mu_m^{el}(\rho_p = 0)$ term). In the salt-free limit, the fg-RPA has been shown to overestimate the correlation energy by up to a factor of $\sqrt{N}/\ln(N)$.[50] For $N = 100$ this overestimation is up to a factor of ≈ 2.2.

Note that Fig. 3.10 is shown on a linear-log plot, highlighting that for sufficiently high concentrations (such that screening is dominated by the polyelectrolytes), the correlation energy is actually *logarithmic* in polymer concentration $\Delta\mu_m^{el} \sim -\ln\rho$. This result can be rationalized by realizing that, at the parameters studied, the chain structure is rod-like in semidilute solutions up until at least some electrostatic persistence length.

The electrostatic fluctuation integrals can then be well approximated by replacing the chain structure factor with the asymptotic high-k expression for rods, $\tilde{S}(k) \sim \pi/k$. Although the resulting integral is not convergent, it is straightforward to work out that the convergent piece of the fluctuation contribution to the Helmholtz free energy has a functional form $-\alpha\rho(\ln\rho - 1)$, which has the same form as translational entropy,

plus a thermodynamically inconsequential logarithmic piece $\propto \ln(a)$ related to the energy of confining charges to a cylinder of microscopic cut-off radius a. As long as the prefactor $-\alpha$ is not overly negative (i.e. yielding negative osmotic pressures), this can be viewed as renormalizing the translational entropy of the counterions into $(1-\alpha)\rho(\ln\rho - 1)$. Thus, $1-\alpha$ can be interpreted as the fraction of "osmotically active" counterions in counterion condensation theories.[75, 88–90]

This effect was previously noted in our paper on the osmotic coefficient of salt-free solutions [50] and outlined in a previous RPA study for rods. [42] We emphasize that we only study conditions *below* the critical Manning condensation parameter. Thus, even at charge densities below the critical Manning charge parameter, our theory effectively describes an atmosphere of ions about the polyelectrolyte backbone.

These results indicate that it is vitally important to capture the correct chain structure at length scales below the correlation lengths. While our chain structure Eq. (3.13) is approximate, it captures the fact that polyelectrolyte chain structures at the conditions studied *do* resemble the WLC reference structures used. [90] A more accurate chain structure can be obtained by performing full single-chain simulations as part of the self-consistent calculation, which will likely yield similar WLC chain structures. However, if one uses the Gaussian uniform expansion structure (commonly used to successfully describe the overall chain size),[54] electrostatic interactions on smaller scales will be artificially suppressed. Within the RGF framework, a uniform expansion approximation will erroneously predict that correlation energies *decrease* (i.e. become more negative) with increasing chain length in semidilute solutions, when they should instead be independent of chain length.

In conjunction with the results in previous sections, we suggest that, at least for the purposes of calculating thermodynamic properties or fitting experimental data of semidilute solutions for the coacervate system, it is possible to use Eq. 3.13 with a *constant* l_{eff} as a fitting parameter, thus bypassing the need for the self-consistent calculations.

3.6 Conclusions

Using the renormalized Gaussian fluctuation (RGF) field theory, which is able to self-consistently describe the intrachain structure and thermodynamics from dilute to semidilute solutions, we have studied the phase behavior for solutions of both a single polyelectrolyte species and a symmetric mixture of oppositely charged polyelectrolytes, in the presence of salt.

Unique to the single polyelectrolyte system is a loop in the phase diagram in the salt-polymer concentration plane. Both the lower critical salt and polymer concentrations vanish with increasing chain length, respectively as N^{-4} and N^{-5}. Interestingly, the spinodal shape near the RGF lower critical point seems to be fairly independent of chain structure. Even the fg-RPA, which assumes an ideal Gaussian structure and may not have a lower critical point at all, can still exhibit a peculiar spinodal featuring an ellipsoidal region with a lower apex near the RGF lower critical point.

For both the single polyelectrolyte and oppositely charged polyelectrolytes, the addition of large amounts of salt eventually salts the polyelectrolyte back into a single phase. The upper critical salt concentration grows with increasing chain length, while the upper critical polymer concentration is non-monotonic in the chain length, reflecting competing chain length dependences between increasing correlation energies and decreasing translational entropy. The phase diagrams for fully-charged flexible chains within the RGF theory are much more similar to those predicted for semiflexible rods than for chains with fixed, ideal Gaussian structures. We also consistently find that increased rigidity decreases the tendency for phase separation.

Even at relatively mild conditions ($f l_b/b \leq 1$ where Manning counterion condensation theory predicts no condensation), we showed that to get a good estimate of the thermodynamics and correlation energies, it is vital to capture correct chain structure. Our calculations confirm that a main consequence of field fluctuations of more highly charged chains is the renormalization of the chain structure, leading to local stiffening and chain swelling even in semidilute solution, and can significantly change the correlation energies and thermodynamics. For such fully-charged chains, in particular at higher salt and polymer concentrations, we see that it is possible to capture the predictions of the RGF theory for the coacervates by using a constant l_{eff}.

At lower charge fractions where the chain structure is only slightly perturbed, the critical point behavior of the oppositely charged symmetric polyelectrolytes predicted by our theory is close to that previously predicted for chains with fractal dimension $d > 3/2$.

In the RGF the nonlinear fluctuations are to a certain degree naturally accounted for through the self-consistent chain structure, which describes the correlated monomer densities associated with the fluctuations. The self-consistent calculation of the chain structure within RGF in essence renormalizes the *entire* chain structure and in doing

so predicts better correlation energies and thermodynamics. Even in neutral melts, fluctuations modify the chain structure. The closely related renormalized one-loop (ROL) theory predicts a *perturbative* correction to the single chain structure factor (the ROL only self-consistently renormalizes the $k \to 0$ value of the interaction χ, but the chain structure correction is calculated perturbatively). [91–94] The RGF's non-perturbative "renormalization" of chain structure self-consistently estimates the electrostatic fluctuations at all sub-chain length scales, and is especially important given the scale-free nature of the Coulomb interaction.

BIBLIOGRAPHY

[1]A. Veis, and C. J. Aranyi, "Phase separation in polyelectrolyte systems. i. complex coacervates of gelatin", Phys. Chem. **64**, 1203 (1960).

[2]A. Veis, "Phase separation in polyelectrolyte solutions. ii. interaction effects", J. Phys. Chem. **65**, 1798 (1961).

[3]A. F. Thünemann, M. Müller, H. Dautzenberg, J.-F. Joanny, and H. Löwen, "Polyelectrolyte complexes", Adv. Comput. Simul. Approaches Soft Matter Sci. I **166**, 113 (2004).

[4]C. G. de Kruif, F. Weinbreck, and R. de Vries, "Complex coacervation of proteins and anionic polysaccharides", Curr. Opin. Colloid Interface Sci. **9**, 340 (2004).

[5]C. L. Ting, J. Wu, and Z.-G. Wang, "Thermodynamic basis for the genome to capsid charge relationship in viral encapsidation", P. Natl. Acad. Sci. USA **108**, 16986 (2011).

[6]D. T. Hallinan Jr, and N. P. Balsara, "Polymer electrolytes", Annu. Rev. Mater. Res. **43**, 503 (2013).

[7]C. Schmitt, and S. L. Turgeon, "Protein/polysaccharide complexes and coacervates in food systems", Adv. Colloid Interface Sci. **167**, 63 (2011).

[8]D. S. Hwang, H. Zeng, A. Srivastava, D. V. Krogstad, M. Tirrell, J. N. Israelachvili, and J. H. Waite, "Viscosity and interfacial properties in a mussel-inspired adhesive coacervate", Soft Matter **6**, 3232 (2010).

[9]F. Pittella, and K. Kataoka, *Polymeric micelles for sirna delivery* (Springer, 2013), p. 161.

[10]D. W. Pan, and M. E. Davis, "Cationic mucic acid polymer-based sirna delivery systems", Bioconjugate Chem. **26**, 1791 (2015).

[11]K. A. Black, D. Priftis, S. L. Perry, J. Yip, W. Y. Byun, and M. Tirrell, "Protein encapsulation via polypeptide complex coacervation", ACS Macro Lett. **3**, 1088 (2014).

[12]M. A. Cohen Stuart, W. T. Huck, J. Genzer, M. Müller, C. Ober, M. Stamm, G. B. Sukhorukov, I. Szleifer, V. V. Tsukruk, and M. Urban, "Emerging applications of stimuli-responsive polymer materials", Nat. Mater. **9**, 101 (2010).

[13]V. Tolstoguzov, "Some physico-chemical aspects of protein processing in foods", Food Hydrocolloids **9**, 317 (1995).

[14]F. Weinbreck, R. de Vries, P. Schrooyen, and C. G. de Kruif, "Complex coacervation of whey proteins and gum arabic", Biomacromolecules **4**, 293 (2003).

[15]L. A. Luzzi, "Microencapsulation", J. Pharm. Sci. **59**, 1367 (1970).

[16]A. Harada, "Chain length recognition: core-shell supramolecular assembly from oppositely charged block copolymers", Science **283**, 65 (1999).

[17]E. Y. Kramarenko, A. R. Khokhlov, and P. Reineker, "Effect of formation of ion pairs on the stability of stoichiometric block ionomer complexes", J. Chem. Phys. **119**, 4945 (2003).

[18]S. van der Burgh, A. de Keizer, and M. A. Cohen Stuart, "Complex coacervation core micelles. colloidal stability and aggregation mechanism", Langmuir **20**, 1073 (2004).

[19]M. E. Davis, "The first targeted delivery of sirna in humans via a self-assembling, cyclodextrin polymer-based nanoparticle: from concept to clinic", Mol. Pharmaceutics **6**, 659 (2009).

[20]M. Delcea, H. Möhwald, and A. G. Skirtach, "Stimuli-responsive lbl capsules and nanoshells for drug delivery", Adv. Drug Delivery Rev. **63**, 730 (2011).

[21]D. V. Pergushov, A. H. E. Müller, and F. H. Schacher, "Micellar interpolyelectrolyte complexes", Chem. Soc. Rev. **41**, 6888 (2012).

[22]H. Zhao, C. Sun, R. J. Stewart, and J. H. Waite, "Natural underwater adhesives", J. Biol. Chem. **280**, 42938 (2005).

[23]H. Shao, K. N. Bachus, and R. J. Stewart, "A water-borne adhesive modeled after the sandcastle glue of p. californica", Macromol. Biosci. **9**, 464 (2009).

[24]R. J. Stewart, C. S. Wang, and H. Shao, "Complex coacervates as a foundation for synthetic underwater adhesives", Adv. Colloid Interface Sci. **167**, 85 (2011).

[25]W. Wei, Y. Tan, N. R. M. Rodriguez, J. Yu, J. N. Israelachvili, and J. H. Waite, "A mussel-derived one component adhesive coacervate", Acta Biomater. **10**, 1663 (2014).

[26]G. Decher, J. Hong, and J. Schmitt, "Buildup of ultrathin multilayer films by a self-assembly process: iii. consecutively alternating adsorption of anionic and cationic polyelectrolytes on charged surfaces", Thin Solid Films **210**, 831 (1992).

[27]M. Castelnovo, and J.-F. Joanny, "Formation of polyelectrolyte multilayers", Langmuir **16**, 7524 (2000).

[28]S. Srivastava, and M. V. Tirrell, "Polyelectrolyte complexation", Adv. Chem. Phys., 499–544 (2016).

[29]C. E. Sing, "Development of the modern theory of polymeric complex coacervation", Advances in Colloid and Interface Science **239**, 2–16 (2017).

[30]M. Muthukumar, "50th anniversary perspective: a perspective on polyelectrolyte solutions", Macromolecules **50**, 9528 (2017) 10.1021/acs.macromol.7b01929.

[31]J. T. G. Overbeek, and M. J. Voorn, "Phase separation in polyelectrolyte solutions. theory of complex coacervation", J. Cell Compar. Phys. **49**, 7 (1957).

[32]P. Debye, and E. Hückel, "De la théorie des électrolytes. i. abaissement du point de congélation et phénomènes associés", Phys. Zeitschrift **24**, 185 (1923).

[33]C. E. Sing, J. W. Zwanikken, and M. O. de la Cruz, "Interfacial behavior in polyelectrolyte blends: hybrid liquid-state integral equation and self-consistent field theory study", Phys. Rev. Lett. **111**, 168303 (2013).

[34]L. Blum, Y. V. Kalyuzhnyi, O. Bernard, and J. N. Herrera-Pacheco, "Sticky charged spheres in the mean-spherical approximation: a model for colloids and polyelectrolytes", J. Phys. Condens. Matter **8**, A143 (1996).

[35]I. Protsykevytch, Y. Kalyuzhnyi, M. Holovko, and L. Blum, "Ion-ion, ion-solvent and solvent-solvent interactions in electrolyte solutions: solution of the polymer mean spherical approximation for the totally flexible sticky two-point electrolyte model", J. Mol. Liq. **73**, 1 (1997) http://dx.doi.org/10.1016/S0167-7322(97)00053-6.

[36]O. Bernard, and L. Blum, "Thermodynamics of a model for flexible polyelectrolytes in the binding mean spherical approximation", J. Chem. Phys. **112**, 7227 (2000) http://dx.doi.org/10.1063/1.481287.

[37]N. von Solms, and Y. C. Chiew, "Analytical integral equation theory for a restricted primitive model of polyelectrolytes and counterions within the mean spherical approximation. i. thermodynamic properties", J. Chem. Phys. **111**, 4839 (1999) http://dx.doi.org/10.1063/1.479246.

[38]N. von Solms, and Y. C. Chiew, "A model for polyelectrolytes", J. Stat. Phys. **100**, 267 (2000) 10.1023/A:1018652031157.

[39]J. Jiang, L. Blum, O. Bernard, and J. M. Prausnitz, "Thermodynamic properties and phase equilibria of charged hard sphere chain model for polyelectrolyte solutions", Mol. Phys. **99**, 1121 (2001).

[40]V. Y. Borue, and I. Y. Erukhimovich, "A statistical theory of weakly charged polyelectrolytes: fluctuations, equation of state and microphase separation", Macromolecules **21**, 3240 (1988).

[41]A. Khokhlov, and K. Khachaturian, "On the theory of weakly charged polyelectrolytes", Polymer **23**, 1742 (1982).

[42]J. Qin, and J. J. de Pablo, "Criticality and connectivity in macromolecular charge complexation", Macromolecules **49**, 8789 (2016).

[43]Y. A. Budkov, A. L. Kolesnikov, N. Georgi, E. A. Nogovitsyn, and M. G. Kiselev, "A new equation of state of a flexible-chain polyelectrolyte solution: phase equilibria and osmotic pressure in the salt-free case", J. Chem. Phys. **142**, 174901 (2015).

[44]K. A. Mahdi, and M. O. de la Cruz, "Phase diagrams of salt-free polyelectrolyte semidilute solutions", Macromolecules **33**, 7649 (2000).

[45]M. Castelnovo, and J.-F. Joanny, "Complexation between oppositely charged polyelectrolytes: beyond the random phase approximation", Eur. Phys. J. E **6**, 377 (2001).

[46]A. V. Ermoshkin, and M. Olvera de la Cruz, "A modified random phase approximation of polyelectrolyte solutions", Macromolecules **36**, 7824 (2003).

[47]A. M. Rumyantsev, and I. I. Potemkin, "Explicit description of complexation between oppositely charged polyelectrolytes as an advantage of the random phase approximation over the scaling approach", Phys. Chem. Chem. Phys. **19**, 27580–27592 (2017).

[48]Y. A. Budkov, A. I. Frolov, M. G. Kiselev, and N. V. Brilliantov, "Surface-induced liquid-gas transition in salt-free solutions of model charged colloids", J. Chem. Phys. **139**, 194901 (2013).

[49]Y. A. Budkov, A. Kolesnikov, E. Nogovitsyn, and M. Kiselev, "Electrostatic-interaction-induced phase separation in solutions of flexible-chain polyelectrolytes", Polymer Science Series A **56**, 697–711 (2014).

[50]K. Shen, and Z.-G. Wang, "Electrostatic correlations and the polyelectrolyte self energy", J. Chem. Phys. **146**, 084901 (2017) DOI:10.1063/1.4975777.

[51]M. Muthukumar, and S. Edwards, "Extrapolation formulas for polymer solution properties", J. Chem. Phys. **76**, 2720 (1982).

[52]M. Muthukumar, "Double screening in polyelectrolyte solutions: limiting laws and crossover formulas", J. Chem. Phys. **105**, 5183 (1996).

[53]J. P. Donley, J. Rudnick, and A. J. Liu, "Chain structure in polyelectrolyte solutions at nonzero concentrations", Macromolecules **30**, 1188 (1997).

[54]A. Yethiraj, "Theory for chain conformations and static structure of dilute and semidilute polyelectrolyte solutions", J. Chem. Phys. **108**, 1184 (1998).

[55]A. Yethiraj, "Conformational properties and static structure factor of polyelectrolyte solutions", Phys. Rev. Lett. **78**, 3789 (1997).

[56]M. Muthukumar, "Phase diagram of polyelectrolyte solutions: weak polymer effect", Macromolecules **35**, 9142 (2002).

[57]A. Kundagrami, and M. Muthukumar, "Effective charge and coil-globule transition of a polyelectrolyte chain", Macromolecules **43**, 2574 (2010).

[58]G. Orkoulas, S. K. Kumar, and A. Z. Panagiotopoulos, "Monte carlo study of coulombic criticality in polyelectrolytes", Phys. Rev. Lett. **90**, 048303 (2003).

[59]Z.-G. Wang, "Fluctuation in electrolyte solutions: the self energy", Phys. Rev. E **81**, 021501 (2010).

[60]G. Fredrickson, *The equilibrium theory of inhomogeneous polymers* (Oxford University Press, USA, 2013).

[61]G. V. Efimov, and E. A. Nogovitsin, "The partition functions of classical systems in the gaussian equivalent representation of functional integrals", Physica A: Statistical Mechanics and its Applications **234**, 506–522 (1996).

[62]S. A. Baeurle, M. Charlot, and E. A. Nogovitsin, "Grand canonical investigations of prototypical polyelectrolyte models beyond the mean field level of approximation", Phys. Rev. E **75**, 011804 (2007).

[63]E. A. Nogovitsyn, and Y. A. Budkov, "Development of the theory of a self-consistent field for polyelectrolyte solutions", Russ. J. Phys. Chem. A **85**, 1363–1368 (2011).

[64]Y. Budkov, E. Nogovitsyn, and M. Kiselev, "The model of a polyelectrolyte solution with explicit account of counterions within a self-consistent field theory", Russ. J. Phys. Chem. A **87**, 638–644 (2013).

[65]A. L. Kolesnikov, Y. A. Budkov, and E. A. Nogovitsyn, "Coarse-grained model of glycosaminoglycans in aqueous salt solutions. a field-theoretical approach", J. Phys. Chem. B **118**, 13037–13049 (2014).

[66]C.-Y. Shew, and A. Yethiraj, "Self-consistent integral equation theory for semi-flexible chain polyelectrolyte solutions", J. Chem. Phys. **113**, 8841 (2000).

[67]C.-Y. Shew, and A. Yethiraj, "Monte carlo simulations and self-consistent integral equation theory for polyelectrolyte solutions", J. Chem. Phys. **110**, 5437 (1999).

[68]M. J. Stevens, and K. Kremer, "The nature of flexible linear polyelectrolytes in salt free solution: a molecular dynamics study", J. Chem. Phys. **103**, 1669 (1995).

[69]P. J. Flory, *Principles of polymer chemistry* (Cornell University Press, 1953).

[70]Z.-G. Wang, "50th anniversary perspective: polymer conformation: a pedagogical review", Macromolecules **50**, 9073 (2017) 10.1021/acs.macromol.7b01518.

[71]D. Yang, and Q. Wang, "Unified view on the mean-field order of coil-globule transition", ACS Macro Lett. **2**, 952 (2013).

[72]O. Ptitsyn, and I. Eizner, "The theory of helix-coil transitions in macromolecules", Biofizika **10**, 3 (1965).

[73]P. G. De Gennes, "Collapse of a polymer chain in poor solvents", J. Phys. Lett. Paris **36**, 55 (1975).

[74]L. D. Landau, E. Lifshitz, and L. Pitaevskii, *Electrodynamics of continuous media*, trans. by J. Bell, M. Kearsley, and J. Sykes, 2nd ed., Vol. 8 (Pergamon Press, 1984).

[75]A. V. Dobrynin, and M. Rubinstein, "Theory of polyelectrolytes in solutions and at surfaces", Prog. Polym. Sci. **30**, 1049–1118 (2005).

[76]P. Zhang, N. M. Alsaifi, J. Wu, and Z.-G. Wang, "Salting-out and salting-in of polyelectrolyte solutions: a liquid-state theory study", Macromolecules **49**, 9720 (2016).

[77]H. Eisenberg, and G. R. Mohan, "Aqueous solutions of polyvinylsulfonic acid: phase separation and specific. interactions with ions, viscosity, conductance and potentiometry", J. Phys. Chem. **63**, 671–680 (1959).

[78]N. Volk, D. Vollmer, M. Schmidt, W. Oppermann, and K. Huber, "Conformation and phase diagrams of flexible polyelectrolytes", Adv. Polym. Sci. **166**, 29 (2004).

[79]D. Priftis, N. Laugel, and M. Tirrell, "Thermodynamic characterization of polypeptide complex coacervation", Langmuir **28**, 15947 (2012).

[80]D. Priftis, and M. Tirrell, "Phase behaviour and complex coacervation of aqueous polypeptide solutions", Soft Matter **8**, 9396–9405 (2012).

[81]A. G. Moreira, and R. R. Netz, "Phase behavior of three-component ionic fluids", Eur. Phys. J. D **13**, 61 (2001).

[82]S. L. Perry, and C. E. Sing, "Prism-based theory of complex coacervation: excluded volume versus chain correlation", Macromolecules **48**, 5040–5053 (2015).

[83]P. Zhang, N. M. Alsaifi, J. Wu, and Z.-G. Wang, "Salt partitioning in complex coacervation of symmetric polyelectrolytes", Macromolecules **51**, 5586 (2018) DOI:10.1021/acs.macromol.8b00726.

[84]K. T. Delaney, and G. H. Fredrickson, "Theory of polyelectrolyte complexation—complex coacervates are self-coacervates", J. Chem. Phys. **146**, 224902 (2017).

[85]J. Qin, D. Priftis, R. Farina, S. L. Perry, L. Leon, J. Whitmer, K. Hoffmann, M. Tirrell, and J. J. de Pablo, "Interfacial tension of polyelectrolyte complex coacervate phases", ACS Macro Lett. **3**, 565 (2014).

[86]L. Li, S. Srivastava, M. Andreev, A. Marciel, J. de Pablo, and M. Tirrell, *Submitted*, 2018.

[87]J. Qin, *Private communications*, 2018.

[88]Q. Liao, A. V. Dobrynin, and M. Rubinstein, "Molecular dynamics simulations of polyelectrolyte solutions: osmotic coefficient and counterion condensation", Macromolecules **36**, 3399 (2003).

[89]A. Deshkovski, S. Obukhov, and M. Rubinstein, "Counterion phase transitions in dilute polyelectrolyte solutions", Phys. Rev. Lett. **86**, 2341 (2001) 10.1103/PhysRevLett.86.2341.

[90]J.-M. Y. Carrillo, and A. V. Dobrynin, "Polyelectrolytes in salt solutions: molecular dynamics simulations", Macromolecules **44**, 5798–5816 (2011).

[91]Z.-G. Wang, "Chain dimensions in amorphous polymer melts", Macromolecules **28**, 570 (1995).

[92]P. Grzywacz, J. Qin, and D. C. Morse, "Renormalization of the one-loop theory of fluctuations in polymer blends and diblock copolymer melts", Phys. Rev. E **76**, 061802 (2007).

[93]J. Qin, and D. C. Morse, "Renormalized one-loop theory of correlations in polymer blends", J. Chem. Phys. **130**, 224902 (2009).

[94]J. Qin, and D. C. Morse, "Fluctuations in symmetric diblock copolymers: testing theories old and new", Phys. Rev. Lett. **108**, 238301 (2012).

Chapter 4

IONIC ATMOSPHERE VS. COUNTERION CONDENSATION: FROM WEAK TO INTERMEDIATE ELECTROSTATIC CORRELATIONS

We give a unified account of electrostatic fluctuations of flexible polyelectrolytes, from ionic atmospheres described by weak coupling (corresponding to the free energy of linear charge density responses) to intermediate coupling (where counterion condensation becomes important). Over a broad range of charge fractions or interaction strengths, electrostatic fluctuations renormalize intrachain structure and couple weak fluctuations with counterion condensation; this adaptive intrachain structure is described by the recently-developed renormalized Gaussian fluctuation (RGF) theory, which self-consistently accounts for the coupling of thermodynamics with changing chain conformations. At higher interaction strengths the chain structure is determined self-consistently alongside counterion condensation, which we treat via a tight-binding population of condensed counterions. We elucidate the relative importance of the ionic atmosphere and counterion condensation, and find that at typical coupling strengths $l_b/b \gtrsim 1$ the relative contribution of counterions is actually found to *decrease* with increasing concentration. From our theory we also identify a comprehensive electrostatic binding constant that describes how screening, chain structure, and degree of condensation modulates the driving force for counterion condensation. The choice of chain model and charge renormalization scheme needs to be made carefully – the typical convention of completely neutralizing the counterion can lead to the unphysical effect of suppressing phase separation in salt-free solutions at all interaction strengths. To remedy this, we retain the discrete nature of the polyelectrolyte backbone and the counterions; in the far field, these counterion-backbone pairs act as dipoles, and their fluctuations lead to phase separation in salt-free polyelectrolyte solutions.

4.1 Introduction

Charge correlations underpin the phenomenology and behavior of charged macromolecules. A particularly provocative effect is when the correlations of the small ions lead to effective attraction [1, 2] and even phase-separation between like-charged macromolecules.[3–7] Physically, charge correlations reflect the fact that

charges are preferentially surrounded by opposite charges (conversely, like-charges are repelled), reducing the effective charge seen away from the charge.

The earliest acknowledgment of such a charge correlation effect is by Debye and Hückel (DH), who calculated the linear density response of simple electrolytes about tagged charges;[8] this formalized the notion of an "ionic atmosphere" and the screened Coulomb (Yukawa) potential. The DH linear response calculation can be applied to integrate out small ion degrees of freedom in colloidal and polymer systems,[5, 8–10] and results in the same pairwise-additive screened Coulomb potential between macromolecular charges. We note that the linear response approach, also known as the Random Phase Approximation can also be used to integrate out macromolecular degrees of freedom.[11–13] In this chapter, we will formally refer to the electrostatic response calculated via linear response approaches as the "linearized fluctuations" or more informally the (generalized) "ionic atmosphere."

It is not hard to see that such linear response theories will be inadequate when stronger electrostatic interactions and correlations are involved. At high enough interaction strengths there will necessarily be counterion condensation, an effect first elucidated by Manning and Oosawa for charged polymers, or polyelectrolytes.[14–18] They idealized the polyelectrolyte as an infinitely long cylinder and found that above a certain linear charge density, counterions are condensed onto the polyelectrolyte and renormalize the effective charge of the cylinder.

Leading-order effects of counterion condensation on thermodynamic quantities like the osmotic coefficient can be readily understood – the condensed counterions lose their translational entropy, resulting in an osmotic coefficient plateau proportional to the fraction of uncondensed counterions; conversely the release of counterions leads to a free energy change of kT per released ion. Overall, counterion condensation has informed many studies of polyelectrolytes – it serves as a way to reason about or heuristically treat the strong-correlations between counterions and highly charged polyelectrolytes, reducing the system to a simpler one with only modestly charged polyelectrolytes.[19–22]

Due to the historic importance and wide application of DH theory, the ionic atmosphere is often used synonymously with electrostatic correlations, but we emphasize again that both counterion condensation and the linearized electrostatic response that underpins the DH ionic atmosphere are different *forms* of electrostatic correlations. Even once the translational entropy reduction effect of counterion condensation is considered, the linearized electrostatic fluctuations (of both small ion and macro-

molecular degrees of freedom), which also reduce the osmotic pressure, must still be accounted for in order to produce effective attractions and/or phase separation.[4, 5, 23, 24]

A complicating factor for flexible polyelectrolytes is that, *well before* counterion condensation sets in, electrostatic fluctuations and correlations first act to change the conformation of polyelectrolyte chains,[23, 25–27] which can also significantly affect thermodynamic properties. Intriguingly, after the renormalization of the chain conformations, the remaining linear-response fluctuations of unbound counterions and electrostatically stiffened chains can produce thermodynamic signatures characteristic of counterion condensation, such as the aforementioned osmotic coefficient plateau.[23, 27] This raises a conceptual question: if both counterion condensation and the ionic atmosphere characterize the accumulation of opposite charges next to each other, and both effects result in similar thermodynamic effects, how should one distinguish between the two? It is an outstanding challenge to construct a theory that self-consistently accounts for the many different ways that charge correlations can manifest: from weak-coupling ionic atmospheres, [5, 8–10] to chain conformational changes that accompany intermediate couplings,[23, 25, 26] to the onset of strong coupling effects like counterion condensation.[14–18]

The most common theoretical treatment of counterion condensation introduces a tightly-bound population of counterions in the vincinity of monomers, alongside an "unbound" population.[9, 12, 28–32] Theories that invoke a tightly-bound population of counterions often introduce the notion of a local binding constant. The binding constant can range from a phenomenological parameter,[33] to an intrinsic piece describing remaining effects after others (i.e. VO-type screening, excluded volume capture) have been estimated,[32] to identification with a bare Coulomb interaction energy or backbone-solvent dielectric mismatch.[12, 30, 31] The simplest estimate of the binding constant $\ln K$ estimate it to be driven by an interaction energy ϵ of order l_b/σ, the *unscreened* electrostatic interaction of two charges,[12] where l_b is the Bjerrum length characterizing the strength of electrostatic interactions and σ is the average ion size. However, this estimate neglects the long-ranged nature of electrostatics and chain connectivity – there will necessarily be interactions with other monomers in the chain and condensed counterions, meaning that counterion binding should be a non-local and cooperative binding effect that reflects chain connectivity and conformations.

After introducing a description of counterion condensation, it is necessary for a the-

ory to account for the correlations of uncondensed charges. (We again note previous work's imprecise terminology separating counterion condensation and electrostatic correlations) These remaining electrostatic correlations have been modeled using a variety of approaches, including Voorn-Overbeek-type approximations [32], Random Phase Approximation [12], and double screening theory [30, 31]).

However, there are still two important contributions to electrostatic correlations. As discussed, one of these important effects is chain conformational changes – this is not a widely appreciated fact and has seen only limited study.[30, 31] Secondly, the electrostatic fluctuations of the *condensed* charges are also important, and will necessitate a more detailed consideration of the charge structure of the bound state. These residual charge fluctuations are important when treating the ion pairing and phase separation of simple electrolytes,[34] and they have also been implicated in the coil-globule phase transitions of polyelectrolytes.[35–39] Yet for simplicity, the tightly-bound counterion population is often accounted for by identically neutralizing both the condensed charges and sites.[12, 29, 31, 32] Such a strict neutralization of the counterion and backbone charges eliminates much of the charge fluctuations of the counterion and its condensation site. To recover these residual charge fluctuation effects, theories have had to supplement their free energy expressions with density-functional expressions,[37, 40] or with added dipole interaction terms.[30, 39]

In this chapter, we strive for a unified exposition of electrostatic interactions that accounts for the aforementioned effects: chain connectivity and fluctuations of *both* condensed and uncondensed charges. In section 4.2 we describe how to combine fluctuations, described using the recently-proposed renormalized Gaussian fluctuation (RGF) framework, which can account for changes in chain structure, with a tight-binding picture. In the vein of colloid charge-renormalization theories,[4, 5, 41–44] we give a thermodynamic interpretation for the loosely bound counterions as those providing the linear density response to the (conformation-adapted)[23, 27] macromolecule and its strongly "bound" population of condensed counterions. Our theory allows us to separate the thermodynamic effects associated with the translational entropy loss of bound counterions from the remaining linearized fluctuations, and compare their relative contributions.

To understand the fluctuations of condensed charges we relax the assumption of identically neutralizing the condensed charges and sites. We retain the discreteness of both the counterion and the charged site, and each condensed pair is characterized

by a length parameter d and in the far field contributes a dipolar electrostatic response; no new dipole interaction terms need to be introduced. Small values of d suppress charge fluctuations and is expected to stabilize the solution against phase separation, while larger (but still reasonable) values of d allow for phase separation. The extent of residual charge fluctuations is thus seen to be an important determinant of phase separation. We also compare to models with continuous backbones and either smeared or discrete condensed counterions.

Crucially, our derivation allows the transparent identification of an effective *electrostatic* binding constant that captures the direct interaction between condensing charges as well as the non-local effects due to chain connectivity and correlation/screening. This careful development of the electrostatic binding coefficient allows us to appreciate the effects of screening and chain-connectivity on the electrostatic binding, and mitigates risks of double-counting physical effects when piecing together different electrostatic theories into a polyelectrolyte theory of counterion condensation. To emphasize the physical content of the electrostatic binding constant, we discuss how other counterion condensation theories in literature can be understood in terms of our expression for the electrostatic binding constant, using Voorn Overbeek-type estimates of the binding constant as a concrete example.

Following, in section 4.3 we present numerical results, first studying the dependence of counterion binding on salt and polymer concentration. Using the self energy we explain differences in counterion binding between different chain structures and charge models, and we decompose the binding constant to distinguish between a bare Coulombic and finite-concentration correlation contributions to the binding constant. We then track the exchange of counterions between the tightly-bound and loosely-bound populations to evaluate the transition from weak to intermediate fluctuation effects, and present the osmotic coefficient contribution of counterion condensation versus the (renormalized) linearized fluctuations. Finally, we discuss the extent to which counterion condensation stabilizes polyelectrolyte solutions, and the degree to which explicit charge structure is needed to produce expected phase separations in polyelectrolyte solutions.

4.2 Theory

We first present the general, renormalized Gaussian fluctuation variational grand free energy. For details of notation and derivation we refer readers to our previous paper [23] or Ch. 2. To focus on electrostatics, the main interaction considered is

the electrostatic interaction, which we model as taking place in a linear dielectric medium with constant scaled electric permittivity $\epsilon = \varepsilon/(\beta e^2)$. We do not consider other interactions like the Flory-Huggins χ interaction, though they can readily be added. To simplify notation, we will use k_BT as the unit of energy and e as the unit of charge, so we set $\beta = 1$ and $e = 1$. For further simplicity, all monomers are taken to have the same volume v, and Kuhn length of the polymer is taken to be $b = 1$, thus setting the unit of length. We then describe how, within the grand canonical ensemble and a tight-binding framework, counterion condensation can be treated by classifying polyelectrolytes and their condensed counterions collectively as new species. We discuss our proposed models for the charge structure and the physical content of the electrostatic binding constant that arises in the theory.

4.2.1 Introducing tight binding into the renormalized Gaussian fluctuations

Given the position configuration of the species, we can introduce the microscopic density $\hat{\rho}_\gamma$, volume fraction $\hat{\phi}_\gamma = v_\gamma \hat{\rho}_\gamma$, and charge density $\hat{\rho}_\gamma^{chg}$ operators for species γ (which indexes over all solvent, polyelectrolyte, and salt ion species). Within our theory, individual monomeric charges are modeled with a short-ranged charge distribution $z\,h(\mathbf{r} - \mathbf{r}')$ for a charged monomer of valence z located at $\mathbf{r}'$. The charge distribution is chosen to be a Gaussian with a radius a (not necessarily the same as the excluded volume size, but for simplicity we take $a = 0.5$ in this chapter). This smearing is reflected in the charge densities $\hat{\rho}_\gamma^{chg}$, and captures the Born solvation energy of individual ions in a dielectric medium, and produces finite-size corrections to the ion correlation energy. [23, 45]

Given the charge densities, the charged interactions are treated as in a linear dielectric medium, mediated by a Coulomb operator C and with energy H_C. Chain connectivity is accounted through a bonded interaction hamiltonian H_B which depends on the relative positions of the monomers in a polyelectrolyte chain. To complete the description of the system, the excluded volume between all the species is accounted for by an incompressibility constraint $\sum_\gamma \hat{\phi}_\gamma(\mathbf{r}) = 1$ that applies at all $\mathbf{r}$.[46] This constraint is enforced by a Dirac δ-function in its familiar representation $\delta(1 - \sum_\gamma \hat{\phi}_\gamma) = \int \mathcal{D}\eta e^{i\eta(1-\sum_\gamma \hat{\phi}_\gamma)}$, which introduces an incompressibility field η.

The RGF is a *non-perturbative* procedure and consists of writing the grand canonical partition function, carrying out standard field-theoretic transformations, and then following the Gibbs-Feynman Bogoliubov approach by introducing a Gaussian reference action characterized by a Green's function G capturing field fluctuations

about a mean $-i\psi$. The resulting variational grand partition function and free energy are:

$$\Xi_{GFB} = \int \mathcal{D}\eta e^{-W_v[G,\psi;\eta]} \tag{4.1}$$

$$\begin{aligned} W_v[G,\psi;\eta] = &-\frac{1}{2}\ln\left(\frac{\det G}{\det C}\right) - \frac{1}{2}\int d\mathbf{r}d\mathbf{r}'\psi\cdot C^{-1}\cdot\psi \\ &+ \frac{1}{2}\int d\mathbf{r}d\mathbf{r}'[C^{-1}-G^{-1}]G \\ &- \int d\mathbf{r}(i\eta - \rho_{\text{ex}}\psi) - \sum_\gamma \lambda_\gamma \left\langle Q_\gamma \right\rangle . \end{aligned} \tag{4.2}$$

Note that at this point the expressions above are completely general and can accommodate any number of species γ. The last term features species fugacities λ_γ and effective (field-averaged) single-molecule partition functions $\left\langle Q_\gamma \right\rangle$, which are the partition functions of a single molecule of species γ interacting via the effective interaction G and mean fields ψ and η.

Equilibrium is determined by solving for G, ψ, η such that the variational free energy is stationary. For a bulk system without background charges, the stationarity condition for ψ yields a charge-neutrality condition. Treating incompressibility at the mean field level, η is pure-imaginary, and we henceforth define a real field $\mathcal{P} = i\eta$ satisfying:

$$\mathcal{P} = -\frac{1}{v}\log(1-\phi) \tag{4.3}$$

defining ϕ as the total volume fraction $\phi = \sum_{\gamma\neq solv}\phi_\gamma$ of non-solvent species. We define $\left\langle Q_\gamma \right\rangle$ below and the equilibrium relation for G in section 4.2.3, but first note that the self-consistency of the RGF method arises because the average molecular behavior, as described by $\left\langle Q_\gamma \right\rangle$, depends on the Green's function G (via the variational condition), which in turn depends on the molecular structure described by $\left\langle Q_\gamma \right\rangle$.[23]

We now specify to a system with polyelectrolyte chains (p), each with chain length N and charge fraction f, monovalent counterions (+), added monovalent salt pairs (+/−), and neutral solvent (s) . For concreteness take the polyelectrolyte chain to be negatively charged, and take the monovalent counterions to be the same as the

cations in the added salt. For solvent (s) and simple electrolytes $\pm$,

$$\langle Q_s \rangle = \int d\mathbf{r}_s \quad \exp\left[-iv_s\eta\right] \tag{4.4}$$

$$\langle Q_\pm \rangle = Vq_\pm \exp\left[-v_\pm\mathcal{P} - z_\pm\psi\right]$$

$$q_\pm = \exp\left[-\frac{1}{2}\int d\mathbf{r}d\mathbf{r}'\; z_\pm h_\pm \cdot G \cdot z_\pm h_\pm\right] \tag{4.5}$$

The polyelectrolyte expression is a bit more involved. Within the tight-binding model, each charged monomer serves as a binding site for a counterion, and a binding state can be specified by the occupation numbers of each of these sites $\{\sigma_i\}$. Each binding state may still have additional internal degrees of freedom of the counterion in its bound state, along with associated constraints due to sterics or other short-range interactions, and can be subsumed in an *internal* partition function ξ to be detailed shortly.

A natural way to incorporate tight binding into the theory is to introduce a different species for every possible binding configuration $\{\sigma_i\}$; this procedure can be justified by carefully tracking all the combinatorial factors associated with partitioning a system of chains and small ions into these new species. Of course, the fugacities of these new species are not independent, but instead related to those of free polyelectrolyte and cations by

$$\lambda_{\{\sigma_i\}} = \lambda_p \lambda_+^m \tag{4.6}$$

where we have defined the occupancy number $m = \sum_i \sigma_i$, and without loss of generality assumed the counterions are positively charged and labeled by '+'. The sum $\sum \lambda_\gamma \left\langle Q_\gamma \right\rangle$ over these new polyelectrolyte species then becomes

$$\sum_{\{\sigma_i\}} \lambda_\gamma \left\langle Q_\gamma \right\rangle = \lambda_p \sum_{\{\sigma_i\}} \lambda^{m(\{\sigma_i\})} \left\langle Q_{\{\sigma_i\}} \right\rangle \tag{4.7}$$

with the average partition function $\left\langle Q_{\{\sigma_i\}} \right\rangle$ for a specific binding configuration $\{\sigma_i\}$ written as:

$$\lambda_+^m \left\langle Q_{\{\sigma_i\}} \right\rangle = \frac{e^{m\mu_+}}{m! v_+^m} e^{\left[-(N_p+m)v\mathcal{P} - (m - Nf_{p\pm})z\psi\right]} V q_p(\{\sigma_i\}) \tag{4.8}$$

$$q_p(\{\sigma_i\}) = \frac{1}{V}\int \mathcal{D}\mathcal{R} \prod^m dr_{+c} \Omega(\{r_{+c}\};\{\sigma_i\}) e^{-H_B}$$

$$\exp\left[-\frac{1}{2}\int d\mathbf{r}d\mathbf{r}'\; \hat{\rho}_{p1}^{\text{chg}}(\mathbf{r};\{r_{+c}\},\{\sigma_i\}) \right.$$

$$\left. \cdot\, G(\mathbf{r},\mathbf{r}') \cdot \hat{\rho}_{p1}^{\text{chg}}(\mathbf{r}';\{r_{+c}\},\{\sigma_i\}) \right] \tag{4.9}$$

where $\Omega(\{r_{+c}\};\{\sigma_i\})$ represents constraints on the configuration space of the condensed counterion coordinates r_{+c}, i.e. single occupancy or other internal degrees of freedom constraints, and $\hat{\rho}^{\text{chg}}_{p1}$ represents the charge density resulting from the chain specified by coordinates $\mathcal{R}$ and condensed counterions r_{+c}.

A convenient result of working in the grand canonical ensemble is that, after summing over all possible binding configurations $\{\sigma_i\}$, one can re-interpret the polyelectrolyte as a *single* species that is itself in grand-canonical equilibrium with the counterions:

$$\lambda_p \left\langle Q_p \right\rangle \equiv \lambda_p \sum_{\{\sigma_i\}} \lambda^{m(\{\sigma_i\})} \left\langle Q_{\{\sigma_i\}} \right\rangle \tag{4.10}$$

Thus the introduction of polyelectrolyte-counterion species was only a temporary tool to account for the binding states associated with the tight-binding model.

In general, the single chain partition functions $q_p(\{\sigma_i\})$ can be estimated using simulation, but for ease of calculation we generalize a one-parameter Flory-type decomposition that was shown to give good results for homopolyelectrolytes.[23, 27]

To proceed we now specify the constraint that counterions are not allowed to condense onto the same site, and that remaining degrees of freedom on configurations of each bound counterion can be summarized by an internal partition function ξ. For example, the "capture volume" described previously [32] would be included in this term. Then, to simplify the summation over all possible binding configurations we first make the common approximation that all configurations with m counterions have similar structures and energies, and hence are well-approximated by an *average* configurational partition function that depends only on the occupancy m:

$$q_p(\{\sigma_i\}) \approx e^{-F(m)+m\ln\xi} \tag{4.11}$$

where the self-energy (or single-chain free energy) $F(m)$ follows from minimization over an effective one-parameter (l_{eff}) Flory-type decomposition:[23]

$$F(m) = \min_{l_{\text{eff}}} \left(F_{\text{ent}}(l_{\text{eff}}) + F_{\text{int}}(l_{\text{eff}};m) \right) \tag{4.12}$$

$$F_{\text{ent}} = -\frac{3}{2} N \ln\left(1 - \frac{\alpha^2}{N}\right) - 3\ln(\alpha) \tag{4.13}$$

$$F_{\text{int}} = \frac{1}{4\pi^2} \int k^2 dk\ \tilde{G}(k) \tilde{S}^{\text{chg}}_p(k; l_{\text{eff}}, m) \tag{4.14}$$

where the chain expansion α^2 is approximated as

$$\alpha^2 = \left\langle R_{ee}^2 \right\rangle / R_{ee,0}^2 = 2(l_{\text{eff}}/b)\left[1 - (l_{\text{eff}}/Nb)\left(1 - e^{-Nb/l_{\text{eff}}}\right)\right], \tag{4.15}$$

and the charge structure S_p^{chg} will be presented in the next subsection 4.2.2. The single chain partition function can then be written

$$\begin{aligned}\left\langle Q_p \right\rangle \approx \sum_m \frac{(Nf)!}{(Nf-m)!}\frac{e^{m(\mu_+ + \ln\xi)}}{m! v_+^m} V \\ \exp\left[-(N_p+m)v\mathcal{P} - (m - Nf_{p\pm})z\psi - F(m)\right]\end{aligned} \tag{4.16}$$

The combinatorial factor enumerates the number of ways m ions can condense onto Nf charged sites, and the second factor $\exp\left[m(\mu_+ + \ln\xi)\right]$ represents the effective fugacity of the m condensed ions. The last factor is the Boltzmann weight of a polyelectrolyte with m condensed ions, including both the mean-field excluded volume, mean electrostatic potential, and free energy $F(m)$ of the polyelectrolyte-condensed counterion species.

4.2.2 Charge Model and Self-Energy Decomposition of Polyelectrolyte With Condensed Counterions

At this point, Eq. (4.14) gives an estimate of the interaction energy provided we know the chain-condensed-counterion charge structure factor $S_p^{\text{chg}}(k; l_{\text{eff}}, m)$, which represents an average over the counterion binding configurations of m condensed counterions and, following previous work, is further parameterized by an effective persistence length l_{eff} that is variationally determined.[23] However, we still have to propose a reasonable approximation for the *charge* structure factor, which will necessitate independent choices for both *chain structure* (i.e. Gaussian, self-consistent flexible chain, or semiflexible rod), described by a function $\tilde{\omega}$ that we present towards the end of this section, and a *charge model*, i.e. the assumption of continuous or discrete charges and a more detailed description of the structure of condensed counterions and their condensation site. Different charge models will lead to different energies of counterion condensation and different residual charge fluctuations.

A common approximation in tight-binding counterion condensation theories is that the condensed counterion coordinates r_{+c} are restricted to *exactly* neutralize polyelectrolyte backbone charges; in such models the polyelectrolyte backbone charge and renormalizing counterions are often treated in a smeared-out fashion with a

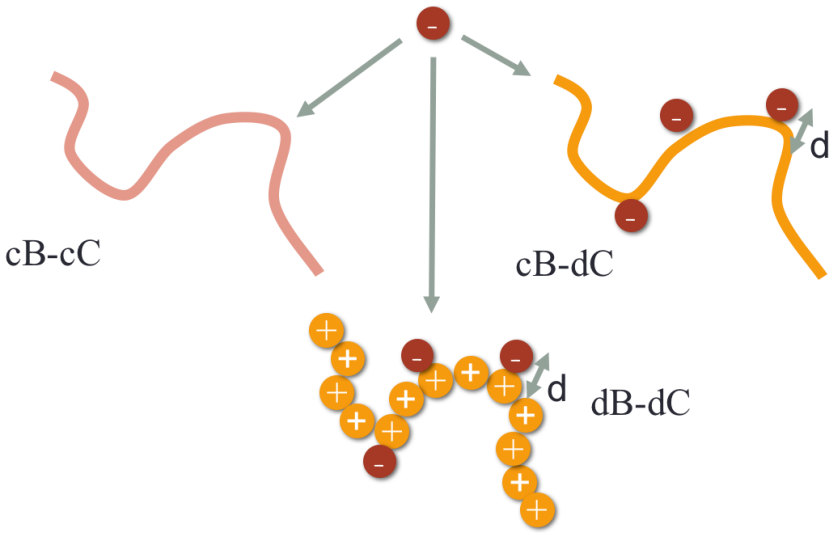

Figure 4.1: Charge model S_p^{chg} of the combined polyelectrolyte-condensed counterions object. We consider continuous-backbone plus continuous counterion (cB-cC), continuous-backbone plus discrete counterion (cB-dC), and discrete-backbone plus discrete counterion (dB-dC). The cB-dC and dB-dC models have a dipole parameter d dictating how much fluctuations are left upon condensation. Uncondensed counterions are always treated as discrete charges with finite size described by a smearing function h.

continuous backbone, which we formally express as

$$\tilde{S}_p^{\text{chg}}(k,x) = (1-x)^2 S_{pp}^{\text{chg}}(k) \tag{4.17}$$

$$S_{pp}^{\text{chg}} = Nf \cdot Nf\tilde{\omega}\tilde{h}^2 \tag{4.18}$$

where $x = m/Nf$ is the fraction of condensed charges, $\tilde{h}$ is the Fourier transform of the spread-charge distribution, (which for simplicity is taken to be the same for all species), and $\tilde{\omega}$ is again the average intra-chain per-monomer structure specified at the end of this section. Note that the continuous nature of the backbone is because there is no self-scattering term. We call Eqs. (4.17) plus Eq. (4.18) the **C**ontinuous-**B**ackbone-**C**ontinuous-**C**ounterion (cB-cC) model.

As we will discuss in the results this exact neutralization over-estimates the degree of charge-stabilization, and can lead to counter-intuitive results. To make transparent the physical assumptions in the cB-cC model and its relations to the new charge models that we will propose, it is helpful to decompose the charge structure of the polyelectrolyte-plus-counterion species into explicit polyelectrolyte-polyelectrolyte (pp), polyelectrolyte-counterion (pc), and counterion-counterion (cc)

contributions:[12]

$$\tilde{S}_p^{\mathrm{chg}}(k; l_{\mathrm{eff}}, x) = S_{pp}^{\mathrm{chg}} - 2S_{pc}^{\mathrm{chg}} + S_{cc}^{\mathrm{chg}} \tag{4.19}$$

The cB-cC charge model then corresponds to the following choices for the partial structure factors:

$$\begin{aligned} S_{pp}^{\mathrm{chg}} &= Nf \cdot Nf \cdot \tilde{\omega}\tilde{h}^2 \\ S_{pc}^{\mathrm{chg}} &= Nfx \cdot Nf \cdot \tilde{\omega}\tilde{h}^2 \\ S_{cc}^{\mathrm{chg}} &= Nfx \cdot Nfx \cdot \tilde{\omega}\tilde{h}^2 \end{aligned} \tag{4.20}$$

Such a decomposition will help comparisons with charge models that have discrete charges.

We now propose two more models of the charge structure. The first presumes a continuous charge distribution on the backbone, as has usually been assumed in the past,[11, 13, 29, 31] but we introduce the discrete nature of the counterions in the counterion-counterion (cc) correlation.

$$\begin{aligned} S_{pp}^{\mathrm{chg}} &= Nf \cdot Nf\tilde{\omega}\tilde{h}^2 \\ S_{pc}^{\mathrm{chg}} &= Nfx \cdot Nf\tilde{\omega}\tilde{\Gamma}\tilde{h}^2 \\ S_{cc}^{\mathrm{chg}} &= Nfx[1 + (Nfx - 1)\tilde{\omega}]\tilde{\Gamma}^2\tilde{h}^2 \end{aligned} \tag{4.21}$$

The discrete nature of the condensed counterions can most easily be seen by looking at the limit when the chain connectivity ω is zero: in such a limit S_{cc}^{chg} is still finite, representing the self-scattering of the explicit counterions. By comparison, the cB-cC model Eq. (4.20) has no such self-scattering.

To model the residual charge fluctuations of ion pairs that do not identically neutralize each other, in Eq. (4.21) we also introduced a "counterion distribution" $\Gamma(r, d) = \delta(|r| - d)$ about condensed sites, that in Fourier space is

$$\tilde{\Gamma}(k, d) = \sin(kd)/kd \tag{4.22}$$

and contains a length d; Γ thus locates charges at a finite distance from a backbone monomer. One might naturally expect d to be roughly the monomer diameter σ, but in practice it is sensitive to other molecular details and we prefer to treat it as a parameter measuring the *degree* of residual charge fluctuations. Importantly, in the $x \to 1$ limit, Eq. (4.19) is no longer identically 0, and charge fluctuations are

retained even when the chain is fully condensed. Although a decomposition of the charge structure into pp, pc, and cc components was proposed previously,[12] the previous work did not consider residual fluctuations and finite d. We call Eq. (4.19) plus Eq. (4.21) the **C**ontinuous-**B**ackbone-**D**iscrete-**C**ounterion (cB-dC) model.

Another approximation can be made if one wishes to retain the discrete nature of the backbone charged sites that the counterions can bind to:

$$\begin{aligned} S_{pp}^{\text{chg}} =& Nf[1 + (Nf - 1)\tilde{\omega}]\tilde{h}^2 \\ S_{pc}^{\text{chg}} =& Nfx[1 + (Nf - 1)\tilde{\omega}]\tilde{\Gamma}\tilde{h}^2 \\ S_{cc}^{\text{chg}} =& Nfx[1 + (Nfx - 1)\tilde{\omega}]\tilde{\Gamma}^2\tilde{h}^2 \end{aligned} \tag{4.23}$$

which, when combined with Eq. (4.19) we term the **d**iscrete-**B**ackbone-**d**iscrete-**C**ounterion (dB-dC) model. In contrast to the cB-dC model Eq. (4.21), note that when $d = 0$, for charges of equal size (i.e. the same ion spread charge distribution h) this discrete backbone model yields a structure factor that is identically zero in the $x \to 1$ limit because the charged site and the counterion exactly overlap and cancel; this $x \to 1, d \to 0$ limit is analogous to the smeared renormalization model Eq. (4.17) in the sense that the charge fluctuations are identically eliminated (if charges are of equal size). In this dB-dC charge model Eq. (4.23), nonzero values of d are required to recover finite-strength dipoles.

A nice feature of the dB-dC model can be seen by first rearranging the sum Eq. (4.19) of the dB-dC terms Eq. (4.23):

$$S_{dBdC}^{\text{chg}} = Nf\tilde{h}^2\Big[(1 - x) + 2x(1 - \tilde{\Gamma}) \tag{4.24}$$

$$+ \tilde{\omega}[Nf - 1 + x(Nfx - 1)\tilde{\Gamma}^2 - 2x\tilde{\Gamma}(Nf - 1)]\Big] \tag{4.25}$$

written this way, we reveal the self-scattering of the $Nf(1 - x)$ condensed charges, the chain connectivity contributions proportional to $\tilde{\omega}$, and the charge structure $2Nfx(1 - \Gamma)$ of the condensed backbone-counterion charge pairs. In the far-field, the charge structure of the pairs behaves as a dipole

$$1 - \tilde{\Gamma} \approx k^2 d^2/6. \tag{4.26}$$

When substituted into the Green's function expression Eq. (4.29) presented in the next section, counterion-backbone charge pairs will naturally screen as dipoles, without the need for explicit introduction of dipole interactions. When $d = 0$, there

is are no more dipolar fluctuations, qualitatively similar to the cB-cC model. It is also instructive to note that the cB-dC model also leads to dipolar screening but, in contrast to the dB-dC model, the cB-dC model delocalizes the backbone charge over the entire chain and yields a counterion-backbone charge pair structure of the form $\tilde{\omega} - \tilde{\Gamma}$, which will yield a dipole length set by the chain size.

Lastly, l_{eff} enters through $\tilde{\omega}$, an averaged per-monomer structure factor that interpolates between Gaussian chains at low k and rodlike behavior at high k,[23]

$$\tilde{\omega}(k) = \frac{\exp[-kl_{\text{eff}}/2]}{1 + k^2 N b l_{\text{eff}}/6} + \frac{1 - \exp[-kl_{\text{eff}}/2]}{1 + kNb/\pi}. \tag{4.27}$$

Eq. (4.19) above defines the average structure at fixed l_{eff} and m, and the final structure factor of the polyelectrolyte species should be averaged over m

$$\tilde{S}_p^{chg}(k) = \frac{\sum_m \tilde{S}_p^{chg}(k,m) \frac{(Nf)!}{(Nf-m)!} \frac{e^{m(\mu_+ + \ln \xi)}}{m! v_+^m} \exp\left[-(N_p + m)v\mathcal{P} - (m - Nf_{p\pm})z\psi - F(m)\right]}{\sum_m \frac{(Nf)!}{(Nf-m)!} \frac{e^{m(\mu_+ + \ln \xi)}}{m! v_+^m} \exp\left[-(N_p + m)v\mathcal{P} - (m - Nf_{p\pm})z\psi - F(m)\right]}. \tag{4.28}$$

As will be seen in section 4.2.3, for finite concentrations of polymer, the charge structure factor will modify the effective solution screening and the free energy $F(m)$ Eq. (4.12), and the two need to be solved self-consistently. To facilitate these calculations we approximate the average Eq. (4.28) with the value of $\tilde{S}_p^{chg}$ at the most-likely value of m, as determined by a maximum-term approximation detailed in section 4.2.4.

4.2.3 Solution Screening and Thermodynamic Quantities

Having defined the charge structure, the RGF condition for Green's function is written in Fourier space as

$$\tilde{G}(k) = \frac{1}{\epsilon[k^2 + \tilde{\kappa}^2(k)]}, \tag{4.29}$$

from which we identify

$$\tilde{\kappa}^2(k) = 2\tilde{I}(k)/\epsilon \tag{4.30}$$

as the *wavevector-dependent* screening *function*, a generalization of the Debye screening constant,[23] with the ionic strength function $\tilde{I}(k)$ given by

$$2\tilde{I}(k) = \sum_\gamma \frac{\rho_\gamma}{N_\gamma} \tilde{S}_\gamma^{chg}(k) \tag{4.31}$$

where $\tilde{S}_\gamma^{chg}(k)$ is the *single-molecule* charge structure factor. Again, for the polyelectrolyte it is Eq. (4.19) averaged over m Eq. (4.28), while for monovalent small ions it is $S_\pm^{chg}(k) = \tilde{h}^2$.

Importantly, the Green's function characterizes the electrostatic field fluctuations in the system and acts as a renormalized (screened) electrostatic interaction. As alluded to earlier, the dB-dC charge model Eq. (4.23) can be rearranged to reveal that at low k, polyelectrolyte charged sites with condensed counterions yield a charge structure that contribute (in addition to connectivity effects) dipolar screening terms $\sim k^2$ Eq. (4.26) to the screening function Eq. (4.30); to leading order these dipolar terms act to renormalize (in the low-k limit) the dielectric constant in the Green's function equation Eq. (4.29).

Evaluating the grand potential Eq. (4.2) at its equilibrium (self-consistent RGF) value yields the osmotic pressure

$$\begin{aligned}\Pi = &-\frac{1}{4\pi^2}\int_0^\infty k^2\, dk\left[\ln\left(1+\frac{\tilde{\kappa}^2(k)}{k^2}\right)-\frac{\tilde{\kappa}^2(k)}{k^2+\tilde{\kappa}^2(k)}\right]\\ &-\frac{1}{v}\Big(1+\log(1-\phi)\Big)+\frac{1-\phi}{v}+\rho_+ +\rho_- +\frac{\rho_p}{N_p}.\end{aligned} \tag{4.32}$$

In the above expression, ρ_+ only refers to the *free* cations, and does not include the bound counterions.

The per-ion and per-*chain* chemical potentials are determined from the relationship $\rho_\gamma = \lambda_\gamma \langle Q_\gamma \rangle$:

$$\begin{aligned}\mu_\pm &= \ln(\rho_\pm v_\pm) \;+\; v\mathcal{P} \;+\; z_\pm\psi \;+u_\pm\\ \mu_p &= \ln\left(\frac{\rho_p v_p}{N_p}\right)+vN_p\mathcal{P}+z_{p\pm}^{tot}\psi+u_p\end{aligned} \tag{4.33}$$

The first three terms in both chemical potential expressions Eq. (4.33) are the same as in a mean-field analysis of a bulk solution. The last terms u_γ are the small ion self energies $u_\pm$ and the non-mean-field contribution u_p to the polymer chemical potential

$$u_\pm = -\ln q_\pm \tag{4.34}$$

$$u_p = -\ln\left[\sum_m \frac{(Nf)!}{(Nf-m)!}\frac{e^{m(\ln\rho_+ v_+ +\ln\xi+u_+)}}{m!v_+^m}e^{-F(m)}\right] \tag{4.35}$$

We remark that Eq. (4.32) has the same terms as the original RGF theory, which does not have an explicit tight binding population. Counterion condensation enters

only through the modification of the loose counterion density ρ_+ and the effective charge structure hiding in the ionic screening function $\tilde{\kappa}^2(k)$ Eq. (4.30). Once the self-consistent $\tilde{\kappa}^2(k)$ is determined, the remaining Fourier integral has the same form as in a linear response theory, and we will call this the "linearized" fluctuation contribution:

$$\beta\Pi^{lin} = -\frac{1}{4\pi^2}\int_0^\infty k^2\, dk \left[\ln\left(1+\frac{\tilde{\kappa}^2(k)}{k^2}\right) - \frac{\tilde{\kappa}^2(k)}{k^2+\tilde{\kappa}^2(k)}\right] \tag{4.36}$$

For point charges, this linearized fluctuation contribution corresponds to a size-corrected Debye-Hückel fluctuation energy describing the correlation energy contained in the ionic atmosphere. Given prescribed chain structure and hence ionic screening function $\tilde{\kappa}^2(k)$, Eq. (4.36) generalizes the ionic atmosphere to polyelectrolytes, and implicitly includes the effect of changing chain structure.

The remaining contribution to the osmotic pressure corresponds to the counterion translational entropy change of condensed counterions, which we term the counterion condensation contribution to the osmotic pressure:

$$\beta\Pi^{cc} = \rho_+ - \rho_+^0 = -\langle x\rangle\,\rho_+ \tag{4.37}$$

where ρ_+^0 is the total counterion concentration, including both bound and unbound ions.

4.2.4 Electrostatic Binding Constant

To define the driving force for counterion condensation it is convenient to use the maximum-term approximation:

$$\begin{aligned}\left\langle Q_p\right\rangle \approx & V e^{-N_p v\mathcal{P} - Nf_{p\pm} z\psi}\cdot \\ & \max_m \frac{(Nf)!}{(Nf-m)!}\frac{e^{m(\ln\rho_+ v_+ + \ln\xi + u_+)}}{m! v_+^m} e^{-F(m)}\end{aligned} \tag{4.38}$$

Using Stirling's approximation for the factorials, and expressing $m = xNf$, the maximum term-condition is equivalent to

$$\begin{aligned}0 = & \ln\rho_+ - \ln\frac{x}{1-x} \\ & + \ln\xi + u_+(G) - \frac{1}{Nf}\frac{\partial F(xNf)}{\partial x}\bigg|_G\end{aligned} \tag{4.39}$$

The first two terms correspond to translational entropy of unbound counterions and combinatorial entropies of bound counterions, and the third term $\ln\xi$ again describes the internal degrees of freedom of the counterion in its bound state.

We *identify* the binding constant for the equilibration of condensed and uncondensed charged sites as

$$K = \frac{x}{1-x} = \rho_+ \xi \cdot K_{el} \tag{4.40}$$

as driven by a non-electrostatic (translational entropy and internal partition function ξ) and an electrostatic K_{el} piece. We focus our attention on the electrostatics and study the electrostatic binding constant K_{el}, given by the last two terms of Eq. (4.39) as

$$\ln K_{el}(x; G) = -\left(\frac{1}{Nf} \frac{\partial F(xNf)}{\partial x}\bigg|_G - u_+(G) \right), \tag{4.41}$$

which can be interpreted as the electrostatic free energy change of condensing a counterion on the polyelectrolyte chain. Our expressions Eqs. (4.12)-(4.14) for F involves a charge structure factor $\tilde{S}$ Eq. (4.19) that can be decomposed into pp, pc, and cc interactions. Chain connectivity and anti-cooperativity arise naturally as long as the respective structure components incorporate a chain structure factor ($\tilde{\omega}$ Eq. (4.27) in our notation).

There is an implicit dependence of $\ln K_{el}$ on G: $\ln K_{el}$ has components u_+ and $\frac{\partial F(xNf)}{\partial Nfx}$ which are both calculated at the *equilibrium* G, i.e. at fixed concentration and chain structure. For single-chain in salt, G is simply that in the bulk salt solution – the final equilibrium value of x of a single chain does not affect G. However, at finite-concentrations of polyelectrolyte each chain is condensing counterions and hence x can significantly affect the solution screening G; when Eq. (4.39) is satisfied by the optimal value x^*, G represents the screening in a solution at the equilibrium x^*, and the two have to be self-consistently determined.

For given x, we fix the free cation concentration by charge neutrality, fix the x value in the structure factor (4.19), and use Eq. (4.12) to calculate the l_{eff} that determines the average chain structure and hence G at the specified (x, ρ_+). This gives the x-dependence of G and thus $K_{el}(x)$, which can be used in Eq. (4.39) to solve for the equilibrium fraction of condensed ions x_{eq}.

To interpret correctly and appreciate the electrostatic binding constant Eq. (4.41), we highlight an apparent paradox that arises when approximating $F(m)$ and u_+ using Voorn-Overbeek (VO) ideas.[32] Such a model, where the condensed charges are neutralized and the electrostatic free energy is estimated only for uncondensed charges using a generalized Debye-Hückel (GDH) expression,[32] essentially models the chain electrostatic free energy as $F(xNf) = (1-x)Nfu_+$, where the electrostatic free energy of the chain is modeled as simply the number of charges times

the self energy of separate ions. In this case, the electrostatic binding constant is $\ln K_{el}^{VO} = 2u_+$. If one further applies the GDH expression $u_+ = -l_b\kappa/2(1+\kappa\sigma)$, which is *negative*, it appears that the resulting (VO-type GDH, or GDH-VO) electrostatic binding constant $\ln K_{el}^{GDH-VO}$ *opposes* counterion condensation and becomes increasingly unfavorable with increasing Bjerrum length (electrostatic interaction strength)!

This result runs counter to expectations and arises from the fact that the GDH free energy expression subtracts out the Born energy of uncondensed ions as its reference energy, leaving only the (negative) correlation energy.[23] Conceptually this is problematic because the reference energy then changes with changing degrees of counterion condensation, even though the total number of charges in the system doesn't change upon condensation. Physically, when charges condense (become "neutralized"), the GDH expression only accounts for the loss of the favorable correlation energy, leading to an electrostatic binding constant that opposes counterion binding.

More generally, when calculating electrostatic correlation energies it is a common regularization practice[12, 13, 47] to subtract reference energies in the form of

$$\frac{1}{4\pi^2}\int k^2 dk\ \tilde{C}(k)\tilde{S}_p^{\text{chg}}(k; l_{\text{eff}}, m) \tag{4.42}$$

where $\tilde{C}(k)$ is the Coulomb operator. This has the side effect of removing the direct, favorable *pc* electrostatic interactions that drive counterion condensation. Such a procedure leaves only the correlation, or screening, effects behind [23] and leads to a binding constant that opposes counterion condensation. We caution that the choice of S^{chg} used in such a regularization is not unique (i.e. connected or disconnected charges),[12, 13, 47] and different choices of S^{chg} correspond to different interactions being removed.

The typical "fix" in such theories is to reintroduce an *additional* electrostatic driving force or binding constant, either empirically [32] or by physical argument. Theoretical estimates of the binding constant have been estimated for simple ion pairing,[34] and in the polyelectrolyte literature has been estimated as $\sim l_b/b$,[12] possibly scaled with a dielectric mismatch parameter,[30, 31] corresponding to the direct counterion-backbone electrostatic interaction. We correspondingly write an

estimate for DH-VO and GDH-VO binding constants as

$$-\ln K_{el}^{DH-VO} \equiv -\frac{l_b}{b} + l_b\kappa \tag{4.43}$$

$$-\ln K_{el}^{GDH-VO} \equiv -\frac{l_b}{b} + \frac{l_b\kappa}{(1+\kappa b)} \tag{4.44}$$

where the DH-VO uses the Debye-Hückel (DH) point charge expression for the correlation energy. However, such an ad hoc binding constant suffers several physical limitations as outlined in the introduction, with an unclear dependence on chain structure (i.e. missing interactions between condensed counterions and both polyelectrolyte charges and other condensed counterions) and the electrostatic environment (i.e. changing screening, described by G).

In contrast, we do not encounter such issues with our expressions Eqs. (4.14) and (4.35) for $F_{\text{int}}(m)$ and u_+, respectively. Our expressions adopt the more natural reference energy of taking the vacuum as the point of zero energy for both $F_{\text{int}}(m)$ and u_+, yielding what is termed the *total* self energy.[23, 40] This reference energy explicitly includes the energy of assembling charges dispersed at infinity into a finite object; for homopolyelectrolytes it accounts for how chain connectivity increases the electrostatic energy of the monomers in the chain.[23]

Further, when we use Eq. (4.14) to evaluate $F(m)$ in $\ln K_{eq}$, the charge structure factor $\tilde{S}_p^{chg}(k;m)$, as seen in the decomposition Eq. (4.19) explicitly describes the spatial arrangement of both polyelectrolyte chain and condensed counterions, thus accounting for intrachain (pp), counterion-chain (pc), *and* counterion-counterion (cc) electrostatic interactions by substituting the respective partial charge structure factor into the interaction energy Eq. (4.14):

$$F_{\text{int,pp/pc/cc}} = \frac{1}{4\pi^2}\int k^2 dk\ \tilde{G}(k)\tilde{S}^{\text{chg}}_{pp/pc/cc}(k; l_{\text{eff}}, m) \tag{4.45}$$

Our expression considers nonlocal interaction effects that arise from chain connectivity via $\tilde{\omega}$ in our expressions for S^{chg}, e.g. Eqs. (4.20), (4.21), (4.23). Further, the Green's function G accounts for how changing solution environment modifies the screening and direct interaction between counterions and their condensed sites.

Even for a single chain in salt, where G is independent of the degree of condensation, $\ln K_{eq}$ still depends on the degree of condensation through S_p^{chg}, reflecting (anti-)cooperative effects due to the previously condensed counterions, described explicitly by the x^2 dependence of S_{cc}^{chg} e.g. Eq. (4.23), and implicitly through the possibly adaptive chain structure $\tilde{\omega}$ Eq. (4.27). This is in contrast to the VO-type

binding constant Eq. (4.44), which approximated $F(xNf) = (1-x)Nfu_+$ and yields a x-independent $\frac{\partial F(xNf)}{\partial x}$ provided that G (and thereby u_+) is independent of the degree of condensation (as it is for a single chain in salt solution).

To summarize, in our theory the electrostatic binding constant contains both chain connectivity *and* finite-concentration correlation (screening) effects in a self-consistent fashion. The electrostatic energies F Eq. (4.14) and u_+ Eq. (4.34) both depend on concentration and chain structure effects implicitly through G. Further, F also contains an explicit dependence on the charge structure of a polyelectrolyte with its associated counterions. The charge structure depends on both the degree of counterion condensation as well as the adaptive chain structure, which is determined variationally by the RGF framework.[23] We will thus be able to see how changing chain conformation mediates and affects counterion binding.

4.3 Numerical Results

We first present results for single chain in salt. In the single chain limit counterion condensation does not change the bulk concentration of free counterions, thus simplifying discussion of the binding constant, though the results carry over to solutions with finite polyelectrolyte concentration with only quantitative differences. We are able to explain differences between different chain structure and charge models in terms of the self energy.

After presenting single chain results, we discuss solutions with finite polyelectrolyte concentration. We first explain quantitative differences between salt-free polyelectrolyte solutions and single polyelectrolyte chains at equivalent salt conditions, appropriately defined. We then consider the thermodynamic effects of counterion condensation on polyelectrolyte solutions, and examine the transition from the regime when entropy effects are dominated by linearized fluctuations to the limit when entropy changes are mostly attributable to the translational entropy loss of the tightly bound population, and explore the consequences of retaining residual dipolar fluctuations on the phase behavior.

To translate our number densities to units of M, we set $b = 0.35nm$ in our conversions. Unless otherwise mentioned, we present most results only for the discrete backbone, discrete counterion (dB-dC) model with a dipole parameter of $d = 0.7a$. In general, qualitative results generalize for both of our proposed charge structure models cB-dC Eq. (4.21) and dB-dC (4.23), and when relevant we compare the two models to show their quantitative differences. When appropriate, we also compare

to continuous backbone, continuous counterion (cB-cC) model Eq. (4.17). Most results are presented for flexible chains with adaptive chain structure; in certain cases we also compare to predictions where the average chain structure is fixed to either a Gaussian or semiflexible rod form, as detailed elsewhere.[27] Unless otherwise noted, to focus on only the electrostatic driving force for counterion condensation, we set $\ln \xi = 0$ such that there is no intrinsic bias favoring or disfavoring counterion condensation – the electrostatics included thus far already provide a driving force for counterion condensation.

4.3.1 Single Chain in Salt

To illustrate the theory, we first present representative probability distributions of the degree of condensation, at two different salt concentrations and for various chain lengths. As the chain length increases, we expect the average degree of condensation to increase due to increasing correlations, before eventually reaching some long-N limit because condensed counterions can only "see" the chain up to the solution screening length – they can not tell how long the chain is if the chain is much longer than the screening length. Further, we expect the probability distribution for x to narrow for long chains. These expectations are borne out in Fig. 4.2, where we can clearly see the mean of the probability distributions converge towards a long-N limit. Further, we see that the convergence of the mean is achieved faster for higher salt concentrations – this again makes sense, because increasing salt means a decreasing screening length, and correspondingly a shorter length scale over which chain connectivity can enhance counterion binding.

This chain length effect can be better visualized by plotting the average counterion condensation as a function of salt concentration in Fig. 4.3a. Similarly to Fig. 4.2, the convergence of different chain lengths is faster for higher salt concentrations. Fig. 4.3a is plotted for $l_b = 2b$. Setting $b = 0.35nm$ such that $l_b = 0.7nm$ corresponds to water at room temperature, at salt concentrations of $\sim 0.01M$ or Debye lengths $\approx 3nm$, chain lengths $N > 100$ have nearly indistinguishable counterion condensation profiles. At the lowest salt concentrations plotted, the curves for $N = 3000$ and $N = 10,000$ chains are nearly indistinguishable. With increasing chain length, the level of counterion condensation also becomes a weaker function of salt concentration, almost approaching a plateau. Still, screening at high salt concentrations eventually slightly reduces the level of counterion condensation.

We can also examine the effect of chain structure and our different proposed models

for the charge structure. As observed in our previous work, fully charged polyelectrolyte chains are locally stiffened, and this results in thermodynamic properties (i.e. correlation energies and binodal values) that more closely resemble those of semiflexible rods rather than (fixed-average-structure) Gaussian chains.[27] Further, previous work showed that, in choosing the reference electrostatic energy as we have, the (total) self energy consists of an infinite-dilution repulsive piece characterizing the work to assemble charge onto the chain. Finite concentration correlation effects screen the repulsive self-energy, such that the total self energy trends towards zero.

In other words, chains with greater self energy stand to benefit more from correlations, whether they take the form of linearized density responses (ionic atmospheres),[23] macroscopic phase separation,[27] or counterion condensation as studied in this chapter. We thus also expect Gaussian chains, which are more compact and hence have higher repulsive self energy to condense more counterions than their rigid counterparts. Adaptive-structure flexible chains, as described by the RGF theory, lie somewhere in between, though for highly charged chains their increased stiffness yields behaviors more similar to rods than continuous Gaussian chains.[27]

We find these self-energy arguments to apply to counterion condensation. In Fig. 4.3b we again plot the average counterion condensation as a function of salt con-

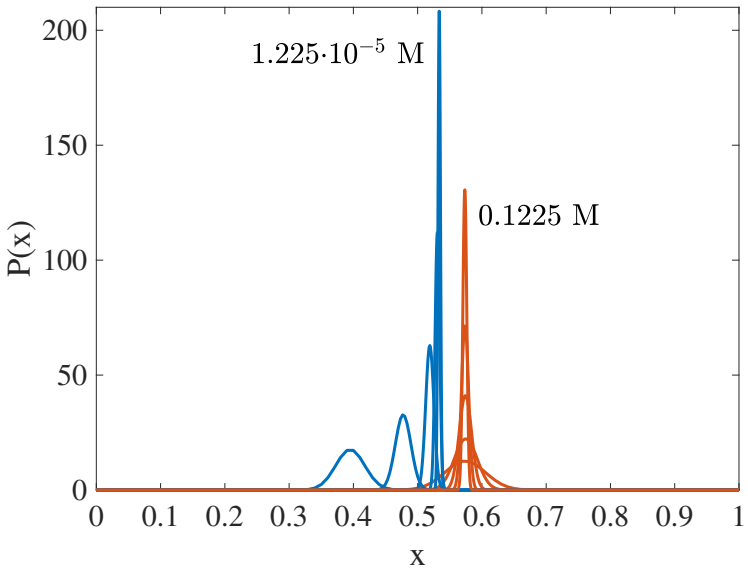

Figure 4.2: Probability distribution of counterion condensation fraction, at $l_b/b = 2$ for chains with $N = 100, 300, 1000, 3000, 10000$, f=1, with the dB-dC charge model.

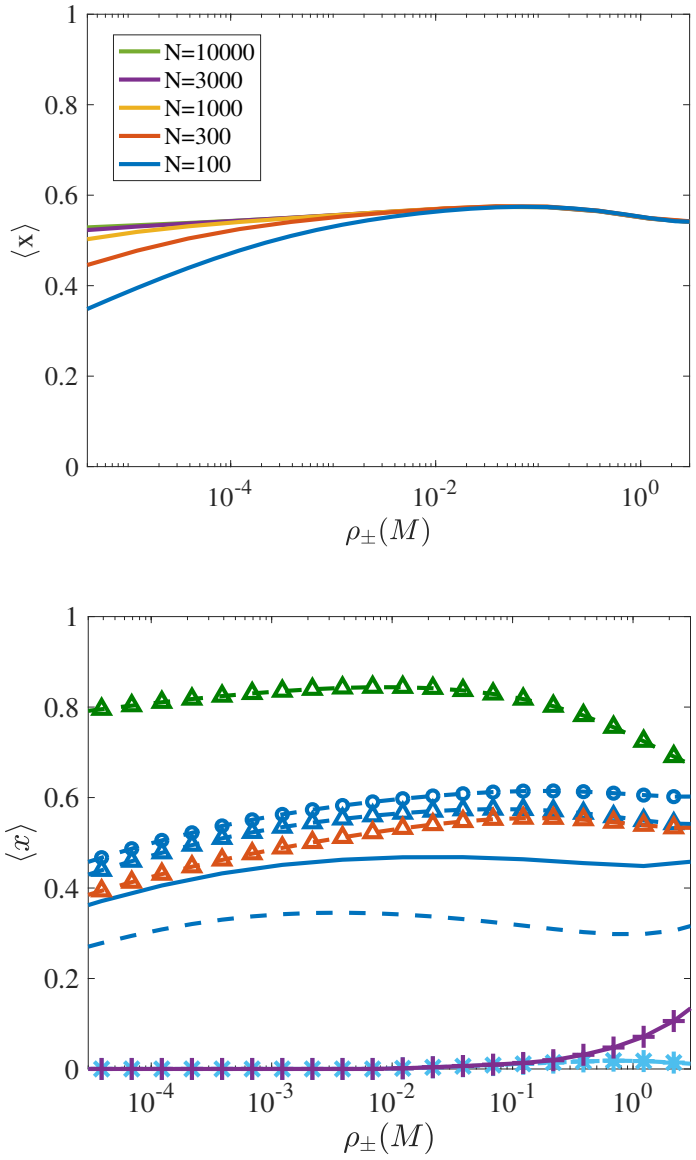

Figure 4.3: a) Chain length effect at $l_b = 2b$ for dB-dC charge model with $d = 0.7a$, for chain lengths $N = 100$ to $N = 10,000$, from bottom to top. b) Single flexible polyelectrolyte chain in salt, effect of different chain models, $N = 100$, $f = 1$, $l_b/b = 2$. DH-VO (light blue, asterisk) and GDH-VO (purple, cross). Discrete backbone and discrete counterion models with dipole parameter $d = 0.7a$ for Gaussian structure (green triangle), self-consistent structure (blue triangle) and semiflexible rod (red triangle). We also present results for self-consistently calculated chains, but with other models of the backbone and counterion charges: dB-dC with $d = 0.0a$ (blue circle); cB-dC with $d = 0.0a$ (blue dashed); cB-cC (blue solid).

centration; the lines with triangles denote calculations using discrete backbone and discrete counterion charges (dB-dC) with parameter $d = 0.7a$. The results for the self-consistent calculation of flexible chains (blue triangles), are much closer to predictions of semiflexible rods (red triangles) than predictions asssuming the chain is fixed in a Gaussian chain structure (green triangles); the latter is seen to greatly overestimate the degree of counterion condensation because it confines the chains to artificially compact chains, increasing the intrachain electrostatic interactions and the tendency to attract counterions.

On the other hand, the VO-assumption Eq. (4.44), which is missing chain-connectivity effects, leads to a drastic *under-estimate* of the amount of counterion condensation, for both the DH (light blue asterisks) and GDH (purple crosses) electrostatic correlation expressions. In particular, the DH expression, which is derived for point charges and is known to give overly strong correlations, suppresses counterion condensation even more than the GDH expression. Accounting for the finite size of ions limits the amount of electrostatic correlations to roughly the infinite dilution self energy,[23] which the GDH expression respects. Our reference energy and spread-charge regularization scheme [45] also behaves correctly with respect to this correlation energy limit.

An interesting feature of all of the models with chain connectivity is that there appears to be a peak in counterion condensation with increasing salt. This means that, initially increasing salt also increases the degree of counterion condensation, but for sufficient salt concentration there is less energy to be gained by condensation. This can be interpreted as screening, or more generally correlation effects, and the non-monotonicity in degree of counterion condensation will be discussed later when we take a closer look at the effective electrostatic binding constant.

We also find that the charge models, which differ in their treatment of residual charge fluctuations of condensed charge and site, differ quantitatively from each other. Like the differences due to chain structure, quantitative differences in the different charge models can also be traced to their different amounts of self energy (the work required to assemble charge into the chain)[23, 27] that can be reduced through correlations or condensation. The dB-dC charge model has the largest self energy because it confines charges into discrete monomers, and correspondingly has the most energy to be gained by condensation (larger driving force). In comparison, the cB-dC model (blue dashed) assumes a continuous backbone, which lowers the self energy and reduces a significant portion of the interaction between a counterion and a backbone

site; the driving force for condensation is weaker and the the average fraction of condensed ions drops. Finally, further delocalizing the counterion charges over the backbone (cB-cC model, blue solid) in a smeared fashion artificially removes much of the Born energy of the counterion upon condensation (counterions are discrete when unbound), producing an artificial driving force relative to the cB-dC model. Thus cB-cC predictions for $\langle x \rangle$ are intermediate between dB-dC and cB-dC results.

An interesting difference between the discrete backbone and continuous backbone models is that, although the degree of charge condensation in both can be non-monotonic, continuous backbones appear to have counterion condensation peaks at lower salt concentrations than the dB-dC model assuming discrete backbone charges. We point out that the continuous backbones also show an increase of counterion condensation at high salt ($> 1M$). This feature actually also exists for the discrete backbone model at even higher salt concentrations, but is less pronounced, and is attributed as an artifact of tight binding models at weak interaction strengths and high concentrations. If one looks at Eq. (4.39) one notices that at sufficiently high salt concentration, the translational entropy piece actually begins *favoring* condensation. Similar issues of spurious "condensation" or "pairing" at high concentrations exist with a popular theory of associating polymers.[48]

Due to chain connectivity effects, the electrostatic driving force depends on the fraction of condensed counterions – the presence of condensed charges will repel uncondensed charges and hence reduce the driving force for counterion condensation. This is in contrast to theories that *a priori* take the counterion condensation binding constant to be constant, or include the x-dependence only if the concentration of counterions is changing (i.e. for finite concentration of polyelectrolyte).[32] Our results are presented in Fig. 4.4a, where one can see that for most counterion condensation fractions, $\ln K_{el}$ changes with x. Interestingly, it appears to be largely linear in x, consistent with the leading x^2 dependence of the counterion-counterion charge structure factor and hence electrostatic self energy F_{int} (recall $\ln K_{el} \sim \partial F_{int}/\partial x$). Only at high values of x does one start to see deviations from the linear behavior. We also plot the zero-salt limit of the electrostatic binding constant (black-dashed)

$$\ln K_{el}^{0}(x) \equiv \ln K_{el}(x; \rho_{\pm} = 0) \tag{4.46}$$

which describes the effective electrostatic driving force due to the direct Coulomb interactions, and will be helpful for isolating changes to the binding constant due

to anti-cooperative counterion binding and due to finite-concentration correlation effects.

Note that $\ln K^0(x)$ implicitly contains much of the chain-connectivity and structure effects – chain connectivity should be most pronounced when the electrostatics are unscreened and long-ranged. In the inset of Fig. 4.4a one can see the significant difference in binding constant between semiflexible rod and Gaussian chains. The fully-charged chains with adaptive structure (black line in inset) are quite close to those of the rod.

To visualize the dependence of $\ln K_{el}$ on the salt concentration, for given salt concentration $\rho_\pm$ in Fig. 4.4b we plot the value of $\ln K_{el}$ at the *equilibrium* extent of counterion condensation $x_{eq}(\rho_\pm)$ at the specified salt concentration. For comparison, we also plot the VO-motivated binding-constants Eq. (4.44). In the inset we compare the full binding constant to the zero-salt binding constant $\ln K^0_{el}$ at the same $x_{eq}(\rho_\pm)$. Noting that that the predominant chain structure effects are embodied in $\ln K^0_{el}$, the difference between $\ln K_{el}$ and $\ln K^0_{el}$ is then attributable to finite-concentration correlation effects, which technically includes both screening *and* adaptive chain structure effects [23]. Over the range of concentrations presented in Fig. 4.4b, the concentration dependence of $\ln K_{el}$ is largely driven by screening effects; this is consistent with Fig. 4.3 where we see that the degree of counterion condensation changes negligibly over the same concentration range. Of course, at even lower concentrations, changes in the binding constant will be predominantly due to increasing bare Coulomb-interactions between the condensed counterions.

The concentration-dependence of the degree of counterion condensation seen in Fig. 4.3 can be understood by examining Eq. (4.40), which makes apparent that there is a competition between translational entropy and the electrostatic driving force. Typical counterion condensation theories predict that the amount of counterion condensation should increase with increasing salt concentration, primarily because as $\rho_\pm$ increases, the counterion translational entropy penalty associated with condensing drops. We find this to be true over most salt concentrations. However, increasing salt also screens electrostatic interactions and decreases $\ln K_{el}$ – at high enough salt, if the electrostatic driving force decreases faster than the translational entropy penalty decreases, then the amount of counterion condensation will decrease. In general, we expect there to be a non-monotonic dependence of $\langle x \rangle$ on the salt density $\rho_\pm$, as observed previously in Fig. 4.3, and this in fact holds for finite concentrations of polyelectrolyte as well.

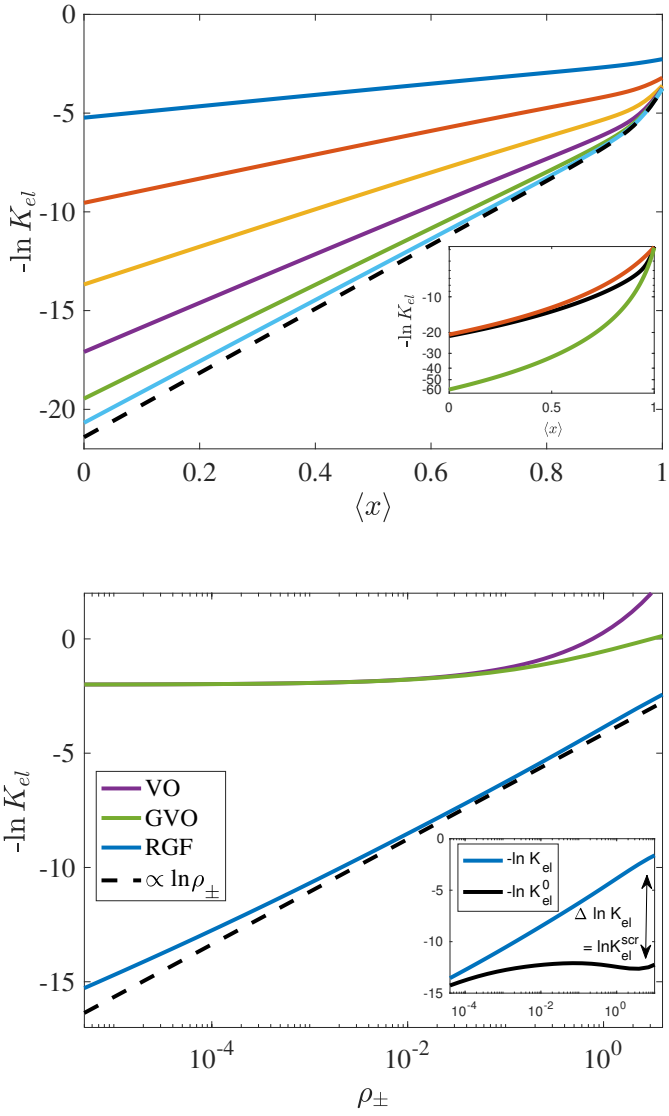

Figure 4.4: (a) Binding driving force as function of condensation fraction, at $l_b/b = 2$, for $N = 100$, $f = 1$. The black dashed line is for the zero salt $\rho_{\pm} = 0M$ limit, while the remaining colored lines are for different concentrations, from $\rho_{\pm} = 1.22M$ (top) to $\rho = 1.22 \cdot 10^{-5}M$ (bottom). Inset: zero-salt binding constants for semiflexible rod (red), Gaussian chain (green), and adaptive chain structure (black). (b) Binding driving force at the average $\langle x \rangle$ of given salt concentration $\rho_{\pm}$. Results are for $N = 100$, $l_b/b = 2$, $f = 1$, with the dB-dC charge model ($d = 0.7a$) and self-consistently-calculated flexible chain (blue), GDH-VO (green), and VO (purple). Inset: binding constant for the adaptive chain structure, compared to the zero-salt binding constant ($\ln K^0$) at the same equilibrium condensation fraction. The difference between the two are attributable to finite-concentration correlation effects.

Generally, the salt concentration at which the (admittedly shallow) peak $\langle x \rangle$ is attained depends on the *rate* at which the entropy penalty and electrostatic driving forces change with salt concentration. Clearly, if both terms changed at the same rate, then the amount of condensed counterions will stay constant with changing salt concentrations. For long chains, we see a flattening of the $\langle x \rangle$ versus $\rho_{\pm}$ curve in Fig. 4.3b, corresponding to a regime where, although increased salt screening decreases the electrostatic driving force for counterion condensation, it decreases at nearly the same rate at which the translational entropy penalty decreases.

The peak in the condensed fraction $\langle x \rangle$ coincides with the salt concentration at which the rate of change of the translational entropy penalty matches the rate of change of the electrostatic driving force. This peak is observed even for the DH-VO theory (which does not consider chain connectivity effects) at $l_b/b = 2$ – at high concentrations the electrostatic driving force decreases sufficiently quickly with increasing salt concentration. Although this non-monotonic dependence of $\langle x \rangle$ on salt concentration is not yet observed for the GDH-VO theory at $l_b/b = 2$, one can see that increasing the Bjerrum length will increase the rate of screening and eventually lead to a non-monotonic dependence of $\langle x \rangle$ on $\rho_{\pm}$.

By examining the salt-dependence of counterion condensation one can further infer the relative rates at which the electrostatic binding constant changes for the different charge models. However, in the interest of brevity we do not pursue such an in-depth comparison.

4.3.2 Finite Concentration: Thermodynamics

Much of the intuition regarding the influence of chain structure and concentration carries over from the single-chain case to the case of solutions with finite-concentrations of polyelectrolytes. To compare the two cases, we define the equivalent single-chain system as that of a single chain in a simple-electrolyte concentration at the same counterion concentration as the salt-free polyelectrolyte solution. Conceptually, the equivalent single-chain system is achieved by disconnecting all polyelectrolytes in the salt-free solution except for one chain.

We first look at the probability distribution $P(x)$ of the condensed counterion fraction. As seen in Fig. 4.5a, the standard deviations are quite similar between the two cases, while the salt-free polyelectrolyte solution (solid lines) has a consistently smaller $\langle x \rangle$ than does the equivalent single-chain in salt system. The primary reason for this is because in the salt-free polyelectrolyte solution, *every* chain is condens-

ing counterions. As a result, the counterion condensation drops as the average condensation fraction increases, *increasing* the translational entropy penalty. This additional translational entropy penalty reduces the average counterion condensed fraction relative to that of a single chain at the equivalent salt concentration.

The effect of this increase in the translational entropy penalty holds true for both discrete backbone and continuous backbone models, across all concentrations, as presented in Fig. 4.5b. Further, in general counterion condensation should push the concentration ρ_p at which $\langle x \rangle$ achieves its peak to higher concentrations. Relative to the equivalent single-chain in salt system, salt free polyelectrolyte solutions face a larger translational entropy penalty to condense ions because *all* chains are condensing counterions. Conversely, the translational entropy penalty also decreases faster as a function of increasing polymer (and counterion) concentration, and higher concentrations must be achieved before the screening reduces the electrostatic driving force faster than the translational entropy penalty decreases. This delay of the counterion condensation peak is true for the discrete backbone model (red dashed). For the continuous backbone model, at the conditions presented in Fig. 4.5b, the translational entropy penalty is large enough to suppress the non-monotonic dependence of $\langle x \rangle$ on $\rho_\pm$ altogether, resulting in a monotonically increasing $\langle x \rangle$.

We now turn our attention to the issue of the distinction between the linearized fluctuations and the translational entropy loss of the condensed counterions. As observed in previous works, over a significant semidilute regime, the linear-response fluctuations of locally stiff polyelectrolytes (i.e. rods or electrostatically extended) predict electrostatic chemical potential contributions that have the same functional form as the translational entropy of small ions, albeit with opposite sign.[27] This suggests that, at the level of linear response, the fluctuation effects of such polyelectrolytes can be understood largely as renormalizing the small ions' translational entropy, or reducing the osmotically active population of small ions.

This renormalization effect of the fluctuations is qualitatively the same as the thermodynamic effect of condensed counterions. We are thus interested in how much of the entropy loss of the system can be associated with the linear response fluctuations, and how much with the condensed counterions. Clearly, at low values of $\langle x \rangle$ (i.e. at low l_b) we expect that the correlations should predominantly come from the linear response. In contrast, at high condensation fractions the correlations are expected to be dominated by the translational entropy loss of condensed counterions. The crossover between these two limits is of great interest – how quickly do the two

contributions cross over? To what extent does the linear fluctuation theory describe counterion condensation?

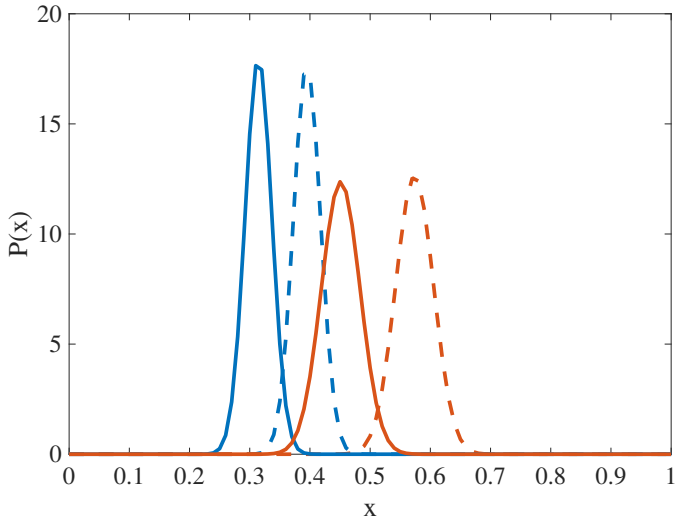

(a)

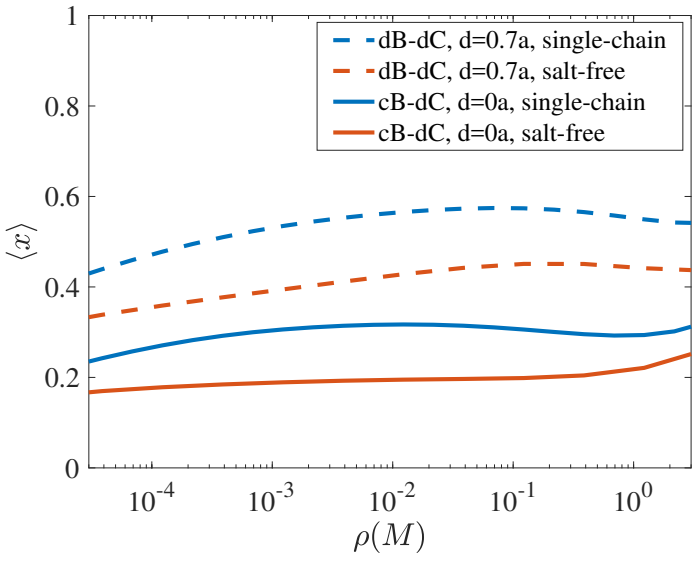

(b)

Figure 4.5: (a) $l_b = 2\sigma$, $N = 100$. Solid lines are for salt-free solutions at $0.0000122M$ (blue) and $0.122M$ (red). Dashed lines, with the same meaning for colors, are for single chains at the equivalent salt concentration. (b) $l_b = 2\sigma$, $N = 100$. Solid lines are for the cB-dC charge model ($d = 0a$) and dashed lines are for dB-dC chains ($d = 0.7a$). Red lines are for salt-free solutions and blue lines are for single chains at the equivalent salt concentration. Translational entropy penalty is larger for salt-free solution than single chains in equivalent salt because all chains collect their counterions, reducing the concentration of free counterions.

We consider the *electrostatic* contributions to the osmotic coefficient, across a range of l_b. In salt-free solution, the osmotic coefficient is $\Phi = \frac{\beta\Pi}{\rho(f+1/N)}$, from which we define the linearized fluctuation and counterion condensation contributions to the osmotic coefficient in accordance with our classification of the osmotic pressure contributions in Eqs. (4.36) and (4.37):

$$\Phi^{lin} = \frac{\beta\Pi^{lin}}{\rho(f + 1/N)} \tag{4.47}$$

$$\Phi^{cc} = \frac{\beta\Pi^{cc}}{\rho(f + 1/N)} \tag{4.48}$$

and define the total *electrostatic* contribution of the osmotic coefficient as $\Phi^{tot} = \Phi^{lin} + \Phi^{cc}$.

At low l_b and low concentrations, the linearized fluctuation theory captures most of the electrostatic contribution to the osmotic coefficient (Fig. 4.6a, compare yellow and purple lines). To emphasize the importance of accounting for changes in chain conformations, we also plot the osmotic coefficient contribution of an RPA theory (where the chains are assumed to on average have a Gaussian structure) without counterion condensation (green line). As can be seen, even for small l_b values, the RPA theory over-estimates the fluctuations. There is thus a very clear regime where chain conformational changes are important, but counterion condensation is not yet important.

With increasing l_b, introduction of counterion condensation reduces the contribution of linearized fluctuations relative to predictions without counterion condensation, and Φ^{lin} becomes a non-monotonic function of l_b/b. Nevertheless, at typical aqueous experimental conditions ($l_b/b < 3$), the transition to the counterion-dominated regime is not yet complete – the linearized fluctuations still contribute an appreciable fraction of the osmotic coefficient drop. In Fig. 4.6b we plot the fraction of the electrostatic contribution to the osmotic coefficient $\Phi^{cc}/\Phi^{tot} = \Phi^{cc}/(\Phi^{cc} + \Phi^{lin})$ assigned to counterion condensation. At $l_b/b = 2$, the counterion condensation contribution is only about 50%.

The above observations indicate that deviations of the osmotic coefficient from 1 are not entirely synonymous with counterion condensation – rather, much of it may come from linearized fluctuations. For example, at the conditions in Fig. 4.6a ($N = 100, f = 1, \rho_p = 0.00122M$), at $l_b/b = 1$ where no counterions are condensed by the Manning criterion, and only $< 5\%$ of ions are condensed as predicted by our theory, there is an appreciable osmotic coefficient drop of ~ 0.3

that arises from the linearized fluctuations alone. The slight upturn at low l_b/b for increasing concentration is a result of the previously-mentioned artifact of the tight binding model, which is also seen when applying such binding theories to associating polymers.[48]

In general, the partitioning of the electrostatic contributions into linearized fluctuations and counterion condensation depends on the polyelectrolyte concentration, and this is also observed in Fig. 4.6b. The transition from an electrostatic osmotic coefficient Φ^{tot} contribution dominated by linearized fluctuations to Φ^{tot} dominated by counterion condensation translational entropy losses follows a sigmoidal shape, and the transition is sharper for lower polymer concentration. A particularly interesting consequence of this concentration dependence is that at higher l_b/b, increasing polymer concentration actually *decreases* the fraction of the electrostatic contribution to the osmotic coefficient that is due to counterion condensation translational entropy losses! This is all the more remarkable because for the concentrations shown in Fig. 4.6b, the degree of counterion condensation is still *increasing* with increasing polymer concentration. Although counterion condensation is increasing with increasing polymer concentration, the linearized fluctuations are increasing at a faster rate.

Finally, we examine the effect of counterion condensation on phase behavior. Previous work suggested that counterion condensation *decreases* the critical Bjerrum length of salt free solutions – i.e. it destabilizes polyelectrolyte solutions.[12, 31]. The explanation for this destabilization is argued to be related to the modulated small ion entropy upon counterion condensation.[31]

However, there is also reason to believe counterion condensation might stabilize the solution – in simple electrolytes, ion pairing is predicted to *increase* the critical electrostatic interaction strength $l_b \propto T^{-1}$ *and* critical density ρ^* [34]. For simple electrolytes, this can qualitatively be understood by the fact that paired ions do not screen as effectively nor contribute as much to fluctuations, thus decreasing the driving force for macroscopic phase separation. Another way to rationalize this trend is that the solution can decrease its electrostatic energy through condensation, which in theories without counterion condensation is only achievable by macrophase separation. A similar qualitative effect can be seen when comparing RPA and RGF theories for flexible chains – the RGF theory allows chains to relax their electrostatic energy through conformational changes, which also has the qualitative effect of stabilizing the solution against macroscopic phase separation.

In our theory, we modulate counterion condensation by tuning the parameter d. Decreasing the dipole parameter d in the discrete backbone (dB-dC) charge model

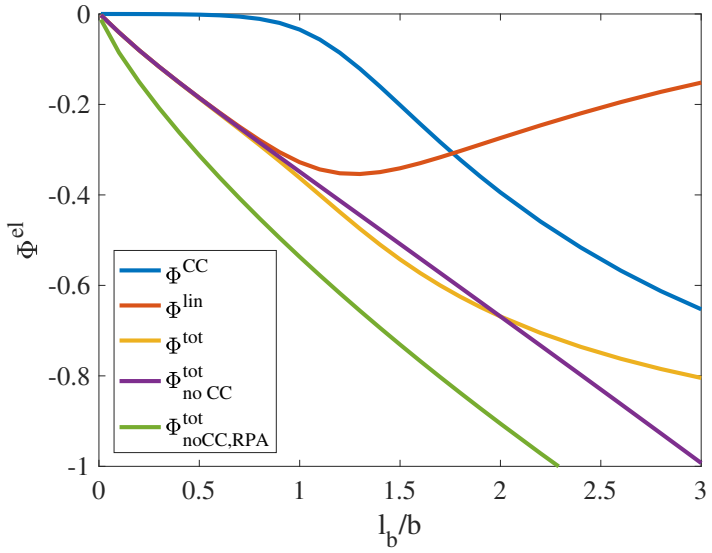

(a)

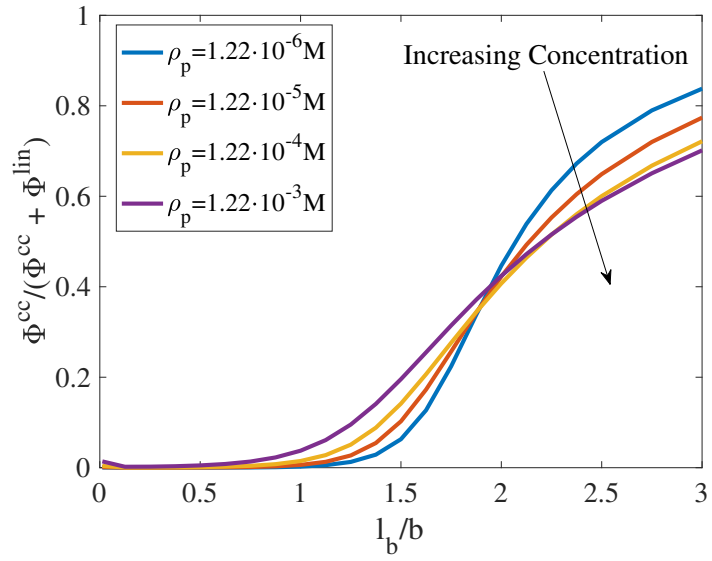

(b)

Figure 4.6: (a) Decomposition of electrostatic osmotic coefficient contributions for at $\rho_p = 0.00122M$. We also compare the total electrostatic contribution for flexible chains with $N = 100$, $f = 1$, calculated for RGF with counterion binding, RGF without counterion binding, and RPA. (b) Fraction of electrostatic osmotic coefficient drop ($\Phi^{cc}/(\Phi^{cc} + \Phi^{lin})$) attributable to translational entropy loss upon counterion condensation, at different densities. For low l_b, the fraction attributable to condensation entropy loss increases with increasing concentration; this trend is reversed for higher l_b.

has two effects: 1) allowing counterion and backbone charge to interact more closely, thus slightly increasing the condensation driving force and increasing the amount of counterion condensation, and 2) decreases the electrostatic fluctuations of the two charges. Large values of d correspond to two essentially non-interacting charges fluctuating as two independent charges, while $d \to 0$ corresponds to two tightly interacting charges whose leading order electrostatic fluctuations are those of a charge dipole that vanishes as d^2 Eq. (4.26). As discussed, we prefer to think of d as a parameter characterizing the degree of fluctuations of the counterion-backbone charge pairs.

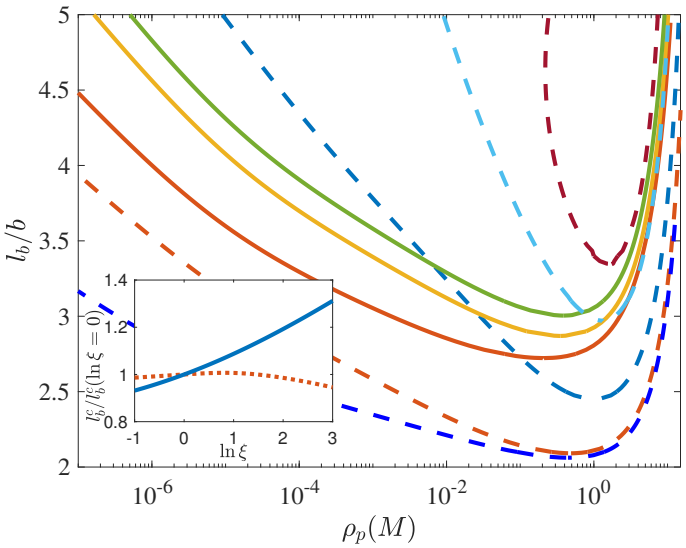

Figure 4.7: Phase diagram for cB-dC (solid lines, from top to bottom d=0.0a, d=1.0a, d=2.0a) and dB-dC (dashed line, from top to bottom d=0.6a, d=0.7a, d=1.0a, d=2.0a, d=100.0a) charge models, with $\ln\xi = 0$. Inset: Critical Bjerrum length l_b^c as a function of non-electrostatic binding strength $\ln\xi$, normalized by its avlue when $\ln\xi = 0$. Lines are for $d = 1.0a$ (blue solid) and $d = 1.5a$ (red dashed).

Our calculations for the phase diagram (4.7) confirm the importance of the residual fluctuations. For large values of d, even when the counterions are condensed, their dipolar fluctuations are still sufficiently strong to produce the expected macroscopic phase separation. For decreasing values of d, which decreases the residual fluctuations, the the critical Bjerrum length l_b and critical concentration ρ_p both increase. For small enough d, the phase window begins shrinking with increasing l_b. In fact, setting the dipole parameter $d = 0$ in the dB-dC charge model completely eliminates

the phase instability of the salt-free polyelectrolyte solution at all Bjerumm lengths considered (up to $l_b/b = 7$).

This over-stabilization arises because setting $d = 0$ in the dB-dC model eliminates electrostatic fluctuations and correlations associated with the condensed charge and the site that it condenses onto. In a similar vein, the cB-cC model, which has a continuous backbone and smeared-out (continuous) condensed counterions, condenses fewer charges than the dB-dC model (see Fig. 4.3b) and also fails to predict phase separation in the salt-free solution even at the highest Bjerrum lengths we considered ($l_b/b = 7$).

For comparison we plot predictions of the cB-dC model in Fig. 4.7 (solid lines). In this model, the same stabilizing trend of increasing l_b^c, ρ_p^c is observed with decreasing d. However, the asymmetry between the continuous backbone and discrete condensed counterions means that in the $d = 0$ limit the cB-dC model still has charge fluctuation contributions of the form $\tilde{\omega}(k) - \tilde{\Gamma}$. Thus, even in the $d = 0$ limit, the cB-dC model can still phase separate, unlike in the dB-dC model.

To more cleanly isolate the effect of residual fluctuations from the extent of counterion condensation, we varied the non-electrostatic driving force $\ln \xi$ at different values of the parameter d. For smaller d, we expect that increasing the driving force acts to further stabilize the system against macroscopic phase separation because of the aforementioned effect of weaker residual fluctuations. Thus, increasing $\ln \xi$ increases the critical interaction strength l_b required to observe phase separation, as seen in the inset of Fig. 4.7 for $d = 1a$. Interestingly, at larger values of d we actually observe that the critical l_b can change non-monotonically with the non-electrostatic driving force $\ln \xi$, eventually de-stabilizing the solution. In such cases, there is sufficient counterion condensation at high polymer concentrations relative to condensation at low polymer concentrations to destabilize the polyelectrolyte solution. In fact, for large enough d this de-stabilization effect is also seen when comparing $\ln \xi = -\infty$ (no counterion condensation) versus $\ln \xi = 0$, though the effect is modest (l_b^c changes by $\sim 3\%$).

Our examination of different charge models reveals that the exact nature of the fluctuating counterion-backbone charge pair should be examined more closely. The interpretation and quantitative determination of our parameter d depends on the exact details of the backbone charge structure (i.e. continuous or discrete) and molecular details not considered in our coarse-grained model, but it is nevertheless clear that retaining the residual, higher order charge fluctuations is vital to reproducing the

phase separation of polyelectrolyte solutions.

4.4 Conclusion

We have discussed the nature of electrostatic fluctuations in solutions of flexible polyelectrolytes within a modified self-consistent renormalized Gaussian fluctuation (RGF) theory augmented with a tight-binding model for counterion condensation. For weak charge interactions or low charge fractions, electrostatic fluctuations are weak and well-described by RPA theories, which essentially describe the free energy changes associated with the linear response of charges. By using the RGF theory for fluctuations, we are able to further cover intermediate interaction strengths when field fluctuations renormalize the polyelectrolyte chain structure[23], to the onset of stronger correlation effects like counterion condensation.

At stronger interaction strengths $l_b/b \gtrsim 1$, Manning condensation theory suggests that there are stronger correlations associated with the physical phenomenon of counterion condensation. In this work we observe that, after renormalizing the chain structure, the remaining fluctuations in the RGF theory are still of the linear response form. It is thus consistent to introduce a tightly bound population of counterions to capture the nonlinear electrostatic fluctuations not described by the RGF theory.

We show that within our theory one can identify a comprehensive electrostatic binding constant as the free energy change of adding a tightly bound counterion to a polyelectrolyte, while short-range, non-electrostatic effects driving counterion binding are included in our derivation as an internal partition function ξ, and is taken as a parameter in our theory. The electrostatic binding constant clarifies the relevant contributions to counterion binding, such as the (anti-)cooperative effect of previously bound counterions, and the RGF framework gives a *unified* way to estimate the coupled effects of correlations (screening) and chain connectivity (including conformational changes) on counterion binding. Further, differences in counterion binding between different chain structure and charge models were explainable in terms the self energy. In general, more compact chains condense more counterions than extended semiflexible rods. In a similar vein, the dB-dC (discrete backbone and discrete counterion) charge model, which confines charges to discrete entities and thereby raising their self energy, condenses more counterions than continuous backbone models that delocalize charges along the entire polyelectrolyte backbone.

In contrast, previous theories often employ electrostatic correlation energy expressions that subtract a condensation-dependent reference energy.[12, 30, 32] As we showed, this is tantamount to subtracting out favorable electrostatic interactions between counterions and backbone charges, which led previous theories to have to re-introduce additional electrostatic binding constants. Further, the reference energies subtracted in such theories are not unique, and represent subtracting different interactions.

We find it much more natural and consistent to use a reference electrostatic energy where the vacuum is the zero-point;[23, 40] combined with our expressions for the electrostatic self energy allows us to naturally describe chain connectivity, anti-cooperativity between counterions, and screening effects. In particular, by breaking down the charge structure into polyelectrolyte-polyelectrolyte, polyelectrolyte-counterion, and counterion-counterion, we were able to explain the electrostatic binding constant's dependence on the degree of counterion condensation x. This cooperativity effect stems from the counterion-counterion interaction energies, which to leading order depends quadratically $\sim x^2$ on the degree of counterion condensation; the binding constant is the first derivative of the electrostatic energy of condensation, and thus is to good approximation linear in x.

To highlight the different faces of electrostatic fluctuations, we compare the thermodynamic contributions of the linearized electrostatic fluctuations with the translational entropy loss of condensed counterions. We see that chain structure renormalization of flexible chains significantly modifies the linearized fluctuations even at low l_b/b, before counterion condensation sets in. The cross-over to the counterion-condensation regime happens when $l_b/b \sim O(1)$, typical for fully-charged polyelectrolytes in aqueous solution. However, under these common aqueous conditions, the linearized fluctuations of the ionic atmosphere can still contribute an appreciable amount to the entropy loss associated with electrostatic correlations. In fact, at higher interaction strengths $l_b/b \gtrsim 1.5 \sim 2$ increasing the polyelectrolyte concentration actually *decreases* the relative contribution of counterion condensation translational entropy losses.

While the onset of counterion condensation is *after* electrostatic fluctuations have already begun renormalizing chain structure, we emphasize that the linearized fluctuations, chain structure, and counterion condensation are all coupled. Counterion condensation theories that ignore the role of chain conformational changes of flexible polyelectrolytes skip a whole regime of fluctuation effects and, depending on

their model of electrostatic correlations, may significantly under or over-estimate counterion condensation.

Lastly, we showed how the choice of how to describe the charge structure (i.e. continuous or discrete backbone, continuous or discrete counterion) upon counterion condensation needs to be made carefully. Specifically, using schemes that identically neutralize the backbone charge and counterion (i.e. the cB-cC continuous backbone-continuous counterion charge model or dB-dC discrete backbone-discrete counterion model we proposed with $d = 0a$) runs the risk of over-stabilizing the electrostatic correlations and eliminating phase separation in salt-free polyelectrolyte solutions. Instead, it is vital to retain the charge fluctuations of counterion-backbone charge pairs, which we capture through the introduction of a dipole parameter d that, to leading order, yields attractive dipolar charge fluctuations; in the past, this was modeled as additional effective short-ranged attractive interactions.[30] Depending on the amount of residual charge fluctuations, counterion condensation can either *stabilize* polyelectrolyte solutions (i.e. increasing l_b^c, consistent with the behavior of simple electrolyte solutions [34], or eventually *destabilize* polyelectrolyte solutions, as reported previously in certain theoretical studies.[12, 31]

We remark that the the sensitivity of polyelectrolyte solutions to the residual charge fluctuations suggests that one should more carefully study the difference between polyelectrolyte charge regularization due to acid/base reactions [49] and counterion condensation (which to leading order is commonly treated as also exactly neutralizing the polyelectrolyte chains). The binding process in both cases will continue to depend on chain structure and exhibit cooperative effects due to chain connectivity. However, the two may have different phase separation behaviors. The exact charge neutralization model is probably a better description of acid/base titration than counterion condensation, with the consequence that acid/base titration is more likely to stabilize polyelectrolyte solutions. Granted, once the chains become neutralized, it will also become important to consider non-electrostatic interactions, such as the χ-interactions – the organic backbone of polyelectrolytes is typically hydrophobic and thus otherwise immiscible with water. One will also have to more carefully consider the difference between any introduced χ interactions and the residual charge fluctuations of the polyelectrolyte – recent work has shown that adding a polarizability, or an effective dipole, to polymer chains naturally leads to attractive interactions, as we have found in our theory, and can be characterized by effective χ interactions.[50]

In the future, it will be important to account for the full spectrum of ion-pairing

effects. For example, at even higher l_b/b than those considered in this study, ion-pairing between small ions may also need to be considered, and the fluctuations of condensed ions and backbone can lead to coil-globule transitions discussed in literature but not considered in this work. Also, at the $O(1)$ values of l_b/b considered here, it will be important to examine the effect of ion pairing between oppositely charged polyelectrolytes.[51] If counterion condensation occurs, then charged monomers on polyelectrolyte chains, which will have enhanced electrostatic interactions due to chain connectivity, will pair as well. It would be interesting to study how such ion pairing would modify predictions of the phase diagram for coacervates.

BIBLIOGRAPHY

[1]B.-Y. Ha, and A. J. Liu, "Counterion-mediated attraction between two like-charged rods", Phys. Rev. Lett. **79**, 1289–1292 (1997) 10.1103/PhysRevLett.79.1289.

[2]J. C. Butler, T. Angelini, J. X. Tang, and G. C. L. Wong, "Ion multivalence and like-charge polyelectrolyte attraction", Phys. Rev. Lett. **91**, 028301 (2003) 10.1103/PhysRevLett.91.028301.

[3]G. Orkoulas, S. K. Kumar, and A. Z. Panagiotopoulos, "Monte carlo study of coulombic criticality in polyelectrolytes", Phys. Rev. Lett. **90**, 048303 (2003).

[4]B. Zoetekouw, and R. van Roij, "Nonlinear screening and gas-liquid separation in suspensions of charged colloids", Phys. Rev. Lett. **97**, 258302 (2006).

[5]A. R. Denton, "Charge renormalization, effective interactions, and thermodynamics of deionized colloidal suspensions", J. Phys. Condens. Matter **20**, 494230 (2008).

[6]H. Eisenberg, and G. R. Mohan, "Aqueous solutions of polyvinylsulfonic acid: phase separation and specific. interactions with ions, viscosity, conductance and potentiometry", J. Phys. Chem. **63**, 671–680 (1959).

[7]P. Zhang, N. M. Alsaifi, J. Wu, and Z.-G. Wang, "Salting-out and salting-in of polyelectrolyte solutions: a liquid-state theory study", Macromolecules **49**, 9720 (2016).

[8]P. Debye, and E. Hückel, "De la théorie des électrolytes. i. abaissement du point de congélation et phénomènes associés", Phys. Zeitschrift **24**, 185 (1923).

[9]C. Mak, and P. S. Henke, "Ions and rnas: free energies of counterion-mediated rna fold stabilities", J. Chem. Theory Comput. **9**, 621–639 (2012).

[10]J.-L. Barrat, and F. Joanny, "Theory of polyelectrolyte solutions", Adv. Chem. Phys.: Polymeric Systems **94**, 1–66 (1996).

[11]V. Y. Borue, and I. Y. Erukhimovich, "A statistical theory of weakly charged polyelectrolytes: fluctuations, equation of state and microphase separation", Macromolecules **21**, 3240 (1988).

[12]A. V. Ermoshkin, and M. Olvera de la Cruz, "A modified random phase approximation of polyelectrolyte solutions", Macromolecules **36**, 7824 (2003).

[13]J. Qin, and J. J. de Pablo, "Criticality and connectivity in macromolecular charge complexation", Macromolecules **49**, 8789 (2016).

[14]G. S. Manning, "Limiting laws and counterion condensation in polyelectrolyte solutions i. colligative properties", J. Chem. Phys. **51**, 924 (1969).

[15]G. S. Manning, "Limiting laws and counterion condensation in polyelectrolyte solutions ii. self-diffusion of the small ions", J. Chem. Phys. **51**, 934–938 (1969).

[16]G. S. Manning, "Counterion binding in polyelectrolyte theory", Accounts of Chemical Research **12**, 443–449 (1979).

[17]G. S. Manning, "The critical onset of counterion condensation: a survey of its experimental and theoretical basis", Berichte der Bunsengesellschaft für physikalische Chemie **100**, 909–922 (1996).

[18]F. Oosawa, "Polyelectrolytes", in *Polyelectrolytes* (Marcel Dekker, 1971).

[19]V. A. Belyi, and M. Muthukumar, "Electrostatic origin of the genome packing in viruses", Proceedings of the National Academy of Sciences **103**, 17174–17178 (2006).

[20]K. M. Beers, D. T. Hallinan Jr, X. Wang, J. A. Pople, and N. P. Balsara, "Counterion condensation in nafion", Macromolecules **44**, 8866–8870 (2011).

[21]J. Kamcev, D. R. Paul, and B. D. Freeman, "Ion activity coefficients in ion exchange polymers: applicability of manning's counterion condensation theory", Macromolecules **48**, 8011–8024 (2015).

[22]J. Kamcev, M. Galizia, F. M. Benedetti, E.-S. Jang, D. R. Paul, B. D. Freeman, and G. S. Manning, "Partitioning of mobile ions between ion exchange polymers and aqueous salt solutions: importance of counter-ion condensation", Physical Chemistry Chemical Physics **18**, 6021–6031 (2016).

[23]K. Shen, and Z.-G. Wang, "Electrostatic correlations and the polyelectrolyte self energy", J. Chem. Phys. **146**, 084901 (2017) DOI:10.1063/1.4975777.

[24]C.-L. Lee, and M. Muthukumar, "Phase behavior of polyelectrolyte solutions with salt", J. Chem. Phys. **130**, 01B608 (2009).

[25]P. G. De Gennes, P. Pincus, R. M. Velasco, and F. Brochard, "Remarks on polyelectrolyte conformation", J. Phys. France **37**, 1461 (1976).

[26]A. V. Dobrynin, R. H. Colby, and M. Rubinstein, "Scaling theory of polyelectrolyte solutions", Macromolecules **28**, 1859 (1995).

[27]K. Shen, and Z.-G. Wang, "Polyelectrolyte chain structure and solution phase behavior", Macromolecules **51**, 1706–1717 (2018) DOI:10.1021/acs.macromol.7b02685.

[28]Z.-J. Tan, and S.-J. Chen, "Electrostatic correlations and fluctuations for ion binding to a finite length polyelectrolyte", J. Chem. Phys. **122**, 044903 (2005).

[29]R. M. Nyquist, B.-Y. Ha, and A. J. Liu, "Counterion condensation in solutions of rigid polyelectrolytes", Macromolecules **32**, 3481–3487 (1999).

[30]M. Muthukumar, "Theory of counter-ion condensation on flexible polyelectrolytes: adsorption mechanism", J. Chem. Phys. **120**, 9343 (2004).

[31]M. Muthukumar, J. Hua, and A. Kundagrami, "Charge regularization in phase separating polyelectrolyte solutions", J. Chem. Phys. **132**, 084901 (2010).

[32]A. Salehi, and R. G. Larson, "A molecular thermodynamic model of complexation in mixtures of oppositely charged polyelectrolytes with explicit account of charge association/dissociation", Macromolecules **49**, 9706–9719 (2016).

[33]T. K. Lytle, and C. E. Sing, "Transfer matrix theory of polymer complex coacervation", Soft Matter **13**, 7001–7012 (2017).

[34]M. E. Fisher, and Y. Levin, "Criticality in ionic fluids: debye-hückel theory, bjerrum, and beyond", Phys. Rev. Lett. **71**, 3826 (1993).

[35]A. Kundagrami, and M. Muthukumar, "Effective charge and coil-globule transition of a polyelectrolyte chain", Macromolecules **43**, 2574 (2010).

[36]Y. A. Budkov, N. N. Kalikin, and A. L. Kolesnikov, "Polymer chain collapse induced by many-body dipole correlations", The European Physical Journal E **40**, 47 (2017).

[37]N. V. Brilliantov, D. V. Kuznetsov, and R. Klein, "Chain collapse and counterion condensation in dilute polyelectrolyte solutions", Phys. Rev. Lett. **81**, 1433 (1998).

[38]A. M. Tom, S. Vemparala, R. Rajesh, and N. V. Brilliantov, "Mechanism of chain collapse of strongly charged polyelectrolytes", Phys. Rev. Lett. **117**, 147801 (2016).

[39]A. G. Cherstvy, "Collapse of highly charged polyelectrolytes triggered by attractive dipole-dipole and correlation-induced electrostatic interactions", J. Phys. Chem. B **114**, 5241–5249 (2010).

[40]A. M. Rumyantsev, and I. I. Potemkin, "Explicit description of complexation between oppositely charged polyelectrolytes as an advantage of the random phase approximation over the scaling approach", Phys. Chem. Chem. Phys. **19**, 27580–27592 (2017).

[41]B. Derjaguin, and L. Landau, "Theory of the stability of strongly charged lyophobic sols and of the adhesion of strongly charged particles in solutions of electrolytes", Prog. Surf. Sci. **43**, 30–59 (1941).

[42]E. J. W. Verwey, "Theory of the stability of lyophobic colloids", J. Phys. Colloid Chem. **51**, 631–636 (1947).

[43]E. Trizac, and Y. Levin, "Renormalized jellium model for charge-stabilized colloidal suspensions", Phys. Rev. E **69**, 031403 (2004).

[44]T. E. Colla, and Y. Levin, "The renormalized jellium model of colloidal suspensions with multivalent counterions", J. Chem. Phys. **133**, 234105 (2010).

[45]Z.-G. Wang, "Fluctuation in electrolyte solutions: the self energy", Phys. Rev. E **81**, 021501 (2010).

[46]G. Fredrickson, *The equilibrium theory of inhomogeneous polymers* (Oxford University Press, USA, 2013).

[47]A. V. Ermoshkin, A. N. Kudlay, and M. Olvera de la Cruz, "Thermoreversible crosslinking of polyelectrolyte chains", J. Chem. Phys. **120**, 11930 (2004).

[48]A. N. Semenov, and M. Rubinstein, "Thermoreversible gelation in solutions of associative polymers. 1. statics", Macromolecules **31**, 1373–1385 (1998).

[49]I. Borukhov, D. Andelman, R. Borrega, M. Cloitre, L. Leibler, and H. Orland, "Polyelectrolyte titration: theory and experiment", The Journal of Physical Chemistry B **104**, 11027–11034 (2000).

[50]J. M. Martin, W. Li, K. T. Delaney, and G. H. Fredrickson, "Statistical field theory description of inhomogeneous polarizable soft matter", J. Chem. Phys. **145**, 154104 (2016).

[51]K. T. Delaney, and G. H. Fredrickson, "Theory of polyelectrolyte complexation—complex coacervates are self-coacervates", J. Chem. Phys. **146**, 224902 (2017).

Chapter 5

FIELD THEORETIC TECHNIQUES TO STUDY FLUCTUATIONS

Variational Gaussian approaches, sometimes termed renormalized Gaussian fluctuations (RGF), are a powerful technique to describe field theoretic formulations of partition sums beyond the perturbative, random phase approximation (RPA). Most recently, it was generalized to study polyelectrolytes, where it was shown to capture fluctuations corresponding to changes in chain conformation. However, while the RGF approach is well-grounded in the Gibbs-Feynman-Bogoliubov (GFB) inequality for real-valued actions, the field theories that it has been recently applied to feature *complex-valued* actions. We show that the RGF self-consistency conditions are the same as those derived from a self-consistent first-order perturbation (sc1P), thus giving another interpretation of the RGF that does not rely on the GFB inequality. Further, we show that the self-consistent conditions derived in our theories all involve a self-consistent determination of the structure factor; this renormalization of structure is a vital contribution of the newly-considered, non-perturbative fluctuations. Specifically, we show that the RGF/sc1P procedure applied in the grand canonical ensemble renormalizes the *intra*chain structure. Next, although the RGF cannot be readily applied in the canonical ensemble, the sc1P can. By exactly re-summing a sub-collection of terms in the perturbation expansion, we obtain transparent self-consistency conditions that incorporate a renormalized *multi-chain* structure factor, including both intra- and inter-chain effects. Our results shed light on previous self-consistent perturbation theories in the canonical ensemble. We close by discussing the relation of the RGF to other self-consistent fluctuation theories.

5.1 Introduction

Statistical mechanics problems are often profitably reformulated as field theories, whereby a partition sum is transformed from a many-body, particle-based representation to a field-theoretic representation via standard mathematical identities [1]. The fields represent a collective description of the system, typically representing density or auxiliary (chemical) potential fields. The resulting action ("Hamiltonian") in the statistical weight is usually complex-valued, and the evaluation of the

field-theoretic partition sum is typically impossible in full but is amenable to several analytical tools. The saddle point of the complex action corresponds to a mean-field solution, while including the leading order harmonic fluctuations about the saddle point yields the random phase approximation (RPA) [1–6].

In many soft matter systems, the fluctuations play a crucial part in the thermodynamics [7–12]. One of the most notable examples is charged systems, where for bulk systems the mean field solution of the free energy is *independent* of the electrostatic interactions due to charge neutrality; electrostatic fluctuations are a crucial part of the thermodynamics. For this reason, studies of charged systems have employed a variety of approaches to study the fluctuations in charged systems [13–28].

One of the most powerful tools to describe fluctuations are variational Gaussian, or renormalized Gaussian fluctuation (RGF) approaches based on the Gibbs-Feynman-Bogoliubov (GFB) bound [29]. We direct interested readers into excellent pedagogical discussions with example applications to toy models involving scalar actions [2, 3]. This approach has been widely used in the study of charged systems [13, 14, 17, 20, 21], and was recently extended to polymers where it was shown to *naturally* produce a self-consistent procedure involving renormalization of the intrachain structure, something that had previously only been done by self-consistent PRISM theories [30, 31].

Despite the success of the various variational Gaussian theories, it is interesting to note that the GFB free energy bound, upon which these variational theories are constructed, only holds if the action in the partition sum is real-valued. In contrast, typical field theories involve complex-valued actions. It is thus desirable to find a more solid basis for such variational Gaussian theories – even if rigorous bounds can not be found, such work would give deeper insight into the mechanics of the GFB procedure.

To this end, recent work by Frydel et al. has explored the connection of variational Gaussian theories to the inhomogeneous Ornstein-Zernicke equations closed by the RPA closure [32], as well as connections with hierarchies of exact relations derived from derivatives of the partition sum [2]. In this paper, we explore the connection of the Gaussian variational procedure to self-consistent first order perturbation (which we will call sc1P for short) theory. We are motivated by the fact that for certain simple scalar theories, the sc1P procedure, which is also sometimes called a self-consistent Hartree renormalization [33], can be shown to give the same self-consistent equations as the RGF [3]. A version of the sc1P procedure has also been

used to study semidilute solutions of polymers [11], where fluctuations beyond the RPA are known to be important.

In Section II, we outline the field theoretic formalism for a generic system of polymers interacting via a pair potential, and recapitulate the RGF procedure in the grand canonical ensemble. In Section III we present the sc1P procedure for both grand canonical and canonical ensembles. In Section IV we compare RGF and sc1P to each other and to the RPA and exact field-theoretic expressions, emphasizing that the new fluctuations considered by the self-consistency approach relate to modifications of the chain structure. Finally, in Section V we close by comparing the non-perturbative, self-consistent approaches derived in this paper with other non-perturbative theories, noting their similarities and differences. Overall, we note the importance of ensembles and whether or not the molecules considered are rigid.

5.2 Field Theoretic Framework

We first derive the field-theoretic representation of a system of homopolymer chains with intramolecular bonded interaction βH_B and under an external field $h(\mathbf{r})$. A particle-based representation describes configurations based on the chain configuration $\mathcal{R}_A \equiv \{\mathbf{r}_{Aj}\}$, where A indexes the A-th molecule and runs up to the total number n of molecules, and j indexes the j-th "monomer" out of a total number N of monomers in the A-th molecule A. The microscopic density operator for the polymer is then defined as

$$\hat{\rho}(\mathbf{r}) = \sum_{A=1}^{n} \sum_{j=1}^{N} \delta(\mathbf{r} - \mathbf{r}_{Aj}), \tag{5.1}$$

For monomeric species, $N = 1$ and the index j only takes the value of 1.

In addition to the intra-chain bonded interaction βH_B, we let the monomers interact through a pair potential U:

$$\beta H_U = \frac{1}{2} \int d\mathbf{r} d\mathbf{r}' \hat{\rho}(\mathbf{r}) U(\mathbf{r}, \mathbf{r}') \hat{\rho}(\mathbf{r}'), \tag{5.2}$$

The canonical partition function is then

$$Q = \frac{1}{n! v^{nN}} \prod_{A,j} \int d\mathbf{r}_{Aj} \exp\left(-\beta H_B - \beta H_U - \sum_{Aj} h(\mathbf{r}_{Aj}) \right). \tag{5.3}$$

We use the monomer volume v_γ instead of the cube of the thermal de Broglie wavelength; this merely shifts the reference chemical potential and does not affect thermodynamic properties.

Next, we use the Hubbard-Stratanovich (HS) transformation to decouple densities in the pair interaction. This introduces an auxiliary potential $\Psi(\mathbf{r})$ and the interaction energy is written as

$$e^{-\beta H_U} = \frac{1}{\Omega_U} \int D\Psi \ \cdot \exp\left[-i \int d\mathbf{r} \hat{\rho}(\mathbf{r}) \Psi(\mathbf{r}) \right] \tag{5.4}$$

$$\exp\left[-\frac{1}{2} \int d\mathbf{r} d\mathbf{r}' \ \ \Psi(\mathbf{r}) U^{-1}(\mathbf{r}, \mathbf{r}') \Psi(\mathbf{r}') \right] \tag{5.5}$$

Note that the argument of the exponential is now *complex-valued*, but is only *linear* in the density ρ. Being linear in ρ, the chains are now decoupled, interacting with each other only vicariously through the auxiliary potential Ψ. Meanwhile, Ω_U is a normalization factor given by

$$\begin{aligned} \Omega_U &= \int D\Psi \exp\left[-\frac{1}{2} \int d\mathbf{r} d\mathbf{r}' \ \ \Psi(\mathbf{r}) U^{-1}(\mathbf{r}, \mathbf{r}') \Psi(\mathbf{r}') \right] \\ &= [\det U]^{1/2} \end{aligned} \tag{5.6}$$

The field-theoretic canonical partition function is then

$$Q = \frac{1}{n! v^{nN}} \int \frac{\mathcal{D}\Psi}{\Omega_U} \exp(-L^c[i\Psi + h]). \tag{5.7}$$

with a complex-valued canonical action

$$L^c[\psi] = \frac{1}{2} \int d\mathbf{r} d\mathbf{r}' \ \ \Psi \cdot U^{-1} \cdot \Psi - n \ln Q[i\Psi + h] \tag{5.8}$$

where the configurational integration is now included in the *independent* single-chain partition functions Q:

$$Q = \int \mathcal{D}\mathcal{R} e^{-H_B - \int d\mathbf{r}(h + i\Psi)\hat{\rho}^{(1)}} \tag{5.9}$$

where the superscript "(1)" in $\hat{\rho}^{(1)}$ is meant to emphasize that this is a *single*-chain version of the microscopic density operator.

Finally, we introduce the chain fugacities λ and transform Q to the grand canonical partition function using a standard mathematical identity for the series representations of the exponential function [1]

$$\Xi = \frac{1}{\Omega_U} \int \mathcal{D}\Psi e^{-L^{gc}[i\Psi + h]} \tag{5.10}$$

with the grand canonical "action"

$$L^{gc}[\Psi] = \frac{1}{2} \int d\mathbf{r} d\mathbf{r}' \ \ \Psi \cdot U^{-1} \cdot \Psi - \lambda Q[i\Psi + h] \tag{5.11}$$

One sees that the canonical and grand canonical field-theoretic partition functions only differ in the term with the chain partition function Q.

The above field theoretic representation is derived only using identities and the partition functions are thus *exact*. We reiterate that the actions in the full field-theory equations are complex-valued. The saddle-point approximation of the partition function is found by the value of the action at the mean field Ψ such that the functional derivative $\delta L/\delta\Psi = 0$ [1]. RPA theory expands about the saddle point in quadratic fluctuations, but results in a *fixed* structure factor determined solely by the saddle-point [1]. For uniform systems, the chain structure factor that enters the RPA is independent of polymer concentration. This is not an issue for rigid molecules, but can be vitally important for semidilute polymer concentrations [30, 31]. As we will see below, an important beyond-RPA physical effect captured by the *non-perturbative* RGF and sc1P approaches will be a concentration-dependent renormalization of polymer conformations.

5.3 Renormalized Gaussian Fluctuations

The RGF theory follows the Gibbs-Feynman-Bogoliubov (GFB) approach by introducing a general Gaussian reference action L_{ref}. The Gaussian fluctuations are not fixed by the saddle point, but rather "renormalized" by a variational condition. For the Ψ field, we use the following Gaussian reference action:

$$L_0 = \frac{1}{2}\int d\mathbf{r}d\mathbf{r}'[\Psi(\mathbf{r}) + i\psi(\mathbf{r})]G^{-1}(\mathbf{r},\mathbf{r}')[\Psi(\mathbf{r}') + i\psi(\mathbf{r}')] \tag{5.12}$$

which is parametrized by a mean electrostatic potential $-i\psi(\mathbf{r})$ and a Green's function $G(\mathbf{r},\mathbf{r}')$. This reference action accounts for the deviation $\delta\psi = \Psi - (-i\psi) = \Psi + i\psi$ with variance G from the mean $-i\psi$.

For reasons that will become clear soon, the GFB procedure is most readily applied to the grand canonical ensemble. We use L_0 to rewrite *exactly* the grand canonical partition function Eq. (5.10) as

$$\begin{aligned}\Xi =& \frac{1}{\Omega_U}\int \mathcal{D}\Psi e^{-L_0[\Psi]}e^{-(L[\Psi]-L_0[\Psi])}\\ =& \frac{\Omega_G}{\Omega_U}\left\langle e^{-(L[\Psi]-L_0[\Psi])}\right\rangle_0\end{aligned} \tag{5.13}$$

where $\langle\cdots\rangle_0$ denotes an average over Ψ with respect to the reference action L_0, and Ω_G the corresponding partition function of L_{ref}, defined analogously to Ω_U in Eq. (5.6) with G in place of U. For notational clarity in this section, we will write $\langle\cdots\rangle_0$ as $\langle\cdots\rangle$.

The GFB procedure proceeds by approximating the field integral over Ψ with a leading order cumulant expansion

$$\Xi \approx \frac{\Omega_G}{\Omega_U} e^{-\langle L - L_0 \rangle} \equiv e^{-W_v} \equiv \Xi_{GFB}. \tag{5.14}$$

which defines $W_v = \frac{\Omega_G}{\Omega_U} e^{-\langle L - L_0 \rangle}$ as the *variational* grand free energy. If the action were real-valued, the cumulant expansion would actually satisfy the GFB inequality and thus produce a free energy bound. Unfortunately, because the action is complex, this bound is no longer true. Nevertheless, the formal steps and stationarity conditions of the GFB procedure can still be followed.

This cumulant expansion in the exponent can be readily evaluated owing to the Gaussian nature of the fluctuating field, and results in the following grand partition function Ξ_{GFB} and *variational* grand free energy W_v:

$$\Xi_{GFB} = e^{-W_v[G,\psi]} \tag{5.15}$$

$$W_v[G,\psi] = -\frac{1}{2} \ln\left(\frac{\det G}{\det U}\right) + \frac{1}{2} \int d\mathbf{r} d\mathbf{r}' [U^{-1} - G^{-1}] G - \frac{1}{2} \int d\mathbf{r} d\mathbf{r}' \psi \cdot U^{-1} \cdot \psi - \lambda \langle Q \rangle . \tag{5.16}$$

Importantly, in the grand canonical ensemble the partition function term $\langle Q \rangle$ can be averaged *exactly*, in contrast to the canonical ensemble which would require performing a Gaussian average on $\langle \ln Q \rangle$. The former is easily performed because the only Ψ dependence in Q is $e^{-i \int \Psi \cdot \hat{\rho}}$, and can be averaged inside of the configurational integral using the identities in the appendix. The averaged single-particle/chain partition function is:

$$\langle Q \rangle = \int \mathcal{D}\mathcal{R} \; e^{-H_B - \int d\mathbf{r} (h+\psi) \cdot \hat{\rho} - \frac{1}{2} \int d\mathbf{r} d\mathbf{r}' \; \hat{\rho}^{(1)} \cdot G \cdot \hat{\rho}^{(1)}} \tag{5.17}$$

The calculation of the single-chain partition function now features $G(\mathbf{r}, \mathbf{r}')$ as an effective *intra*chain instantaneous interaction

$$u_p^{\text{inst}}(\mathcal{R}) \equiv \frac{1}{2} \int d\mathbf{r} d\mathbf{r}' \hat{\rho}^{(1)}(\mathbf{r}) G(\mathbf{r}, \mathbf{r}') \hat{\rho}^{(1)}(\mathbf{r}'). \tag{5.18}$$

This interaction is conformation dependent. We emphasize that the fluctuation-mediated effective intra-particle/chain interaction $G(\mathbf{r}, \mathbf{r}')$ is missing in self-consistent mean-field (SCMF) theories. For polymeric species, it is precisely this intrachain interaction that allows chain structure to adapt to solution conditions.

It remains to determine the self-consistent set of equations for ψ and G. The RGF conditions for ψ and G require that Eq. (5.16) be stationary with respect to both. The condition arising from ψ yields the mean-field condition:

$$0 = \frac{\delta W_v}{\delta \psi} = -\int d\mathbf{r}' U(\mathbf{r}, \mathbf{r}')\psi(\mathbf{r}') + \rho(\mathbf{r}) \tag{5.19}$$

where we have used the system density $\rho(r) = -\lambda \delta Q[\psi]/\delta\psi(r)$. This mean-field condition might appear trivial, but $\rho(r)$ depends on the external field h, the mean electrostatic field ψ, *and* the effective intrachain interaction mediated by G. Thus although the expression appears simple, in general the mean ψ will *not* be the same as the saddle-point value.

Similarly, the functional differentiation with respect to G yields

$$0 = -G^{-1} + U^{-1} + \lambda \langle Q \rangle \left\langle \hat{\rho}^{(1)}(r)\hat{\rho}^{(1)}(r') \right\rangle \tag{5.20}$$

where $\left\langle \hat{\rho}^{(1)}(r)\hat{\rho}^{(1)}(r') \right\rangle_1$ is a single-chain structure factor determined by the single-chain averaged partition function $\langle Q \rangle$, i.e. it is the single-chain structure of a chain under external fields ψ and h, and interacting with itself via the pair interaction G. The above two conditions constitute the self-consistent equations of the RGF theory. Importantly, the Green's function G depends on the single-chain structure factor, which in turn implicitly depends on G through $\langle Q \rangle$. Thus the self-consistent equations require a self-consistent solution of the single-chain structure as well.

This chain-structure self-consistency is *missing* in the RPA procedure. For simple electrolytes, the RGF and RPA were shown to be equivalent [2], but this is no longer true when the chain has intramolecular flexibility that allows it to adapt its chain configuration to the the external field h and the variational parameters ψ and G.

We acknowledge that the exact evaluation of single-chain partition functions is difficult even for simpler pair interactions, and in general can be done by numerical simulation [34], or by other simple variational approaches [11, 30, 31, 34]. However, the particular way by which one evaluates the single-chain partition function is not necessary for the discussions in this paper, and we refer interested readers to the aforementioned references or Ch. 2.

5.4 Self-Consistent First Order Perturbation (sc1P)

The self-consistent first order perturbation involves evaluating the partition integral with a reference action $L_0[\psi]$. Then, the average of any observable A can be exactly

written as

$$\langle A \rangle = \frac{\left\langle A e^{-(L-L_0)} \right\rangle_0}{\left\langle e^{-(L-L_0)} \right\rangle_0} \tag{5.21}$$

where the reference average $\langle \cdot \rangle_0$ is:

$$\langle \cdot \rangle_0 = \frac{\int D\Psi(\cdot) e^{-L_0[\Psi]}}{\int D\Psi e^{-L_0[\Psi]}} \tag{5.22}$$

The first-order perturbation expands (5.21) to first order in ΔL:

$$\langle A \rangle = \langle A \rangle_0 - \langle A \Delta L \rangle_0 + \langle A \rangle_0 \langle \Delta L \rangle_0 + \ldots \tag{5.23}$$

The self-consistent procedure comes from setting $\langle A \rangle = \langle A \rangle_0$, i.e. requiring the leading order first order perturbation to vanish

$$0 = - \langle A \Delta L \rangle_0 + \langle A \rangle_0 \langle L \rangle_0 . \tag{5.24}$$

By setting the observable A to Ψ and $\delta\psi\delta\psi$, we can self-consistently respectively estimate the two parameters of the reference action: ψ and G^{-1}. The physical motivation for doing so is to essentially "renormalize" the first order perturbation correction into the reference Gaussian action and into the leading order $\langle A \rangle_0$ contribution. This is most clearly understood when $A = \delta\psi\delta\psi$, and $\langle \delta\psi\delta\psi \rangle_0 = G$. In other words, we want the reference action's Green's function to approximate the actual system's second order response as closely as possible.

5.4.1 sc1P in Grand Canonical Ensemble

We first consider the Grand Canonical Ensemble, where, like the RGF, it is convenient to use a Gaussian reference action

$$L_0[\Psi] = \frac{1}{2} \int_{12} \delta\psi_1 G_{12}^{-1} \delta\psi_2 . \tag{5.25}$$

For economy of notation we use subscripts to denote the arguments of the functions and integration variables.

Applying the sc1P to the mean field $\langle \Psi \rangle = -i\psi + \delta\psi$, the sc1P condition is

$$\begin{aligned} 0 &= - \langle \Psi \Delta L \rangle_0 + \langle A \rangle_0 \langle L \rangle_0 \\ &= - \langle -i\psi + \delta\psi \Delta L \rangle_0 + \langle -i\psi + \delta\psi \rangle_0 \langle L \rangle_0 \\ &= - \langle \delta\psi \Delta L \rangle_0 + \langle \delta\psi \rangle_0 \langle L \rangle_0 \\ &= - \langle \delta\psi \Delta L \rangle_0 \end{aligned} \tag{5.26}$$

where we note that ψ cancels in the two contributions because it is a constant and can be can be taken out of the averaging, and under the Gaussian reference action $\langle \delta\psi \rangle_0 = 0$.

The reference averages will require averages over the chain partition function Q. We introduce the shorthand notation

$$\int_R (\cdot) \equiv \int \mathcal{D}\mathcal{R} e^{-\beta H_B - \int_1 h_1 \cdot \hat{\rho}_1^{(1)}} (\cdot) \tag{5.27}$$

in order to focus on the effects of the averaging on the auxiliary field. Like in the RGF derivation, the Gaussian averaging of the partition function yields $\langle Q \rangle_0 = \int_R \exp[-\int_1 \hat{\rho}_1^{(1)} \cdot \psi_1 - \int_{12} \frac{1}{2} \hat{\rho}_1^{(1)} \cdot G_{12} \cdot \hat{\rho}_2^{(1)}]$ and $\lambda \langle Q \rangle_0 = n$ the number of chains. In this section we denote configurational averages with this effective single chain partition function as $\langle \cdot \rangle_R$. The chain density operators involved are to be understood as the single-chain density operator.

In detail, we evaluate the first order term to be:

$$\begin{aligned}
\langle \delta\psi_1 \Delta L \rangle_0 &= \left\langle \delta\psi_1 \left(-\frac{1}{2} \int_{34} \psi_3 U_{34}^{-1} \psi_4 - i \int_{34} \psi_3 U_{34}^{-1} \delta\psi_4 + \frac{1}{2} \int_{34} \delta\psi_3 (U_{34}^{-1} - G_{34}^{-1}) \delta\psi_4 - \lambda Q[\Psi] \right) \right\rangle_0 \\
&= \left\langle \delta\psi_1 \left(-i \int_{34} \psi_3 U_{34}^{-1} \delta\psi_4 - \lambda Q[\psi] \right) \right\rangle_0 \\
&= \left[-i \int_{34} \psi_3 U_{34}^{-1} \langle \delta\psi_1 \delta\psi_4 \rangle_0 - \lambda \int_R \left\langle \delta\psi_1 e^{-\int_1 \hat{\rho}^{(1)} \psi_1 - i \int_1 \hat{\rho}_1^{(1)} \delta\psi_1} \right\rangle_0 \right] \\
&= \left[-i \int_{34} \psi_3 U_{34}^{-1} G_{14} - \lambda \int_R (-i) e^{-\int_1 \hat{\rho}_1^{(1)} \psi_1 - \frac{1}{2} \int_{12} \hat{\rho}_1^{(1)} \cdot G_{12} \cdot \hat{\rho}_2^{(1)}} \int_4 \hat{\rho}_4^{(1)} G_{14} \right] \\
&= -i \left[\int_{34} \psi_3 U_{34}^{-1} G_{14} - \int_4 \langle \rho_4 \rangle G_{14} \right] \\
&= -i \int_4 G_{14} \left[-\langle \rho_4 \rangle + \int_3 U_{34}^{-1} \psi_3 \right]
\end{aligned} \tag{5.28}$$

In the second line we have used the fact that terms that are odd in $\delta\psi$ disappear after Gaussian averaging, and in the third line we wrote out the single-chain partition function in full to identify the portion of the partition sum integrand that is averaged by the reference action. The fourth line makes use of a Gaussian averaging identity presented in the appendix, and the fifth line makes use of the fact that, in the grand canonical ensemble

$$\lambda \langle Q \rangle_0 \frac{1}{\langle Q \rangle_0} \int_R \hat{\rho}^{(1)} e^{-\int_1 \hat{\rho}_1^{(1)} \psi_1 - \frac{1}{2} \int_{12} \hat{\rho}_1^{(1)} \cdot G_{12} \cdot \hat{\rho}_2^{(1)}} \tag{5.29}$$

$$= \lambda \langle Q \rangle_0 \left\langle \hat{\rho}^{(1)} \right\rangle_R \equiv \langle \rho \rangle \tag{5.30}$$

where $\left\langle \hat{\rho}^{(1)} \right\rangle_R$ is the average density of a *single* chain and is proportional to N/V. When combined with the number of chains factor $\lambda \langle Q \rangle_0 = n$, one gets the *system* average density $\langle \rho \rangle$

Finally, setting the term in the brackets to zero yields

$$0 = -\langle \rho_1 \rangle + \int_2 U_{12}^{-1} \psi_2 \tag{5.31}$$

which is the same expression as Eq. (5.19) obtained previously for the RGF! Importantly, the sc1P requires the same effective single-chain partition function $\int_R \exp[-\int_1 \hat{\rho}_1^{(1)} \psi_1 - \frac{1}{2} \int_{12} \hat{\rho}_1^{(1)} \cdot G_{12} \cdot \hat{\rho}_2^{(1)}]$ as the RGF, and thus also contains the same self-consistent renormalization of chain structure and G that is described in the RGF.

To complete the correspondence between the sc1P and RGF for grand canonical systems of chains, we consider the sc1P estimate of $G = \langle \delta\psi \delta\psi \rangle$. The first order perturbation terms that we have to evaluate are:

$$\langle \delta\psi\delta\psi \rangle_0 \langle \Delta L \rangle_0 = G_{12} \left[\frac{1}{2} \int_{34} [U^{-1} - G^{-1}]_{34} G_{34} - \frac{1}{2} \int_{34} \psi_3 U_{34}^{-1} \psi_4 - \lambda \langle Q \rangle_0 \right] \tag{5.32}$$

$$\begin{aligned}
\langle \delta\psi\delta\psi (L - L_0) \rangle_0 =& \frac{1}{2} \int_{34} \left\langle \delta\psi_1 \delta\psi_2 (\delta\psi_3 - i\psi_3) U_{34}^{-1} (\delta\psi_4 - i\psi_4) \right\rangle_0 \qquad (5.33) \\
& - \lambda \langle \delta\psi\delta\psi Q[\psi] \rangle_0 - \frac{1}{2} \int_{3,4} \left\langle \delta\psi_1 \delta\psi_2 \delta\psi_3 G_{34}^{-1} \delta\psi_4 \right\rangle_0 \\
=& \quad \frac{1}{2} \left[G_{12} \int_{34} G_{34} U_{34}^{-1} + 2 \int_{34} G_{13} G_{24} U_{34}^{-1} \right] - \frac{1}{2} G_{12} \int_{34} \psi_3 U_{34}^{-1} \psi_4 \\
& - \frac{1}{2} \left[G_{12} \int_{34} G_{34} G_{34}^{-1} + 2 \int_{34} G_{13} G_{24} G_{34}^{-1} \right] \\
& - \lambda \int_R e^{-\int_1 \hat{\rho}_1^{(1)} \psi_1 - \frac{1}{2} \int_{12} \hat{\rho}_1^{(1)} \cdot G_{12} \cdot \hat{\rho}_2^{(1)}} \left[G_{12} - \int_{34} G_{13} G_{24} \rho_3^{(1)} \rho_4^{(1)} \right] \\
=& \frac{1}{2} \left[G_{12} \int_{34} G_{34} (U_{34}^{-1} - G_{34}^{-1}) + 2 \int_{34} G_{13} G_{24} (U_{34}^{-1} - G_{34}^{-1}) \right] \\
& - \frac{1}{2} G_{12} \int_{34} \psi_3 U_{34}^{-1} \psi_4 - G_{12} \lambda \langle Q \rangle_0 + \lambda \langle Q \rangle_0 \int_{34} G_{13} G_{24} \langle \rho_3 \rho_4 \rangle_R
\end{aligned}$$

We have again used the Gaussian averaging identities presented in the appendix, and similarly to before identified

$$\frac{1}{\langle Q \rangle_0} \int_R e^{-\int_1 \hat{\rho}_1^{(1)} \psi_1 - \frac{1}{2} \int_{12} \hat{\rho}_1^{(1)} \cdot G_{12} \cdot \hat{\rho}_2^{(1)}} \rho_1^{(1)} \rho_2^{(1)} = \left\langle \rho_1^{(1)} \rho_2^{(1)} \right\rangle_R \tag{5.34}$$

as the *single-chain* structure, of a chain under an interaction mediated by the Green's function G and the mean field ψ. Finally, the self-consistency condition requires

$$\begin{aligned} 0 &= \langle \delta\psi\delta\psi(L - L_0)\rangle_0 - \langle \delta\psi\delta\psi\rangle_0 \langle L - L_0\rangle_0 \\ &= \int_{34} G_{13}G_{24}(U_{34}^{-1} - G_{34}^{-1}) + \lambda \langle Q\rangle_0 \int_{34} G_{13}G_{24} \left\langle \rho_3^{(1)}\rho_4^{(1)} \right\rangle_0 \end{aligned} \tag{5.35}$$

which is satisfied by

$$0 = U^{-1} - G^{-1} + \lambda \langle Q\rangle_0 \left\langle \rho^{(1)}\rho^{(1)} \right\rangle_0 . \tag{5.36}$$

which is the same as Eq. (5.20) derived in the RGF theory. We have thus shown, within the grand canonical ensemble, the equivalence of the self-consistency conditions derived from the RGF and from the sc1P procedures.

5.4.2 sc1P in Canonical Ensemble

The field theoretic action for the canonical ensemble features a $n \ln Q[i\Psi + h]$ term. The RGF procedure requires Gaussian averaging over this natural logarithm $\langle \ln Q\rangle_0$, which unfortunately can not be simply carried out (one could perform a series expansion about a reference partition function, but this will involve products of the partition function and becomes unwieldy).

If one were to use the same Gaussian reference action as in the grand canonical ensembles, the sc1P would run into a similar problem as the RGF, where a Gaussian average of $\langle \ln Q\rangle_0$ is required. Instead of carrying out the configurational integrals which produce the $\ln Q$ term in the field-theoretic action, we preliminarily opt to explicitly keep all chain coordinate degrees of freedom, such that we have a hybrid particle-field partition function

$$Z = \int \mathcal{D}\{\mathcal{R}\} \int \mathcal{D}\Psi e^{-H[\Psi,\{\mathcal{R}\}]} \tag{5.37}$$

with canonical action

$$\begin{aligned} H[\Psi, \{\mathcal{R}\}] = \sum_A H_c[\mathcal{R}_A] &+ \int_1 \hat{\rho}_1(h_1 + i\Psi_1) \\ &+ \frac{1}{2}\int_{12} \Psi_1 U_{12}^{-1}\Psi_2 \end{aligned} \tag{5.38}$$

where the sum runs over the chains in the system and $\hat{\rho} = \sum_A \hat{\rho}_A$ is again the *system* instantaneous density. It will also be convenient to introduce the notation

$$\int_R = \int \mathcal{D}\{\mathcal{R}\} e^{-\sum_A H_c[\mathcal{R}_A] - \int_1 \hat{\rho}_1 h_1}. \tag{5.39}$$

To carry out the sc1P procedure we use the same Gaussian action as before:

$$L_0[\Psi] = \frac{1}{2}\int_{12} \delta\psi_1 \cdot G_{12}^{-1} \cdot \delta\psi_2 \tag{5.40}$$

and we define Gaussian averages $\langle\cdot\rangle_0$ just as before:

$$\langle\cdot\rangle_0 = \frac{1}{\Omega_G}\int \mathcal{D}\Psi e^{-L_0[\Psi]} \tag{5.41}$$

The perturbation theory requires the difference in the action, which we partition as:

$$\begin{aligned} H - L_0 &= \sum_A H_c[\mathcal{R}_A] + \frac{1}{2}\int_{12} \delta\psi_1 \cdot (U^{-1} - G^{-1})_{12} \cdot \delta\psi_2 + \int_1 \hat{\rho}_1(-i\psi_1 + \delta\psi_1) \\ &\quad - i\int_{12} \delta\psi_1 \cdot U_{12}^{-1} \cdot \psi_2 - \frac{1}{2}\int_{12} \psi_1 \cdot U_{12}^{-1} \cdot \psi_2 + \int_1 h_1\hat{\rho}_1 \\ &\equiv \sum_A H_c[\mathcal{R}_A] + \int_1 h_1\hat{\rho}_1 + H_1 + H_2 + H_3 \end{aligned}$$

with the following definitions:

$$H_1 \equiv \frac{1}{2}\int_{12} \delta\psi_1 \cdot [U^{-1} - G^{-1}] \cdot \delta\psi_2 = \frac{1}{2}\int_{12} \delta\psi_1 \cdot \zeta_{12} \cdot \delta\psi_2 \tag{5.42}$$

$$H_2 \equiv \int_1 [\hat{\rho}_1\psi_1 + i\int_1 \delta\psi_1(\hat{\rho}_1 - \int_{12} U_{12}^{-1} \cdot \psi_2) \tag{5.43}$$

$$H_3 \equiv -\frac{1}{2}\int_{12} \psi_1 \cdot U_{12}^{-1} \cdot \psi_2 \tag{5.44}$$

where in H_1 we defined $\zeta \equiv U^{-1} - G^{-1}$ to save space. With these definitions, the full partition function is

$$Z = \frac{\Omega_G}{\Omega_U}\int_R \left\langle e^{-H_1-H_2-H_3}\right\rangle_0 \tag{5.45}$$

and averages in the full partition function are

$$\langle\cdot\rangle = \frac{\int_R \left\langle(\cdot)e^{-H_1-H_2-H_3}\right\rangle_0}{\int_R \left\langle e^{-H_1-H_2-H_3}\right\rangle_0}. \tag{5.46}$$

Instead of carrying out the perturbation to first order in $H - L_0$, we only expand to first order in H_1. This is because we observe that H_3 is a constant (for prescribed ψ), and that H_2 has a simple form that can be averaged with respect to L_0 even when exponentiated. For comparison, an earlier first-order perturbation analysis (with a slightly different reference action) studied only the case where $\psi = 0$ and could be ignored, kept the expansion with respect to the $i\hat{\rho}\delta\psi$ term in H_2 to all powers, while

excluding terms corresponding to the product of H_1 and higher orders of H_2 [11, 24]. Our approach, by keeping H_2 and H_3 exponentiated, goes further and exactly resums all terms that are first order in H_1 but of higher order in H_2 and H_3.

Such an expansion scheme essentially sets the reference system about which we perturb to one where $H_1 = 0$. The partition function of this reference system can be written as:

$$\begin{aligned}\frac{1}{n!}\left\langle \int_R e^{-H_2-H_3}\right\rangle_0 =& \frac{1}{n!}e^{-H_3}\int_R \left\langle e^{-H_2}\right\rangle_0 \\ =& \frac{1}{n!}e^{-H_3}\int_R e^{-\int_1 \hat{\rho}_1\psi_1 - \frac{1}{2}\int_{12}\delta\hat{\rho}_1 G_{12}\delta\hat{\rho}_2} \\ \equiv& e^{-H_3}Z_R = Y \end{aligned} \tag{5.47}$$

where we define $\delta\hat{\rho}_1 = \hat{\rho}_1 - \int_2 U_{12}^{-1}\cdot\psi_2$. The factor of $\exp(-H_3)$ can be factored out because it does not depend on the configurations $\mathcal{R}$ nor the fluctuating field Ψ. Z_R or Y can be thought of the partition function of a system of chains interacting with the pair interaction G, and under external potential $\psi_1 - \int_{23} G_{12}U_{23}^{-1}\psi_3$. When the external potential is constant, i.e. bulk systems, due to the constant number of chains in the canonical ensemble, the external potential terms can be factored out of the partition sum and Z_R or Y are essentially the partition function of a system of chains interacting via G.

We write averages with respect to this new effective reference as

$$\langle O\rangle_{ref} = \frac{1}{n!Y}\int_R O\left\langle e^{-H_2-H_3}\right\rangle_0 = \frac{1}{n!Y}\frac{1}{n!}e^{-H_3}\int_R Oe^{-\int_1\hat{\rho}_1\psi_1-\frac{1}{2}\int_{12}\delta\hat{\rho}_1 G_{12}\delta\hat{\rho}_2} \tag{5.48}$$

Our perturbation scheme for an observable O thus amounts to

$$\langle O\rangle = \frac{\int_R \left\langle Oe^{-H_1-H_2-H_3}\right\rangle_0}{\int_R\left\langle e^{-H_1-H_2-H_3}\right\rangle_0} \tag{5.49}$$

$$\begin{aligned}\approx& \frac{\int_R\left\langle O(1-H_1)e^{-H_2-H_3}\right\rangle_0}{\int_R\left\langle(1-H_1)e^{-H_2-H_3}\right\rangle_0} \\ =& \frac{\int_R\left\langle Oe^{-H_2-H_3}\right\rangle_0 - \int_R\left\langle OH_1e^{-H_2-H_3}\right\rangle_0}{\int_R\left\langle e^{-H_2-H_3}\right\rangle_0 - \int_R\left\langle H_1e^{-H_2-H_3}\right\rangle_0} \\ =& \frac{\int_R\left\langle Oe^{-H_2-H_3}\right\rangle_0 - \int_R\left\langle OH_1e^{-H_2-H_3}\right\rangle_0}{n!Y(1-\frac{1}{n!Y}\int_R\left\langle H_1e^{-H_2-H_3}\right\rangle_0)} \\ \approx& \langle O\rangle_{ref} - \langle OH_1\rangle_{ref} + \langle O\rangle_{ref}\langle H_1\rangle_{ref}\end{aligned} \tag{5.50}$$

We now apply the self-consistent perturbation to determine the condition for the mean field ψ. Evaluating the terms in the perturbation, we obtain:

$$\langle \Psi \rangle_{ref} = -i\psi + \langle \delta\psi \rangle_{ref} \tag{5.51}$$

$$\langle \Psi H_1 \rangle_{ref} = -i\psi \langle H_1 \rangle_{ref} + \langle \delta\psi H_1 \rangle_{ref} \tag{5.52}$$

$$\langle \Psi \rangle_{ref} \langle H_1 \rangle_{ref} = -i\psi \langle H_1 \rangle_{ref} + \langle \delta\psi \rangle_{ref} \langle H_1 \rangle_{ref} \tag{5.53}$$

and

$$\langle \Psi \rangle = -i\psi + \langle \delta\psi \rangle_{ref} - \langle \delta\psi H_1 \rangle_{ref} + \langle \delta\psi \rangle_{ref} \langle H_1 \rangle_{ref} \tag{5.54}$$

Consider the leading perturbation term $\langle \delta\psi \rangle_{ref}$:

$$\begin{aligned}
\langle \delta\psi \rangle_{ref} =& \frac{1}{n!Y} \int_R \left\langle \delta\psi_1 e^{-H_2 - H_3} \right\rangle_0 \\
=& -\frac{ie^{-H_3}}{n!Y} \int_R e^{-\int_1 \hat{\rho}_1 \psi_1} e^{-\frac{1}{2}\int_{12} \delta\hat{\rho}_1 G_{12} \delta\hat{\rho}_2} \int_2 G_{12} \left(\hat{\rho}_2 - \int_3 U_{23}^{-1} \cdot \psi_3 \right) \\
=& -i \int_2 G_{12} \left\langle \hat{\rho}_2 - \int_3 U_{23}^{-1} \cdot \psi_3 \right\rangle_{ref} \\
=& -i \int_2 G_{12} \left(\langle \hat{\rho}_2 \rangle_{ref} - \int_3 U_{23}^{-1} \cdot \psi_3 \right)
\end{aligned} \tag{5.55}$$

An intuitively appealing self-consistency condition arises if we require $0 = \langle \delta\psi \rangle_{ref}$, or

$$0 = \langle \hat{\rho}_2 \rangle_{ref} - \int_3 U_{23}^{-1} \cdot \psi_3 \tag{5.56}$$

which is a mean-field like expression. It also motivates our previous definition of $\delta\hat{\rho} = \hat{\rho} - U^{-1} \cdot \psi$, and the identification $\langle \hat{\rho} \rangle = U^{-1} \cdot \psi$ and interpretation of Y as the partition function of a system of chains feeling external potentials h and ψ, while *deviations* of density from the mean interact via the effective interaction G. Alternatively, we can consider this as a system of chains interacting with each other through G, along with external field h and mean-field $\psi_1 - \int_{23} G_{12} U_{23}^{-1} \psi_3$.Note that this reference system is *multi*-chain, and thus the structure factors involved contain *inter*-chain correlation information.

Next we check the remaining perturbation contribution $\langle \delta\psi H_1 \rangle_{ref}$:

$$\langle \delta\psi H_1 \rangle_{ref} = \frac{1}{n!Y} \int_R \left\langle \delta\psi_1 H_1 e^{-H_2 - H_3} \right\rangle_0 \tag{5.57}$$

$$= \frac{1}{n!Y} \int_R \left\langle \delta\psi_1 \frac{1}{2} \int_{23} \delta\psi_2 \zeta_{23} \delta\psi_3 e^{-H_2 - H_3} \right\rangle_0 \tag{5.58}$$

$$= \frac{1}{2} \int_{23} \zeta_{23} \frac{e^{-H_3}}{n!Y} \int_R \left\langle \delta\psi_1 \delta\psi_2 \delta\psi_3 e^{-H_2} \right\rangle_0$$

$$= \frac{1}{2} \int_{23} \zeta_{23} \frac{e^{-H_3}}{n!Z_R X} \int_R (-i) e^{-\int_1 \hat{\rho}_1 \psi_1} e^{-\frac{1}{2}\int_{12} \delta\hat{\rho}_1 G_{12} \delta\hat{\rho}_2} \ldots \tag{5.59}$$

$$\left[- \int_{456} G_{14} G_{25} G_{36} \delta\hat{\rho}_4 \delta\hat{\rho}_5 \delta\hat{\rho}_6 \ldots \right.$$

$$\left. + \int_4 \delta\hat{\rho}_4 (G_{12} G_{34} + G_{13} G_{24} + G_{23} G_{14}) \right]$$

$$= \frac{-i}{2} \int_{23} \zeta_{23} \left[- \int_{456} G_{14} G_{25} G_{36} \left\langle \delta\hat{\rho}_4 \delta\hat{\rho}_5 \delta\hat{\rho}_6 \right\rangle_{ref} \ldots \right. \tag{5.60}$$

$$\left. + \int_4 \left\langle \delta\hat{\rho}_4 \right\rangle_{ref} (G_{12} G_{34} + G_{13} G_{24} + G_{23} G_{14}) \right]$$

Where we have defined correlation functions $\langle \delta\rho\delta\rho\delta\rho \rangle_{ref}$ of the system with partition function Y. The second term in Eq. (5.61) is zero because of the aforementioned condition, which is equivalent to $\langle \delta\rho \rangle_{ref} = 0$. Meanwhile, we expect the first term in Eq. (5.61) to be smaller than the second term because it involves higher order terms in both $\delta\psi$ (via G) and $\delta\rho$. We thus propose to neglect the first term.

If we neglect these higher order terms in $\delta\psi$ and $\delta\rho$, we satisfy the self-consistency condition that $\langle \Psi \rangle = \langle \Psi \rangle_0 = -i\psi$, with the mean-field condition Eq. (5.56). Note that this is slightly different from requiring $\langle \Psi \rangle = \langle \Psi \rangle_{ref}$, but is, in addition to being more tractable, still physically reasonable and in the spirit of renormalizing the leading perturbation into the *Gaussian reference* action L_0.

Finally, we present the self-consistent first order perturbation results for the fluctuations. The perturbation expansion requires evaluating:

$$\langle \delta\psi_1 \delta\psi_2 \rangle_{ref} = \frac{1}{n!Y} \int_R \left\langle \delta\psi_1 \delta\psi_2 e^{-H_2 - H_3} \right\rangle_0 \tag{5.61}$$

$$= \frac{e^{-H_3}}{n!Y} \int_R e^{-\int_1 \hat{\rho}_1 \psi_1 - \frac{1}{2}\int_{12} \delta\hat{\rho}_1 G_{12} \delta\hat{\rho}_2} \left[G_{12} - \int_{34} G_{13} G_{24} \delta\hat{\rho}_3 \delta\hat{\rho}_4 \right]$$

$$= G_{12} - \int_{34} G_{13} G_{24} \left\langle \delta\hat{\rho}_3 \delta\hat{\rho}_4 \right\rangle_{ref}$$

$$
\begin{aligned}
\langle \delta\psi_1 \delta\psi_2 H_1 \rangle_{ref} =& \frac{1}{n!Y} \int_R \left\langle \delta\psi_1 \delta\psi_2 H_1 e^{-H_2 - H_3} \right\rangle_0 \qquad (5.62)\\
=& \frac{1}{2} \int_{34} \zeta_{34} \frac{e^{-H_3}}{n!Y} \int_R \left\langle \delta\psi_1 \delta\psi_2 \delta\psi_3 \delta\psi_4 e^{-H_2} \right\rangle_0 \\
=& \frac{1}{2} \int_{34} \zeta_{34} \frac{e^{-H_3}}{n!Y} e^{-\int_1 \hat{\rho}_1 \psi_1 - \frac{1}{2} \int_{12} \delta\hat{\rho}_1 G_{12} \delta\hat{\rho}_2} \ldots \\
& \left[G_{12} G_{34} + 2 G_{13} G_{24} + \int_{5678} G_{15} G_{26} G_{37} G_{48} \delta\hat{\rho}_5 \delta\hat{\rho}_6 \delta\hat{\rho}_7 \delta\hat{\rho}_8 \ldots \right. \\
& \quad - \int_{56} \delta\hat{\rho}_5 \delta\hat{\rho}_6 (G_{12} G_{35} G_{46} + G_{34} G_{15} G_{26} \ldots \\
& \quad \left. + G_{13} G_{25} G_{46} + G_{14} G_{25} G_{36} + G_{23} G_{15} G_{46} + G_{24} G_{15} G_{36}) \right] \\
=& \frac{1}{2} \int_{34} \zeta_{34} \left[G_{12} G_{34} + 2 G_{13} G_{24} + \int_{5678} G_{15} G_{26} G_{37} G_{48} \left\langle \delta\hat{\rho}_5 \delta\hat{\rho}_6 \delta\hat{\rho}_7 \delta\hat{\rho}_8 \right\rangle_{ref} \ldots \right. \\
& \quad - \int_{56} \left\langle \delta\hat{\rho}_5 \delta\hat{\rho}_6 \right\rangle_{ref} (G_{12} G_{35} G_{46} + G_{34} G_{15} G_{26} \ldots \\
& \quad \left. + G_{13} G_{25} G_{46} + G_{14} G_{25} G_{36} + G_{23} G_{15} G_{46} + G_{24} G_{15} G_{36}) \right]
\end{aligned}
$$

$$
\begin{aligned}
\langle H_1 \rangle_{ref} =& \frac{1}{n!Y} \int_R \left\langle H_1 e^{-H_2 - H_3} \right\rangle_0 \qquad (5.63)\\
=& \frac{1}{n!Y} \int_R \left\langle \frac{1}{2} \int_{34} \delta\psi_3 \zeta_{34} \delta\psi_4 e^{-H_2 - H_3} \right\rangle_0 \\
=& \frac{1}{2} \int_{34} \zeta_{34} \frac{e^{-H_3}}{n!Y} \int_R \left\langle \delta\psi_3 \delta\psi_4 e^{-H_2} \right\rangle_0 \\
=& \frac{1}{2} \int_{34} \zeta_{34} \left[G_{34} - \int_{56} G_{35} G_{46} \left\langle \delta\hat{\rho}_3 \delta\hat{\rho}_4 \right\rangle_{ref} \right]
\end{aligned}
$$

where we have used the Gaussian identities to evaluate the Gaussian averages.

Piecing everything together, we get:

$$\begin{aligned}
\langle \delta\psi\delta\psi\rangle =& \langle \delta\psi_1\delta\psi_2\rangle_{ref} - \langle \delta\psi_1\delta\psi_2 H_1\rangle_{ref} + \langle \delta\psi_1\delta\psi_2\rangle_{ref}\langle H_1\rangle_{ref} \qquad (5.64)\\
=& G_{12} - \int_{34} G_{13}G_{24}\langle \delta\hat{\rho}_3\delta\hat{\rho}_4\rangle_R \\
&- \frac{1}{2}\int_{34}\zeta_{34}\Big[G_{12}G_{34} + 2G_{13}G_{24} + \int_{5678} G_{15}G_{26}G_{37}G_{48}\langle \delta\hat{\rho}_5\delta\hat{\rho}_6\delta\hat{\rho}_7\delta\hat{\rho}_8\rangle_R \ldots \\
&\quad - \int_{56}\langle \delta\hat{\rho}_5\delta\hat{\rho}_6\rangle_R (G_{12}G_{35}G_{46} + G_{34}G_{15}G_{26}\ldots \\
&\quad + G_{13}G_{25}G_{46} + G_{14}G_{25}G_{36} + G_{23}G_{15}G_{46} + G_{24}G_{15}G_{36})\Big] \\
&+ G_{12}\frac{1}{2}\int_{34}\zeta_{34}\Big[G_{34} - \int_{56} G_{35}G_{46}\langle \delta\hat{\rho}_3\delta\hat{\rho}_4\rangle_R\Big] \\
&- \int_{56} G_{15}G_{26}\langle \delta\hat{\rho}_5\delta\hat{\rho}_6\rangle_R \frac{1}{2}\int_{34}\zeta_{34}\Big[G_{34} - \int_{78} G_{37}G_{48}\langle \delta\hat{\rho}_7\delta\hat{\rho}_8\rangle_R\Big] \\
=& G_{12} - \int_{34} G_{13}G_{24}\ldots \\
&\langle \delta\hat{\rho}_3\delta\hat{\rho}_4\rangle_R - \frac{1}{2}\int_{34}\zeta_{34}\Big[2G_{13}G_{24} + \int_{5678} G_{15}G_{26}G_{37}G_{48}\langle \delta\hat{\rho}_5\delta\hat{\rho}_6\delta\hat{\rho}_7\delta\hat{\rho}_8\rangle_R \ldots \\
&\quad - \int_{56}\langle \delta\hat{\rho}_5\delta\hat{\rho}_6\rangle_R (G_{13}G_{25}G_{46} + G_{14}G_{25}G_{36} + G_{23}G_{15}G_{46} + G_{24}G_{15}G_{36})\Big] \\
&+ \frac{1}{2}\int_{34}\zeta_{34}\int_{56} G_{15}G_{26}\langle \delta\hat{\rho}_5\delta\hat{\rho}_6\rangle_R \int_{78} G_{37}G_{48}\langle \delta\hat{\rho}_7\delta\hat{\rho}_8\rangle_R \\
=& G_{12} - \int_{34} G_{13}G_{24}\langle \delta\hat{\rho}_3\delta\hat{\rho}_4\rangle_R - \frac{1}{2}\int_{34}\zeta_{34} 2G_{13}G_{24}\ldots \qquad (5.65)\\
&- \frac{1}{2}\int_{34}\zeta_{34}\Big[\int_{5678} G_{15}G_{26}G_{37}G_{48}\langle \delta\hat{\rho}_5\delta\hat{\rho}_6\delta\hat{\rho}_7\delta\hat{\rho}_8\rangle_R \\
&\quad - \int_{5678} G_{15}G_{26}\langle \delta\hat{\rho}_5\delta\hat{\rho}_6\rangle_R G_{37}G_{48}\langle \delta\hat{\rho}_7\delta\hat{\rho}_8\rangle_R \\
&\quad - \int_{56}\langle \delta\hat{\rho}_5\delta\hat{\rho}_6\rangle_R (G_{13}G_{25}G_{46} + G_{14}G_{25}G_{36} + G_{23}G_{15}G_{46} + G_{24}G_{15}G_{36})\Big]
\end{aligned}$$

Consistent with our self-consistency condition for the mean field ψ, we set $\langle \delta\psi\delta\psi\rangle = G$, i.e. every term after the first in Eq. (5.65) vanishes. The self-consistency condition is satisfied if

$$\zeta_{34} + \langle \delta\hat{\rho}_3\delta\hat{\rho}_4\rangle_{ref} = 0 \qquad (5.66)$$

and, like before, we neglect all higher order terms (in $\delta\hat{\rho}$ or $\delta\psi$). The above

self-consistency condition leads to the Green's function equation:

$$\begin{aligned} 0 =& U^{-1} - G^{-1} + \langle \delta\hat{\rho}\delta\hat{\rho} \rangle_{ref} \\ =& U^{-1} - G^{-1} + \langle \hat{\rho}\hat{\rho} \rangle_{ref} - \langle \hat{\rho} \rangle_{ref} \langle \hat{\rho} \rangle_{ref} \end{aligned} \tag{5.67}$$

In the bulk, the $\langle \hat{\rho} \rangle \langle \hat{\rho} \rangle$ term is immaterial for the Green's function equation because it leads to a delta function in Fourier space, thus only modifying the $k = 0$ mode, and arises as a consequence of maintaining constant particle number when working in the canonical ensemble. The Green's function is then essentially determined by the density-density pair correlation function $\langle \hat{\rho}\hat{\rho} \rangle_{ref}$ (related to the structure factor $\sim \rho S$ in Fourier space).

Eqs. (5.56) and (5.67) constitute the sc1P conditions in the canonical ensemble, using a hybrid particle-field partition function derivation. Importantly, there is a complicated self-consistency hidden in the fact that the chain structure $\langle \delta\rho\delta\rho \rangle_{ref}$ depends on G and ψ, and vice versa. A further complication is that the structure factor involved is a *multi*-chain structure.

5.5 Connection to Exact Field Theory and RPA

Our derived self-consistency equations for the RGF Eqs. (5.19), (5.20) and sc1P Eqs. (5.31), (5.36), (5.56) and (5.67) bear striking resemblance to mean-field and RPA expressions, which are based on the saddle-point approximation and a second order perturbation about the saddle-point, respectively. To understand the connection on a deeper level it is helpful to compare these expressions to the *exact* field-theoretic relations for systems with a bare pair interaction U and auxiliary field Ψ (Eq. 4.53 and 4.56 in [1]):

$$\langle \hat{\rho}_1 \rangle = \frac{i}{\beta} \int_2 U_{12}^{-1} \langle \Psi_2 \rangle \tag{5.68}$$

$$\langle \Psi_1 \Psi_2 \rangle = U_{12} - \int_{34} U_{13} \langle \hat{\rho}_3 \hat{\rho}_4 \rangle U_{24} \tag{5.69}$$

$$\begin{aligned} \langle \delta\psi_1 \delta\psi_2 \rangle =& \langle \Psi_1 \Psi_2 \rangle - \langle \Psi_1 \rangle \langle \Psi_2 \rangle \\ =& U_{12} - \int_{34} U_{13} \langle \delta\hat{\rho}_3 \delta\hat{\rho}_4 \rangle U_{24} \end{aligned} \tag{5.70}$$

where in the last equation $\delta\psi \equiv \Psi - \langle \Psi \rangle$, and these averages are all *system* averages. Eq. (5.68) has the exact same form as the self-consistency conditions Eqs. (5.19), (5.31), and (5.56), except that the averages are taken in the reference ensemble instead of the true ensemble. In the saddle-point approximation (and the RPA),

the reference ensemble is a single chain in an external field. Meanwhile, for the self-consistent relations derived in this chapter, the reference ensemble is either a single chain or system of chains interacting with a mean field and with each other through some effective interaction G. A crucial effect of the added pair-interactions in the reference ensemble is to modify chain structure.

For completeness we also look at the relation for the fluctuations – by inverting Eq. (5.70)

$$\langle \delta\psi_1 \delta\psi_2 \rangle^{-1} = U_{12}^{-1} + \int_3 \langle \delta\hat{\rho}_1 \delta\hat{\rho}_3 \rangle \left(\delta_{23} - \int_4 U_{24} \langle \delta\hat{\rho}_3 \delta\hat{\rho}_4 \rangle \right)^{-1} \tag{5.71}$$

$$\approx U_{12}^{-1} + \langle \delta\hat{\rho}_1 \delta\hat{\rho}_2 \rangle \tag{5.72}$$

The RPA, RGF, and sc1P approximate the fluctuations $\langle \delta\psi_1 \delta\psi_2 \rangle = G_{12}$. The RPA tries to approximate the chain structure term with a scaled *single* mean-field chain structure $n \left\langle \hat{\rho}^{(1)} \hat{\rho}^{(1)} \right\rangle_0$, while the RGF and grand-canonical sc1P approximate it with a renormalized single-chain structure $n \left\langle \hat{\rho}^{(1)} \hat{\rho}^{(1)} \right\rangle$. Lastly, the canonical-ensemble sc1P uses a multi-chain reference system $\langle \delta\hat{\rho}_1 \delta\hat{\rho}_2 \rangle_{ref}$.

5.6 Discussion and Conclusion

In the grand canonical ensemble, RGF and sc1P yield equivalent self-consistent relations. Importantly, for flexible molecules both procedures involve an adaptive chain structure that must be solved self-consistently with the reference action's field fluctuations; this chain structure renormalization accounts for the leading effect of fluctuations beyond the RPA-level.

We take a moment to compare our results with several others reported in the literature. Interestingly, for simple electrolytes, it was previously shown that a variational Gaussian approach yielded the same self-consistent conditions as an inhomogeneous Ornstein-Zernicke theory with the RPA closure [32]. In a similar vein, for rigid molecules the RGF and sc1P can be seen to give the same equations as the RPA, because there will no longer be chain-structure self-consistency [30].

However, for flexible molecules it is doubtful that the Ornstein-Zernicke theory with the RPA closure will yield the RGF and sc1P conditions, as neither the Ornstein-Zernicke equations nor the RPA closure describe how chain structure should *change* in response to different mean fields ψ or fluctuations G. Typically, self-consistent chain structure must be *added* into a theory by ansatz, such as in the self-consistent PRISM [34, 35] or RPA theories [36]. The RGF and sc1P approaches *naturally* prescribe equations to effect this self-consistent chain structure calculation.

Another interesting work considered derivatives of the grand canonical partition function with respect to the fugacity and an external source term [2]. The real partition function must satisfy these derivative relationships for self-consistency, thus yielding self-consistency conditions for any proposed variational action. Importantly, this work showed that there are two possible second-order conditions to satisfy, and thus the variational Gaussian self-consistency approach is *not* unique. Interestingly, the linearized second-order condition in this approach was shown to be satisfied by the variational Gaussian approach. By extension, the sc1P grand canonical theory derived in our work also satisfies the same linear second-order condition. Our preliminary (unpublished) explorations with this self-consistency scheme suggest that it can also renormalize chain conformations in the grand canonical ensemble, and it would be interesting to consider what this method of constructing self-consistent conditions might say about the canonical ensemble.

We were also able to apply the sc1P procedure to the canonical ensemble, which the RGF is ill-suited for. A key step in our analysis was to carry out the perturbation only on the harmonic term $H_1 = \int_{12} \delta\psi_1 \cdot (G^{-1} - U^{-1})_{12} \cdot \delta\psi_2$ Eq. (5.42), leaving the action term that is linear in density $\int_1 \delta\psi_1 \cdot \hat{\rho}_1$ Eq. (5.43) exponentiated, and to apply the Gaussian averaging over Ψ *before* carrying out the configurational integration. We were motivated to do this because the resulting Gaussian integrals can be evaluated *exactly*, and leads to a transparent and more accurate perturbation expansion where the reference action is that of a system of chains interacting via the Green's function G and under the action of an external field $\psi_1 - \int_{23} G_{12} U_{23}^{-1} \psi_3$.

One key feature of this perturbation approach is that the reference system is *multi*-chain, in contrast to the effective *single*-chain reference system in the grand canonical ensemble. This is important because the grand canonical theories derived in this paper can only renormalize intra-chain structural effects of the fluctuations, whereas the canonical ensemble theory in principle also includes a renormalization of the *inter*-chain structure. A detail of our derived canonical-ensemble self-consistent conditions is that for given perturbation order in H_1, the averaging with respect to the reference system yields terms that are to mixed order in $\delta\psi$ and $\delta\rho$. To effect the self-consistency conditions, we opted to collect terms by their order in $\delta\psi$ and $\delta\rho$, and renormalize the leading perturbation terms into the variational Gaussian action parameters ψ and G.

We compare our results to a previous first-order perturbation theory applied to the canonical ensemble [11, 24]. In addition to only considering the bulk and tacitly

setting the average $\psi = 0$, for its reference action this theory neglected the energy term $\left(\int_1 \delta\psi_1\hat{\rho}_1\right)$ linear in the density. This reference state hence does not explicitly couple the chain conformations with field fluctuations, and is essentially that of *n independent* chains (with prescribed structure) and an independently fluctuating auxiliary field. In order to incorporate inter-chain structural or screening effects, this theory performed a perturbation calculation and Gaussian averaging on the $\exp[-H_1 - \int_1 \delta\psi_1\hat{\rho}_1]$ Boltzmann factor, kept H_1 to first order, and resummed only the higher order $\delta\psi\hat{\rho}$ terms that did not mix H_1 and $\delta\psi\hat{\rho}$ (in contrast to our theory, where we Gaussian average $\exp\left[-H_1 - \int_1 \delta\psi_1\hat{\rho}_1\right] \approx (1 - H_1)\exp\left[-\int_1 \delta\psi_1\hat{\rho}_1\right]$ exactly). Finally, self-consistent chain structure was re-introduced by a separate argument requiring those the reference system's non-interacting chains' structures be the same as that of single chains interacting via the effective interaction mediated by G. Again, whereas the chain structure self-consistency arises naturally out of our self-consistent derivation, it had to be introduced by a separate physical argument in this previous work.

Thus we consider the canonical ensemble sc1P theory described in our paper, because of its use of a more accurate reference system than the previous theory, to be a closer approximation of the actual system. However, the previous theory should not be underestimated – the simpler reference action and accompanying approximations allow for greater analytical tractability and a reduction of the multi-chain reference system to calculations involving just an effective single chain [11]. This reduction to an effective single chain problem is a very powerful result.

We note that the self-consistent first order perturbation theory procedure shares similarities to Hartree approximations [3, 33]. The Hartree approximation has been effected in several different ways in literature [1, 7, 9, 37], but like the sc1P, involves renormalizing higher order perturbation responses into the functional form of a higher order, typically mean-field response function, i.e. the leading order mean-field response is renormalized. The self-consistency scheme is then effected by requiring that the bare response used in calculating the perturbation contribution be set to the renormalized mean-field response.

To make things more concrete, for example, for neutral polymer solutions one way to effect the Hartree approximation is to demand that the fluctuation contribution to the renormalized virial coefficient B_r be calculated using B_r instead of the bare interaction strength B [1]. Similar analyses have been done for studying binary polymer blends [7–9, 37], where the Hartree approximation was effected by consid-

ering the perturbation correction to the $k \to 0$ response function $\chi(k)$ and termed a renormalized one loop (ROL) theory. While technically the response function should be renormalized at all wavelengths, for simplicity it is often only performed for the long wavelength contribution $\chi(k \to 0)$. One interesting observation is that the response $\chi(k)$ can be related to the system's structure factor [9], such that a Hartree renormalization of $\chi(k \to 0)$ can be understood as a renormalization of the long wavelength structure factor. Such long wavelength renormalizations are vitally important near critical points. However, for systems where a finite length scale emerges, a Hartree approximation would have to be performed for $k \neq 0$.

In a similar vein to the Hartree, the canonical ensemble sc1P theory also renormalizes inter-chain interactions, and so will renormalize the long wavelength $k \to 0$ solution structure. In contrast, the grand canonical RGF or sc1P only renormalizes *intrachain* structure, but does so for all $k > 1/R$ where R is some characteristic chain size. Thus the grand canonical RGF and sc1P complement the $k \to 0$ ROL theories. In fact, in this thesis we will demonstrate that the long-range nature of electrostatic interactions renders *intra*-chain structural renormalizations very important. Thus, the RGF is ideally suited for studying polyelectrolyte systems.

Lastly, we would be remiss if we did not mention a series of works using a "Gaussian Equivalent Representation"(GER) method that was previously developed for quantum physics [38] and later applied to study polyelectrolytes [39–41]. Like the RGF, the GER seeks to find the closest Gaussian representation of a field-theoretic partition function as possible. However, in its derivation the GER does not explicitly incorporate a chain conformation self-consistency condition like in the RGF. Instead, like previous canonical-ensemble sc1P theories, chain conformation self-consistency had to be added in by additional physical arguments [42].

To conclude, we have derived that an important physical effect of self-consistent (i.e. non-perturbative) Gaussian fluctuations *beyond* the RPA (a second order perturbative theory) correspond to renormalizations of both intra and inter-chain structure. Further, the grand canonical RGF theory can be understood as a self-consistent first order perturbation where we require the reference action's mean field ψ and response function G to simultaneously match, to first order, the full system's mean field and response. Thus, even though the GFB bound – upon which variational Gaussian approaches are built – is not satisfied for the complex actions found in many field-theoretic statistical mechanics formulations, the variational procedure can nevertheless be grounded in its satisfaction of intuitive self-consistent condi-

tions.

We also highlight that our canonical ensemble sc1P theory includes renormalizations of the inter-chain structure factor. Our derivation helps bring transparency to previous self-consistent perturbation theories, and can serve as a more accurate foundation upon which future work on the coupling between structure and fluctuations can be built.

5.7 Appendix

Both the RGF and sc1P procedures rely on the *exact* evaluation of certain Gaussian averages. Some particular useful ones involve evaluating moments that are exponentially-weighted by $\exp\left[-i\int_1 f_1\delta\Psi_1\right]$:

$$\left\langle e^{-i\int_1 f_1\delta\psi_1}\right\rangle_0 = \exp\left[-\frac{1}{2}\int_{12} f_1 G_{12} f_2\right] \tag{5.73}$$

$$\left\langle \delta\psi_1 e^{-i\int_1 f_1\delta\psi_1}\right\rangle_0 = \exp\left[-\frac{1}{2}\int_{12} f_1 G_{12} f_2\right](-i)\int_2 G_{12} f_2 \tag{5.74}$$

$$\left\langle \delta\psi_1\delta\psi_2 e^{-i\int_1 f_1\delta\psi_1}\right\rangle_0 = \exp\left[-\frac{1}{2}\int_{12} f_1 G_{12} f_2\right]\left(G_{12} - \int_{34} G_{13}G_{24}f_3 f_4\right) \tag{5.75}$$

$$\begin{aligned}\left\langle \delta\psi_1\delta\psi_2\delta\psi_3 e^{-i\int_1 f_1\delta\psi_1}\right\rangle_0 = \exp&\left[-\frac{1}{2}\int_{12} f_1 G_{12} f_2\right](-i)\ldots \\ &\cdot\Bigg[-\int_{456} G_{14}G_{25}G_{36}f_4 f_5 f_6\ldots \\ &\quad + G_{12}\int_4 G_{34}f_4 + G_{13}\int_4 G_{24}f_4\ldots \\ &\quad + G_{23}\int_4 G_{14}f_4\Bigg]\end{aligned} \tag{5.76}$$

$$\begin{aligned}\left\langle \delta\psi_1\delta\psi_2\delta\psi_3\delta\psi_4 e^{-i\int_1 f_1\delta\psi_1}\right\rangle_0 = \exp&\left[-\frac{1}{2}\int_{12} f_1 G_{12} f_2\right]\ldots \\ &\cdot\Bigg[(G_{12}G_{34} + 2G_{13}G_{24})\ldots \\ &\quad -\int_{56} f_5 f_6[G_{12}G_{35}G_{46} + G_{34}G_{15}G_{26}\ldots \\ &\qquad + G_{13}G_{25}G_{46} + G_{14}G_{25}G_{36}\ldots \\ &\qquad + G_{23}G_{15}G_{46} + G_{24}G_{15}G_{36}]\ldots \\ &\quad + \int_{5678} f_5 f_6 f_7 f_8 G_{15}G_{26}G_{37}G_{48}\Bigg]\end{aligned} \tag{5.77}$$

where in the last identity we have assumed symmetry between the (explicit) arguments (1 and 2), (3 and 4), as will be the case in our derivations. In the text of the chapter, f was typically $\delta\hat{\rho}_1 = \hat{\rho}_1 - \int_2 U_{12}^{-1} \cdot \psi_2$.

The above identities can be easily proven be Taylor-expanding the exponential, performing the averages, and re-summing, being careful to keep track of all the permutations of the Wick terms. This re-summation can be done exactly, yielding the effective interaction terms $\frac{1}{2}\int_{12} f_1 \cdot G_{12} \cdot f_2$ in the exponent.

BIBLIOGRAPHY

[1]G. Fredrickson, *The equilibrium theory of inhomogeneous polymers* (Oxford University Press, USA, 2013).

[2]D. Frydel, "Introduction to statistical field theory: from a toy model to a one-component plasma", Eur. J. Phys. **36**, 065050 (2015).

[3]Z.-G. Wang, "Variational methods in statistical mechanics: a pedagogical introduction", in *Variational methods in molecular modeling*, edited by J. Wu, (Springer Singapore, Singapore, 2017) Chap. 1, pp. 1–29.

[4]V. Y. Borue, and I. Y. Erukhimovich, "A statistical theory of weakly charged polyelectrolytes: fluctuations, equation of state and microphase separation", Macromolecules **21**, 3240 (1988).

[5]A. V. Ermoshkin, and M. Olvera de la Cruz, "A modified random phase approximation of polyelectrolyte solutions", Macromolecules **36**, 7824 (2003).

[6]K. A. Mahdi, and M. O. de la Cruz, "Phase diagrams of salt-free polyelectrolyte semidilute solutions", Macromolecules **33**, 7649 (2000).

[7]Z.-G. Wang, "Concentration fluctuation in binary polymer blends: χ parameter, spinodal and ginzburg criterion", The Journal of Chemical Physics **117**, 481–500 (2002).

[8]P. Grzywacz, J. Qin, and D. C. Morse, "Renormalization of the one-loop theory of fluctuations in polymer blends and diblock copolymer melts", Phys. Rev. E **76**, 061802 (2007).

[9]J. Qin, and D. C. Morse, "Renormalized one-loop theory of correlations in polymer blends", J. Chem. Phys. **130**, 224902 (2009).

[10]S. F. Edwards, "The theory of polymer solutions at intermediate concentration", P. Phys. Soc. **88**, 265 (1966).

[11]M. Muthukumar, and S. Edwards, "Extrapolation formulas for polymer solution properties", J. Chem. Phys. **76**, 2720 (1982).

[12]F. S. Bates, J. H. Rosedale, G. H. Fredrickson, and C. J. Glinka, "Fluctuation-induced first-order transition of an isotropic system to a periodic state", Phys. Rev. Lett. **61**, 2229–2232 (1988) 10.1103/PhysRevLett.61.2229.

[13]R. R. Netz, and H. Orland, "Variational charge renormalization in charged systems", The European Physical Journal E **11**, 301–311 (2003).

[14]Z.-G. Wang, "Fluctuation in electrolyte solutions: the self energy", Phys. Rev. E **81**, 021501 (2010).

[15]M. Kanduč, A. Naji, J. Forsman, and R. Podgornik, "Dressed counterions: strong electrostatic coupling in the presence of salt", The Journal of Chemical Physics **132**, 124701 (2010).

[16]A. Naji, M. Kanduč, J. Forsman, and R. Podgornik, "Perspective: coulomb fluids—weak coupling, strong coupling, in between and beyond", The Journal of Chemical Physics **139**, 150901 (2013).

[17]L. Lue, "Variational methods in statistical mechanics: a pedagogical introduction", in *Variational methods in molecular modeling*, edited by J. Wu, (Springer Singapore, Singapore, 2017) Chap. 5, pp. 137–154.

[18]R. Netz, "Electrostatistics of counter-ions at and between planar charged walls: from poisson-boltzmann to the strong-coupling theory", The European Physical Journal E **5**, 557–574 (2001).

[19]A. G. Moreira, and R. R. Netz, "Phase behavior of three-component ionic fluids", Eur. Phys. J. D **13**, 61 (2001).

[20]S. Buyukdagli, M. Manghi, and J. Palmeri, "Variational approach for electrolyte solutions: from dielectric interfaces to charged nanopores", Phys. Rev. E **81**, 041601 (2010).

[21]Z. Xu, M. Ma, and P. Liu, "Self-energy-modified poisson-nernst-planck equations: wkb approximation and finite-difference approaches", Phys. Rev. E **90**, 013307 (2014).

[22]A. W. C. Lau, D. B. Lukatsky, P. Pincus, and S. A. Safran, "Charge fluctuations and counterion condensation", Phys. Rev. E **65**, 051502 (2002).

[23]A. W. C. Lau, and P. Pincus, "Counterion condensation and fluctuation-induced attraction", Phys. Rev. E **66**, 041501 (2002).

[24]M. Muthukumar, "Double screening in polyelectrolyte solutions: limiting laws and crossover formulas", J. Chem. Phys. **105**, 5183 (1996).

[25]M. Muthukumar, "Phase diagram of polyelectrolyte solutions: weak polymer effect", Macromolecules **35**, 9142 (2002).

[26]M. Muthukumar, "Theory of counter-ion condensation on flexible polyelectrolytes: adsorption mechanism", J. Chem. Phys. **120**, 9343 (2004).

[27]I. I. Potemkin, and V. V. Palyulin, "Complexation of oppositely charged polyelectrolytes: effect of discrete charge distribution along the chain", Phys. Rev. E **81**, 041802 (2010).

[28]A. M. Rumyantsev, and I. I. Potemkin, "Explicit description of complexation between oppositely charged polyelectrolytes as an advantage of the random phase approximation over the scaling approach", Phys. Chem. Chem. Phys. **19**, 27580–27592 (2017).

[29]D. Chandler, *Introduction to modern statistical mechanics* (Oxford University Press, 1987).

[30]K. Shen, and Z.-G. Wang, "Electrostatic correlations and the polyelectrolyte self energy", J. Chem. Phys. **146**, 084901 (2017) DOI:10.1063/1.4975777.

[31]K. Shen, and Z.-G. Wang, "Polyelectrolyte chain structure and solution phase behavior", Macromolecules **51**, 1706–1717 (2018) DOI:10.1021/acs.macromol.7b02685.

[32]D. Frydel, and M. Ma, "Density functional formulation of the random-phase approximation for inhomogeneous fluids: application to the gaussian core and coulomb particles", Phys. Rev. E **93**, 062112 (2016).

[33]P. M. Chaikin, and T. C. Lubensky, *Principles of condensed matter physics*, Vol. 1 (Cambridge University Press Cambridge, 1995).

[34]C.-Y. Shew, and A. Yethiraj, "Monte carlo simulations and self-consistent integral equation theory for polyelectrolyte solutions", J. Chem. Phys. **110**, 5437 (1999).

[35]A. Yethiraj, "Theory for chain conformations and static structure of dilute and semidilute polyelectrolyte solutions", J. Chem. Phys. **108**, 1184 (1998).

[36]J. P. Donley, J. Rudnick, and A. J. Liu, "Chain structure in polyelectrolyte solutions at nonzero concentrations", Macromolecules **30**, 1188 (1997).

[37]D. C. Morse, and J. Qin, "Relationships among coarse-grained field theories of fluctuations in polymer liquids", J. Chem. Phys. **134**, 084902 (2011).

[38]G. V. Efimov, and E. A. Nogovitsin, "The partition functions of classical systems in the gaussian equivalent representation of functional integrals", Physica A: Statistical Mechanics and its Applications **234**, 506–522 (1996).

[39]S. A. Baeurle, M. Charlot, and E. A. Nogovitsin, "Grand canonical investigations of prototypical polyelectrolyte models beyond the mean field level of approximation", Phys. Rev. E **75**, 011804 (2007).

[40]E. A. Nogovitsyn, and Y. A. Budkov, "Development of the theory of a self-consistent field for polyelectrolyte solutions", Russ. J. Phys. Chem. A **85**, 1363–1368 (2011).

[41]Y. Budkov, E. Nogovitsyn, and M. Kiselev, "The model of a polyelectrolyte solution with explicit account of counterions within a self-consistent field theory", Russ. J. Phys. Chem. A **87**, 638–644 (2013).

[42]A. L. Kolesnikov, Y. A. Budkov, and E. A. Nogovitsyn, "Coarse-grained model of glycosaminoglycans in aqueous salt solutions. a field-theoretical approach", J. Phys. Chem. B **118**, 13037–13049 (2014).